Syntheses of Luciferins and Their Bioluminescent Evaluation

Marwaan Rylands

Department of Chemistry

University of Cape Town

August 2018

Syntheses of Luciferins and Their Bioluminescent Evaluation

Thesis presented for the degree of

Doctor of Philosophy

by

Marwaan Rylands

Supervisor: Assoc. Prof. M. A. Jardine

Department of Chemistry

University of Cape Town

Rondebosch, 7701

Cape Town

South Africa

August 2018

Declaration

I know the meaning of plagiarism and declare that "***Syntheses of Luciferins and Their Bioluminescent Evaluation"*** is my original work and to the best of my knowledge has not been presented for the award of any degree at any university. I declare that all of the work in this document, except for that which is properly acknowledged, is my own.

SIGNATURE: _____

DATE: August 2018

I would like to dedicate this thesis to my Grandmother, Gawa Van Dyk – For her love that stays with me even now after she has gone. Memie, I wish you could have been here for this!

Acknowledgements

First and foremost, I acknowledge my lord and creator (*Allah*) – I thank the almighty *Allah* for guiding me on this journey, for granting me all that I've needed, and for using those most dear to me as his instruments for enriching my life with goodness, love and faith.

To my parents, Hiemie and Gayba – I never once felt that I was in any way disadvantaged, to this day, I have never felt that I could not compete, and I most certainly never felt that I could not succeed. The two of you have given me everything I have ever needed and there are no words that can express the depths of my gratitude and love. I thank you and I love you.

To my supervisor, Anwar Jardine – There are many people who contributed to this body of work, but you Dr AJ, you helped shape not only this thesis but also me as an individual and for that I will be forever grateful. I sincerely thank you for your guidance and support.

To the AJ research group and the members of Lab 7A, past and present – Thank you all for guiding me in the lab as well as for helping me grow as a scientist. A special thank you to Shakeela Sayed and Nadia Baartzes for your friendship and support, you both had a huge impact on me and on my time on the 7th floor, thank you.

A sincere thank you to Prof Hunter, Sophie Reese-Jones and the rest of the Hunter research group for their contribution to this thesis and for allowing me to join in on the Hunter group meetings.

Thank you to Shankari Nair for the useful discussions and for taking the time to read this thesis, and to Daniel Kuzsa and Zaheer Timol for their guidance, company and friendship.

To my family – I am proud of who I am because of who you all are. Thank you for your support.

To my wife and best friend, Laa-iqa – Liefling, you have been a constant source of encouragement and support for me from the very start of this journey. I thank you for your patience and sacrifice. Thank you for understanding and struggling through "the student life" with me. I could not have been granted a better partner, I love you.

Lastly, to those who have helped me financially – My pursuit of this degree would not have been possible without the NRF and David and Elaine Potter foundation. I sincerely thank both organisations for their respective contributions, and I would like to thank the David and Elaine Potter Foundation in particular, for not only their generous financial support, but also for taking an interest in my life story.

Thank you all, I was truly blessed to have had such love, care and support.

Outputs

Results from this thesis have been presented at the following conferences;

The Development of Luciferin-Based Bioluminescent Probes, 18th Tetrahedron Symposium, MCEC, Melbourne, Australia, 23-26 July **2017** – Poster presentation

The Development of Luciferin-Based Bioluminescent Probes, RACI Centenary Congress 2017, MCEC, Melbourne, Australia, 24-28 July **2017** – Poster presentation

The Development of Luciferin-Based Bioluminescent Probes, 6th International Conference for Young Chemists, School of Chemical Sciences, University of Sains Malaysia, Penang, Malaysia, 16-18 August **2017** – Poster presentation

The Development of Luciferin-Based Bioluminescent Probes, 14th Frank Warren Conference, Rhodes University, South Africa, 4-8 December **2016** – Oral presentation

Synthesis and Bioluminescent Evaluation of D-luciferin and Related analogues, UCT Post Graduate Science Students' Colloquium 2016, University of Cape Town, South Africa, 31 August **2016** – Oral presentation

Synthesis and Bioluminescent Evaluation of D-luciferin and Related analogues, SACI/RSC Young Chemists' Symposium 2015, University of Cape Town, South Africa, 13 November **2015** – Poster presentation

One-pot, metal free synthesis of substituted benzothiazoles, 2nd Annual Meeting of the G2C2 Network, Cape Town, South Africa 24-26 August **2014** – Poster presentation

Synthesis and Bioluminescent Evaluation of D-luciferin and Related analogues, 2nd International Symposium on Natural Products, Cape Town, South Africa, 23-25 September **2014** – Poster presentation

One-pot, metal free synthesis of substituted benzothiazoles, SACI/ACS Bi-National Organic Chemistry Conference, Stellenbosch, South Africa, 30th November - 4th December **2014** – Poster presentation

The following patent has been filed based on results from this thesis;

"***DERIVATIVES OF LUCIFERIN AND METHODS FOR THEIR SYNTHESIS***", M. Rylands, M. A. Jardine, GB17l 1983.5, PCT specification filed 25th July **2017**

Abstract

Luciferins are a class of light emitting small molecule substrates. These molecules are oxidised to produce visible light in a reaction catalysed by the luciferase enzymes. The combination of this luminescent reaction coupled with charge-coupled device (CCD) cameras, has produced revolutionary technologies that enable measurements of mammalian gene expression in cells, as well as protein-protein interactions, biochemical labelling, and small molecule flux, to name a few. Of all the luciferin molecules, D-luciferin is the most widely researched. D-Luciferin is the light emitting molecule isolated from the American firefly *Photinus pyralis (Ppy)*. Synthetic D-luciferin has become increasingly valuable since its incorporation into a growing number of commercially available assay kits where the molecule is used as a sensitive reporter both in vitro and in vivo.

This thesis focuses on improved methods of preparing synthetic D-luciferin and related C6-analogues, as well as exploring the bioluminescent properties of a novel C6-thio analogue of D-luciferin. The novel analogue was targeted to provide an alternative or complementary substrate for bioluminescence imaging, that would allow for bioluminescence to be applied in systems where traditional D-luciferin application was limited.

In the first part of the thesis, D-luciferin and a C6-amino analogue of D-luciferin, D-aminoluciferin, were prepared and evaluated for the luciferase catalysed bioluminescent reaction. Both D-luciferin and D-aminoluciferin were prepared from *para*-substituted anilines, with overall yields ranging between 8 and 20 %. The poor overall yield was attributed to a low yielding C-S coupling reaction, that was common in both luciferin syntheses. Thus, modifications to the synthetic routes were subsequently explored, based on disadvantages and limitations that became apparent during initial luciferin preparation, these included among others; low yields and reliance on classical transition metal catalysed reactions. To address the synthetic shortcomings of the previous routes, a more efficient and scalable method for synthesising C6-substituted 2-cyanobenzothiazoles was developed. The C6-substituted 2-cyanobenzothiazoles were identified as key intermediates to the bioluminescent substrates. The new methodology employed easily prepared and inexpensive *ortho*-brominated anilines as starting materials. These anilines were subsequently converted to thioanilides and thereafter cyclised using base-mediated intra-molecular cyclisation reactions to generate the desired C6-substituted 2-cyanobenzothiazoles, resulting in improved overall yields for both D-luciferin and D-aminoluciferin (50-85 %). It was further demonstrated that these reactions, unlike their palladium-based equivalents, are more scalable, have better functional group tolerability and are relatively greener.

The second part of the thesis focuses on the preparation and bioluminescent evaluation of a novel C6-thio analogue of D-luciferin. Initial attempts at forming the C6-thio analogue, D-thioluciferin, were met with various challenges, including undesired *S*-oxidation and *S*-protecting group instability. Eventually a synthetic route based on a thiol-protecting group strategy proved successful. The method allowed for the preparation of pure D-thioluciferin over six steps (34 % yield) using an unconventional thioacrylate *S*-protecting group. The new luminogenic substrate displayed a lower K_m (0.1 µM relative to the 8 µM of D-luciferin) and a more red-shifted maximum emission (λ_{max} 600 nm compared to the 557 nm of D-luciferin), but with a much lower luminescent output relative to D-luciferin. The homodisulfide and sulfide of D-thioluciferin were also evaluated for their ability to produce light in the luciferase catalysed reaction. Both substrates were found to emit much more weakly relative to the free thiol, with the sulfide producing a non-statistically significant signal barely different from the background emission, while the disulfide produced a bioluminescence emission that was under 25 % of D-thioluciferin in emission intensity.

The thiol handle of D-luciferin and its bioluminescence properties were then explored for potential glutathione reductase (GSR) monitoring. The technology was based on an increase in bioluminescence emission resulting from disulfide reduction. A mixed disulfide of D-thioluciferin and the low molecular weight thiol glutathione (GSH) was prepared, where the disulfide functionality resulted in a weaker bioluminescent signal relative to free D-thioluciferin. Then, when the disulfide was reduced by GSR, a detectable bioluminescent signal in the presence of luciferase was produced. The D-Thioluciferin GSH hetero-disulfide was demonstrated to be a good substrate for GSR (K_m of 0.89 mM relative to 0.51 mM for GSSG) and, further to that, the hetero-disulfide was demonstrated to have successfully coupled its resulting luminescence signal to disulfide reduction, upon treatment with luciferase at increasing concentrations of GSR in a physiological buffer. In these examples, increased luminescence was observed at increasing concentrations of GSR and the data obtained was found to be comparable to commonly used colorimetric GSR assays, where induced changes in GSR activity were observed as fluctuations in sample absorbance.

Abbreviations

Ar	Aromatic
BET	Back-electron transfer
Bs	Broad singlet (NMR)
BLI	Bioluminescence imaging
CCD	Charge-coupled device
D	Doublet (NMR)
DBU	1,8-Diazobycyclo[5.4.0]undec-7-ene
Dd	Doublet of doublets
D-Cys	D-Cysteine
DME	1,2-Dimethoxyethane
DTT	Dithiothreitol
EA	Elemental analysis
EDG	Electron donating group
EDTA	Ethylenediaminetetraacetic acid
ee	Enantiomeric excess
EI	Electron impact
ESI	Electronspray ionisation
EtOAc	Ethyl acetate
EtOH	Ethanol
Eq.	Equivalent(s)
EWG	Electron withdrawing group
GSH	Glutathione
GSR	Glutathione reductase
GSSG	Glutathione disulfide
GST	Glutathione *S*-transferase
H	Hour(s)
HSQC	Heteronuclear single quantum coherence
HRMS	High resolution mass spectrometry
Hz	Hertz
IR	Infrared
J	Coupling constant
LMWTs	Low molecular weight thiols

LRMS	Low resolution mass spectrometry
Luc	Luciferase
M	Multiplet (NMR); Medium intensity (IR)
MeOH	Methanol
Min	Minute(s)
Mp	Melting point
MS	Mass spectrometry
m/z	Mass to charge ratio (MS)
NADPH	Nicotinamide adenine dinucleotide phosphate
NMP	*N*-methyl-2-pyrrolidone
NMR	Nuclear magnetic resonance
Pet. Ether	Petroleum ether
PG	Protecting group
PT	Proton transfer
Ppm	Parts per million
Ppy	*Photinus pyralis*
Q	Quartet (NMR)
R_f	Retention factor
RLU	Relative light units
ROS	Reactive oxygen species
Rt	Room temperature
S	Singlet (NMR); Strong intensity (IR)
SD	Standard deviation
SE	Standard error
SET	Single electron transfer
S_NAr	Nucleophilic aromatic substitution
T	Triplet (NMR)
TBAB	Tetrabutylammonium bromide
TD-DFT	Time-dependant density functional theory
TFA	Trifluoroacetic acid
TLC	Thin layer chromatography
TMS	Tetramethylsilane
t_R	Retention time

Contents

Chapter 1

Introduction to Bioluminescence

Abstract

Imaging technologies have been developed and refined to advance our understanding of biological processes by revealing cellular and molecular features of biology and disease, in real-time. One rapid and increasingly accessible technology for in vivo analysis employs internally generated light emitted from photobiological reactions. Luminous substrates, luciferins, are catalysed by enzymes, luciferases, and utilised for various imaging applications. The combination of this luminescent reaction with charge-coupled device (CCD) cameras has allowed for sensitive in vivo measurements of mammalian gene expression in cells, protein-protein interactions, biochemical labelling, and small molecule flux, to name a few. This chapter serves to introduce the subject of bioluminescence and its exploitation in bioluminescence imaging (BLI), as well as to provide perspective for subsequent sections.

Chapter 1

Introduction to Bioluminescence

Luminescence

Luminescence is the emission of light that does not directly depend on the temperature of the emitting substance and it is therefore considered the opposite of incandescence. For centuries luminescence has fascinated mankind and over many years this phenomenon has been noted in different forms and settings. From the extraordinary Northern Lights (*Aurora Borealis*) to the humble dim glow of the railroad worm (*Phengodidae*). Of course, many theories arose to explain these phenomena. The glowing tide (also known as sea light) for example, was at first attributed to the ignition of sea salt (Papin, 1647) or the rubbing together of salt molecules that gave off flint like sparks (Oartesius, 1648). It was the German physicist Eilhard Wiedmann, among others, who helped make the connection between the different forms of light emitting phenomena and coined the term *luminescence* to collectively describe them. He theorised that all light emitted from materials which did not require heating and did not evolve heat were being emitted by a similar mechanism, which in turn was also dissimilar from the evolution of light from incandescent bodies, such as burning wood or molten iron. Eilhard Wiedmann went on to further categorise the distinct types of luminescence (Figure 1.1). He studied the phenomena and generalised luminescence into two main groups; Photoluminescence and Chemiluminescence.

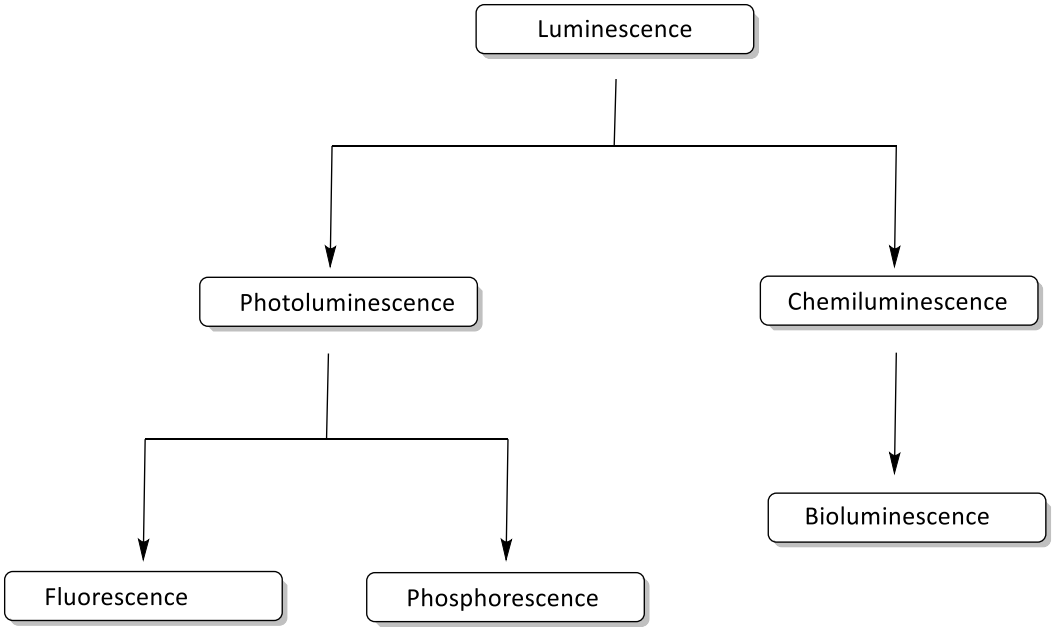

Figure 1.1. Luminescence as defined by Eilhard Wiedmann[1]

Both types of luminescence occur when a substance releases energy in the form of visible light. In the case of photoluminescence, the energy released is derived from the absorption of energy in the form of UV or visible light, which is then re-emitted as light of a longer wavelength. The light absorbing/emitting component of a substance is called its luminophore. Photoluminescence is further divided into fluorescence and phosphorescence. Fluorescence occurs when visible light is absorbed to raise the emitting material's fluorophore (molecular component/compound responsible for fluorescence) to a higher state of energy, and light then gets rapidly re-emitted when the material returns to its ground state (i.e. its energy state before the absorption of light). The light emitted is usually longer in wavelength relative to the light absorbed. Fluorescence is widely observed in the natural world, and many organisms are highly fluorescent. Phosphorescence is closely related to fluorescence, but unlike fluorescence, the energy absorbed is not immediately re-emitted. This results in phosphorescence having a much slower re-emission time scale that is associated with "forbidden" energy state transitions in quantum mechanics. Phosphorescence is less common in nature, there are however many everyday examples of phosphorescent materials, such as glow-in-the dark paints and glow sticks. These materials are characterised by their ability to 'store' light. Chemiluminescence is arguably the most interesting branch of luminescence. It is the evolution of light as a result of a chemical reaction (Scheme 1.1) and therefore, can be produced in complete darkness. The generation of light in its absence is a truly fascinating phenomenon, however, the light generated is by no means produced *ex nihilio*.

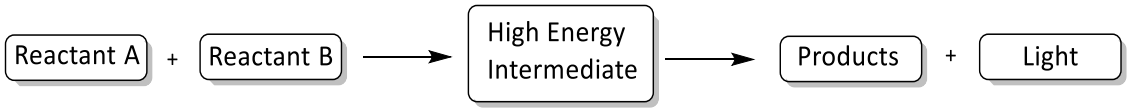

Scheme 1.1. General reaction for chemiluminescence

For chemiluminescence to be observed two or more substances must react to afford a high energy intermediate that relaxes to the ground state with the emission of visible light. One very famous example of a chemiluminescent reaction is that of luminol with blood. Forensic investigators commonly use luminol to detect trace amounts of blood at crime scenes, as it reacts with the iron in haemoglobin. Chemiluminescence is also observed widely in nature, where it is termed bioluminescence or 'living light'.

Bioluminescence remains one of Nature's most admired showcases. It is indeed a splendid display of her mastery over chemistry and has inspired many human endeavours.

Bioluminescence - living light

"…a world without a sun and without fire would by no means be a dark world"
LIVING LIGHT, E. N. HARVEY

When a chemical reaction results in the emission of light, it is termed chemiluminescent and when a chemiluminescent reaction is derived from a biological source, it is termed bioluminescent. Bioluminescence is therefore the chemical production of light by living organisms and is widely distributed among animal groups, particularly marine organisms. The biochemical reaction involves an enzyme and a small molecule substrate and, unlike photoluminescence, can be achieved in total darkness. The substrates used by luminous organisms for the light emitting reaction are collectively, and rather appropriately referred to as luciferins, derived from the Latin word *Lucifer* which means light bearing/bearer.[2] Luciferins are considered a class of structurally diverse small molecules that are oxidised in the presence of highly specific enzymes to produce light.[3] Figure 1.2 shows the structures of selected luciferins. These compounds are naturally produced by many different organisms and examples of such organisms include; the firefly *Photinus pyralis* (*Ppy*), the jelly fish *Aequorea victoria*, and glow worm larvae *Lampyris noctiluca,* to name a few.[4-7]

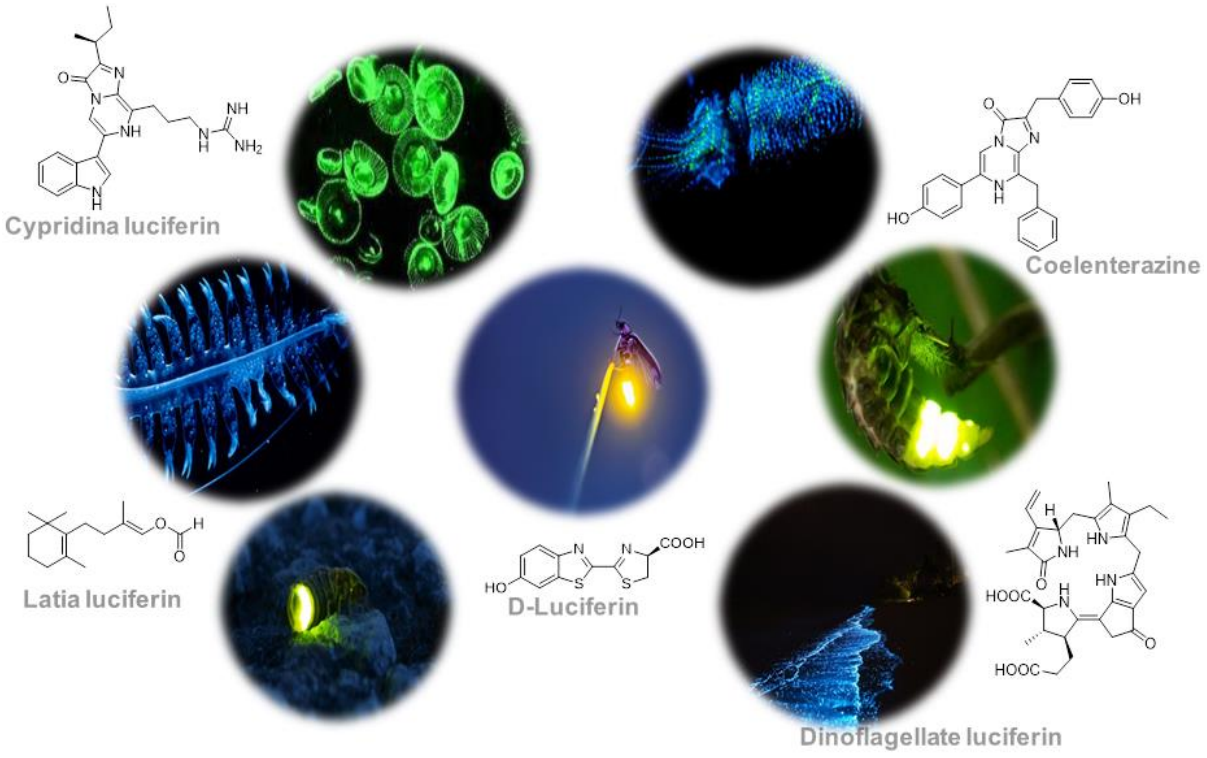

Figure 1.2. Bioluminescent organisms and their corresponding luciferins

Luciferin producing organisms make use of this biochemical reaction to produce light of different colours and intensities, often seen as spectacular bioluminescent displays. Indeed, bioluminescence has many wondrous applications in nature. Certain insects, such as the fire fly *Photinus pyralis*, may

use the light emitted from its tail for courtship signals.[8] Where distinct flashes of light in different patterns are used by the insects to indicate their locality and availability, thus it acts as a form of communication.[8-9] Jellyfish make use of the light emitting reaction to startle and deter potential predators,[5] and many other organisms have evolved to use this particular chemoenzymatic reaction in different and interesting ways. While many different organisms make use of the reaction they do not necessarily make use of the same luciferin. In fact, it has been proposed that there is genetic homology between different organisms using the same luciferin and that sufficiently structurally unique luciferin systems have evolved separately (albeit for the same purpose) and therefore, the evolution of bioluminescence is non-linear.[10-11]

The enzymes that catalyse the bioluminescent reaction are collectively referred to as luciferases. The observed green/yellow light emitted from the tail of the firefly *Ppy*, is due to the reaction of D-luciferin, with the enzyme luciferase in the presence of ATP, O_2 and magnesium ion.[12] In the crustacean *Cypridina hilgendorfii* bioluminescence is due to the reaction of a tryptamine derivative, cypridina luciferin, with its corresponding luciferin. The luciferin in freshwater snails, *Latia neritodes*, is latia luciferin and that in the sea pansy, *Renilla reniformis*, is coelenterazine. Dinoflagellate luciferin is a chlorophyll derivative and is found in some dinoflagellates, which are responsible for the observed night-time glowing of waves. Selected bioluminescent organisms and the wavelength at which the light emission is observed for specific luciferin/luciferase pairs are summarised in Table 1.1 below.

Table 1.1. Selected luciferin-utilising bioluminescent species and their corresponding luciferases

Luminous species	Luciferase	Luciferin	λ_{max} (nm)
P. fischeri, P. logei, P. phosphoreum, P. leiognathi[13]	Bacterial luciferases; heterodimeric with molecular weights in the range of 76 000 ± 4000	a reduced riboflavin phosphate ($FMNH_2$) and a corresponding long chain aldehyde	465/475
Photinus pyralis	Firefly luciferase, Family lampyridae	D-luciferin	560
Luciola mingrelica		D-luciferin	570
Luciola lateralis		D-luciferin	552
Luciola cruciata		LcLuc1	554
Luciola cruciata		LcLuc2	543
Luciola italica		D-luciferin	566/614
Hotaria unmunsana		D-luciferin	-
Hotaria tsushimana		D-luciferin	-
Hotaria parvula		D-luciferin	568

Lampyris noctiluca		D-luciferin	550
Lampyris turkestanicus		D-luciferin	-
Nyctophyla caucasica		D-luciferin	-
Pyrocoelia rufa		D-luciferin	-
Pyrocoelia miyako		D-luciferin	550
Diaphanes pectinealis		D-luciferin	-
Cratomorphus distinctus		D-luciferin	550
Photuris pennsylvanica		D-luciferin	-
Amydetes vivianii		D-luciferin	538
Microlampis sp.		D-luciferin	569
Pyrearnus termitilluminans	Click beetle luciferase, family Elateridae	D-luciferin	537
Pyrophorus plagiophthalamus		D-luciferin	540
Pyrophorus mellifluus		D-luciferin	549
Pyrophorus angustus		D-luciferin	566
Fulgeochizus bruchi		D-luciferin	540
Photophorus jansoni		D-luciferin	559
Ragopthalmus ohbai	Railroad worm luciferase, family Phengodidae	D-luciferin	550
Phrixothrix hirtus		D-luciferin	630
Phrixothrix vivianii		D-luciferin	542
Oplophorus gracilinostris	Coelenterazine utilising luciferase	Coelenterazine	454
Renilla reniformis		Coelenterazine	480
R. muelleri		Coelenterazine	485/479
Gaussia princeps		Coelenterazine	473
Metridia longa		Coelenterazine	480
M. pacifica		Coelenterazine	485
Cypridina (Vargula hilgendorfii)	Cypridina luciferase	Cypridina luciferin	465
Cypridina noctiluca		Cypridina luciferin	465
Periphylla peryphilla		Cypridina luciferin	
Benthosema pterotum		Cypridina luciferin	475
Gonyaulax polyedra, Pyrocystis lunula, Noctiluca scintillians	Dinoflagellate luciferase	Dinoflagellate luciferin	475
Latia neritoides	Latia luciferase	Latia luciferin	536

It is clear from the above table that the wavelength of the light emitted is highly dependent on the luciferin/luciferase pair (570 – 465 nm). Substantial research has gone into the various luciferin/luciferase systems, culminating in a wealth of research that has spanned decades from all scientific domains. The result of this has been that many of these bioluminescent systems have been explored within and outside of a biological setting to both probe our understanding of the mechanism and to also search for potential applications. Currently, there are approximately nine unique luciferin/luciferase systems that account for all known bioluminescence. The underlying mechanism of how light is emitted in these various systems have been well studied and it is accepted that light is emitted by the same mechanism in all instances.

Mechanism of Bioluminescence

Although the biological purpose of luminescence varies from species to species, the chemical mechanism for the generation of the electronically excited-state, responsible for the emission of light, appears to be common to all known bioluminescent organisms. Typically, the generation of light from a chemiluminescent reaction involves the formation of an electronically excited state product, which decays to the ground state while emitting light of a specific wavelength corresponding to the difference in energies between the excited and ground states. Figure 1.3 shows a general pathway for the generation of light from a chemical reaction. Important to note is that a reaction that occurs with enough energy to generate an electronically excited state molecule may generate light through the decay of the said molecule, or through the transfer of energy to an acceptor molecule or moiety (this may be achieved inter- or intramolecularly) which in turn would also decay with emission of light.

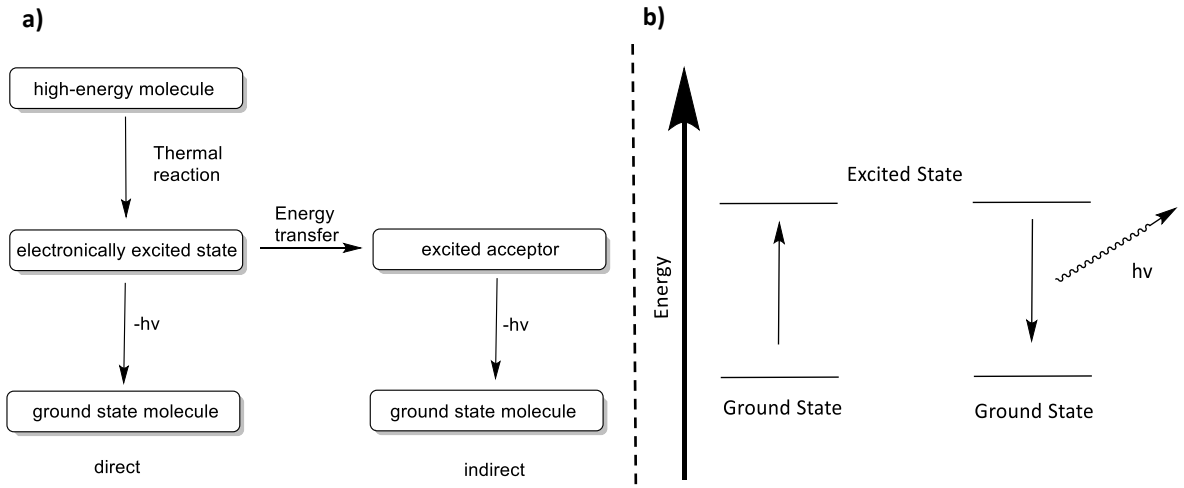

Figure 1.3. a) Proposed mechanism for chemiluminescence and b) its corresponding energy diagram

In most cases, bioluminescence is a result of the breakdown of a high energy cyclic peroxide molecule (dioxetane or dioxetenone) to an excited species, in the form of a decarboxylated or deoxygenated molecule, which relaxes to the ground-state with the expulsion of a photon. There are a number of publications which describe the chemical mechanism for the formation of electronically excited-state molecules. The proposed mechanism involves the luciferase mediated synthesis of a luciferin peroxy adduct and subsequent chemically-initiated electron exchange luminescence (CIEEL) or charge transfer induced luminescence (CTIL).[14-15] In the former case, an electron from either a heteroatom or aromatic pi-system is donated into the anti-bonding orbital of the peroxy O-O bond (π,σ*) resulting in a weakening of the bonding O-O molecular orbital and subsequent cleavage to afford the alpha-alkoxy acid radical anion. The generation of the electronic singlet excited state via the donation of one electron from the electron rich reservoir is shown (Scheme 1.2).

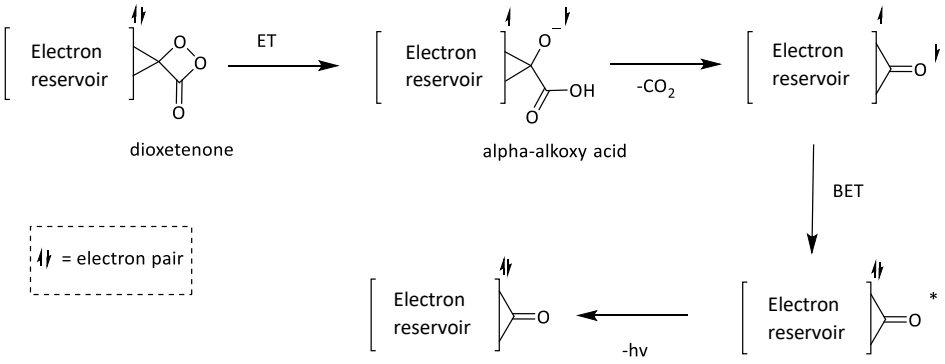

Scheme 1.2. CIEEL mechanism demonstrating the electron transfer process

The mechanism (initially proposed Gary B. Schuster and co-workers in 1977) relates the chemi-excitation to the electron transfer process and proposes that the energy for chemiluminescence results from intramolecular electron transfer in the decarboxylated product. Advances in quantum mechanical modelling have, however, called for a shift away from the CIEEL mechanism to the computationally supported CTIL mechanism.[15] The cyclic peroxy molecules and related dioxetanones have been investigated in great detail in a number of synthetic and mechanistic studies and the observation that the thermal reactions of these high-energy compounds lead to the formation of electronically excited-state carbonyl compounds is taken as strong circumstantial evidence for the involvement of similar intermediates in bioluminescence. In addition, it has also been observed that the thermal reaction of simply substituted dioxetanes and dioxetanones give rise to the non-luminescent triplet excited state of the carbonyl compound. On the other hand, the luminescent singlet excited-state was observed (at almost 100 %) for dioxetanones substituted with activated aromatic hydrocarbons. It was thus hypothesised that the aromatic group acted as an electron donor in the reaction and was crucial for the singlet-excited state formation. The two mechanisms named

were both proposed to account for the role of an electron donating group in the formation of the luminescent singlet-excited state. Both mechanisms start with a partial charge transfer from the electron donating fragment to the chemiluminophore dioxetanone moiety. In the step-wise CIEEL mechanism, a radical anion pair is formed through a single electron transfer (SET) followed by a back electron transfer (BET). In the CTIL, the fragmentation of the C-C and O-O bonds are concerted with the back charge transfer process. The CIEEL mechanism has met challenges concerning its potential for unwanted reactions involving radicals.[15]

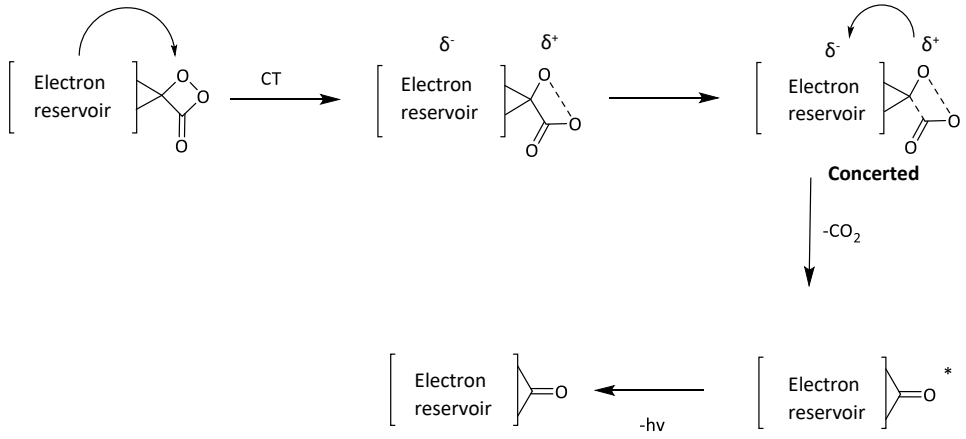

Scheme 1.3. CTIL mechanism demonstrating charge transfer mechanism

Both these mechanisms have contributed significantly to our understanding of how the bioluminescent reaction works, as well as in the development of new, non-natural and often improved bioluminescent substrates for applications in bioluminescent imaging (BLI). These mechanisms have also proved useful in rationalising the effects of different electron reservoirs on the wavelength of emission and how this can be exploited to design luciferins that emit at a specific wavelength. It also informs on what kind of derivatives can be made from natural luciferins by allowing for the identification of molecular components crucial for the light emitting reaction and components that are less so. All of this affects how bioluminescent systems are modified for new applications. One such application is bioluminescence imaging (BLI) which concerns the repurposing of natural bioluminescent systems to image biological analytes or processes.

Bioluminescence imaging has also evolved to observe biological processes as they are happening in real-time, and there is an increasing number of cellular assays based on various bioluminescent technologies where a reporter molecule, whose activity can be measured and imaged, is employed to monitor specific cellular analytes.[16-26]

Applications of Bioluminescence

Two major breakthroughs marked the start of the era of bioluminescence technologies. The first was the first total synthesis of a luciferin and the second was the determination of the nucleotide sequence of the *Ppy* luciferase gene. Together, these two events ushered in the era of applied bioluminescence and research concerning the applications of Nature's bioluminescence grew exponentially. Non-luminescent organisms were transfected to express luciferase and new luciferins were engineered to supplement and/or provide alternatives to conventional imaging modalities.

To gauge the importance of these developments we need only look at the list of Nobel Prizes awarded in Chemistry, where the most recent Nobel Prize (2017) was awarded to Richard Hendersen, Joachim Frank, Jacques Dubochet for their contribution to molecular imaging.[27-28] The prize was also awarded to Eric Betzig, Stefan W. Hell and William E. Moerner (2014) for their contribution to molecular imaging through fluorescence microscopy.[29] There are a number of imaging modalities that constitute molecular imaging, including; magnetic resonance imaging (MRI), near infra-red imaging, single photon emission tomography (SET), positron photon emission tomography (PET) and optical imaging. The term optical imaging relates to the use of bioluminescence, fluorescence and absorption/reflectance as applied to molecular imaging. Optical imaging has been used extensively in science and medicine and its applications are steadily growing. One of the benefits of optical imaging relative to other molecular imaging techniques is its comparatively benign nature. Generally, optical imaging and the imaging agents used are not harmful in a biological sense. Bioluminescence imaging in particular is extraordinarily biocompatible, which is expected given its origin.

Bioluminescence imaging (BLI) is the use of bioluminescent reactions for optical imaging. BLI makes use of the light emitting luciferase/luciferin interaction to monitor cellular and bio-molecular processes. How this works is that luciferase can be genetically engineered into organisms which formerly lacked the gene for the enzyme (can also be introduced ex vivo). Then, when the appropriate substrates and cofactors are introduced, emission of visible light at variable wavelengths can be detected by charge-coupled device (CCD) cameras. Information may then be obtained by coupling the emission of light to specific biological events. In conventional in vivo experiment strategies, temporal information about biological processes is often obtained through repeated, time stacked animal sacrifice. With BLI however, information can be obtained continuously over the duration of the event of interest. Many BLI systems have been developed to address the challenges faced in the broader field of molecular imaging.

These include; i) the development of reporter systems and probes that are able to reveal cellular and molecular processes over a designated time period, ii) the development of probes that are sufficiently sensitive to small changes in cell function and distribution over time, and iii) probes that do not significantly alter/ interfere with the biological process of interest. Many BL systems have since been developed based on the above-mentioned points and cover a wide area of applications.

in vivo BLI is now considered a cornerstone technology for preclinical molecular imaging. It is generally coupled to a specific biological process through enzyme-substrate interactions that become biological indicators that can be studied non-invasively in living animals. Different substrates exhibit different kinetic properties and different intracellular accumulation profiles due to differences in their molecular structure, which in turn influence their bio-distribution in animals. The most widely used applications of BLI includes its use in the study of gene expression, gene delivery, cell viability, cell physiology, in vivo cell trafficking, tumour burden, and protein-protein interactions.[30]

Bioluminescence imaging vs fluorescence imaging

Imaging techniques routinely used in clinical studies include: magnetic resonance imaging (MRI scan), radionuclide imaging (e.g. Gallium scan), ultrasound imaging (sonogram) and computed tomography (CAT scan).[31] In contrast to these techniques, optical imaging has been found to be very useful in terms of research and development. Thus far, its utility has been limited to studying small animals and plants. However, optical imaging remains the more cost-effective, and rapid technique, and can be easily applied to the study of various processes at a cellular level.

There are two major classes of optical imaging, Bioluminescence imaging (BLI) and Fluorescence imaging (FLI). FLI requires an external light source to excite a fluorophore and enable luminescence (fluorophores are chemical compounds or scaffolds which absorb and reemit electromagnetic radiation, most often in the form of visible light). In FLI, a fluorescent probe containing a fluorophore is introduced into a subject and an external light source is used to excite the probe resulting in luminescence. Fluorescent tagging is a practical example of this technology. Fluorescent probes can be tethered to drug like molecules and then, using FLI, one can determine the locality of the drugs in the organism, and even within cells. Similarly, the simultaneous use of two different fluorescent tags can allow for the determination of protein-protein, protein-DNA, and/or protein-substrate interactions. Despite its many applications and continued use, there are limitations associated with FLI. The limitations of FLI include auto-fluorescence (self-induced fluorescence) which arises from endogenous molecules in mammalian tissue. Auto-fluorescence occurs when endogenous molecules interfere with target resolution by scattering and absorbing light at the same wavelengths as the

exogenous fluorophores. For example, haemoglobin whose signals have to be distinguished from administered exogenous molecules.[32-34] However, studies are being done on the selection of appropriate wavelengths for the external light source to minimise background noise.

As previously discussed, bioluminescence imaging involves the production of light as a result of a biochemical reaction. BLI uses enzyme/substrate systems such as the *Ppy* luciferase/D-luciferin interaction to emit light. Unlike FLI, BLI is independent of external light sources required to induce luminescence. In addition, the enzyme luciferase has to be genetically engineered into non-luciferase expressing organisms in order for BLI to be used. Bioluminescence imaging (BLI) is gaining preference over FLI due to the opaque nature of mammalian tissue as well as the presence of endogenous fluorophores which may undesirably fluoresce upon excitation and interfere with FLI.[33] Luciferase based BLI was found to be more sensitive than green fluorescent protein (GFP) imaging. An example is reported where luciferase expressing tumours were detected as early as 1 day after tumour-cell inoculation, whereas GFP expressing tumours were only detectable after 7 days.[35] Limitations to the BLI technique include rapid depletion of the luciferin upon administration for diagnostic purposes. Thus, there is a need for a cheap and industrially sustainable synthetic route toward luciferins or cheaper analogues thereof.

Scope of this study

Of all known luciferins, D-luciferin, the molecule responsible for the emission of light from the tail of the American firefly *Ppy* (figure 1.4), is by far the most widely researched luciferin for its applications in bioluminescence imaging.

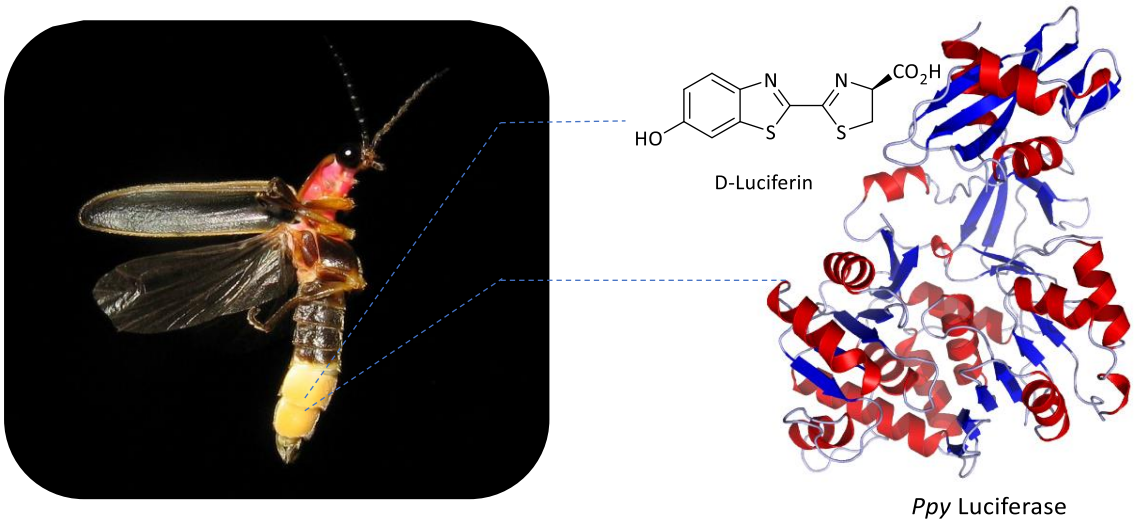

Figure 1.4. Bioluminescence of the American firefly (*Ppy*) and the structures of the enzyme, *Ppy* luciferase, and substrate, D-luciferin, responsible for the bioluminescent reaction.

Broadly, the aim of this study was to investigate the synthetic preparation of D-luciferin and its analogues and, further to that, to explore how the bioluminescent molecule could be exploited in terms of bioluminescent assay development. D-Luciferin was chosen as the luciferin of interest because of its growing use in the development of luciferin-based assays.

The synthetic preparation of D-luciferin was of particular interest since its cost and synthesis were well-known limiting factors to its practical applications. When this project was first proposed, the cost of D-luciferin was approximately R 8 000 for 10 mg (Sigma-Aldrich, March 2014). It was therefore of interest to explore and evaluate the synthetic routes that were available at the time and, thereafter, to propose and develop more efficient routes to the sought-after D-luciferin molecule.

Having an efficient and reliable procedure for luciferin preparation was necessary since further studies, involving the design and synthesis of D-luciferin derivatives, were also envisioned. It was therefore an early goal of this study to develop synthetic routes that would ensure rapid access to the required bioluminescent material.

It has been four years since the projects inception and the cost of D-luciferin has since been reduced to less than half of its initial price. The decrease in cost is largely due to the development of improved luciferin analogues as well the development of cheaper and more efficient synthetic sequences. This project aimed to contribute to these developments by producing a more efficient synthesis of D-luciferin and by introducing new luciferin analogues with improved properties.

Currently, there are a number of commercially available D-luciferin based BLI technologies and this study focused on further adding to the existing BLI arsenal, by developing BL alternatives to existing technologies. Of course, most of these BL technologies were based on *Ppy* D-luciferin whose synthesis is described subsequently (Chapter 2).

Structure of the thesis

The thesis has been divided into unique but related chapters, each with its own abstract, introduction and discussion. Each chapter has its own defined aim which highlights the focus of the research for that specific chapter.

This first chapter serves as an introduction to luminescence and bioluminescence, while subsequent chapters (Chapters 2-3) deal with the synthetic preparation of D-luciferin and its analogues, as well as their reported applications. These chapters also highlight the limitations of existing synthetic sequences and employed methodologies, so as to emphasise the relevance of research relating to improvements on the synthesis of D-luciferin and its derivatives. Accordingly, the following chapter

(Chapter 4) then deals with the study of novel and improved syntheses and synthetic methods. The study then shifts focus from the synthesis of the luciferin scaffold, to the preparation of a new luciferin derivative using the methods highlighted in the preceding chapter. The subsequent chapter (Chapter 5) covers the synthesis of a new derivative and extensively explores its bioluminescent properties. The remaining chapters (Chapters 6-7) focus on the potential applications of the new derivative, with an emphasis on applications where the new derivative offers greater utility than its predecessors.

As per the outlined structure, the next chapter will introduce the bioluminescent molecule D-luciferin.

References

1. Wiedemann, E., Ueber Fluorescenz und Phosphorescenz I. Abhandlung. *Annalen der Physik* **1888,** *270* (7), 446-463.
2. Murthy, K.; Virk, H. S., In Luminescence Phenomena: An Introduction, Defect and Diffusion Forum, *Trans Tech Publ* **2014,** 1-34.
3. Goto, T.; Kishi, Y., Luciferins, bioluminescent substances. *Angewandte Chemie International Edition in English* **1968,** *7* (6), 407-414.
4. White, E. H.; McCapra, F.; Field, G. F.; McElroy, W. D., The structure and synthesis of firefly luciferin. *Journal of the American Chemical Society* **1961,** *83* (10), 2402-2403.
5. Kendall, J. M.; Badminton, M. N., bioluminescence moves into an exciting new era. *Trends in biotechnology* **1998,** *16* (5), 216-224.
6. De Cock, R.; Matthysen, E., Glow-worm larvae bioluminescence (Coleoptera: Lampyridae) operates as an aposematic signal upon toads (Bufo bufo). *Behavioral Ecology* **2003,** *14* (1), 103-108.
7. Lee, J., Bioluminescence of the Australian Glow-Worm, Arachnocampa Richardsae Harrison. *Photochemistry and photobiology* **1976,** *24* (3), 279-285.
8. Carlson, A. D.; Copeland, J., Flash communication in fireflies. *Quarterly review of biology* **1985**, 415-436.
9. Lloyd, J. E., Bioluminescent communication in insects. *Annual Review of Entomology* **1971,** *16* (1), 97-122.
10. Branham, M. A.; Wenzel, J. W., The evolution of bioluminescence in cantharoids (Coleoptera: Elateroidea). *Florida Entomologist* **2001**, 565-586.
11. Bocakova, M.; Bocak, L.; Hunt, T.; Teräväinen, M.; Vogler, A. P., Molecular phylogenetics of Elateriformia (Coleoptera): evolution of bioluminescence and neoteny. *Cladistics* **2007,** *23* (5), 477-496.
12. DeLuca, M., Firefly luciferase. *Adv Enzymol Relat Areas Mol Biol* **1976,** *44*, 37-68.
13. Nealson, K.; Hastings, J. W., Bacterial bioluminescence: its control and ecological significance. *Microbiological reviews* **1979,** *43* (4), 496.
14. Koo, J.; Schmidt, S. P.; Schuster, G. B., Bioluminescence of the firefly: key steps in the formation of the electronically excited state for model systems. *Proceedings of the National Academy of Sciences* **1978,** *75* (1), 30-33.

15. Navizet, I.; Liu, Y. J.; Ferre, N.; Roca-Sanjuán, D.; Lindh, R., The chemistry of bioluminescence: an analysis of chemical functionalities. *ChemPhysChem* **2011,** *12* (17), 3064-3076.
16. Hooper, C. E.; Ansorge, R.; Browne, H. M.; Tomkins, P., CCD imaging of luciferase gene expression in single mammalian cells. *Luminescence* **1990,** *5* (2), 123-130.
17. White, M.; Masuko, M.; Amet, L.; Elliott, G.; Braddock, M.; Kingsman, A. J.; Kingsman, S. M., Real-time analysis of the transcriptional regulation of HIV and hCMV promoters in single mammalian cells. *Journal of Cell Science* **1995,** *108* (2), 441-455.
18. Rutter, G. A.; White, M. R.; Tavare, J. M., Involvement of MAP kinase in insulin signalling revealed by non-invasive imaging of luciferase gene expression in single living cells. *Current Biology* **1995,** *5* (8), 890-899.
19. White, M. R.; Wood, C. D.; Millar, A. J., Real-time imaging of transcription in living cells and tissues. *Portland Press Limited* **1996**.
20. Brandes, C.; Plautz, J. D.; Stanewsky, R.; Jamison, C. F.; Straume, M.; Wood, K. V.; Kay, S. A.; Hall, J. C., Novel features of Drosophila period transcription revealed by real-time luciferase reporting. *Neuron* **1996,** *16* (4), 687-692.
21. Plautz, J. D.; Straume, M.; Stanewsky, R.; Jamison, C. F.; Brandes, C.; Dowse, H. B.; Hall, J. C.; Kay, S. A., Quantitative analysis of Drosophila period gene transcription in living animals. *Journal of biological rhythms* **1997,** *12* (3), 204-217.
22. Sala-Newby, G.; Taylor, K. M.; Badminton, M. N.; Rembold, C.; Campbell, A. K., Imaging bioluminescent indicators shows Ca2+ and ATP permeability thresholds in live cells attacked by complement. *Immunology* **1998,** *93* (4), 601-610.
23. Wilson, T.; Hastings, J. W., Bioluminescence. *Annual review of cell and developmental biology* **1998,** *14* (1), 197-230.
24. Maire, E.; Lelièvre, E.; Brau, D.; Lyons, A.; Woodward, M.; Fafeur, V.; Vandenbunder, B., Development of an ultralow-light-level luminescence image analysis system for dynamic measurements of transcriptional activity in living and migrating cells. *Analytical biochemistry* **2000,** *280* (1), 118-127.
25. Sala-Newby, G. B.; Badminton, M. N.; Evans, W. H.; George, C. H.; Jones, H. E.; Kendall, J. M.; Ribeiro, A. R.; Campbell, A. K., Targeted bioluminescent indicators in living cells. *Methods in enzymology* **2000,** *305*, 479-IN1.

26. McFerran, D.; Stirland, J.; Norris, A.; Khan, R.; Takasuka, N.; Seymour, Z.; Gill, M.; Robertson, W.; Loudon, A.; Davis, J., Persistent Synchronized Oscillations in Prolactin Gene Promoter Activity in Living Pituitary Cells. *Endocrinology* **2001,** *142* (7), 3255-3260.
27. Frank, J., Advances in the field of single-particle cryo-electron microscopy over the last decade. *Nature protocols* **2017,** *12* (2), 209-212.
28. Cyranoski, D., The secret war against counterfeit science. *Nature News* **2017,** *545* (7653), 148.
29. Möckl, L.; Lamb, D. C.; Bräuchle, C., Super-resolved Fluorescence Microscopy: Nobel Prize in Chemistry 2014 for Eric Betzig, Stefan Hell, and William E. Moerner. *Angewandte Chemie International Edition* **2014,** *53* (51), 13972-13977.
30. Shinde, R.; Perkins, J.; Contag, C. H., Luciferin derivatives for enhanced in vitro and in vivo bioluminescence assays. *Biochemistry* **2006,** *45* (37), 11103-11112.
31. Branchini, B. R.; Murtiashaw, M. H.; Magyar, R. A.; Portier, N. C.; Ruggiero, M. C.; Stroh, J. G., Yellow-green and red firefly bioluminescence from 5, 5-dimethyloxyluciferin. *Journal of the American Chemical Society* **2002,** *124* (10), 2112-2113.
32. Blincko, S.; Anzetse, J.; Edwards, R., Measurement of glycated haemoglobin in whole blood by a novel fluorescence quenching assay. *Annals of clinical biochemistry* **2000,** *37* (4), 492-497.
33. Bhaumik, S.; DePuy, J.; Klimash, J., Strategies to minimize background autofluorescence in live mice during noninvasive fluorescence optical imaging. *Lab animal* **2007,** *36* (8), 40.
34. Gopalkrishnapillai, B.; Nadanathangam, V.; Karmakar, N.; Anand, S.; Misra, A., Evaluation of autofluorescent property of hemoglobin-advanced glycation end product as a long-term glycemic index of diabetes. *Diabetes* **2003,** *52* (4), 1041-1046.
35. Honigman, A.; Zeira, E.; Ohana, P.; Abramovitz, R.; Tavor, E.; Bar, I.; Zilberman, Y.; Rabinovsky, R.; Gazit, D.; Joseph, A., Imaging transgene expression in live animals. *Molecular Therapy* **2001,** *4* (3), 239-249.

Chapter 2

Synthesis and Evaluation of D-Luciferin Bioluminescence

Abstract

D-Luciferin, the light emitting molecule isolated from the American firefly *Photinus pyralis (Ppy)*, was synthesised from commercially available *p*-anisidine with an overall yield of 12 %. Modifications to the synthetic route were subsequently explored, based on disadvantages and limitations that became apparent during the synthesis, these included among others; low yields and reliance on classical transition metal catalysed reactions. The optimised method unfortunately did not provide the target compound in an improved manner. An improved synthesis was, of course, of interest in the development of cost effective imaging modalities. Instead, both the employed and modified methods remain generally low yielding but do offer other opportunities for improvement which are explored in subsequent Chapters. This Chapter details the synthesis of D-luciferin based on reported synthetic procedures and thereafter, the evaluation of D-luciferin bioluminescence is described.

Chapter 2

Synthesis and Evaluation of D-Luciferin Bioluminescence

D-Luciferin: An Introduction

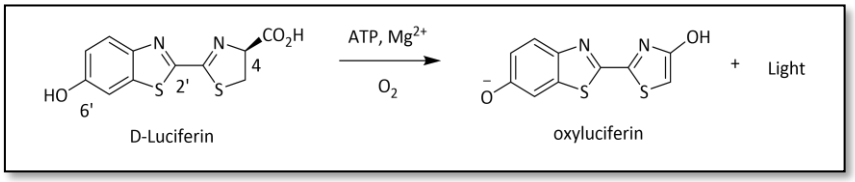

Scheme 2.1. Luciferase-catalysed light emitting reaction of D-luciferin

D-Luciferin is the molecule responsible for the emission of light from the tail of the American firefly, *Photinus pyralis* (*Ppy*). Currently, it is the most widely researched luciferin for its applications in bioluminescence imaging and its exploitation forms the main focus of this study. As shown in scheme 2.1, D-luciferin reacts with oxygen to produce light in a decarboxylative oxidation reaction catalysed by the enzyme luciferase (luc). Part of D-luciferin's appeal concerns its broad emission spectrum, which contains a significant near-IR component (over 650 nm), ideal for imaging in biological systems. D-Luciferin was first isolated in 1957, and a total synthesis to confirm its proposed structure followed shortly thereafter.[1] Structurally, it is a relatively simple heterocyclic molecule comprising of a C6'-hydroxybenzothiazole C2-linked dihydroxythiazole carboxylic acid. There is however, a degree of synthetic complexity resulting from the stereogenic centre at C4 of the 4,5-dihydrothiazole ring. Natural D-luciferin is found in an almost enantiopure form, where only one enantiomer is bioactive and naturally synthesised.[2] In fact, it has been found that the enantiomer L-luciferin, whilst not effective for the light emitting reaction, is a potent competitive inhibitor of luminescence for both natural and commercially available mutant luciferases.[1-2] Consequently, any proposed synthesis must account for the necessary stereoselectivity to achieve the desired stereochemistry at C4.

Biosynthesis of D-luciferin

The biosynthesis of D-luciferin has yet to be fully elucidated. It is generally accepted that D-luciferin is synthesised from 6-hydroxy-2-cyanobenzothiazole and the amino acid L-cysteine (L-Cys). Studies involving the treatment of *Ppy* luc expressing cells with 6-hydroxy-2-cyanobenzothiazole showed that the exogenous precursor was used, in vivo, to produce D-luciferin.[3] However, it is well established that the reaction of 6-hydroxy-2-cyanobenzothiazole and natural L-Cys produces L-luciferin, and not the bioactive D-isomer. Since D-Cys is not produced in any eukaryotes, the biosynthesis for D-luciferin may involve a stereoisomeric bio-inversion. There are studies which support the possible conversion of

L-Cys via L-luciferin into D-luciferin, suggesting that the biosynthesis is enzymatically regulated by the isomerisation of L-luciferin.[3-4] Other studies suggest that D-luciferin may in fact be synthesised from achiral oxyluciferin (formed from the decarboxylation of L-luciferin). A recent publication by Oba *et al* demonstrated that the biosynthesis involved the condensation of *p*-benzoquinone and two L-Cys molecules. Oba *et al* employed isotope-labelled compounds that were injected into the adult lantern of live Japanese firefly *Luciola lateralis* to confirm their incorporation in the biosynthetic pathway.[5] There are a number of studies that make similar suggestions through similar experiments, however, until the associated biosynthetic enzymes are isolated the biosynthesis remains uncertain.

D-Luciferin bioluminescence

Imaging techniques have become widely used diagnostic tools in chemical and medicinal research. The luciferase/luciferin system has been successfully applied in bio imaging, in which cells containing the luciferase enzyme can be visualized when supplied with free D-luciferin.[11] Research involving D-luciferin bioluminescence and the applications thereof is ongoing and an impressive foundation has already been laid by the many pioneers of the BLI field.[6-8] The mechanism by which luciferase catalyses the emission of light is shown in scheme 2.2, where luciferase binds its substrate, D-luciferin, and catalyses the emission of yellow-green or red light in a decarboxylation reaction in the presence of ATP, Mg^{2+} and oxygen.[2, 9]

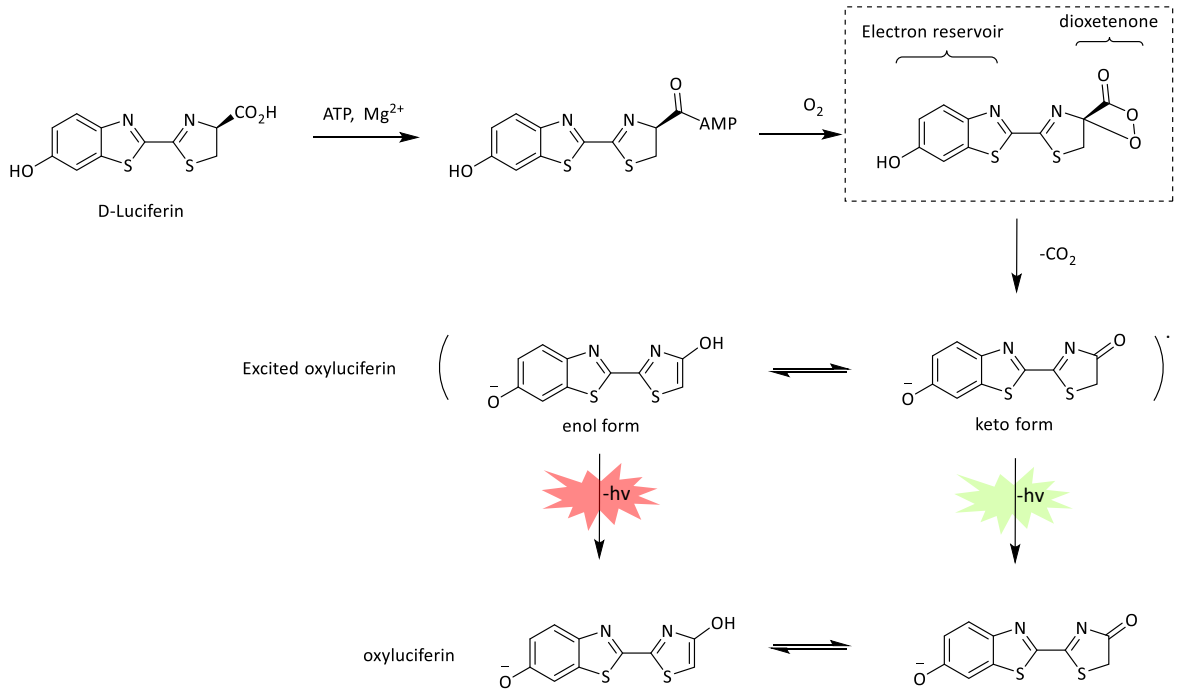

Scheme 2.2. Proposed mechanism for the luciferase-catalysed emission of light

The first step of the luciferase bioluminescence reaction is the luciferase catalysed conversion of luciferin to luciferyl adenosine monophosphate (luciferin-AMP). The thiazolane ring is then reacted with oxygen to form the dioxyethanone/dioxetanone complex, and subsequent decarboxylation results in excited oxyluciferin species. When the excited complex returns to its electronic ground state, energy is released in the form of visible light. Depending on the difference in energy between the ground state and excited state, light of different wavelengths may be emitted. It has been established that the decarboxylation is responsible for the chemi-excitation of the molecule and mechanism for decarboxylation proceeds via the previously described CTIL or CIEEL mechanisms. Interestingly, luciferase is capable of emitting both red and yellow-green light depending on the pH of the media in which the reaction takes place. However, the underlying mechanism affecting the wavelength of the emitted light has yet to be fully understood. It has been proposed that the different wavelengths of light emitted is due to keto-enol tautomerism of oxyluciferin in the excited state, as shown in the above scheme. Keto-enol tautomers are isomeric forms which are related by the transfer of an α-proton and the shifting of bonding electrons. Da Silva et al proposed that the keto and enol form of oxyluciferin have different energies in their excited states and thus emit light of different wavelengths upon returning to their respective ground states.[10] Other studies have also supported the idea that oxyluciferin is produced in a singlet excited state, and that relaxation to its corresponding ground state results in the emission of light.[11] Computational and experimental studies further support that the degree of chemi-excitation determines the degree of bioluminescence and that the angle between the dihydrothiazole and benzothiazole may also influence the excitation energy.[12] Both chemi-excitation and luciferin conformation are of course regulated/mediated by the enzyme luciferase.

Firefly Luciferase

Firefly luciferase *Ppy* luc is a 62 kDa protein found in the light-emitting organ within the abdomen of the firefly. *Ppy* luc was first characterised via crystal structure analysis by Conti et al in 1996.[13] Structurally, the protein is folded into two compact domains. The large N-terminal domain consists of a β-barrel and two β-sheets and the sheets are flanked by α-helices. The C-terminal portion of the molecule forms a distinct domain, which is separated from the N-terminal domain by a wide cleft. The structure of the enzyme is shown in figure 2.1 below.

Functionally, the 62 kDa molecular weight enzyme is considered to be an oxygenase and it is well established that all known bioluminescent reactions require oxygen.[14] However, while all known luciferases isolated from varying species all make use of an oxidation reaction, it is important to note that these reactions involve a variety of different cofactors and often structurally unrelated substrates.

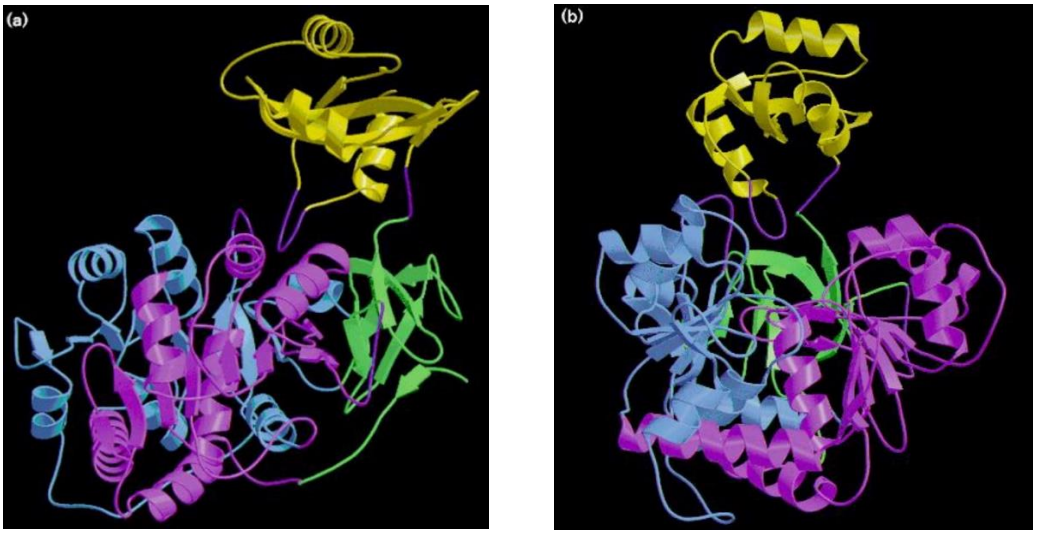

Figure 2.1. Ribbon representations of the firefly luciferase molecule shown in two orthogonal views. The three subdomains of the large N-terminal domain are shown in blue (β-sheet A), purple (β-sheet B) and green (β-barrel) and the small C-terminal domain is shown in yellow. Disordered loops are drawn in violet.[13]

In terms of its amino acid sequence, *Ppy* luc shows extensive sequence homology with a number of enzymes that utilize ATP in adenylation reactions, including acyl-CoA ligases[15] and various other enzymes involved in the synthesis of linear and cyclic polypeptides found in fungi and bacteria.[16]

With regards to the light emitting reaction that *Ppy* luc catalyses, the quantum yield (which is the percentage of the observed photons emitted relative to the expected maximum) is the highest of all known bioluminescent reactions.[17] The *Ppy* luc catalysed reaction does however display unusual kinetics, in that firefly luciferase has a relatively slow turn-over.[18] After an initial flash of light, the luminescence rapidly decreases to a low level of emission, due to product inhibition of the enzyme.

D-Luciferin/luciferase burst kinetics

When the enzyme luciferase is injected into a solution containing D-luciferin, there is a burst of light within the first few seconds, followed by a rapid decay and then sustained levels of light emission.[18] This emission profile is termed burst kinetics and is characteristic of Luciferase-catalysed reactions. The initial burst and subsequent decay in light emission is due to product inhibition where products formed from the light emitting reaction, specifically oxyluciferin and luciferin-AMP also inhibit the enzyme (oxyluciferin Ki = 0.50 $\pm$ 0.03 µM, Luciferin-AMP Ki = 3.8 + 0.7 nM).[11, 19] Nakatsu et al reports that the enzyme is forced into a closed conformation through non-competitive inhibition that was shown to be relieved upon the addition of CoA, which reacts with luciferin-AMP to form luciferin-CoA, a less potent inhibitor.[20]

Figure 2.2 shows how a rapid injection of luciferase to D-luciferin produces a burst of light followed by a decay caused by product inhibition. The addition of CoA at 60 s relieves some product inhibition, resulting in a second burst and a decrease in the subsequent decay (Figure adapted from Fraga, 2008).

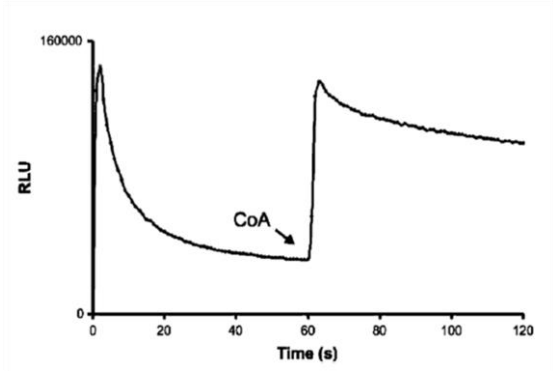

Figure 2.2. Burst

The burst kinetics profile
system in bioluminescen
assays that have been developed require that readings be taken one-minute post enzyme addition to substrate. In this way, error related to burst kinetics is minimised.

D-Luciferin gene reporter assay principle

Possibly the most famous application of D-luciferin/luciferase in science and biology relate to its use as a reporter in the evaluation of gene expression. There are a number of luciferin-based assay kits commercially available, most of which are directly used in gene reporter assays. These assays measure luciferase activity via treatment with D-luciferin, or a salt thereof (Scheme 3.2).

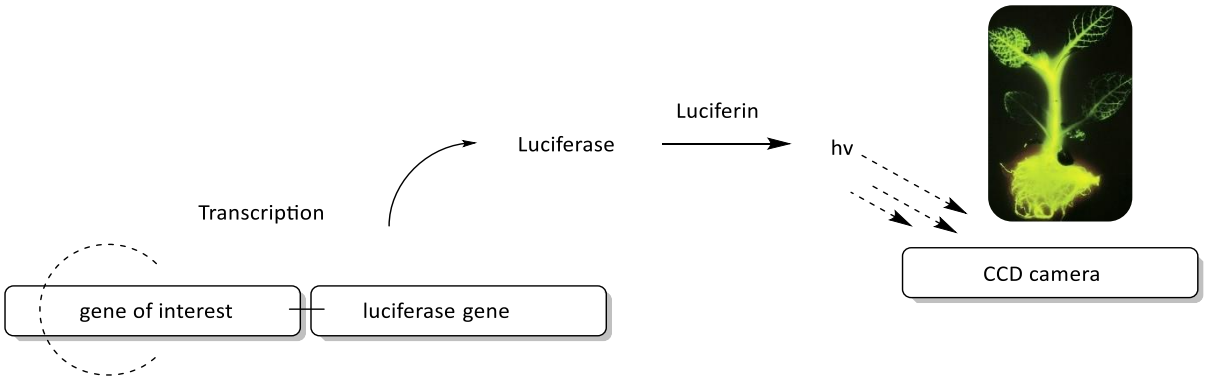

Scheme 2.3. Luciferase-fused gene activity measured through luciferase activity

Genetic reporters are used to study gene expression and related cellular events. They are widely used in cellular and molecular biology as well as clinical pharmacology. Typically, a reporter gene (luc) is cloned with a DNA sequence of interest into an expression vector that is then transferred into cells. Following transfer, the cells are assayed for the presence of the reporter by measuring resultant enzyme activity. In the case of D-luciferin, the enzyme activity is related to light output. As a gene reporter system, the D-luciferin/luciferase has been found to be more sensitive (anywhere from 10 to 1000-fold) than fluorescent reporters making ideal for the study of complex biological systems. These Luciferase-based genetic reporter assays provide sensitive methods for assaying gene expression, enabling the accurate quantification of small changes in transcription resulting from subtle changes in biology. One of the most common applications of reporter genes is the analysis of a cloned mutated promoter sequence. This is done by measuring the effects of mutations and deletions in the promoter region through the coupling of the promoter to a reporter gene.[21]

An example of the use of a luc reporter assay is given below. How this works is that luciferase is genetically engineered into cells which formerly lacked the gene for the enzyme. Cloning the regulatory region of a gene-of-interest upstream of the luciferase gene then allows for the measure of the protein transcription/expression using a luminometer. Since the gene of interest is fused to the luciferase reporter gene, the luciferase activity can be directly correlated with the expression of that particular gene. Of course, the appropriate substrates and cofactors are also needed *in vivo* for the emission of visible light which can be detected by charge-coupled device (CCD) cameras.

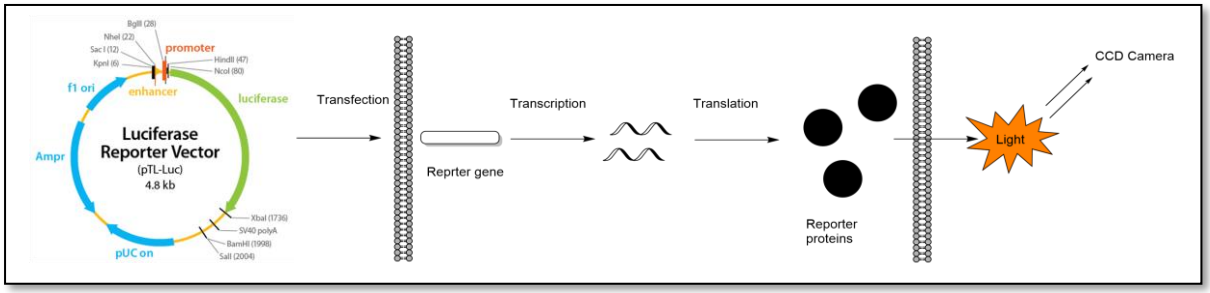

Figure 2.3. Example of a luciferase reporter vector

As described, the luciferin-luciferase reaction requires ATP, Mg^{2+}, and oxygen for bioluminescence and the degree of luminescence is directly correlated to the most limiting of the reactants in the light emitting reaction. This has allowed for the assays to be developed whereby all of the reactants, save one, ATP for example, are introduced in excess to a particular system. Any observable luminescence is then attributed to ATP in the system. Apart from the many luciferase based assays, there have also been a number of assays that have been developed by modifying the luciferase substrate, D-luciferin.

D-Luciferin assays based on modified substrates

It was discovered quite early in the history of D-Luciferin bioluminescence research that chemical modifications to its core structure significantly altered its luminescent activity. White et al discovered that moving the hydroxyl from the C6' position to either C5' or C7' resulted in the loss of luminescent activity. White further demonstrated that alkylation and acylation of the C6-hydroxyl also resulted in the loss of luciferin activity. This very important experiment formed the basis of many D-luciferin based assays, some of which are commercially available today.

The foundation of D-luciferin assays follows an ON/OFF logic, where D-luciferin is modified at the C6-hydroxyl, turning off luminescent activity. The modification is cleverly designed to be removed by specific agents which, through the removal process, liberates free D-luciferin. The light emitted by the D-luciferin can then be related to the removal process and the associated removal agents. Scheme 2.4 illustrates this process.

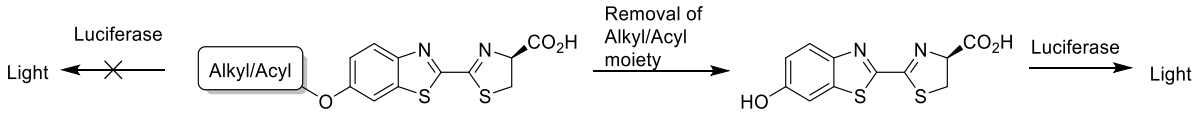

Scheme 2.4. Mechanism of action of modified luciferin assays

D-Luciferin conjugated to a phenylboronic acid (PCL-1) has been used to image tumor cells. The idea here was that the luciferin-boronic acid conjugate, when reacted with hydrogen peroxide, would release free D-luciferin which can be detected by a luminometer, as shown in figure 2.4. Since tumor cells have increased concentrations of peroxides, the degree of luminescence due to D-luciferin would be higher in these cells relative to non-tumor cells.[18] PCL-1 has since been patented and is currently used in medical- and biochemical research to monitor tumor growth and regression.

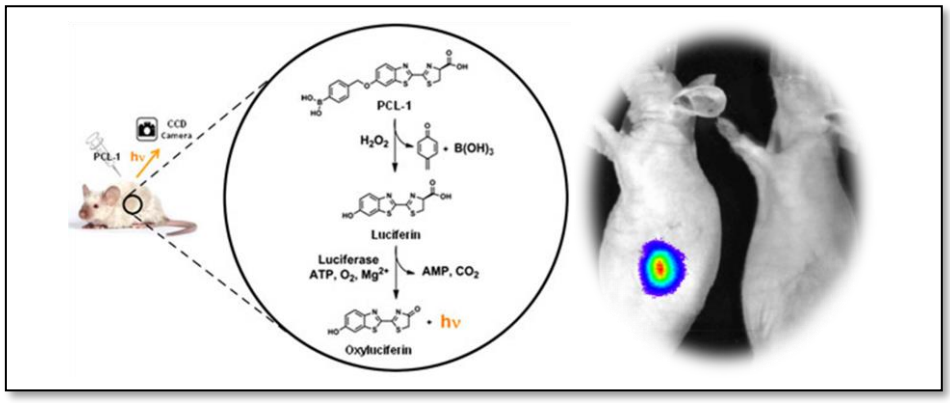

Figure 2.4. The luciferase-PCL-1 assay used for imaging tumor cells

The use of luciferase for optical molecular imaging, as a tag to track grafted cells, as a transgenic marker, to monitor gene expression, to assess protein stability, to sense bioactive small molecules, and to image drug delivery mechanisms have also been documented.[11, 14, 19] It is evident that this particular chemoenzymatic reaction and its application to imaging has become an area of great interest. Thus, luciferin has become a popular synthetic target as ease of access to this particular compound would contribute significantly to the development of rapid, cost effective imaging techniques.

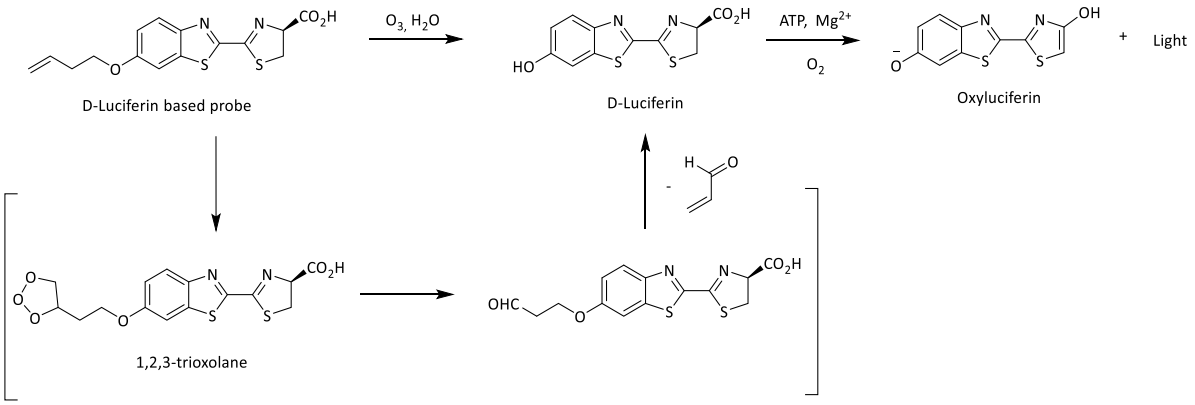

Scheme 2.5. Bioluminescence detection of O_3 by a D-luciferin based probe

A D-luciferin homoallylic ether was reported as a highly selective and sensitive bioluminescent probe that emitted light in the presence of ozone but not other ROS.[22] The probe is a modified D-luciferin where the activity is turned off through alkylation of the C6 hydroxyl with a butenyl chain containing a terminal alkene. The terminal alkene reacts with ozone to produce a 1,2,3-trioxolane that further undergoes a retro [3+2] cycloaddition eliminating acrolein and D-luciferin. The generated luciferin is then oxidised to oxyluciferin with the emission of light. In this way D-luciferin was used to measure concentrations of ozone in environmental and biological samples.[22]

Various modified D-luciferin esters have been prepared, as seen in figure 2.5. These esters were found to be bioluminescent inactive and were used to measure specific esterase activity.[23] Phosphate esters were produced similarly where the C6-hydroxyl was phosphorylated resulting in the loss of bioluminescent activity. The hydroxyl was liberated upon alkaline phosphatase (ALP) mediated dephosphorylation and the resultant luminescence measured. The luminescence was then related to ALP activity.[24] D-Luciferin carbonate derivatives have also been reported.[25] The D-luciferin carbonate derivative was prepared by covalently tethering D-luciferin to a transporter molecule that would then transport the conjugate across the cell membrane after which the linker would be reduced by glutathione (GSH), liberating free luciferin. In this way, luminescence can be used to evaluate cellular uptake of the D-luciferin conjugate.

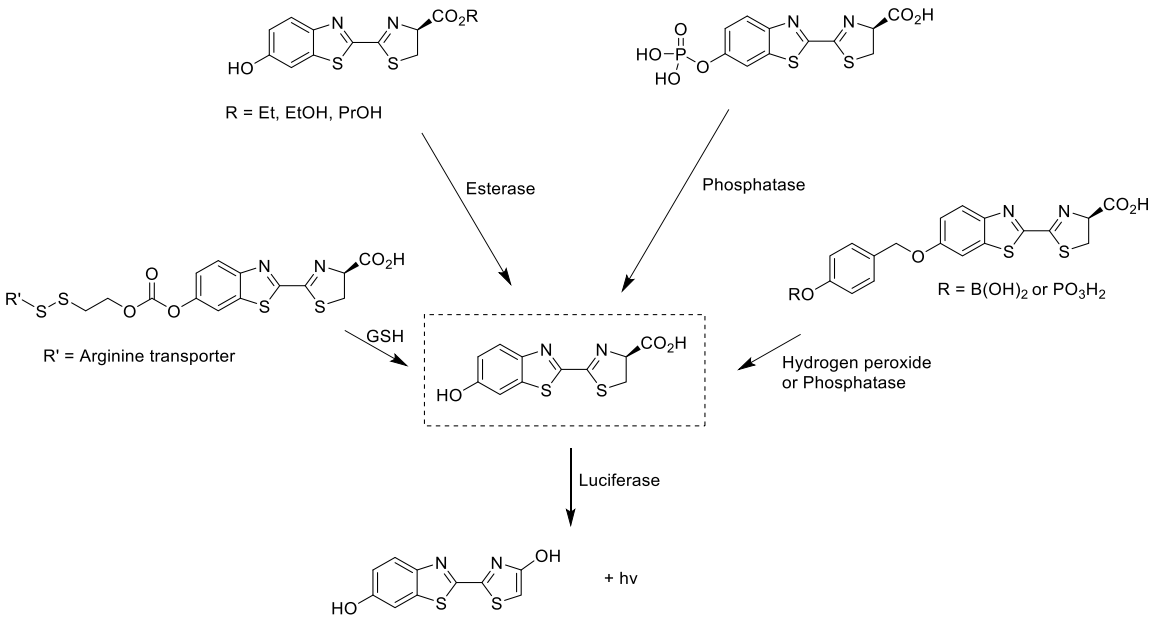

Figure 2.5. Structures of D-luciferin ester, carbonate and phosphate derivatives

There are many other examples of D-luciferin probes, each uniquely modified for a specific function. Most of the latter are synthesised from commercially obtained D-luciferin. There are numerous publications that describe the use of D-luciferin to produce luciferin-based probes,[26-28] there are however much less publications that concern the synthesis of D-luciferin itself.

Review on the syntheses of D-luciferin

Structurally, there are two key components to D-luciferin; the benzothiazole ring and the dihydrothiazole carboxylic acid moiety. As previously mentioned, C4 of the dihydrothiazole ring is a stereogenic centre and, as such, due consideration should be given to its configuration. The first total synthesis of D-luciferin was achieved by White et al in the early 60's. Inspired by what was known of the biosynthesis of D-luciferin at the time, White et al made use of L-Cys to form the dihydrothiazole carboxylic acid ring. He then discovered that L-Cys afforded the undesired enantiomer, L-luciferin. Subsequent reactions using non-naturally occurring D-Cys afforded the correct stereoisomer. In some cases, the White synthetic route is still followed for commercial preparation of D-luciferin.

The White synthesis uses *p*-anisidine **2.1** as a starting material.[1] The thiazoline component of the benzothiazole ring is then formed using ethyl oxalate. The reaction of *p*-anisidine with ethyl oxalate forms the amide ester **2.2**. Thionation and hydrolysis then gives the thio-acid **2.4**, which subsequently undergoes an oxidative cyclisation which results in the key benzothiazole intermediate **2.5**. Several functional group transformations are then employed to form 2-cyano-6-hydroxybenzothiazole which is then reacted with D-Cys to form D-luciferin, in an almost quantitative reaction.

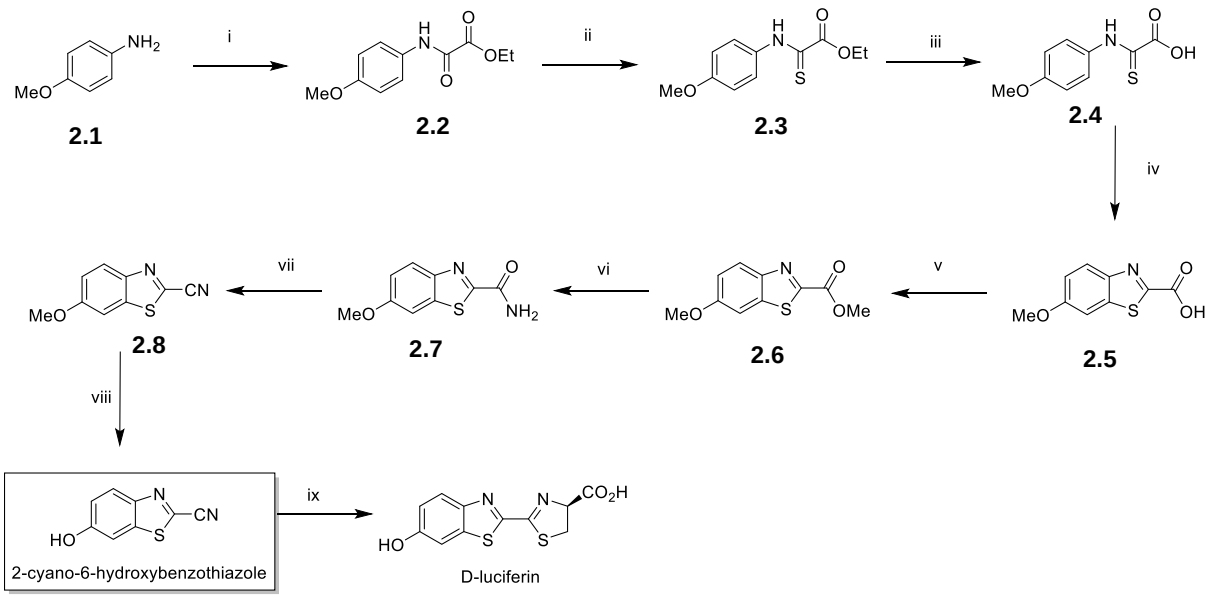

Scheme 2.6. Reagents and conditions: i) ethyl oxalate / 180 ^{0}C / 5 min, 87 %, ii) P_2S_2 / Δ / 40 min, 60 %, iii) NaOH / 0 ^{0}C / HCl, 99 %, iv) $K_3[Fe(CN)_6]$ / NaOH / 0 ^{0}C / 11 h, 61 %, v) CH_2N_2 / 0 ^{0}C / 15 min, 89 %, vi) NH_3 / MeOH / Δ / 30 min, 62 %, vii) $POCl_3$ / MeOH / rt / 30 min, 64 %, viii) PyHCl / 200 ^{0}C / 1 h, 90 %, ix) D-Cys / H_2O:MeOH (1:1) / rt / 30 min, 9 % overall yield

The White et al synthetic approach (Scheme 2.6) has an overall yield of 9 % over 9 steps, arguably making the synthesis of D-luciferin costly and wasteful. Thus, commercially relevant, alternate approaches to D-luciferin are still under investigation. Uninterestingly, most attempts at improving on the synthesis of D-luciferin retained the same general strategy as that developed by White and co-workers. Wherein the benzothiazole is formed first, followed by C6 and C2 functionalisation, generating a nitrile functionality, to which D-Cys is added. In fact, most of the subsequent syntheses of luciferin differ only in their construction of the 2-cyanobenzothiazole nucleus. One of the lower yielding steps in the commercial synthesis of D-luciferin is the benzothiazole forming cyclisation. Seto et al developed an alternate synthetic route (Scheme 2.7), which forms the benzothiazole **2.7** from the thioamide **2.12** to generate the benzothiazole directly. Dehydration then yields the cyanobenzothiazole **2.8**, a key intermediate for luciferin synthesis.[29]

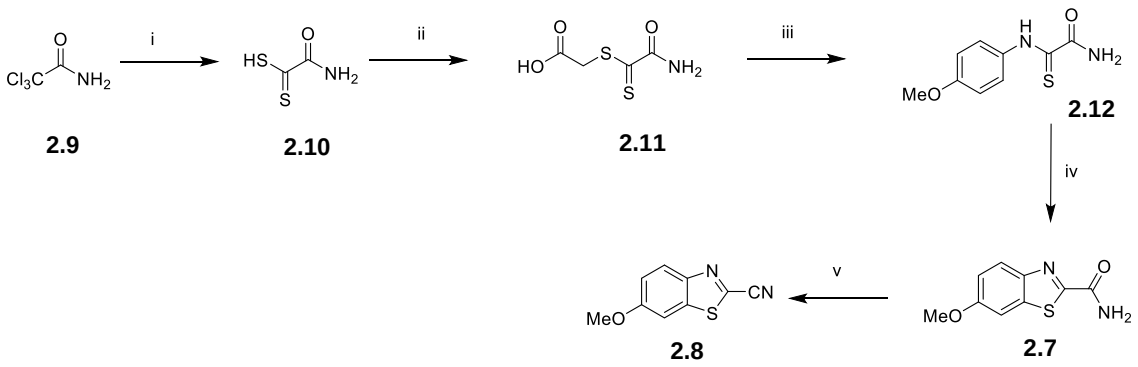

Scheme 2.7. Reagents and conditions: i) KOH(aq) / H_2S, ii) $ClCH_2CO_2H$, iii) *p*-anisidine / MeOH(aq), 29 % iv) $K_3[Fe(CN)_6]$ / NaOH, 65 %, v) $POCl_3$ / Δ, 63 % and 12 % overall

The Meroni synthesis also identified the 2-cyano-6-hydroxybenzothiazole as a key intermediate for the synthesis of D-Luciferin. However, unlike most luciferin synthesis that incorporate *p*-anisidine, the Meroni reaction sequence instead makes use of commercially available 1,4-benzoquinone **2.13**. The benzoquinone was reacted with L-cysteine ethyl ester to afford a quinone thiophenol adduct **2.14**, which was then subjected to an oxidative-cyclization reaction to afford 2-carbethoxy-6-hydroxybenzothiazole **2.15**.

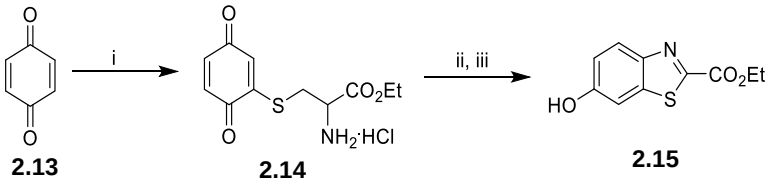

Scheme 2.8. Reagents and conditions: i) L-Cysteine ethyl ester hydrochloride / MeOH:H_2O (1:1) / rt / 1 h, ii) $K_3(FeCN)_6$ / NaOH / EtOH / rt / 1 h, iii) 1 M HCl / EtOH / rt / 24 h, 32 % overall yield

Subsequent C2-functional group conversion afforded the nitrile with an overall yield of 32 %. The latter is one of the highest yields when compared with previously reported procedures that ranged between 6-29 %. Furthermore, by starting with benzoquinone to construct the benzothiazole, Meroni was able to directly form the C6-hydroxyl, as opposed to the *p*-anisidine utilising syntheses which instead form the methyl ether (2-cyano-6-methoxybenzothiazole) that requires demethylation. Meroni was however, unable to convert the C2-ester to the nitrile without protecting the C6 hydroxyl group. An arguably more versatile synthon for D-luciferin synthesis was developed by Hrobàrik et al, in the form of a 2-cyano-6-iodobenzothiazole ring. The iodo derivative allows for versatile functionalisation at the C6 position of any synthesised luciferin. Giving access to a myriad of C6 substituted Luciferin analogues. Moreover, the iodo functionality allows for cross coupling reactions for forming luciferin-small molecule conjugates, of relevance in various assays. Thus, in a recent study toward the synthesis of triphenylamine-based chromophores involving benzothiazole-based systems,[34] a shorter route to

the benzothiazole scaffold was achieved compared to the relatively longer commercial preparation. In this study, *p*-iodoaniline **2.16** was used as the starting material. *p*-Iodoaniline was acetylated to form an iodoanilide **2.17** and subsequent thionation formed a thioamide **2.18**, which underwent cyclisation to afford the benzothiazole intermediate, 6-iodo-2-methyl-benzothiazole **2.19**. Oxidation of the methyl group at C2 afforded the aldehyde, 6-iodobenzothiazole-2-carbaldehyde **2.20**. Hrobàrik et al were able to successfully prepare a 2-cyanobenzothiazole-6-carboxaldehyde in relatively good yield (25 %), however, it was not further transformed into the 2-cyanobenzothiazole **2.21** and was therefore not used in the context of luciferin preparation. Despite this, it is still worth noting the synthesis for its potential use in luciferin analogue construction.

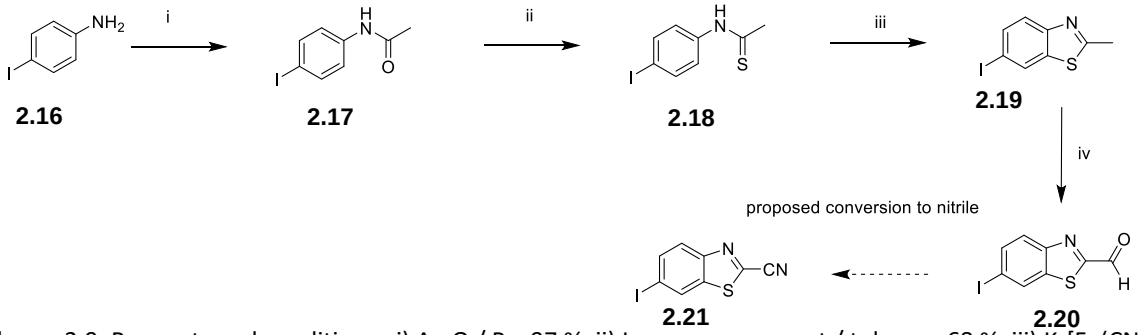

Scheme 2.9. Reagents and conditions: i) Ac_2O / Py, 97 %, ii) Lawessons reagent / toluene, 68 %, iii) $K_3[Fe(CN)_6]$ / NaOH, 59 %, iv) SeO_2 / dioxane / Δ, 25 % overall yield

C6 Functionalisation has been used to prepare luciferin conjugates (such as PCL-1) which, upon exposure to certain reactants or reaction conditions, release luciferin. In this way, the release of bioluminescent luciferin can be coupled to varying biochemical processes and, through the degree of bioluminescence, these processes can be measured. The Hrobàrik et al route was particularly attractive because part of the aims of this research project was to couple the release of luciferin to varying biochemical processes through 6'-modification, which one could easily envisage through a 2-cyano-6-iodobenzothiazole.

Proposed Synthesis of D-Luciferin

Based on the previous syntheses of D-luciferin[28], the 2-cyanobenzothiazole core was identified as a key intermediate in the synthesis of D-luciferin and related compounds. In most cases, the 2-cyanobenzothiazole core was prepared from the cyclisation and functionalisation of an acetamide. However, it can also be directly prepared from the cyclisation of an already functionalised cyanothioformanilide (Route A, Scheme 2.10).[30] Such highly functionalised anilides are not easy to prepare because of their greater reactivity and reports on their synthesis are limited. A rather interesting approach for their preparation has been reported by Reese et al, where the thioanilide was

accessed from the fragmentation of a dithiazolimine prepared from the condensation of Appel's salt and aniline.[31] Recently, the Appel's salt approach has been singled out as the premier methodology for preparing cyanothioformanilides from substituted anilines.[32] Other synthetic approaches are notably longer and some include relatively toxic cyanide reagents. The reported synthesis of the 2-cyanobenzothiazole core and D-luciferin in this study initially followed route B (Scheme 2.10), the Appel's salt approach, adapted from Prescher et al in their recent synthesis of D-luciferin. Prescher et al impressively used Appel's salt to form a dithiazolimine that was subsequently fragmented to afford the cyanoformanilide. The cyanoformanilide was then cyclised using a C-S intra-molecular coupling to afford the 2-cyanobenzothiazole (84 %) and thereafter D-luciferin. To date, the Prescher et al synthesis (route B) clearly towers far above all its predecessors.

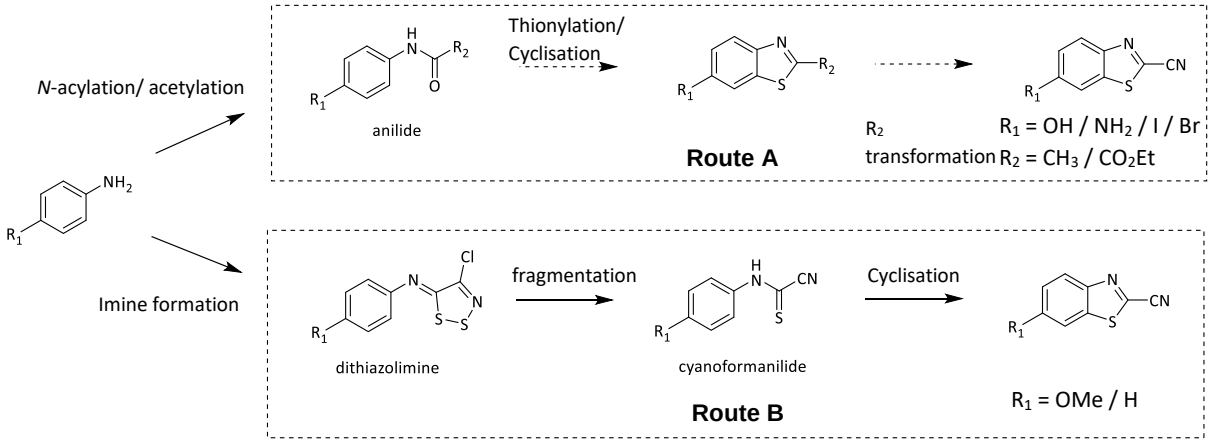

Scheme 2.10. Synthetic routes toward C6-substituted 2-cyanobenzothiazoles; route A involves formation of the benzothiazole first followed by subsequent C2 functional group transformations, while route B installs desired functionality pre-cyclisation

Aims and Objectives

The aim of this work was to explore and evaluate various reported synthetic routes to D-luciferin in terms of overall yield and accessibility and to then synthesise D-luciferin by choosing an appropriate route based on that evaluation. Thereafter, the aim was to investigate whether any improvements could be made to the chosen reported synthetic procedure, since it would help in both securing access to a ready supply of D-luciferin and possibly lead to the development of a unique and improved synthetic route. A further aim involved effectively evaluating the luminescence of the synthesised material by reacting the synthesised luciferin with the enzyme luciferase in the presence of ATP, Mg^{2+}, and O_2 and recording the resultant luminescence

The specific objectives were thus:

i) The synthesis and characterisation of D-luciferin using spectroscopic and analytical characterisation techniques, including; NMR, MS, IR and melting point analyses.

ii) The bioluminescent evaluation of the synthesised D-luciferin using purified luciferase bioluminescence assays where the luciferase was expressed and purified from *E. coli*.

iii) The identification of key limiting steps in the synthetic sequence used, where an improvement was expected to result in a much higher overall yield and a generally improved synthesis.

Synthesis and Bioluminescent Evaluation of D-Luciferin

One of the more recent and most efficient routes to D-luciferin was reported by McCutcheon, Prescher and co-workers.[32-33] As discussed, their synthesis was aimed at forming the nitrile functionality prior to cyclisation. This was done using dithiazolimine fragmentation, a reaction that was refined by Thierry Besson and Charles W. Reese (both well known for their work in field of heteroaromatic synthesis).[30-31, 34-35] The methodology used to form the dithiazolimine was actually first reported by Rolf Appel (of the Appel reaction) where he reacted various substituted anilines with 2,3-dithiazole chloride (later known as Appel's salt).[36] After extensive evaluation and deliberation, this route was chosen as a starting point for the synthesis of D-luciferin.

Prescher et al Synthesis of D-Luciferin

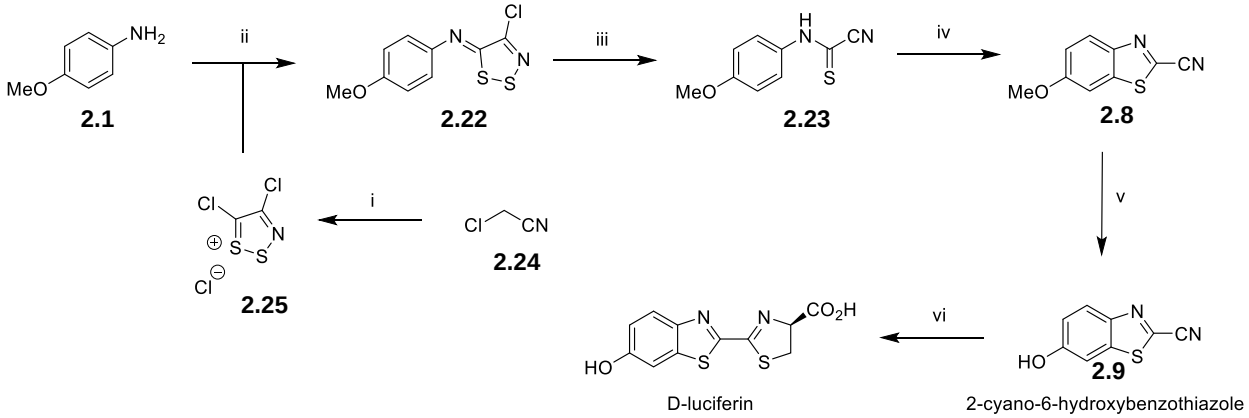

Scheme 2.11. Reagents and conditions: i) S_2Cl_2 / DCM / rt / 24 h, ii) Appel's salt **2.25** / DCM / pyr / rt / 3 h, iii) DBU / DCM / 5 °C / 30 min, iv) $PdCl_2$ / CuI / TBAB / DMF:DMSO (1:1) / 110 °C / 3 h, v) PyHCl / DMF / 150 °C / 1 h, vi) D-cys / K_2CO_3 / MeOH:H_2O / 20 min

The detailed synthetic route used by Prescher et al is outlined in scheme 2.11. The synthesis of D-luciferin was achieved from the condensation of 4,5-dichloro-1,2,3-dithiazolium chloride (Appel's salt) **2.25** with *p*-anisidine **2.1**, generating an *N*-arylimino-1,2,3-dithiazole **2.22**, which then further underwent DBU mediated dithiazole fragmentation to afford the corresponding cyanothioformanilide **2.23**. A copper iodide/palladium chloride catalysed C-S cross-coupling reaction was then used to form the benzothiazole **2.8** from the thioacetamide precursor. Subsequent *O*-alkyl deprotection generated 6-hydroxy-2-cyanobenzothiazole and D-Cys addition on the nitrile functionality of **2.9** generated the carboxy-thiazoline ring of D-luciferin with the correct stereochemistry required for luminescent activity.

To start the synthesis, warrants the preparation of Appel's salt. This was done following literature methods as seen below. Appel's salt **2.25** was prepared from the addition of sulfur monochloride to a solution of chloroacetonitrile in anhydrous DCM at room temperature (Scheme 2.12).

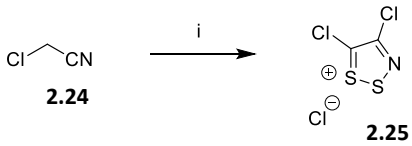

2.24 **2.25**

Scheme 2.12. Reagents and conditions: i) S_2Cl_2 / DCM / rt / 18 h

The solution was swirled a few times and left to stand for 24 h under an inert nitrogen atmosphere. The resulting green-brown crystals were filtered under vacuum and washed copiously with DCM. The crystals were then dried under vacuum and stored at room temperature. Appel's salt was found to be extremely hygroscopic. The formation of Appel's salt was confirmed only by mass spectrometry and its melting point, since it is a known compound with a well-documented poor solubility profile. The proposed mechanism of the formation of Appel's salt is not well understood. However, varying mechanisms of the salt's formation have been previously proposed. Although, there is very little evidence to support any one particular mechanism. It is generally accepted that the reaction proceeds *via* the addition of S_2Cl_2 to the cyano group, followed by cyclisation and ionisation. With the Appel's salt formed, the dithiazolimine was then prepared for subsequent fragmentation.

p-Anisidine **2.1** was reacted with a slight excess of previously prepared Appel's salt in DCM at room temperature, to generate an imine **2.22**. The mechanism involves a nucleophilic substitution at the carbon centre of the thionium (also referred to as sulfenium) functionality, in which the chlorine at position C5 on the dithiazoline ring is replaced by the amine nitrogen of *p*-anisidine, as shown in scheme 2.13.

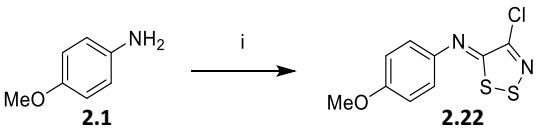

2.1 **2.22**

Scheme 2.13. Reagents and conditions: i) Appel's salt **2.25** / DCM / Py / 3 h

The reaction was monitored by thin layer chromatography, which revealed complete consumption of *p*-anisidine **2.1** after one hour. The reaction then required that two equivalents of pyridine be added; one to abstract the thioamide proton and the other to quench the resulting HCl, as shown in scheme 2.14.

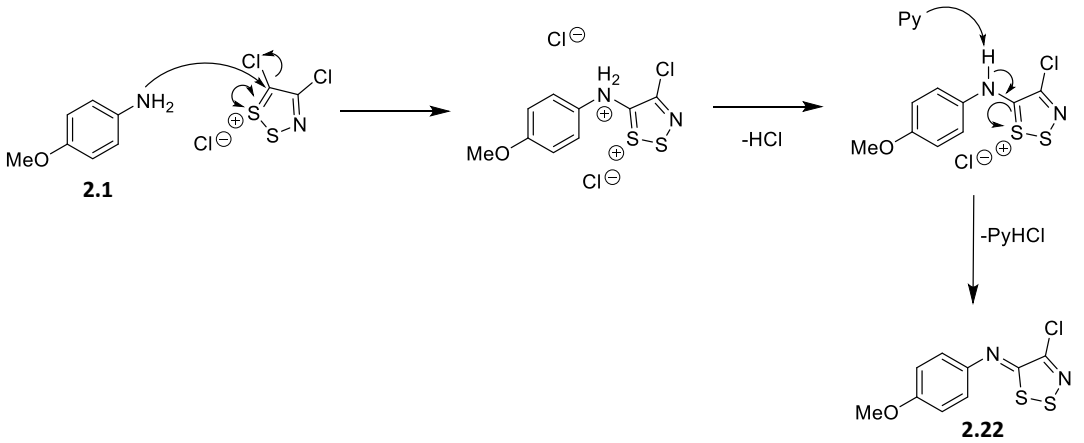

Scheme 2.14. Proposed mechanism for the formation of an *N*-arylimino-1,2,3-dithiazole

The *N*-aryliminodithiazole **2.22** was isolated and purified by chromatography in relatively good yield (>70 %). The ^{1}H-NMR spectrum of **2.22** (Figure 2.5) showed a distinct downfield shift in the aromatic proton signals relative to the starting material, from 6.70-6.78 ppm to 6.98-7.27 ppm. The downfield shift in aromatic proton resonances is reasoned to be the result of a decrease in electron density within the aromatic ring due to the conversion of the heavily donating amine group, to the lesser electron donating imine functionality. Additionally, the ^{1}H-NMR spectrum of **2.22** did not display the amine resonance previously observed in the starting material, further supporting the formation of an imine. A slight downfield shift in the *O*-methyl singlet from 3.75 to 3.85 ppm was also observed. This again was reasoned to be the result of electron density being siphoned from the benzene ring in the imine product by the newly formed dithiazole ring to which it is linked. The ^{13}C-NMR spectrum (Figure 2.6) displayed the expected total of 7 signals, further confirming the formation of **2.22**. The ^{13}C-NMR spectrum revealed resonances at 147.8 and 156.9 ppm confirming the presence of the dithiazole ring. The melting point of the product was found to be 111-112 ^{0}C, corresponding to the recorded literature melting point of 113 ^{o}C.

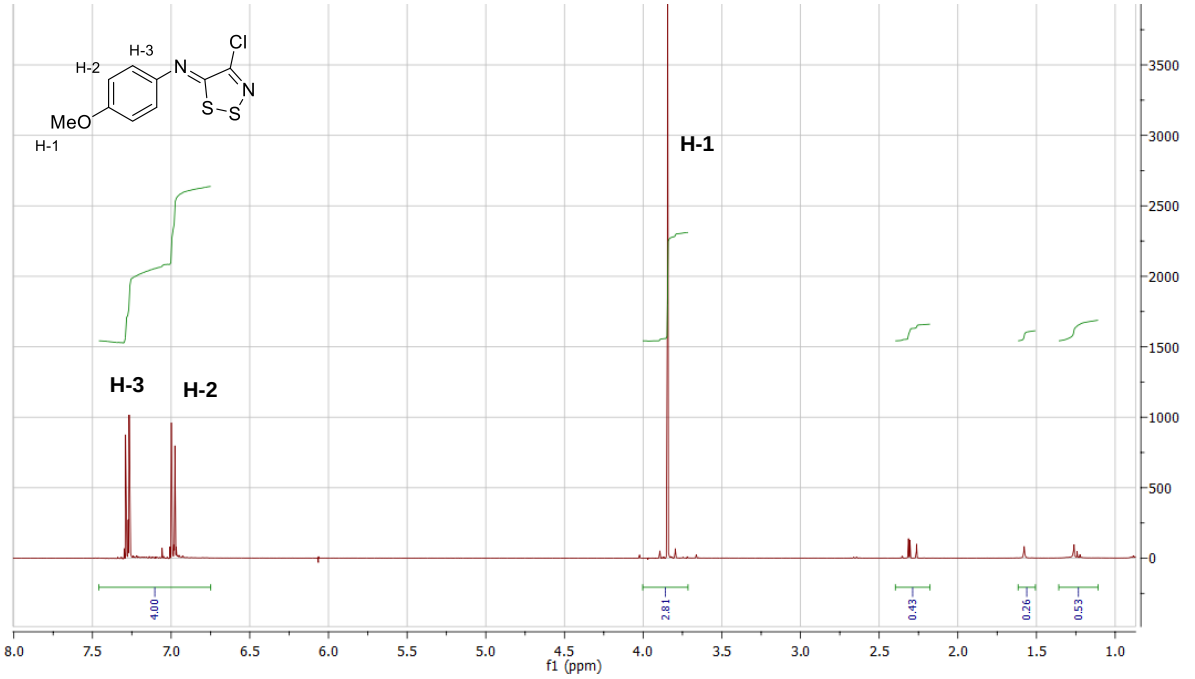

Figure 2.5. ^{1}H-NMR spectrum of dithiazolimine **2.22** in $CDCl_3$

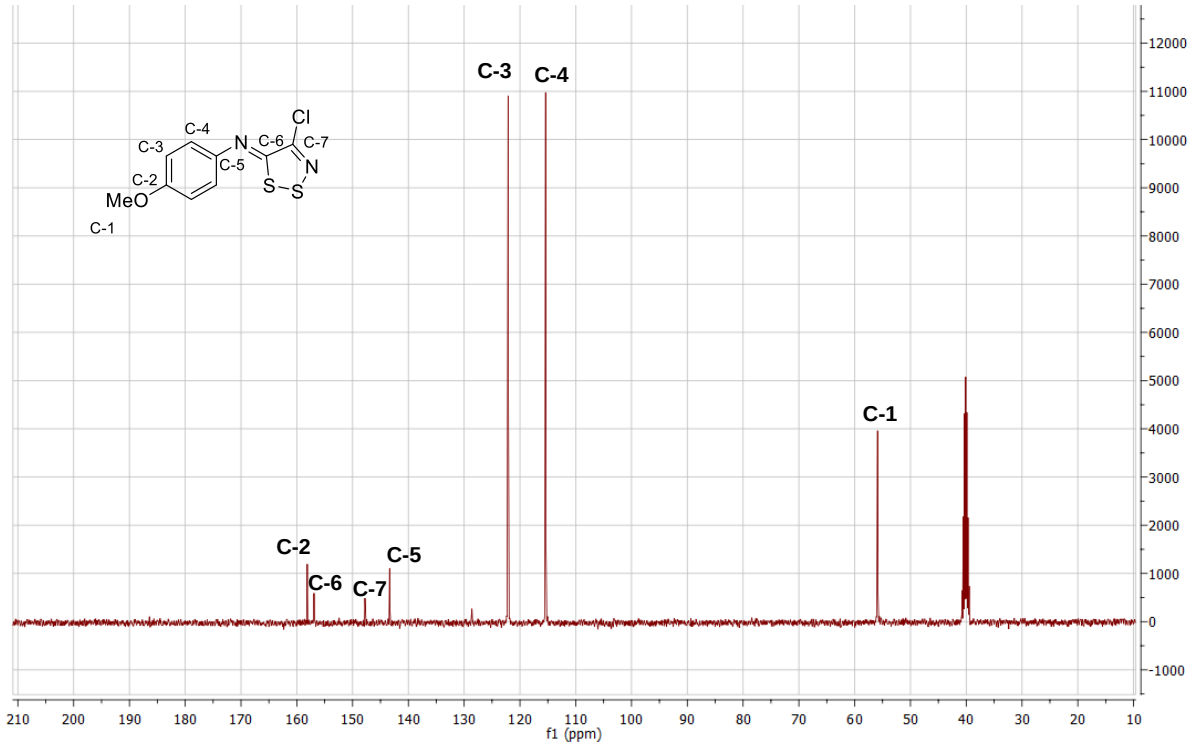

Figure 2.6. ^{13}C-NMR spectrum of dithiazolimine **2.22** in DMSO

A sharp melting point along with ^{1}H-NMR and ^{13}C-NMR spectral data indicated that the product **2.22** was sufficiently pure to be used in the subsequent cyanothioformanilide **2.23** synthesis.

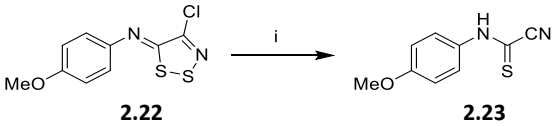

2.22 **2.23**

Scheme 2.15. Reagents and conditions: i) DBU / DCM / 5 °C / 30 min

Base-mediated fragmentation of **2.22** was used to prepare the cyanothioformanilide **2.23** required for the benzothiazole synthesis. 1,8-Diazobicyclo[5.4.0]undec-7-ene (DBU) was slowly added to a stirred solution of imine **2.22** in DCM at 5 °C, over a period of 30 min. After the addition, TLC analysis of the solution showed the complete conversion of the non-polar imine, to multiple products, observed as several relatively more polar spots, very similar in R_f (0.5 in 30% EtOAc). The reaction mixture was allowed to warm to room temperature, and the solvent reduced *in vacuo*. The crude product was purified on a silica gel column, eluting with EtOAc:Hexane (50:50) to afford thioacetamide **2.23** as a red-brown solid in good yield (66 %). The mechanism by which fragmentation occurs has previously been proposed and is shown in scheme 2.16.

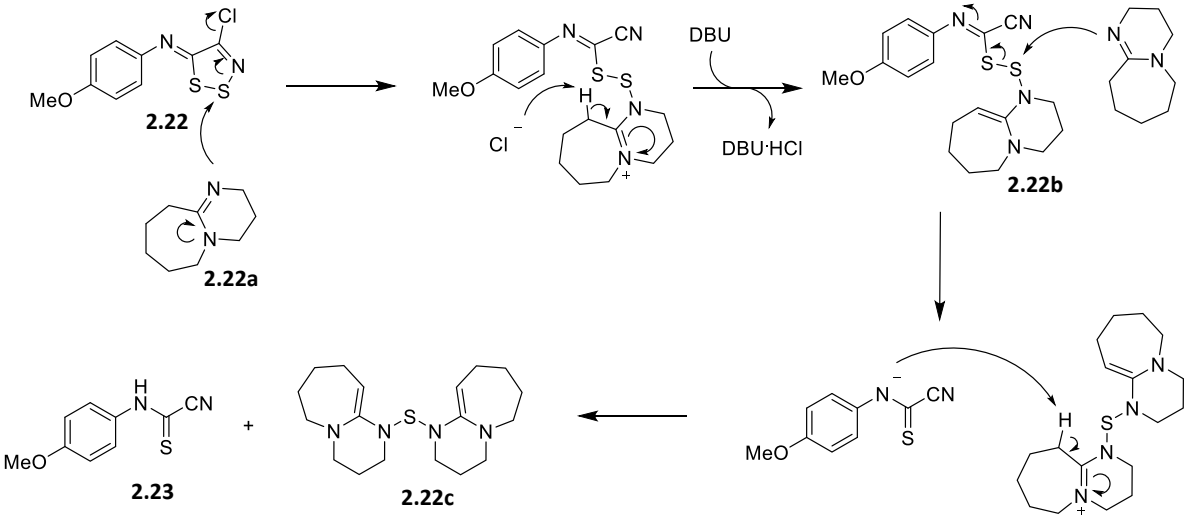

Scheme 2.16. Proposed mechanism of dithiazoline fragmentation

The mechanism involves nucleophilic attack by the DBU **2.22a** amidine nitrogen at the dithiazole S2 ring sulfur and subsequent ring opening to afford the disulfide **2.22b**. A second equivalent of DBU then abstracts HCl from the reaction mixture, followed by a nucleophilic attack by a third equivalent of DBU which cleaves the disulfide bond to give the cyanothioformanilide **2.23** and the neutral sulfane **2.22c**. The sulfane was not isolated from the reaction mixture and thus could not be used to reinforce the proposed mechanistic rationale. However, the need for three equivalents of DBU was confirmed, since the use of less than three equivalents resulted in incomplete conversion of the starting dithiazolimine. The ^{1}H-NMR spectrum of the fragmented product, figure 2.7, shows a significant change in the appearance of the aromatic proton signals relative to the starting material.

The ^{1}H-NMR spectrum of **2.23** displayed three distinct aromatic signals instead of the doublet of doublets expected of a 1,4-disubstituted benzene ring. These signals integrate for the expected total of four protons. The appearance of the aromatic resonances was reasoned to be due to cis/trans-isomers or, more likely, a form of keto-enol tautomerism in the product. This suggests that **2.23** has two interconverting isomeric forms which exist in equilibrium. The chemical equilibrium between the isomeric thione and thioenol (or iminothiol) forms of **2.23** involves the transfer of the thioamide proton and shifting of the bonding electrons. The proton ortho to the methoxy group appears to be less affected by the tautomerism and, as such, a distinct signal integrating for its two protons are observed, assigned in figure 2.7 as H-3. In contrast, the protons ortho to the tautomerising thioanilide moiety are significantly affected resulting in separate signals for protons in the thione and thioenol forms. Both signals are observed as doublets, with *J* = 11.9 Hz, as a result of their coupling to proton H-3. Interestingly, proton H-3 is observed as an apparent triplet (*J* = 11.9 Hz) reasoned to be as a result of its coupling to proton H-2 and H-2'. The ratio of signals H-2 and H-2' indicated that compound **2.23** favours one form more than the other. Two broad singlets integrating for one proton collectively were also observed at 9.54 and 9.79 ppm with the more acidic proton assigned to the thioanilide proton H-1' and the less acidic as H-1 respectively, and were based on predicted pKa calculations. Similarly, these protons are distinct signals representative of the thione and thioenol isomers and the ratio of the two signals correspond to that previously calculated from H-2 and H-2'.

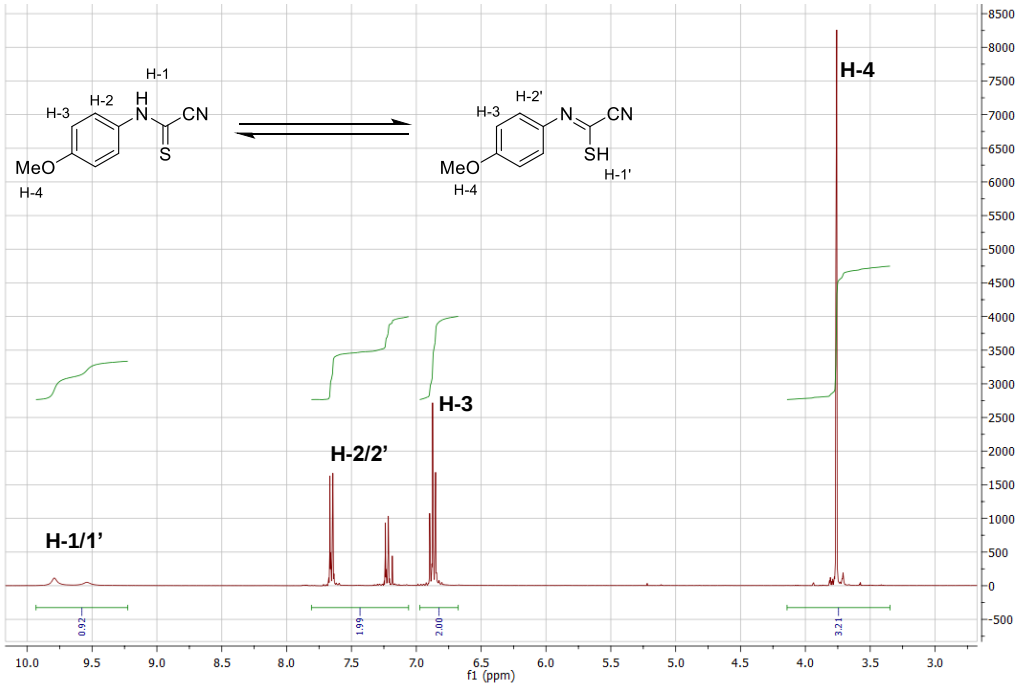

Figure 2.7. ^{1}H-NMR spectrum of 4-methoxy-2-cyanothioformanilide **2.23** in $CDCl_3$

Further supporting that approximately 60 % of the thioanilide is in the iminothiol form by ^{1}H-NMR spectroscopy. This tautomerism is very important in terms of reactivity, as the iminothiol form is required for cyclisation. Cyclisation of the thioamide intermediate **2.23** to the corresponding benzothiazole **2.8** was achieved via a C-S intramolecular cross coupling reaction shown in scheme 2.17.

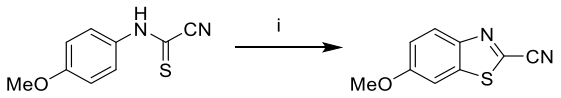

2.23 **2.8**

Scheme 2.17. Reagents and conditions: i) $PdCl_2$ / CuI / TBAB / DMF:DMSO (1:1) / 110 ^{o}C / 3h

The thioamide **2.23** was dissolved in a solution of DMF and DMSO, to which copper iodide, palladium chloride, and tetrabutyl ammoniumbromide (TBAB) were added. The reaction was then heated at 110 ^{o}C for 3 h under N_2. TLC analysis of the reaction revealed the conversion of the starting material to multiple products, observed as a myriad of non-polar spots, where the spot that was most intense in appearance (R_f 0.9 and 0.95 in 10% EtOAc) was thought to be the major product from the cyclisation reaction. After completion of the reaction, the crude mixture was diluted with EtOAc and washed with brine, ammonium chloride and water to remove the metal salts. However, TLC analysis of the organic layer revealed the persistence of trace amounts of highly polar impurities, possibly derived from metal adducts. After the aqueous wash, the organic layer was concentrated and purified on a silica column, eluting with hexanes to afford the 6-methoxy-2-cyanobenzothiazole product as a pale-yellow solid in a poor yield of 13 %. The proposed mechanism for benzothiazole cyclisation involves the directed insertion of the palladium catalyst into a C-H bond ortho to the anilide moiety. It is believed that the anilide functionality facilitates insertion of the metal into the C-H bond, which might explain why insertion occurs at only the proton ortho to the anilide. It is noted that TBAB acts as a ligand as well as a base via the bromide ion. TBAB facilities formation of the thioenolate form which is subsequently stabilised by the copper(I) catalyst. Subsequent oxidative addition and transmetalation results in the formation of a six membered metallocycle which undergoes reductive elimination of Pd(0), thus affording the benzothiazole ring, as shown in scheme 2.18.

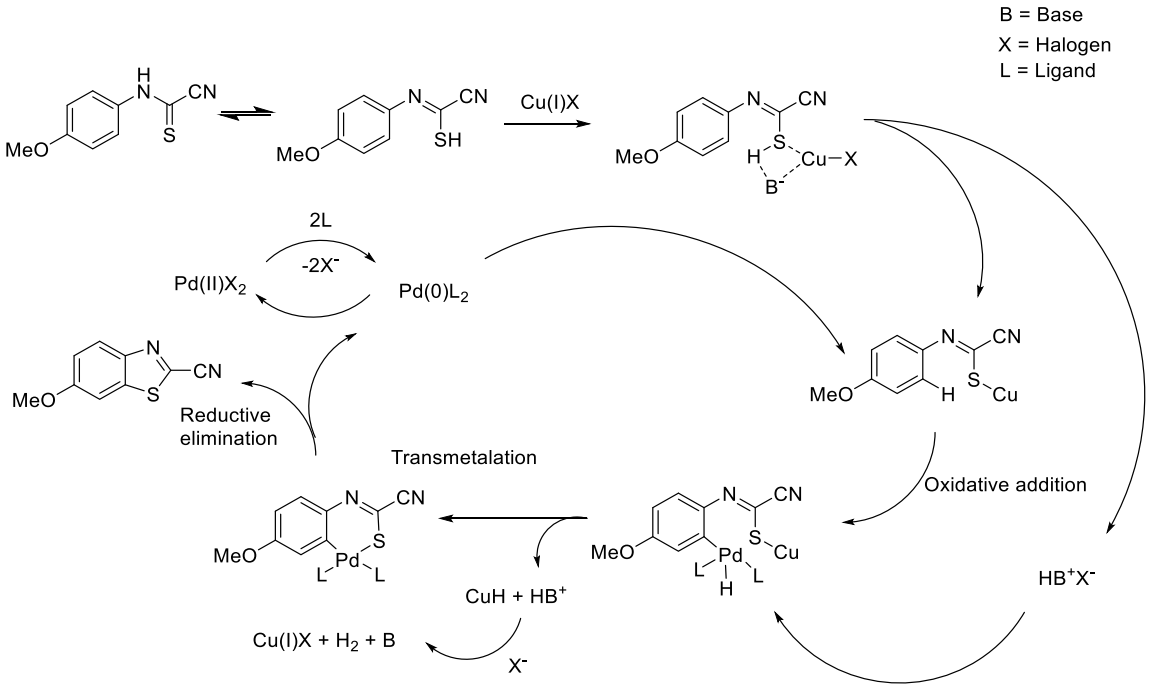

Scheme 2.18. Proposed mechanism for the C-S oxidative coupling reaction

The cyclisation reaction was based on a previously reported literature method with a yield of 87 %, but despite its reported efficacy, the reaction consistently afforded the product in poor yield (~10 %). This forced deviations from the method where increased catalyst loading and alternate Pd(II) catalysts where used, namely; $Pd(OH)_2$, $Pd(dppf)_2$, and $Pd(OAc)_2$. In all instances the product recovery remained low, with little to no improvement, as shown in table 2.1.

Table 2.1. Attempted optimisations for C-S cyclisation reaction

Catalyst	Catalyst loading, mol eq.	Co-catalyst	Co-catalyst loading, mol eq.	Yield, %
$PdCl_2$	0.1	CuI	0.5	13
$PdCl_2$	0.2	CuI	0.5	10
$PdCl_2$	0.5	CuI	0.5	12
$PdCl_2$	1	CuI	0.5	16
$PdCl_2$	0.1	CuI	0	-
$PdCl_2$	0.1	CuI	1	<10
$Pd(OH)_2$	0.1	CuI	0.5	<10
$Pd(OH)_2$	0.5	CuI	0.5	<10
$Pd(OAc)_2$	0.1	CuI	0.5	-
$Pd(OAc)_2$	0.5	CuI	0.5	-
$Pd(dppf)_2$	0.1	CuI	0.5	-

***Based on average isolated yields**

The ^{1}H-NMR spectrum of the isolated benzothiazole product displayed a singlet at 3.93 ppm integrating for 3 protons due to the C6-methoxy group as well the three aromatic resonances expected of a C6-substituted benzothiazole ring system, integrating for one proton each. The ^{1}H-NMR spectrum of the benzothiazole product is shown in figure 2.8.

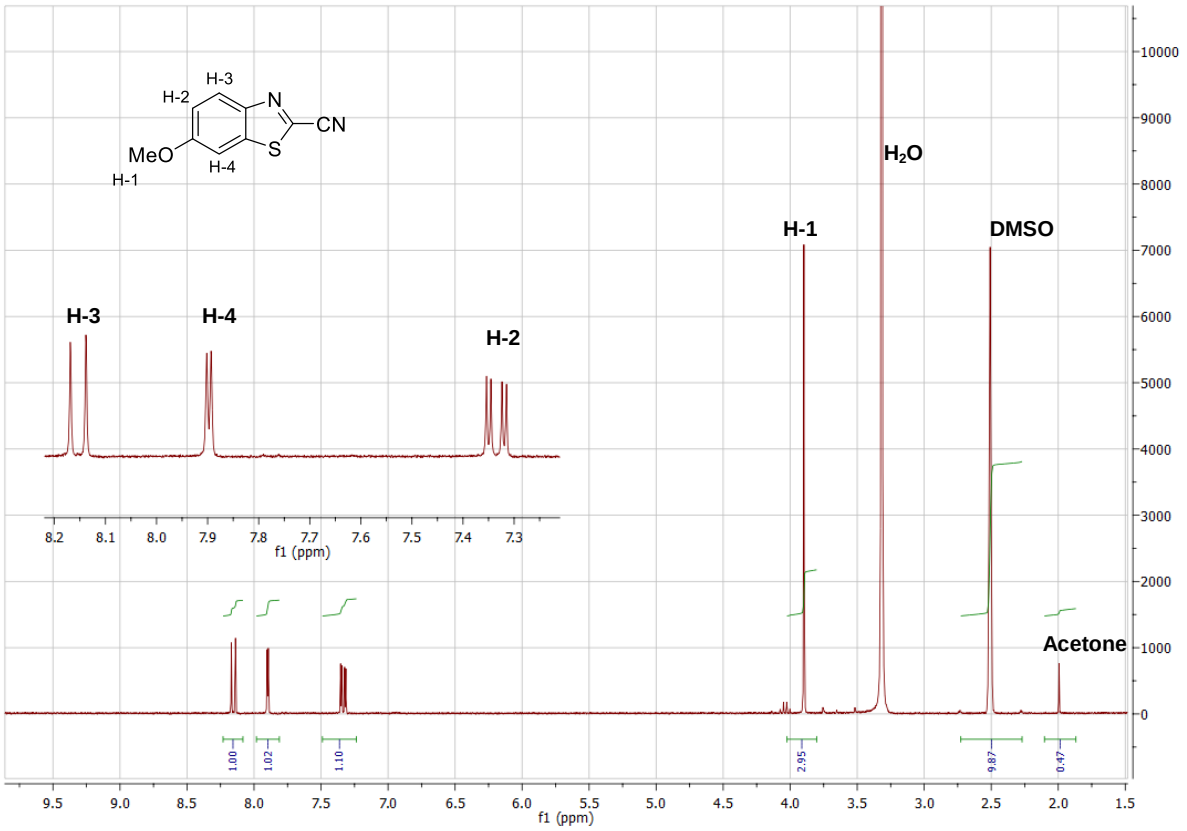

Figure 2.8. ^{1}H-NMR spectrum of 2-cyano-6-methoxybenzothiazole **2.8** in DMSO

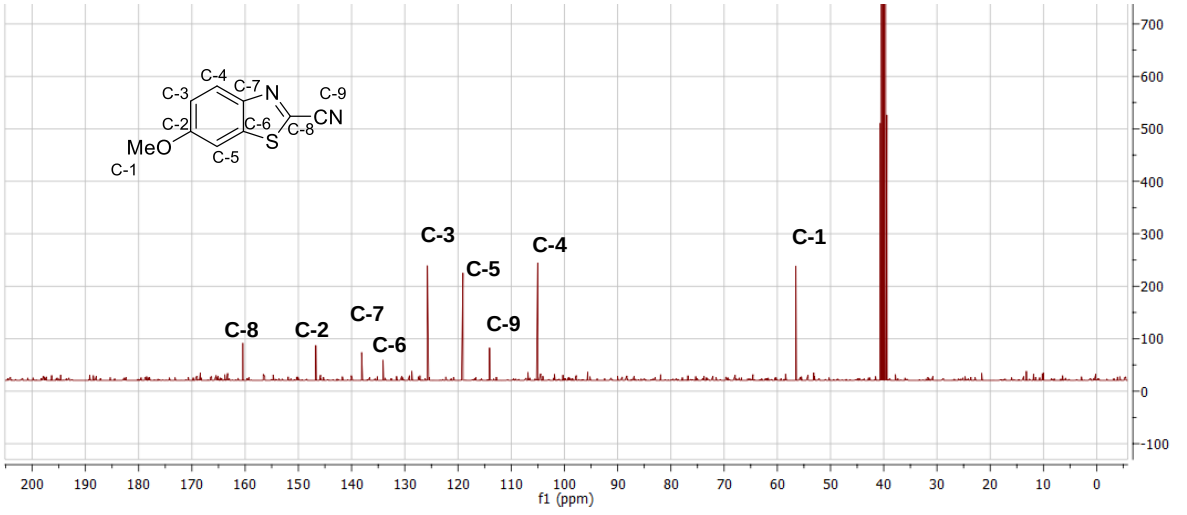

Figure 2.9. ^{13}C-NMR spectrum of 2-cyano-6-methoxybenzothiazole **2.8** in DMSO

The ^{1}H-spectrum of the benzothiazole scaffold showed 3 distinct aromatic signals. The observed coupling constants of individual signals were used to determine their locality. The most obvious assignment was that of H-4, which appeared as a doublet (J = 2.4 Hz) due to long range coupling with H-3. Normally, long range couplings are less than 1 Hz, however, such long-range couplings become more significant when dealing with aromatic compounds. Interactions of C-H bonds with pi electrons of aromatic rings along the coupling pathway resulted in an increase in the magnitude of the long-range coupling. This can be seen in figure 2.8, where the resonance at 7.90 ppm (H-4) displays a small coupling of 2.4 Hz, despite having no vicinal protons to couple to. This long-range coupling constant of J = 2.4 Hz, is also observed in H-2. Thus, signal H-2 appears as a doublet of doublets integrating for 1 proton due to its ^{3}J coupling to H-3 and its ^{4}J coupling to H-4. The ^{13}C-NMR spectrum of **2.8** displayed the expected total of 9 resonances and its IR spectrum revealed a sharp absorption band at 2200 cm^{-1}, further supporting the presence of the nitrile functionality. The melting point of **2.8** was found to be in the range of 123-130 °C, which was in close agreement with the recorded literature value of 129-131 °C. The broad melting point and elemental analysis data of compound **2.8** suggested possible traces of impurities. However, since the reaction was low yielding and the crude material had already been subjected to column chromatography, it was decided that the trace impurities would be dealt with in the next synthetic purification step. *O*-Methyl deprotection was used to prepare 4-hydroxy-2-cyanobenzothiazole. The *O*-alkyl precursor was heated at 110 °C with pyridinium hydrochloride (PyHCl) in DMF for 1 h. TLC analysis of the reaction showed the conversion of the non-polar starting material to a single, more polar product (R_f 0.3 in 30% EtOAc). After completion of the reaction, as evidenced by TLC analysis, the mixture was diluted with EtOAc, washed with brine and the organic layer concentrated and purified using silica column chromatography to afford **2.9**. Most obvious in the analysis of the ^{1}H-NMR spectrum of **2.9** is the absence of the *O*-methyl singlet previously observed in the starting material. All other ^{1}H-NMR signals were conserved in the transformation.

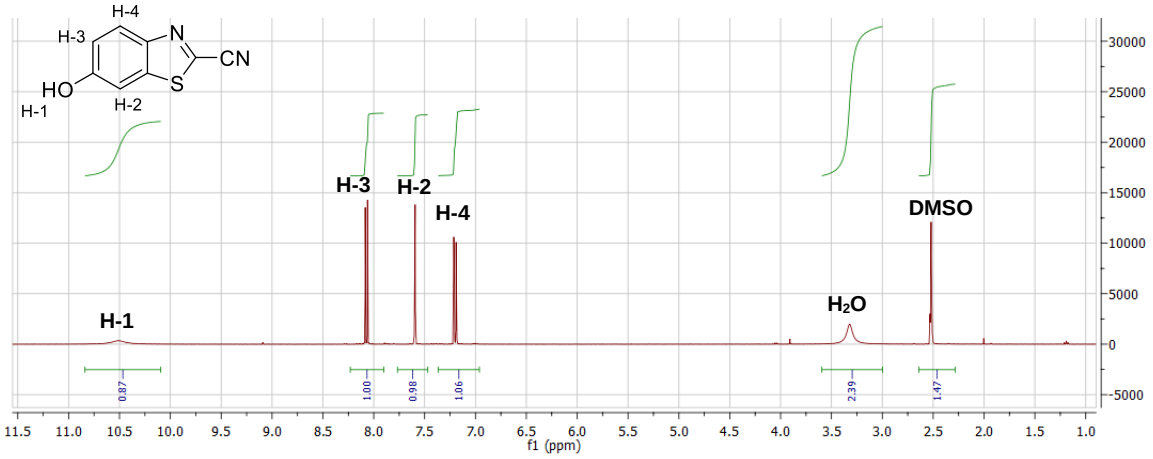

Figure 2.10. ^{1}H-NMR spectrum of 6-hydroxy-2-cyanobenzothiazole **2.9** in DMSO

A noticeable upfield shift in the aromatic proton resonances of the deprotected product relative to the starting material was also observed. The shift upfield concerns the greater electron donating effect of the hydroxyl group, relative to the methoxy precursor (It is well known that the hydroxyl group is a more strongly electron donating substituent than the methoxy group). The IR spectrum of **2.9** indicated that the nitrile functionality was conserved in the transformation and the melting point of the product was in close agreement with that of the recorded literature value (206-207 °C, lit. 205-207 °C).

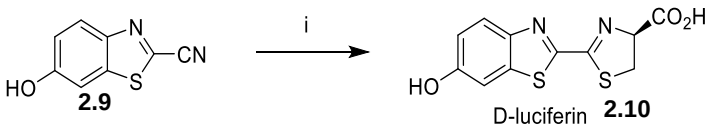

Scheme 2.19. Reagents and conditions: i) D-Cys / K_2CO_3 / MeOH:H_2O / 20 min / rt

The final step was the synthesis of D-luciferin **2.10**, which comprises of a benzothiazole C2-linked thiazoline ring. The thiazole ring has a carboxyl group at the C4 position and, notably, the carbon bearing the carboxyl group is a stereogenic centre with defined stereochemistry. The activity of D-luciferin is highly dependent on the configuration at the C4 position, meaning only one of the two enantiomers are biologically active. To generate a thiazole ring with the correct stereochemistry, 4-hydroxy-2-cyanobenzothiazole was reacted with enantiomerically pure D-Cys (99 % *ee*) in the presence potassium carbonate. The mechanism involves nucleophilic addition of the thiolate of D-Cys on the carbon of the nitrile group to generate an imine. A second attack by the free amine of D-Cys on the same carbon, now bearing an imino functionality, followed by elimination of ammonia generates the thiazoline ring (Scheme 2.20).

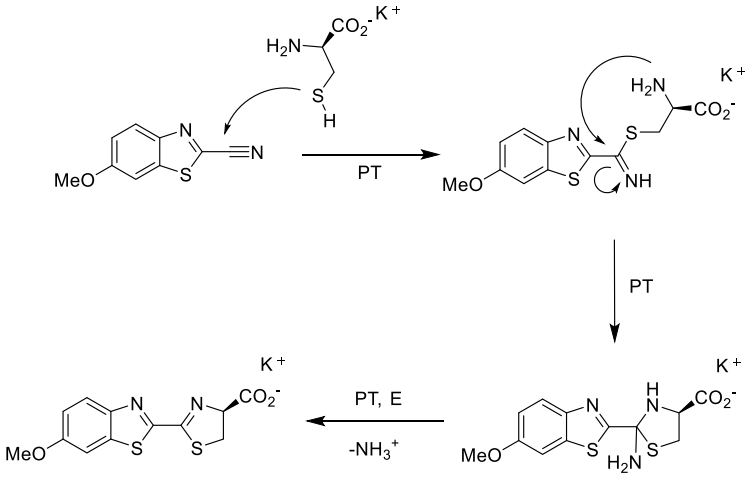

Scheme 2.20. Proposed mechanism for formation of D-Luciferin

An acidic work up protonates the carboxylate moiety to afford D-luciferin. The described cysteine coupling was achieved by adding potassium carbonate to a stirring solution of D-Cys and benzothiazole in a water/methanol mixture under an inert nitrogen atmosphere. TLC analysis of the reaction revealed conversion of the starting material to a new product, seen as the formation of a new, more polar spot (R_f 0.3 in 5 % MeOH). In cases where incomplete conversion of the starting material was observed, an acid-base extraction was employed to selectively isolate **2.10**. The theory behind this technique is that the potassium salt of **2.10**, formed from the base mediated D-Cys addition, is ionic and thus water soluble. Undesired neutral compounds, such as unreacted **2.8**, are extracted from the aqueous layer using diethyl ether. The aqueous layer is then acidified to form a neutral compound, which is then extracted into an organic solvent such as EtOAc, rendering the acid > 95 % pure (based on ^{1}H-NMR spectroscopy and LCMS). The acidification was done at 0 ^{o}C to limit decarboxylation and racemisation, well known reactions undergone by **2.10** reported in both basic and acidic media. The acid form of **2.10** was isolated as a pale-yellow solid in excellent yield (86 %), and was unstable at room temperature. Such instability was revealed by TLC where the polar acid converted to a much less polar product, believed to be due to decarboxylation which is favoured entropically by increasing temperatures. Therefore compound **2.10** was maintained at low temperatures at all times.

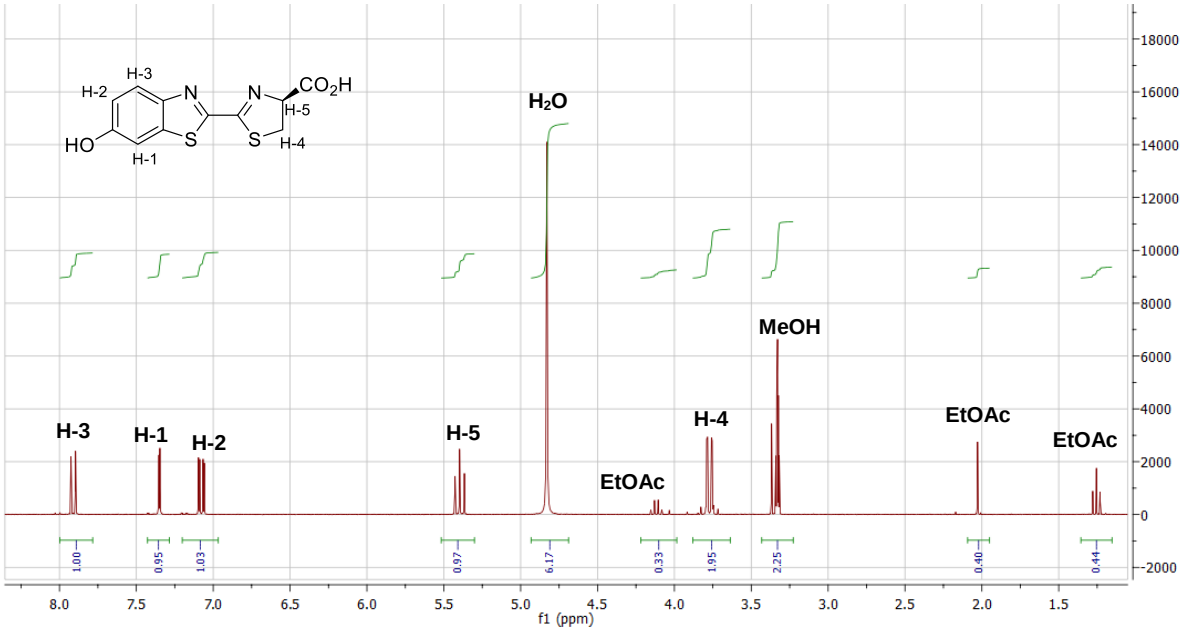

Figure 2.11. ^{1}H-NMR spectrum of D-luciferin **2.10** in MeOD, with trace amounts of EtOAc

The ^{1}H-NMR spectrum of D-luciferin showed all the expected proton signals, formerly reported for the isolated natural product. The spectrum (Figure 2.11) displays three distinct signals in the aromatic region (7-8 ppm) integrating for one proton each. These resonances were assigned to the aromatic protons (H-1,2,3). What appeared to be a well-defined triplet at 5.40 ppm, integrating for one proton,

was assigned the proton alpha to the carboxyl group (H-5). The triplet was found to be highly deshielded, most likely due to the electron withdrawing effects of the geminal carboxyl group. This particular resonance is very interesting because of D-luciferin's chiral character. This chirality differentiates the H-4 protons by their environment and potential. Consequently, a doublet of doublets is expected instead of the observed triplet for proton H-5. A possible reason for the apparent triplet may be due to the carboxythiazoline ring interconverting between two different puckered conformations and that the observed coupling constants are an average over these conformations. Another possible explanation could be that the triplet H-5 is in fact two overlapping doublets. If the signal H-5 is indeed a triplet, then each H-4 coupling will have a 9 Hz coupling constant, which can be seen from the 1H-NMR spectrum.

It is evident from the ^{1}H-NMR spectrum that H-4 has two distinct coupling partners. The coupling constants were found to be 9.0 Hz, and 3.0 Hz. The smaller coupling constant is due to the vicinal coupling of H-4 to H-5. The larger coupling constant is due to the geminal coupling between the two H-4 protons. This further indicated that the two protons are magnetically non-equivalent and are thus said to be diastereotopic. Diastereotopicity confirmed the presence of a stereogenic element and by extension that it is optically active. However, the ^{1}H-NMR data of course gave no indication of the optical purity of D-luciferin, since the enantiomers are equivalent by ^{1}H- and ^{13}C-NMR experiments. For this reason, the optical rotation of D-luciferin was determined.

The $[\alpha]_D^{20}$ was found was found to be in good agreement with that recorded for enantiomerically pure D-luciferin ($[\alpha]_{D\,\text{obs.}}^{20}$ = -29^0, $[\alpha]_{D\,\text{lit.}}^{20}$ = -34^0, DMF, c = 1), which indicated only a small degree of racemisation (85 % optical purity, 92.5 % D-luciferin, 7.5 % L-luciferin). The formation of D-luciferin was further confirmed by ^{13}C-NMR spectroscopy (vide infra), and melting point analysis, all of which were in good agreement with the data on the previously isolated natural product. The ^{13}C-NMR spectrum displayed the correct number of carbon resonances.

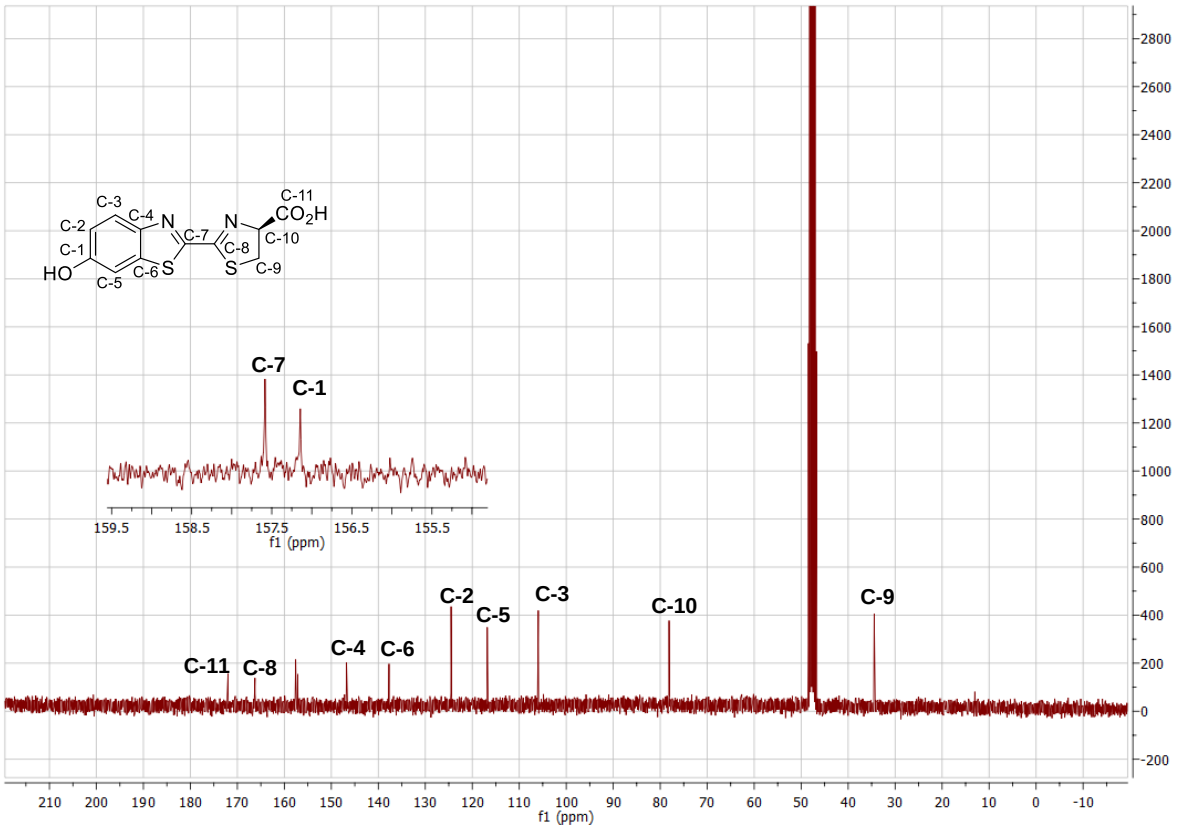

Figure 2.12. ^{13}C-NMR spectrum of D-luciferin **2.10** in MeOD

The purity of the material was further assessed using elemental analysis and LCMS, both of which supported that analytically pure D-luciferin had been produced and with the synthesis of D-luciferin complete, attention was then turned to potential synthetic improvements and bioluminescent evaluation.

Modifications to Prescher et al Synthesis of D-luciferin

The step that was found to be most limiting in the Prescher sequence was the C-S coupling reaction, despite it having been reportedly high yielding (86 %).[32] The lower yielding step was therefore further investigated.

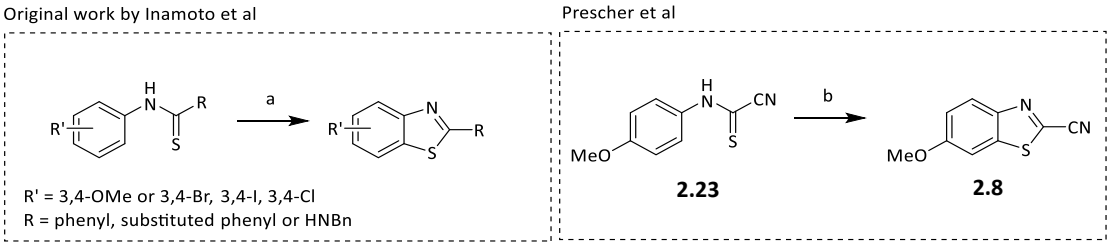

Scheme 2.21. Reagents and conditions: a) $PdCl_2$ / CuI / TBAB / NMP:DMSO (1:1) / 120 °C / 2 h b) $PdCl_2$ (0.1 eq)/ CuI (0.5 eq)/ TBAB / DMF:DMSO (1:1) / 110 °C / 3h

The cyclisation reaction was originally developed by Inamoto et al who reported a Pd-catalysed, CuI co-catalysed C-S cross coupling reaction in 1:1 mixture of DMSO and an appropriate co-solvent.[37] The addition of TBAB reportedly enhanced the transformation as lower yields were observed in its absence and NMP was found to be the best co-solvent. The reaction was originally done exclusively with aryl and amine substituents as shown in scheme 2.21. Prescher et al then used the same reaction on the cyano precursor **2.23** to afford the 2-cyano-6-methoxybenzothiazole **2.8** with the following changes to the cyclisation reaction; DMF was used as a co-solvent instead of NMP, the reaction was heated to 110 °C instead of 120 °C. These changes were not at all explained in any of their publications and afforded consistently low yields under the described conditions. Thus, warranting the use of the original, optimised reaction conditions (described by Inamoto et al) in an attempt to improve the yield and, perhaps, better understand why Prescher et al decided to make those particular changes to the Inamoto method.

The cyclisation reaction starting from **2.23** was therefore repeated using NMP as the co-solvent instead of DMF and the reaction was repeated at 110, 120 and 150 °C. From these reactions it was found that there was a negligible difference between the use of NMP and DMF as both reactions afforded similar average isolated yields with identical TLC profiles. There was however a slight increase in the average yield for the reactions done at 150 °C relative to those done at 110/120 °C (from 10-13 % to 25 %). Furthermore, it was also found that relatively consistent yields were afforded for the same reaction up to 600 mg starting scale, but reduced isolated yields were observed when cyclising gram quantities (1 and 2 g reactions afforded 8 and 10 % of the cyclised product, respectively).

Since both the reaction conditions used by Inamoto et al and Prescher et al afforded equally low yields, it was not possible to determine why Prescher et al made use of DMF instead of NMP or carried out the reaction at reduced temperatures. What was also quite interesting was that Prescher et al continued to work on improving their reportedly high yielding coupling reaction, suggesting that they too were perhaps aware of its limitations in the context of 2-cyanobenzothiazole syntheses. Another possible explanation for the low yields could be the absence of an effective oxidant that could more effectively regenerate the catalysts. Both the Prescher and Inamoto methods report that the reactions were carried out under dry and inert conditions. These conditions could in fact have been retarding catalyst regeneration. Unfortunately the reaction was not attempted with any oxidant additive to confirm this theory, however, it should be noted that Prescher et al later moved away from the limiting C-S coupling method.

Prescher et al Improved and Scalable Synthesis of D-luciferin

McCutcheon and Prescher et al subsequently developed an improved synthesis that bypassed the need for a C-S Pd-catalysed coupling reaction claiming that it improved the overall sequence since it improved both overall yield and scalability.[33] The improved reaction sequence is shown in scheme 2.22.

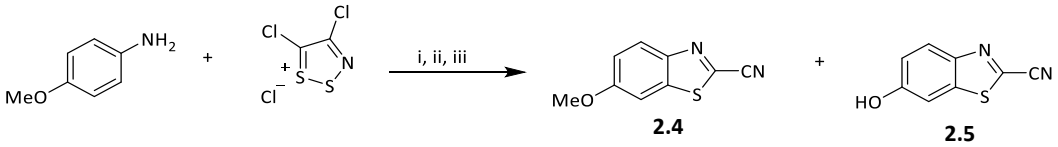

Scheme 2.22. Reagents and conditions: i) Appel's salt / Sulfolane / 40 °C / 3 h, ii) 180 °C / 20 min, iii) PyHCl (10 eq) / 180 °C / 1 h, (**2.4**: 21 %, **2.5**: 51 %)

The reaction involved forming a dithiazolimine from the condensation of *p*-anisidine and Appel's salt followed by dithiazolimine thermolysis and electrocyclisation to afford the cyclised benzothiazole.[33, 38] This publication encouraged a move away from the metal mediated C-S coupling methodology and to further explore dithiazolimine electrocyclisation, discussed in Chapter 4 in the context of the development of a unique and improved general luciferin synthetic sequence. Ultimately, efforts toward optimising the Pd and Cu catalysed reaction were abandoned and focus was instead shifted to developing novel modes of 2-cyanobenzothiazole cyclisation and to the bioluminescent evaluation of the prepared materials.

Bioluminescent Evaluation of D-Luciferin

In general, the bioluminescence properties of luciferin substrates are evaluated by either purified luciferase bioluminescence assays or by using luciferase expressing mutant cell lines. In the case of the purified luciferase assay, if the synthesised material is indeed luminescent, then it will produce a detectible luminescent output when treated with luciferase. This is usually done by dissolving the substrate in a neutral buffer, containing all the elements required for the light emitting reaction, such as Mg^{2+} and ATP. The enzyme (usually also dissolved in a stabilising buffer) then gets added to the substrate and the resulting luminescence is recorded using a luminometer. In the case of luciferase expressing cell lines, luminescence is measured similarly, with the only difference being that buffers containing magnesium and ATP are not required since they are already present in the cells. The D-luciferin that was prepared was evaluated in two ways, the first involved using a purified luciferase bioluminescence assay and the second involved using luciferase expressing tobacco plants.

Purified enzyme assay: The synthesised D-luciferin was reacted with luciferase and the resultant luminescence measured using a Luminoskan Ascent luminescence plate reader. The luciferase enzyme was prepared as a 10 nM solution in enzyme buffer where luciferase lyophilised powder was dissolved in previously prepared luciferase enzyme buffer (20 mM Tris [pH 7.4], 0.1 mM EDTA, 1 mM DTT, and 0.8 mg/mL BSA). Luminescence assays were initiated by adding 30 µL of luciferase in luciferase enzyme buffer to 60 µL of 0.1 µM or 3.56 µM D-luciferin in substrate buffer (20 mM Tris [pH 7.4], 0.1 mM EDTA, 8 mM $MgSO_4$, and 4 mM ATP) in a white 96-well plate. The RLU were then determined 1 min post-enzyme addition and were recorded in triplicate and are represented as the mean ± SEM.

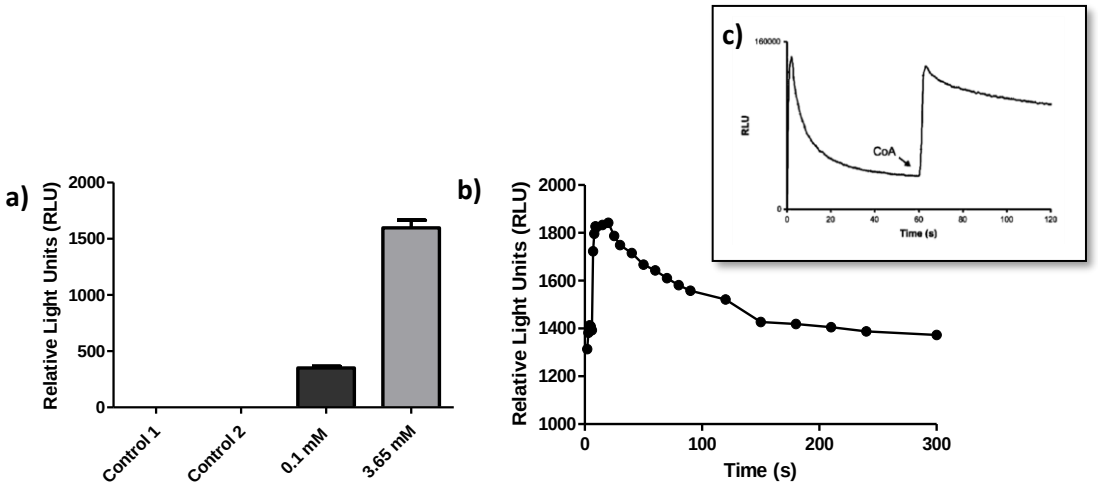

Figure 2.12. a) Graph of D-luciferin bioluminescence and b) Luminescence over time demonstrating Burst kinetics and c) Burst Kinetics as demonstrated by Fraga et al

For the standard evaluation of luminescence, figure 2.12 graph (a), two control readings were recorded. Control 1 contained 90 µL of 10 nM the enzyme luciferase in enzyme buffer, control 2 contained 90 µL of 0.1 µM D-luciferin in substrate buffer. In both instances, no significant luminescence was observed. Only when both the enzyme and substrate were present, was luminescence observed. When 30 µL of the 10 nM enzyme was injected into 60 µL of 0.1 µM D-luciferin an output of 480 RLU was observed after 1 min. A threefold increase in luminescence was observed when the concentration of D-luciferin was increased to 3.65 µM. Graph (b) showed the luminescence profile of D-luciferin over time. It is evident from the graph that there was a spike in luminescence in the first minute, which then decayed to produce a steadier luminescent output over time. This is characteristic of the luciferase enzyme and, as previously discussed by Fraga et al, is caused by inhibition of the enzyme by by-products formed in the light emitting reaction.[11] Graph (c) shows the burst kinetic profile of luciferase reported by Fraga et al for comparison purposes.

Live imaging using luciferase expressing tobacco plants: The synthesised D-luciferin was further evaluated using transgenic luciferase expressing *N. Tabacum* plants. The plants were transfected with a previously prepared luciferase coupled stress inducible promotor, *XvSap1*. Luciferase expression was then induced by subjecting mature *N. Tabacum* plants to a 6-day dehydration period, after which leaves were taken from plants for bioluminescence imaging.

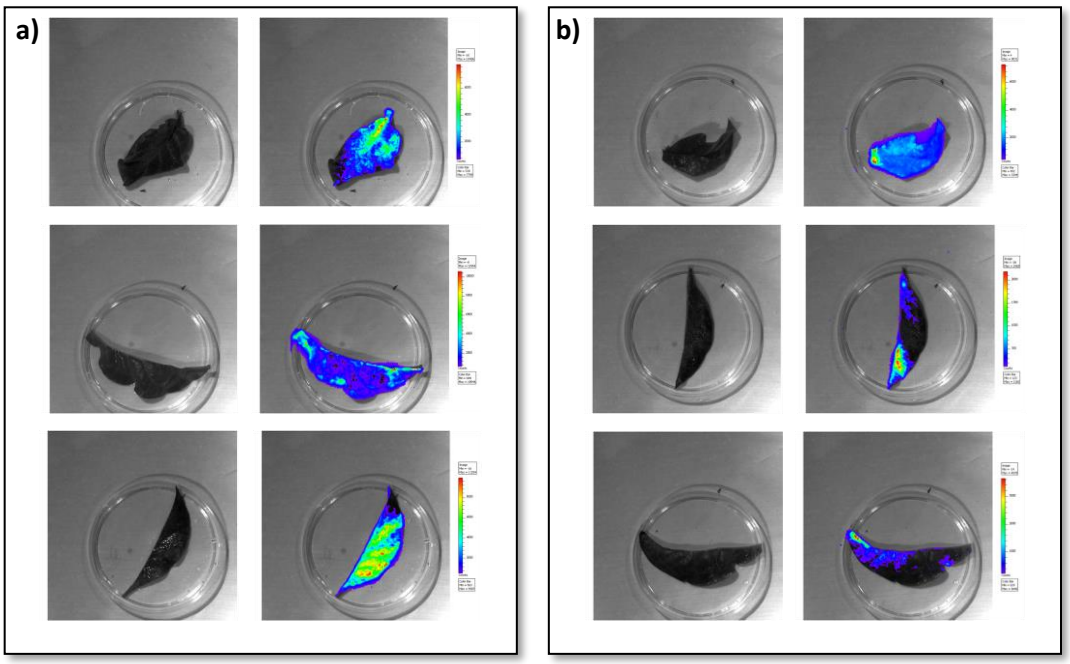

Figure 2.13. BL images of luciferase expressing *N. Tabacum* leaves treated with a 5 mM aqueous solution of a) D-luciferin potassium salt and b) D-luciferin free acid

Leaves were individually sprayed with equal amounts of 5 mM D-luciferin and D-luciferin potassium salt after which Luciferase activity was imaged with a 3D-luminometer at an exposure time of 300 s per leaf. Photon or count emission by luciferase expressing leaves were quantified using the Living Image software (Caliper, USA) and are shown in figure 2.13. Luminescence was recorded before and after the treatment with luciferin and was used to evaluate luciferase expression and by extension luc-coupled promotor activity. The fact that luminescence was observed provided evidence that *XvSAP1* had been upregulated in response to dehydration, since negligible luc activity had been reported prior to dehydrating. As a control, non-luc expressing tobacco leaves were also treated with D-luciferin and as predicted, luminescence was not observed, figure 2.14.

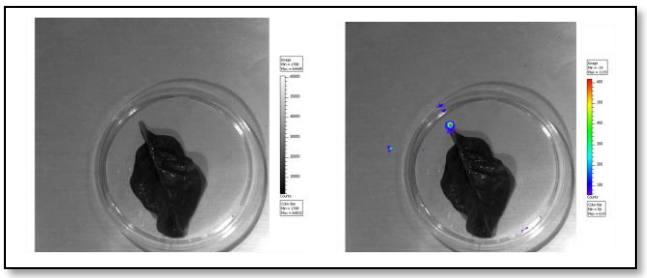

Figure 2.14. Non-luciferase expressing control

Summary and Conclusions

The synthesis of D-luciferin was achieved over 6 steps with a 23 % overall yield. All spectroscopic and analytical data were in good agreement with that previously reported for the natural product. The metal mediated cyclisation to form the benzothiazole was limiting and an alternative methodology for the formation of the benzothiazole from the thioanilide would be advantageous. In terms of its luminescence properties, D-luciferin was found to be luminescent active when treated with luciferase. The synthesised D-luciferin was evaluated alongside commercially sourced D-luciferin, as a positive control, where no significant difference in luminescent output was observed between commercial and synthetic luciferin, further supporting that D-luciferin had been successfully synthesised. In conclusion, pure D-luciferin had been prepared and was primed for use as a luminescent standard.

References

1. White, E. H.; McCapra, F.; Field, G. F.; McElroy, W. D., The structure and synthesis of firefly luciferin. *Journal of the American Chemical Society* **1961,** *83* (10), 2402-2403.
2. White, E. H.; Rapaport, E.; Seliger, H. H.; Hopkins, T. A., The chemi-and bioluminescence of firefly luciferin: an efficient chemical production of electronically excited states. *Bioorganic chemistry* **1971,** *1* (1), 92-122.
3. Niwa, K.; Nakamura, M.; Ohmiya, Y., Stereoisomeric bio-inversion key to biosynthesis of firefly D-luciferin. *FEBS letters* **2006,** *580* (22), 5283-5287.
4. McCapra, F.; Razavi, Z., Biosynthesis of luciferin in Pyrophorus pellucens. *Journal of the Chemical Society, Chemical Communications* **1976,** (5), 153-154.
5. Oba, Y.; Yoshida, N.; Kanie, S.; Ojika, M.; Inouye, S., Biosynthesis of Firefly Luciferin in Adult Lantern: Decarboxylation of L-Cysteine is a Key Step for Benzothiazole Ring Formation in Firefly Luciferin Synthesis. *PloS one* **2013,** *8* (12), e84023.
6. Van de Bittner, G. C.; Bertozzi, C. R.; Chang, C. J., Strategy for dual-analyte luciferin imaging: in vivo bioluminescence detection of hydrogen peroxide and caspase activity in a murine model of acute inflammation. *Journal of the American Chemical Society* **2013,** *135* (5), 1783-1795.
7. Van de Bittner, G. C.; Dubikovskaya, E. A.; Bertozzi, C. R.; Chang, C. J., In vivo imaging of hydrogen peroxide production in a murine tumor model with a chemoselective bioluminescent reporter. *Proceedings of the National Academy of Sciences of the United States of America* **2010,** *107* (50), 21316-21321.
8. Honigman, A.; Zeira, E.; Ohana, P.; Abramovitz, R.; Tavor, E.; Bar, I.; Zilberman, Y.; Rabinovsky, R.; Gazit, D.; Joseph, A., Imaging transgene expression in live animals. *Molecular Therapy* **2001,** *4* (3), 239-249.
9. Prescher, J. A.; Contag, C. H., Guided by the light: visualizing biomolecular processes in living animals with bioluminescence. *Current opinion in chemical biology* **2010,** *14* (1), 80-89.
10. Pinto da Silva, L.; Esteves da Silva, J. C. G., Study on the effects of intermolecular interactions on firefly multicolor bioluminescence. *ChemPhysChem* **2011,** *12* (16), 3002-3008.

11. Fraga, H., Firefly luminescence: A historical perspective and recent developments. *Photochemical & Photobiological Sciences* **2008,** *7* (2), 146-158.
12. Pinto da Silva, L. s.; Santos, A. J. M.; Esteves da Silva, J. C. G., Efficient Firefly Chemi/Bioluminescence: Evidence for Chemiexcitation Resulting from the Decomposition of a Neutral Firefly Dioxetanone Molecule. *The Journal of Physical Chemistry A* **2012,** *117* (1), 94-100.
13. Conti, E.; Franks, N. P.; Brick, P., Crystal structure of firefly luciferase throws light on a superfamily of adenylate-forming enzymes. *Structure* **1996,** *4* (3), 287-298.
14. De Wet, J. R.; Wood, K. V.; Helinski, D. R.; DeLuca, M., Cloning of firefly luciferase cDNA and the expression of active luciferase in Escherichia coli. *Proceedings of the National Academy of Sciences* **1985,** *82* (23), 7870-7873.
15. Schröder, J., Protein sequence homology between plant 4-coumarate: CoA ligase and firefly luciferase. *Nucleic acids research* **1989,** *17* (1), 460.
16. Toh, H., N-terminal halves of gramicidin S synthetase 1, and tyrocidine synthetase 1 as novel members of firefly luciferase family. *Protein sequences & data analysis* **1990,** *3* (6), 517-521.
17. Seliger, H. H.; McElroy, W. D., Spectral emission and quantum yield of firefly bioluminescence. *Archives of biochemistry and biophysics* **1960,** *88* (1), 136-141.
18. DeLuca, M.; McElroy, W. D., Kinetics of the firefly luciferase catalyzed reactions. *Biochemistry* **1974,** *13* (5), 921-925.
19. da Silva, L. P.; da Silva, J. C. E., Kinetics of inhibition of firefly luciferase by dehydroluciferyl-coenzyme A, dehydroluciferin and L-luciferin. *Photochemical & Photobiological Sciences* **2011,** *10* (6), 1039-1045.
20. Nakatsu, T.; Ichiyama, S.; Hiratake, J.; Saldanha, A.; Kobashi, N.; Sakata, K.; Kato, H., Structural basis for the spectral difference in luciferase bioluminescence. *Nature* **2006,** *440* (7082), 372-376.
21. Figueiredo, M. S.; Brownlee, G. G., cis-acting elements and transcription factors involved in the promoter activity of the human factor VIII gene. *Journal of Biological Chemistry* **1995,** *270* (20), 11828-11838.

22. Nam, Y.; Kim, B. S.; Shin, I., Highly sensitive and selective bioluminescence based ozone probes and their applications to detect ambient ozone. *Chemical Communications* **2016,** *52* (6), 1128-1130.

23. Craig, F. F.; Simmonds, A.; Watmore, D.; McCapra, F.; White, M., Membrane-permeable luciferin esters for assay of firefly luciferase in live intact cells. *Biochemical journal* **1991,** *276* (3), 637-641.

24. Zhou, W.; Andrews, C.; Liu, J.; Shultz, J. W.; Valley, M. P.; Cali, J. J.; Hawkins, E. M.; Klaubert, D. H.; Bulleit, R. F.; Wood, K. V., Self-Cleavable Bioluminogenic Luciferin Phosphates as Alkaline Phosphatase Reporters. *ChemBioChem* **2008,** *9* (5), 714-718.

25. Jones, L. R.; Goun, E. A.; Shinde, R.; Rothbard, J. B.; Contag, C. H.; Wender, P. A., Releasable Luciferin− Transporter Conjugates: Tools for the Real-Time Analysis of Cellular Uptake and Release. *Journal of the American Chemical Society* **2006,** *128* (20), 6526-6527.

26. Li, J.; Chen, L.; Du, L.; Li, M., Cage the firefly luciferin!–a strategy for developing bioluminescent probes. *Chemical Society reviews* **2013,** *42* (2), 662-676.

27. Kaskova, Z. M.; Tsarkova, A. S.; Yampolsky, I. V., 1001 lights: luciferins, luciferases, their mechanisms of action and applications in chemical analysis, biology and medicine. *Chemical Society Reviews* **2016,** *45* (21), 6048-6077.

28. Meroni, G.; Rajabi, M.; Santaniello, E., D-Luciferin, derivatives and analogues: synthesis and in vitro/in vivo luciferase-catalyzed bioluminescent activity. *Arkivoc* **2009,** *1*, 265-288.

29. Seto, S.; Ogura, K.; Nishiyama, Y., A convenient synthetic method of 2-carbamoyl-6-methoxybenzothiazole, one of intermediates for the synthesis of firefly luciferin. *Bulletin of the Chemical Society of Japan* **1963,** *36* (3), 331-333.

30. Besson, T.; Dozias, M.-J.; Guillard, J.; Rees, C. W., New route to 2-cyanobenzothiazoles via N-arylimino-1, 2, 3-dithiazoles†. *Journal of the Chemical Society, Perkin Transactions 1* **1998,** (23), 3925-3926.

31. Besson, T.; Emayan, K.; Rees, C. W., 1, 2, 3-Dithiazoles and new routes to 3, 1-benzoxazin-4-ones, 3, 1-benzothiazin-4-ones and N-arylcyanothioformamides. *J. Chem. Soc., Perkin Trans. 1* **1995,** (17), 2097-2102.

32. McCutcheon, D. C.; Paley, M. A.; Steinhardt, R. C.; Prescher, J. A., Expedient synthesis of electronically modified luciferins for bioluminescence imaging. *Journal of the American Chemical Society* **2012,** *134* (18), 7604-7607.

33. McCutcheon, D. C.; Porterfield, W. B.; Prescher, J. A., Rapid and scalable assembly of firefly luciferase substrates. *Organic & Biomolecular Chemistry* **2015,** *13* (7), 2117-2121.

34. Besson, T.; Rees, C. W., Some chemistry of 4, 5-dichloro-1, 2, 3-dithiazolium chloride and its derivatives. *Journal of the Chemical Society, Perkin Transactions 1* **1995,** (13), 1659-1662.

35. Besson, T.; Guillard, J.; Rees, C. W., Rapid synthesis of 2-cyanobenzothiazole, isothiocyanate and cyanoformanilide derivatives of dapsone. *Journal of the Chemical Society, Perkin Transactions 1* **2000,** (4), 563-566.

36. Appel, R.; Janssen, H.; Siray, M.; Knoch, F., Synthese und Reaktionen des 4, 5-Dichlor-1, 2, 3-dithiazolium-chlorids. *Chemische Berichte* **1985,** *118* (4), 1632-1643.

37. Inamoto, K.; Hasegawa, C.; Hiroya, K.; Doi, T., Palladium-catalyzed synthesis of 2-substituted benzothiazoles via a C− H functionalization/intramolecular C− S bond formation process. *Organic letters* **2008,** *10* (22), 5147-5150.

38. Besson, T.; Dozias, M.-J.; Guillard, J.; Rees, C. W., New route to 2-cyanobenzothiazoles via N-arylimino-1, 2, 3-dithiazoles. *Journal of the Chemical Society, Perkin Transactions 1* **1998,** (23), 3925-3926.

Chapter 3

Synthesis and Bioluminescent Evaluation of D-Aminoluciferin

Abstract

D-Aminoluciferin, a C6'-amino variant of D-luciferin, was identified to have more favourable luminescent properties relative to natural D-luciferin; in terms of it having a more red-shifted maximum wavelength of emission (λ_{max} of 557 nm for D-luciferin and 594 nm for D-aminoluciferin using natural luciferase, *Ppy* luc) and in terms of luminescence half-life and binding affinity for the luciferase enzyme. The amino group also provides a unique handle for coupling D-aminoluciferin with other molecules of interest, particularly peptides, to form amides and carbamates of relevance in the development of probes based on amide and carbamate hydrolysis. This chapter concerns the preparation, characterisation and bioluminescent evaluation of D-aminoluciferin, which was prepared from *p*-nitroaniline in 6 steps in a 20 % yield.

Chapter 3

Synthesis and Bioluminescent Evaluation of D-Aminoluciferin

D-Aminoluciferin: An Introduction

Fluorogenic and chromogenic substrates are used commonly in analytical methods for determining enzyme activities. The substrates are cleaved, generally by a target enzyme, to release a detectible analyte. For example, such an analyte could be a bioluminescent active molecule that would luminesce upon release. In this way, the measured luminescence can be used to determine the analyte concentration and hence correlate to enzyme activity.[1] D-Luciferin has been used extensively in this regard[2-4] and, in an effort to diversify its bioluminescent applications, amino derivatives of D-luciferin were developed. D-Aminoluciferin was first prepared by Emile White and co-workers following on their successful synthesis of D-luciferin and some regio-isomers thereof (figure 3.1).[5]

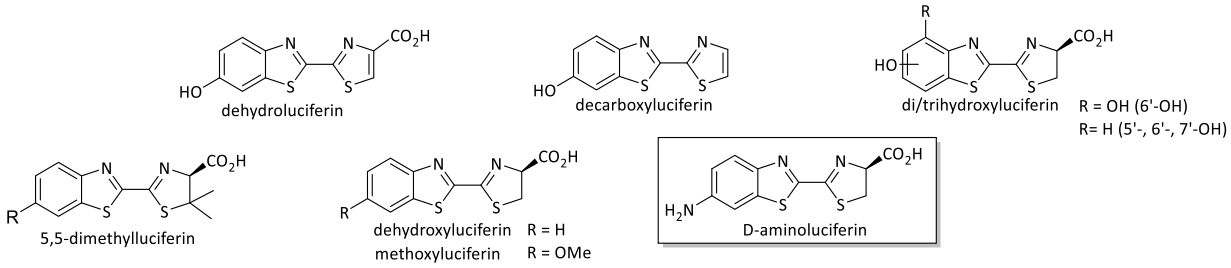

Figure 3.1. The structures of the first synthetic analogues of D-luciferin prepared by Emile White and William McElroy

From these analogues, White and McElroy established that the C6'-hydroxyl of D-luciferin could be replaced with an amino group and still retain luminescent activity.[5] They also reported that C6'-aminoluciferin emits light at a longer wavelength (λ_{max} of 594 nm, relative to 557 nm for D-luciferin) and that it has a 10-fold higher affinity for luciferase than natural D-luciferin.[5-6] Additionally, it was demonstrated that light was not emitted when the amino group was acylated. Much like how D-luciferin loses its luminescent activity when the 6'-hydroxyl is removed, alkylated or acylated. Reportedly, this is not due to a lack of binding, in fact, these and many other modifications are well tolerated by the enzyme. Instead, the modifications prevent light emission by causing the light emitting reaction to generate a singlet excited state as opposed to the triplet excited state required for luminescence.[7]

The replacement of the C6'-hydroxyl of D-luciferin with the more strongly electron-donating amino group red shifts the spectral properties of the luciferin chromophore while maintaining affinity for the enzyme. The red-shifted emission is of course desirable for deep tissue imaging, but what has actually made D-aminoluciferin so popular is the added option of peptide chemistry at the terminal amino group.

Bioluminescent properties of D-aminoluciferin and related analogues

In nature there are approximately thirty different forms of BL systems, of which nine have been established to be unique. Each of the nine BL systems has its own limitations (reactivity, solubility, λ_{max}, etc), which forms the rationale behind the need for new BL systems based on novel or existing luciferins and/or luciferases. For example, a D-luciferin-utilising BL system may be preferable to a coelenterazine BL system due to the lower cost and better bioavailability of the D-luciferin substrate. Unlike D-luciferin, coelenterazine cannot effectively overcome the blood brain barrier which may limit its applications accordingly. On the other hand, D-luciferin has a relatively low stability in solution and hence new luciferins are constantly being investigated.

As previously detailed, all luciferins emit light by the same mechanism of oxidative decarboxylation that results in a high energy excited state intermediate that relaxes to the ground state with the emission of light (CTIL/CIEEL). The energy associated with the excited state is derived, in part, from the electron rich reservoir that is the benzothiazole moiety. In the case of D-aminoluciferin, the amine raises the energy of the electron rich benzothiazole resulting in a lower energy excited state and ultimately a smaller energy gap between the excited and ground state. This smaller energy gap is observed as a longer wavelength of emission as seen in figure 3.2.

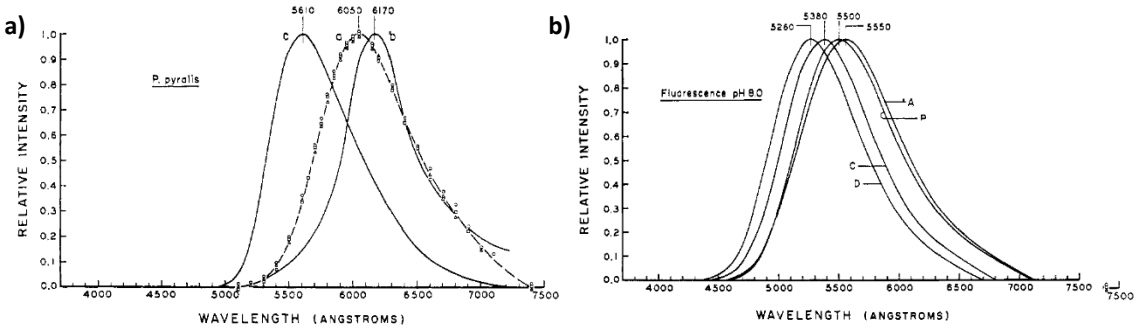

Figure 3.2. a) Bioluminescence emission spectra of *Ppy* luciferase treated with aminoluciferin at pH 6.0, pH 7.7 and pH 8.55, and b) the fluorescence emission spectra of dehydroluciferin (A), 4'-hydroxyluciferin (B), D-luciferin (C), and aminoluciferin (D) in glycylglycine buffer at pH 8.0. The spectra are adapted from White et al and normalised to 1 at peak emission[5]

The spectral properties of various other substituted aminoluciferins were studied independently. It was demonstrated that mono- and di-substituted alkylaminoluciferins **3.2a-d** as well as cyclo-aminoluciferins **3.3a-b** were all substrates for natural *Ppy* luc. All of the amino-derivatives, shown in figure 3.3, displayed greater affinity for luciferase than D-luciferin and D-aminoluciferin and a significant bathochromic shift in the BL maxima in the spectra of alkylaminoluciferins (in vitro) relative to D-luciferin and D-aminoluciferin was also observed. However, the total light output of the enzymatic reactions with the luciferin analogues were significantly reduced relative to D-luciferin.

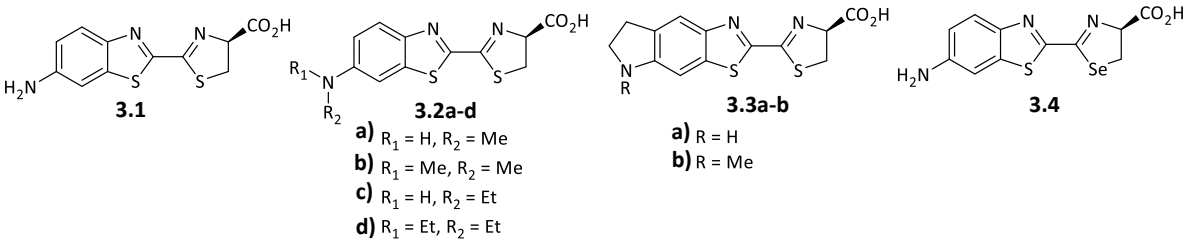

Figure 3.3. The structure of various substituted aminoluciferins

Interestingly, tests with the mutant Ultra-Glo luciferase in P450-Glo buffer solution demonstrated increases of 5.7 and 4.7 times, respectively, in the luminescence intensity and the total light output for cycloluciferin **3.3a** and *N*-methylcycloluciferin **3.3b**.[8] Unfortunately, the mutant Ultra-Glo luc is currently not available for transformation in living cells and hence cannot be used for in vivo imaging. The combination of an electron donating amino group and a polarisable selenium atom was used by Conley et al to expand the range of red-shifted D-luciferin analogues whose emission maxima are shown in figure 3.4. The selenazole **3.4** emits red light in vitro and in vivo (λ_{max} 600 nm), thus it's emission is easily distinguishable from the yellow green light of D-luciferin (λ_{max} 550 nm) making it ideal for use in dual sensing applications.

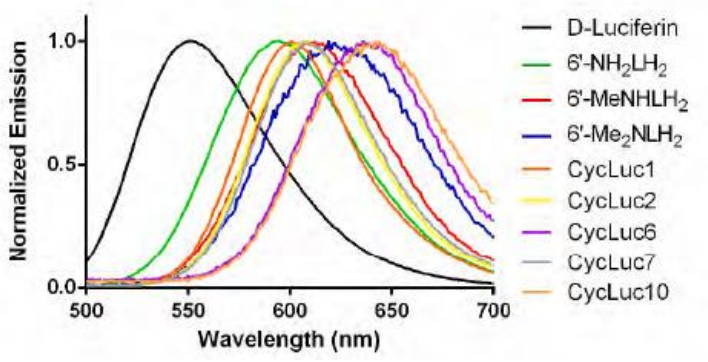

Figure 3.4. Bioluminescence emission spectra of D-luciferin, D-aminoluciferin (6'-NH_2LH_2) and various amino analogues demonstrating increasing λ_{max}

Another interesting example of a 6'-amino derivative of D-luciferin was reported by Zhou et al, who prepared a series of *N*-cycloalkylated luciferins.[9] Of these luciferins, CybLuc demonstrated a 20-fold increase in luminescence intensity relative to D-luciferin and D-aminoluciferin (Figure 3.5).

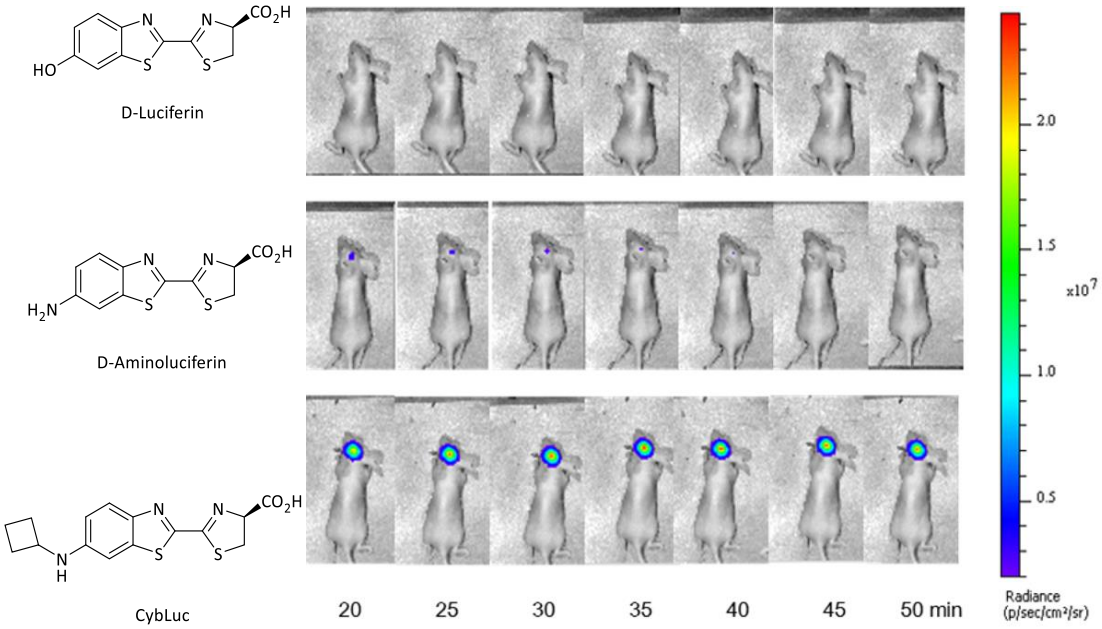

Figure 3.5. Bioluminescence imaging of D-luciferin, D-aminoluciferin and CybLuc in a nude mouse brain that was implanted with ES-2-Fluc cells, to generate tumour xenografts. Structures and representative bioluminescence images after intraperitoneal injection of D-luciferin, D-aminoluciferin, and CybLuc (1 mM, 0.2 mL) over time are shown

In the study by Zhou et al, it was not only demonstrated that CybLuc and related *N*-cycloalkyl luciferins were effective substrates for native *Ppy* luciferase, but also that CybLuc could be used for deep tissue imaging since it produced elevated bioluminescent signals in vivo when compared to the known luciferins. Moreover, CybLuc demonstrated a more red-shifted BL emission maxima (607 nm), similar to that of the previously reported amino-analogues, which again is of significance for tissue penetration in live animal imaging.

While the effects of the different modifications on the emission intensity and BL maxima are interesting and can be exploited to various ends, it must be reiterated at this point that aminoluciferins are generally valued not for their BL wavelength of emission but rather for the unique chemical handle that the amine provides.

Applications of D-aminoluciferin and related analogues

The amino functionality allows for the formation of amides. These amides are non-luminescent active until hydrolysed (either selectively or non-selectively) and luminescence allows for measuring the hydrolysis process (scheme 3.1). A number of technologies have been developed on this premise, some of which are highlighted here.

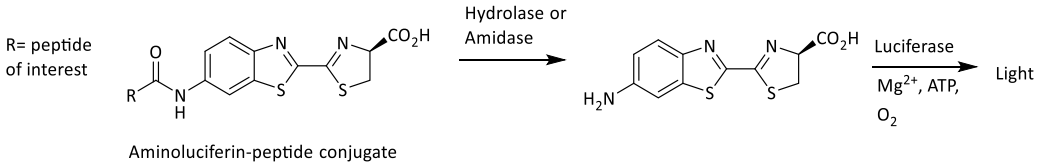

Scheme 3.1. D-Aminoluciferin-peptide conjugates

Specific peptidase activity can be monitored by coupling D-aminoluciferin to specific peptide sequences that are recognised by specific enzymes. An example of such a coupled conjugate is the commercially available Vivoglo® Caspase-3/7 substrate. This luciferin conjugate is recognised by the caspase enzymes which hydrolyses the conjugate to afford aminoluciferin, which further reacts in the presence of luciferase to emit light. In this way, the light output can be correlated to caspase activity and can therefore be used to image apoptotic cells (Scheme 3.2).[10] The Promega caspase-3/7 assay has been used extensively in cancer biology research where caspase activity is of interest.

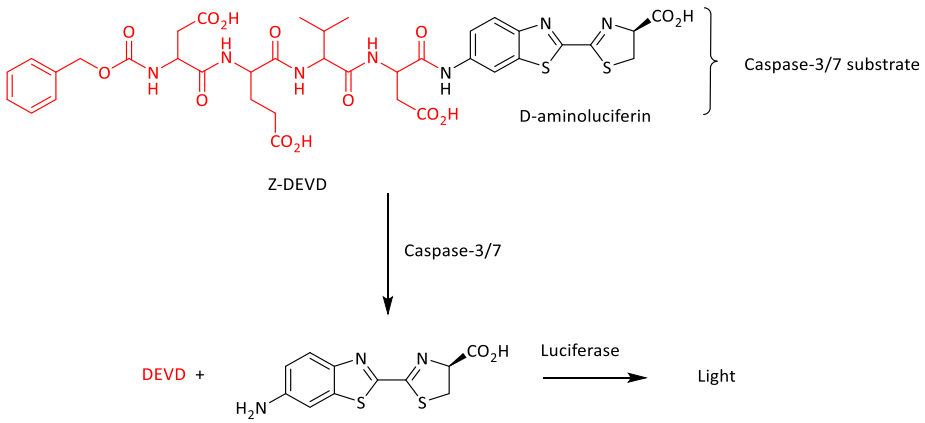

Scheme 3.2. Luciferin-linked caspase-3/7 assay

In a study concerning the characterisation of apoptotic cells Z-DEVD-aminoluciferin, the substrate in the Promega caspase-3/7 assay, was cleaved by caspase-3 to liberate aminoluciferin, which then reacted with luciferase to generate a luminescent signal. In two oncology models (namely SKOV3-luc and MDA-MB-231-luc-LN, at 24, 48, and 72 h after treatment with docetaxel) cells were injected with Z-DEVD-aminoluciferin and the resultant bioluminescence was recorded. Significantly more light was detected in the docetaxel-treated group compared with the vehicle-treated group. This was expected

since docetaxel is a well-known inducer of apoptosis. Interestingly, significant differences between the docetaxel treated and untreated groups were detected as early as 24 h after treatment by bioluminescence imaging, whereas caliper measurements were unable to detect a difference for 4–5 additional days. The results from this study are highlighted in figure 3.6, where increasing luminescence is observed upon increasing docetaxel concentration.[11]

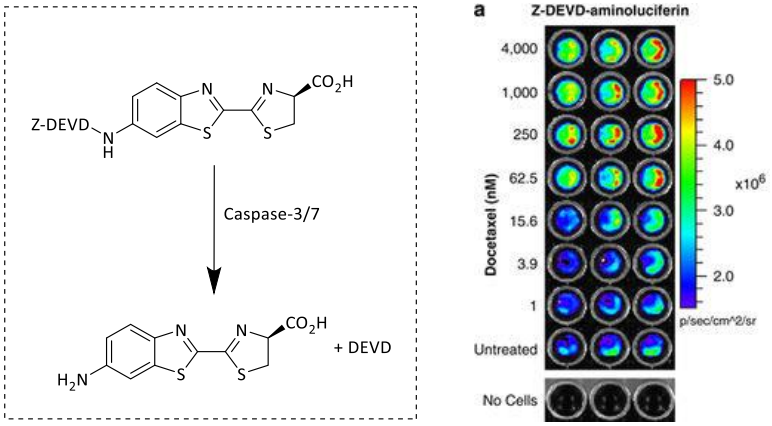

Figure 3.6. VivoGlo® modified aminoluciferin substrate for monitoring caspase-3/7 activity

This report suggests that in vivo imaging of apoptosis using Z-DEVD-aminoluciferin could provide a sensitive and rapid method for early detection of drug efficacy, with potential applications in pre-clinical therapeutic programs. Similarly, various other luciferin amides have been used as substrates for fatty acid amide hydrolase (FAAH). These luciferin amides reportedly enable highly sensitive and selective bioluminescent detection of FAAH activity in vitro and in vivo. The potency and tissue distribution of FAAH inhibitors can be imaged in live mice, and luciferin amides serve as exemplary reagents for greatly improved bioluminescence imaging in FAAH-expressing tissues such as the brain.[12] Other interesting analogues formed from nitroluciferin were demonstrated to be active substrates for specific reductase enzymes that reduced the nitro moiety to form luminescent active aminoluciferin.[13] In a study concerning the imaging of cell-cell contacts a nitroluciferin derivative, Luntr, was used to measure bacterial nitroreductase (NTR) activity in cells.[13] Some of the results from this study are highlighted in figure 3.7.

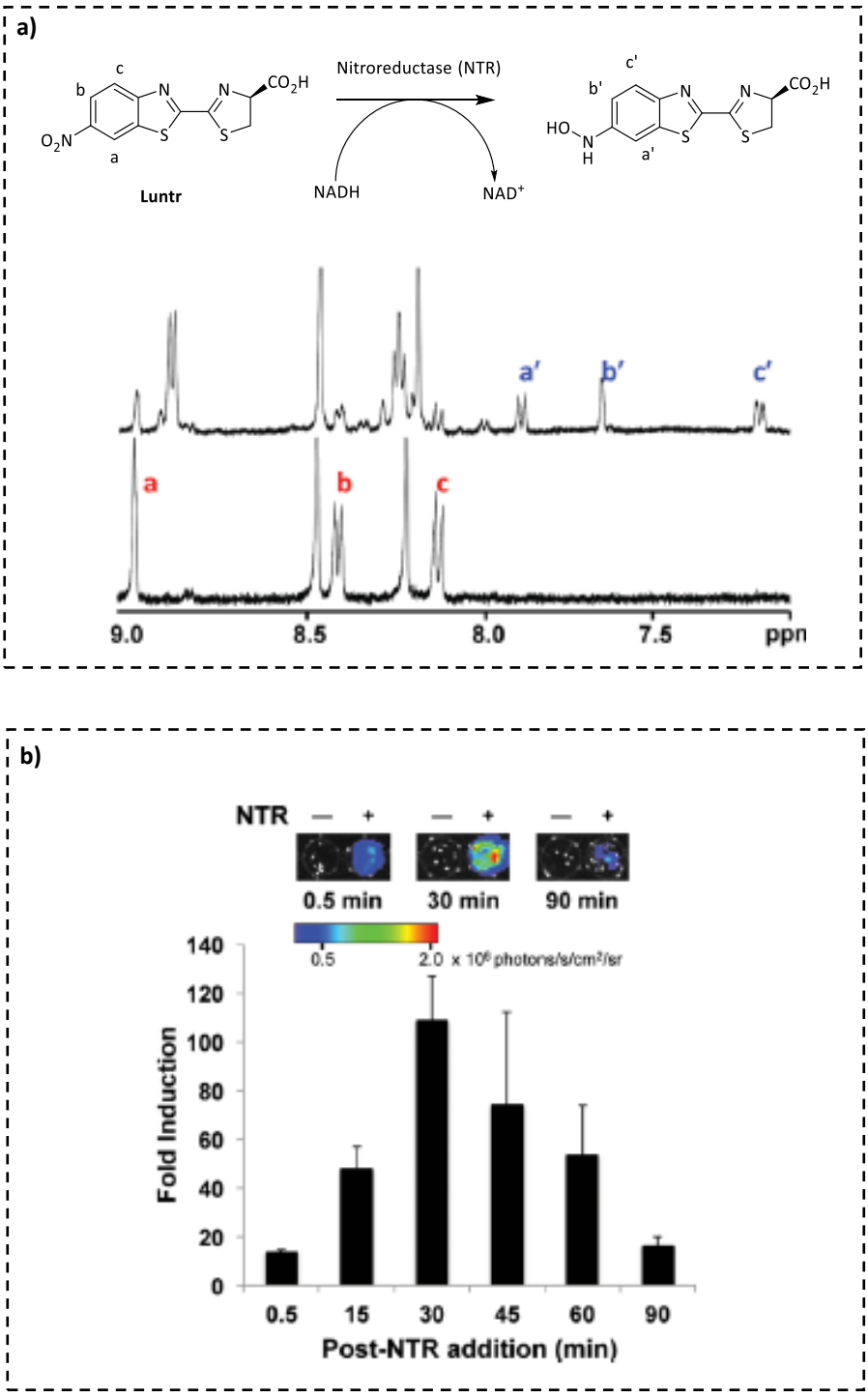

Figure 3.7. NTR-mediated reduction of Luntr produces a light-emitting luciferin; a) ^{1}H-NMR spectra of Luntr combined with NTR and NADH in deuterated PBS, b) Luntr was incubated with NADH in the presence (+) or absence (-) of NTR for 0−90 min and a graph that demonstrates the fold induction in bioluminescent signal (from reporter vs control cells) is displayed

There are many other examples of D-aminoluciferin based probes, most of which are recognised and hydrolysed by aminopeptidase to produce luminescence. Figure 3.8 shows the first examples of bioluminescent probes for imaging aminopeptidase activity in deep tissue and living cells.[14]

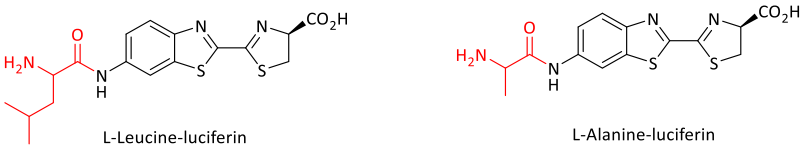

Figure 3.8. Structures of aminoluciferin aminopeptidase probes

All of the probes reviewed here and, for the most part, luciferin probes in general are designed to be substrates for enzymes that are of interest because of their dysregulation as a result of a diseased or abnormal state. For example, studies have shown that aminopeptidase is clearly dysregulated in numerous human malignancies, mainly solid tumours.[15] Thus aminopeptidase has been identified as a potential biomarker for anticancer therapy.

In the previously described reductase probe it was noted that the reductase activity is coupled to NADH/NAD^+ status, which in turn is closely associated with redox imbalances related to oxidative stress. A non-specific or specific reductase probe is therefore of interest in monitoring oxidative stress which is significantly increased in diseased cells and disordered states.

Similarly, the Promega Caspase-3/7 probe was designed to monitor changes in the enzyme activity of the Caspase enzymes whose up-regulation is linked to increased oxidative stress and an associated redox imbalance.

It should now be apparent that the various probes are in fact also sensors for redox imbalance, although they are designed to monitor the affected downstream enzymes and analytes. Interestingly, an aminoluciferin probe that directly monitors changes in redox status has yet to be reported. Linking aminoluciferin luminescence, or even D-luciferin luminescence, to the direct measurement is therefore of interest. However, the functional groups (-OH, $-NH_2$) that would be used to link luminesce offer very limited access to redox chemistry, which is more synonymous with the thiol functionality (-SH). In any case, exploration of aminoluciferin applications in such a way would require ready access to D-aminoluciferin which, because of its synthetic preparation, makes its use in synthetic probe development relatively costly.

Although D-aminoluciferin clearly offers many advantageous over the D-luciferin parent, its cost is equally prohibitively expensive. The cost of course is associated with the synthetic routes used to prepare D-aminoluciferin, many of which have been noted as relatively low yielding.

Review on the synthesis of D-aminoluciferin

The first synthetic route toward D-aminoluciferin differed significantly from that reported by White et al for D-luciferin. The synthesis involved the formation of 6-amino-2-cyanobenzothiazole **3.7** (Scheme 3.3 a) from the substitution of a 2-chloro precursor **3.5** with cyanide. It is not explicitly stated why the D-luciferin synthetic sequence was not or could not be used to prepare D-aminoluciferin, but it can reasonably be assumed that it concerned the relatively more reactive C6-amine.

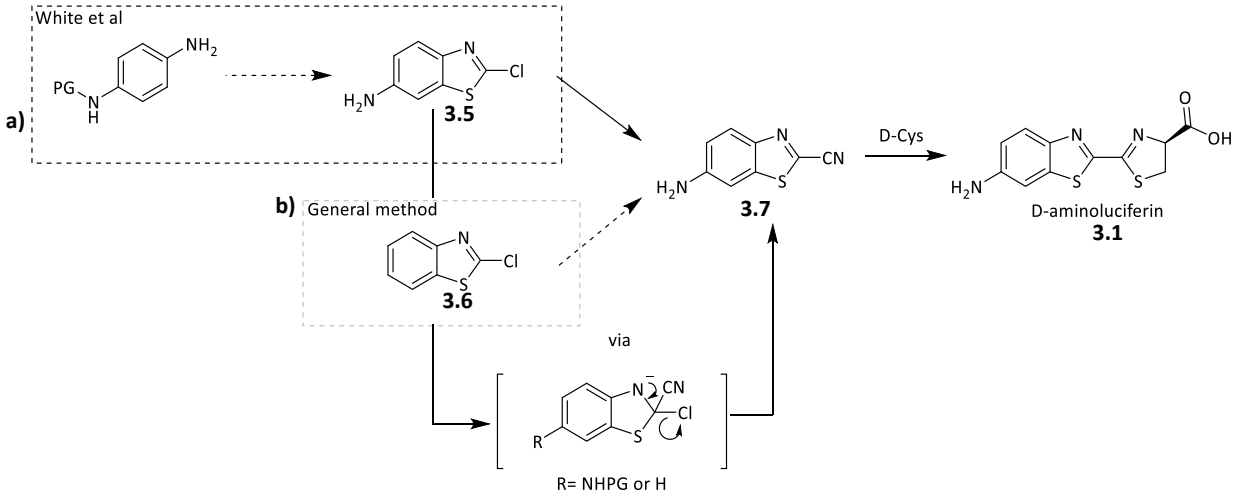

Scheme 3.3. Synthesis of 6-amino-2-cyanobenzothiazole

Most of the reported synthesis of 2-cyanobenzothiazoles make use of a C2-chloro intermediate which reacts in the presence of cyanide to afford the 2-cyanobenzothiazole (scheme 3.3 b). This reaction works particularly well with C6-nitrobenzothiazoles (Scheme 3.4), since the nitro functionality is able to better facilitate chloro substitution by stabilising the resultant Meisenheimer-like complex.

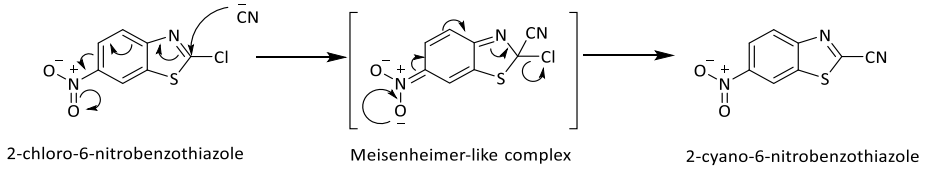

Scheme 3.4. Proposed mechanism for C6-nitro mediated substitution of C2-chloro-6-nitrobenzothiazole by cyanide

A US patent reported the preparation and applications of D-aminoluciferin, prepared via the regioselective nitration of an unsubstituted benzothiazole **3.8** and its subsequent conversion into an ethyl ester (scheme 3.5). [16]

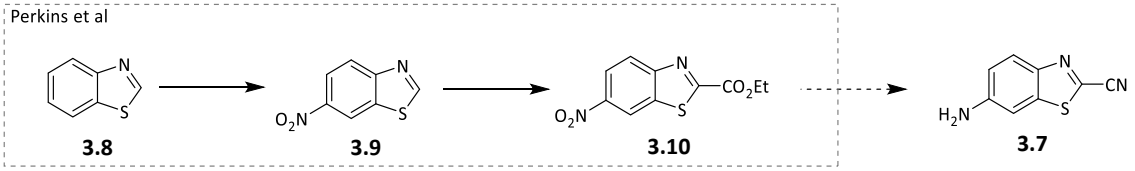

Scheme 3.5. Perkins et al synthesis of D-aminoluciferin

The ester **3.10** was converted to an amide which then underwent dehydration to afford the C-2 nitrile. Thereafter, chemoselective reduction of the nitro group afforded the 6-amino-2-cyanobenzothiazole molecule **3.7**, to which D-cysteine was added to generate D-aminoluciferin.[16] Interestingly, at the time, there were no reports on the use of the Appel's salt methodology in the context of an aminoluciferin synthesis. However, its use in the synthesis of D-nitroluciferin **3.14** was later demonstrated by Prescher et al, as shown in scheme 3.6 a. Prescher et al, who first used the Appel methodology to prepare D-luciferin later reported on the synthesis of a nitroluciferin **3.14** for imaging cell-cell contacts. The nitrobenzothiazole **3.13** was formed from the cyclisation of cyanoformanilide **3.12**, which in turn was formed, in one-pot, from *p*-nitroaniline **3.11**.[13] Prescher et al also reportedly replaced the fragmenting base DBU, with the less nucleophilic sodium thiosulfate which resulted in an increased overall yield of 50 % for both D-luciferin and eventually D-aminoluciferin.[17]

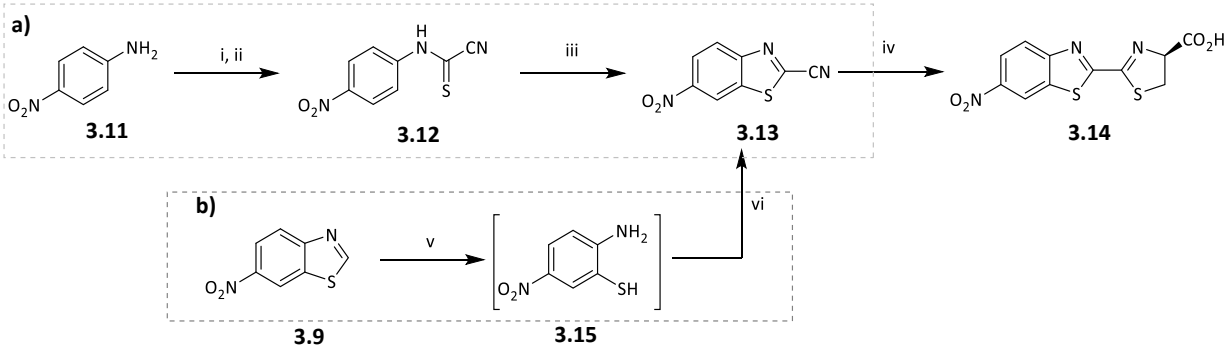

Scheme 3.6. Reagents and conditions: i) Appel's salt/ (1:2) THF:CH_3CN, ii) $Na_2S_2O_3$ (3 eq) / H_2O / rt / 3 h (80 %), iii) $PdCl_2$ / CuI / TBAB / (1:1))DMF:DMSO / 130 °C / 3 h (74 %), iv) D-Cys / K_2CO_3 / CH_3CN:H_2O (2:1) / rt / 2 h (100 %), v) $NH_2NH_2{\cdot}H_2O$ / EtOH / rt / 12 h, vi) Appel's salt / DCM / reflux / 12 h (62 %)

A follow up publication then reported on a new scalable one-pot method which made use of the condensation of 1,2-aminothiophenol **3.15** (generated in situ from the iminolysis of **3.9**) and Appel's salt to form the 2-cyano-6-nitrobenzothiazole **3.13** directly, as shown in scheme 3.6 b.[17]

It is worth noting that the metal-free scalable method developed by McCutcheon and Prescher et al for D-aminoluciferin (Scheme 3.6 b) was markedly different from the scalable procedure developed for D-luciferin (described in Chapter 2, shown in scheme 3.7).

This was because the methodology that was used for D-luciferin synthesis mechanistically involved a thermolytic electrocyclisation reaction, which only produces the 2-cyanobenzothiazole when the C6-substituent is electron donating in character.[18-20] The same reaction could thus not be used to prepare 2-cyano-6-nitrobenzothiazole **3.13**.

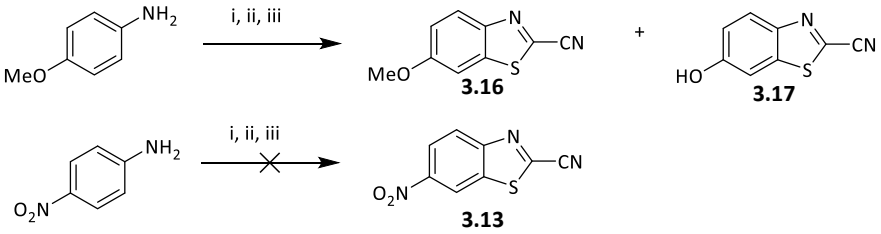

Scheme 3.7. Reagents and conditions: i) Appel's salt / Sulfolane / 40 °C / 3 h, ii) 180 °C / 20 min, iii) PyHCl (10 eq) / 180 °C / 1 h, (**3.16**: 21 %, **3.17**: 51 %)

The toxicity of the cyanide routes and the limitations associated with Appel's salt methodologies meant that there was indeed scope for an improved D-aminoluciferin synthesis and, perhaps, for the development of a more general, scalable route that would allow equally efficient access to both D-luciferin and D-aminoluciferin.

With this in mind, it was decided to first evaluate the previously used D-luciferin synthetic route (described in Chapter 2) to also prepare D-aminoluciferin, since the same method was already reported in the preparation of D-nitroluciferin by Prescher et al.

Aims and Objectives

The aim was to synthesise D-aminoluciferin and, thereafter, to evaluate the bioluminescence of the synthesised material, whilst also investigating whether any improvements could be made to the reported synthetic procedure.

The specific objectives were thus:

i) The synthesis and characterisation of D-aminoluciferin using standard analytical and spectroscopic techniques, including; NMR, MS, IR and melting point analyses.

ii) The bioluminescent evaluation of prepared D-aminoluciferin using purified luciferase enzyme assays.

iii) The identification of key limiting steps in the synthetic sequence where an improvement could result in an improved overall yield and a more efficient synthesis.

Synthesis and Bioluminescent Evaluation of D-Aminoluciferin

Synthesis of D-aminoluciferin

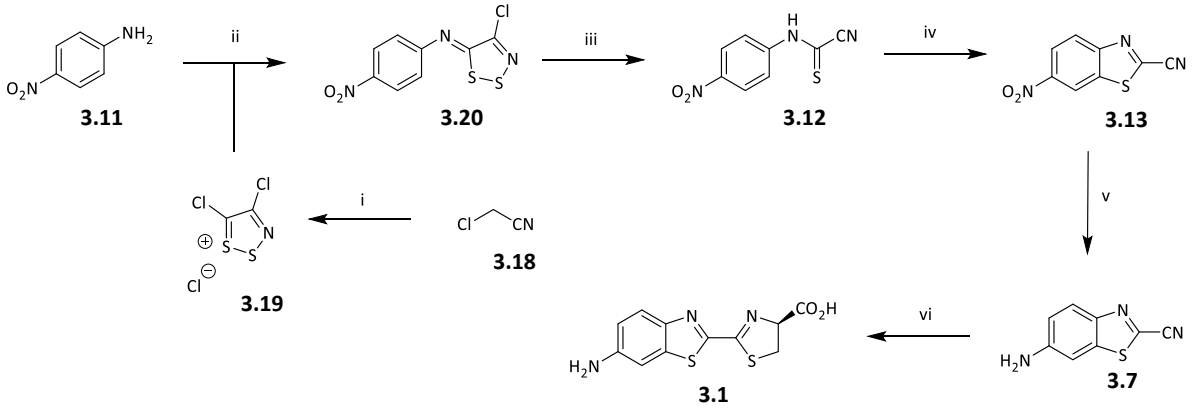

Scheme 3.8. Reagents and conditions: i) S_2Cl_2 / DCM / rt / 24 h, ii) Appel's salt / DCM / Py / rt / 4 h, iii) DBU / DCM / 5 ^oC / 30 min, iv) $PdCl_2$ / CuI / TBAB / DMF:DMSO (1:1) / 120 ^oC / 4 h, v) Zn / NH_4Cl / MeOH / rt / 20 min, vi) D-Cys / K_2CO_3 / MeOH:H_2O / 20 min

D-Aminoluciferin was initially prepared similarly to D-luciferin whereby *p*-nitroaniline **3.11** was reacted with Appel's salt **3.19** to afford a dithiazolimine **3.20**, which further underwent base mediated fragmentation to yield the cyanoformanilide **3.12**. The key difference in the synthesis of D-aminoluciferin and the nitroluciferin synthesis by Prescher et al was the use of DBU to fragment the dithiazolimine instead of sodium thiosulfate, all other reactions were performed as previously described. Intra-molecular cyclisation and subsequent chemoselective reduction afforded the 6-amino-2-cyanobenzothiazole core **3.7** and, as before, D-Cys addition to the cyanobenzothiazole generated D-aminoluciferin **3.1**.

Of note in the synthesis of D-aminoluciferin, was that the formation of the nitrodithiazolimine **3.20** was much slower when compared to the methoxydithiazolimine formed from *p*-anisidine. The fragmentation reaction also differed significantly from what was observed in the D-luciferin synthesis, as the major product formed from this reaction was not the desired product **3.12**, but possibly an intermediate DBU adduct (characterised by MS and ^{1}H-NMR spectroscopy). The DBU adduct made isolation of the fragmented product challenging and prompted an investigation into alternative bases for fragmentation (detailed in chapter 5). Key signals were inspected for in the analysis of the NMR spectra of **3.20** and **3.12**. The carbon resonances in the ^{13}C-NMR spectrum of **3.20**, observed at 145 and 157 ppm, were diagnostic of successful dithiazolimine formation. In the subsequent fragmentation of the imine **3.20** to the cyanoformamide **3.12** (figure 3.9), a significant shift for C-6 was observed in the product relative to the starting material (from 157 ppm to 114 ppm). This corresponded to the conversion of the sp^2 imine carbon to the more shielded sp^3 nitrile.

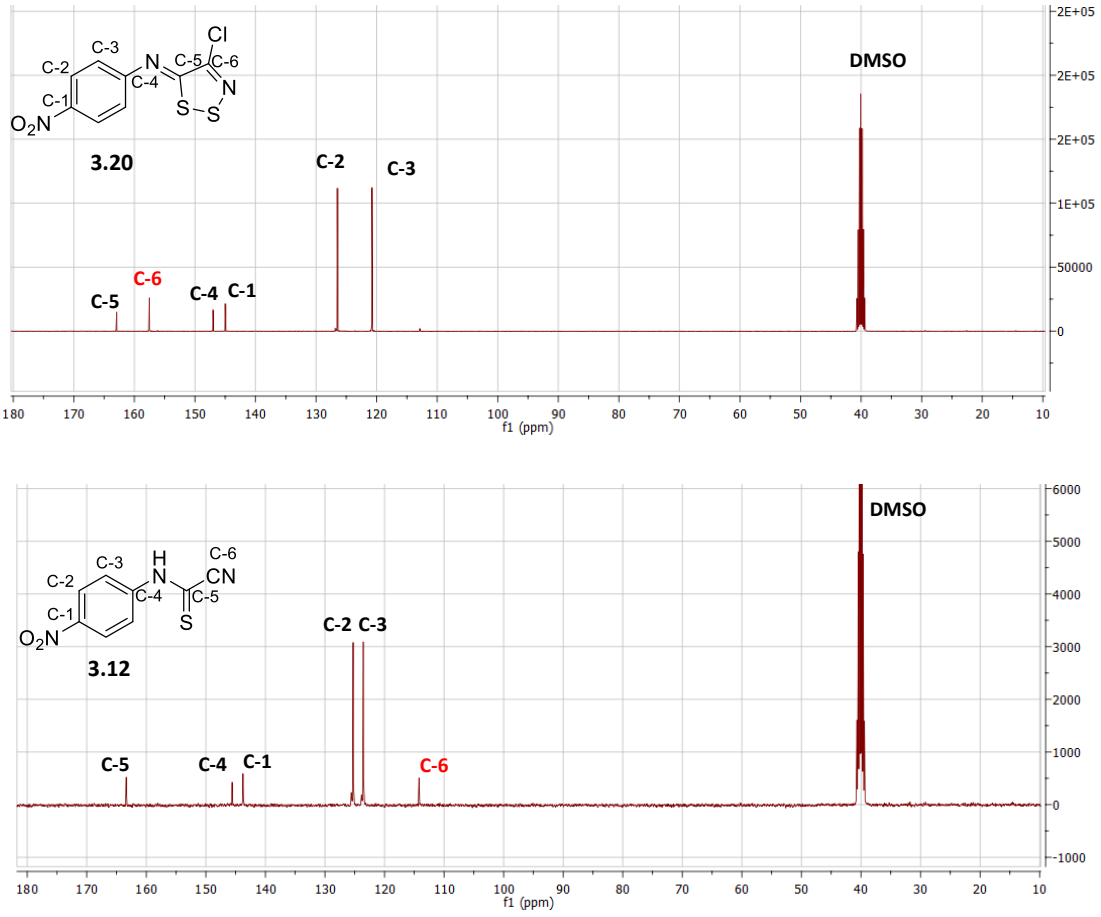

Figure 3.9. ^{13}C-NMR spectra of nitrodithiazolimine **3.20** and nitrocyanoformamide **3.12** in DMSO

The palladium chloride/copper iodide intramolecular C-S cross-coupling reaction that afforded the nitrocyanobenzothiazole worked, as expected, with the nitrocyanoformamide substrate. However, the product was only formed upon increasing the amounts of palladium(II) and copper(I) added (from the reported 10 and 50 % to 20 and 100 %, respectively). The ^{1}H-NMR spectrum of **3.13** (Figure 3.10) showed the expected three proton resonances and the ^{13}C-NMR spectrum displayed the expected eight carbon signals, with a conspicuous signal at 112.5 ppm (C-8) due to the conserved nitrile moiety.

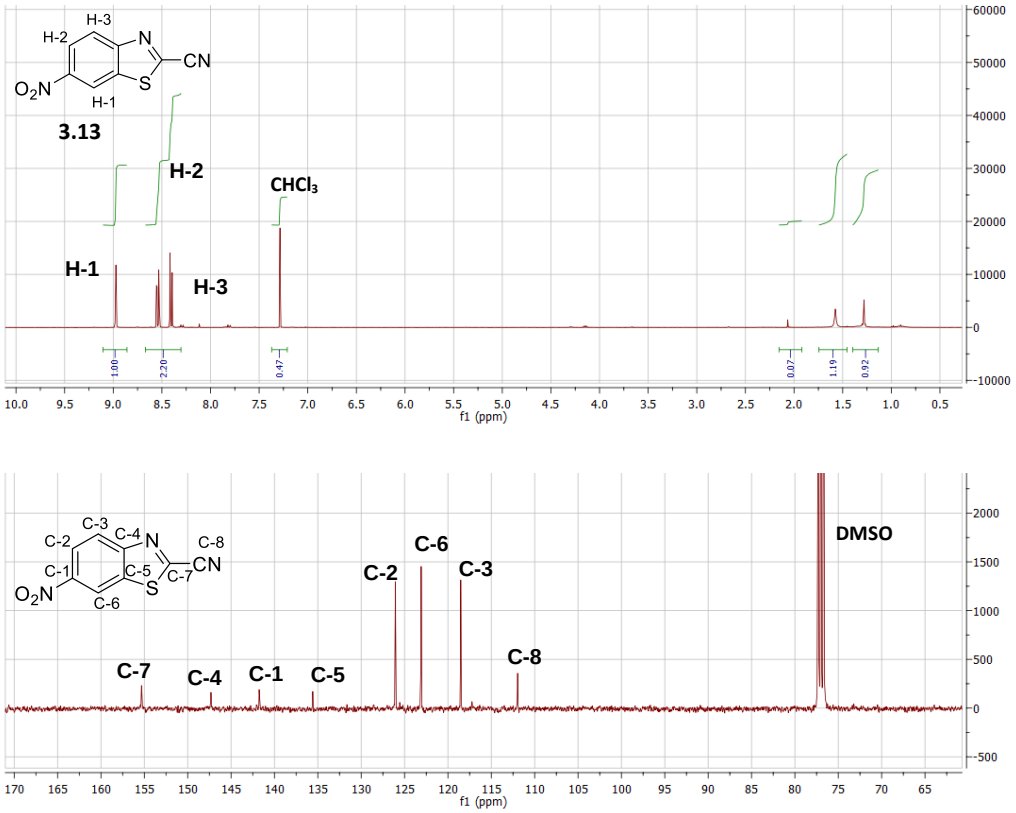

Figure 3.10. ^{1}H- and ^{13}C-NMR spectra of 2-cyano-6-nitrobenzothiazole **3.13** in $CDCl_3$ and DMSO, respectively

Supplementary support for the formation of **3.12** was found in its mass spectrum which displayed a base peak that corresponded to the molecular weight of **3.13** (*m/z* 204.9715, corresponding to M^{+}). The nitro group then had to be chemo-selectively reduced to the amine. To this end, two methods were used, the first of which made use of a solution of $SnCl_2$ in HCl and EtOH. This reaction afforded the desired product, but in very low yield, presumably due to the hydrolysis of the nitrile functionality. The second method proved to be milder and more efficient, resulting in the isolation of the amine in high yield (>95 %). The second method involved stirring the nitrobenzothiazole in a mixture of Zn powder and NH_4Cl in MeOH. The reaction also proved to be much faster, with complete consumption of the starting material within twenty minutes, as evidenced by TLC analysis. Interestingly, the ^{1}H-NMR spectrum of the reduced product **3.7** (figure 3.11) displayed a second set of mirroring aromatic resonances (H-1', H-2', and H-3'), despite TLC analysis having suggested the isolation of one

supposedly pure product. These extra signals did not correspond to starting material, nor were they expected to since TLC analysis of the reaction had revealed total consumption of the starting material.

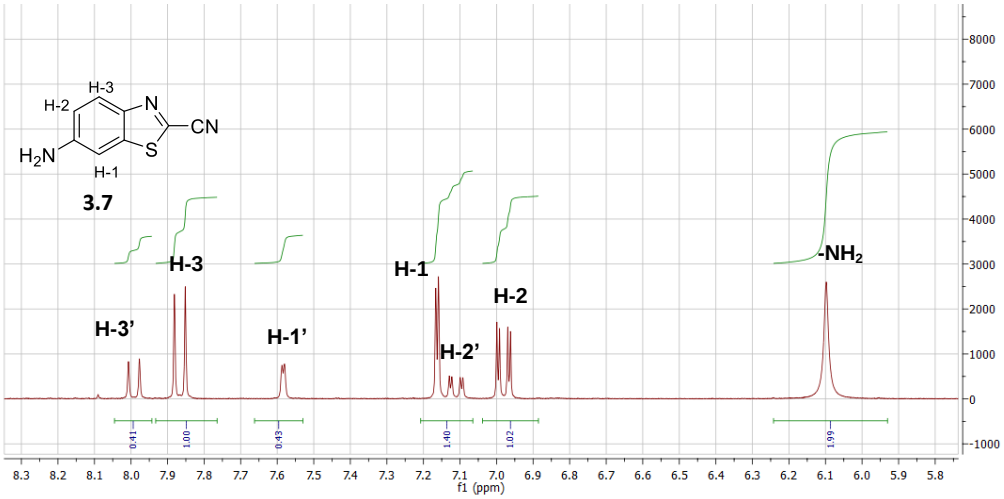

Figure 3.11. ^{1}H-NMR spectrum of 6-amino-2-cyanobenzothiazole **3.7** in DMSO

The mass spectrum of the compound displayed a mass ion peak corresponding to the molecular weight of 6-amino-2-cyanobenzothiazole **3.7** (*m/z* 176.0115, corresponding to [M+H]) and LCMS studies also supported that the reaction had indeed gone to completion, since a single elution band (not corresponding to starting material) was observed. It was proposed that the doubling signals were perhaps due to the formation of an ammonium salt or as a result of incomplete reduction to the hydroxylamine. This was further reinforced when the elemental analysis was carried out, where differences in the calculated and experimental percentages were observed. The elemental analysis of **3.7** was not in agreement with what was expected, and therefore indicated that compound **3.7** was not analytically pure. Despite the obvious doubling of signals observed in the ^{1}H-NMR spectrum of the 2-cyano-6-aminobenzothiazole, the material was used as is (although repeated washes with various bases were carried out in attempt to further purify **3.7**) and reacted with one equivalent of both D-Cys and potassium carbonate to afford the D-aminoluciferin potassium salt. The ^{1}H-NMR spectrum for the D-aminoluciferin potassium salt is shown in figure 3.12 and displays all the signals previously reported by White et al and, gratifyingly, did not display any doubling of aromatic resonances observed previously in the starting material.

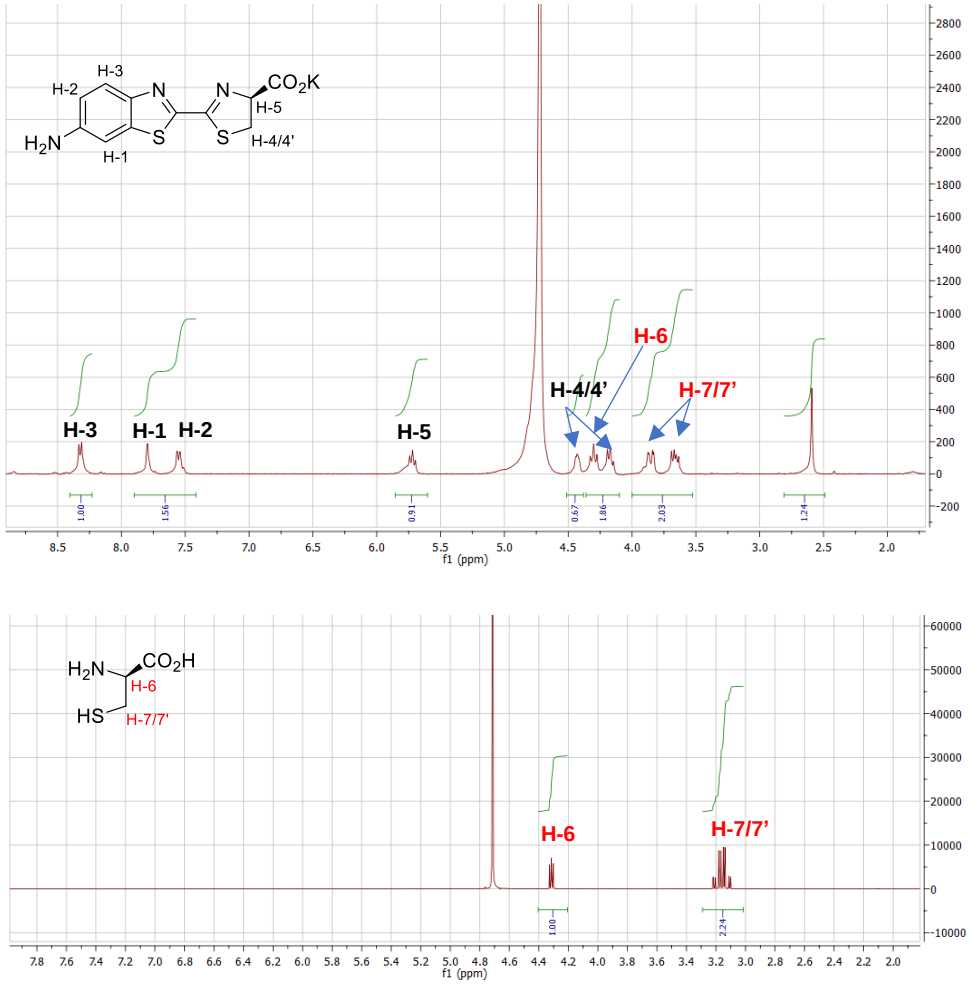

Figure 3.12. ^{1}H-NMR spectra of D-aminoluciferin potassium salt and D-cysteine in D_2O

Unfortunately, unreacted D-Cys was also observed in the NMR spectrum and was reasoned to be the result of having formed the D-aminoluciferin D-Cys ammonium carboxylate salt. This was corrected by resuspending the material in $NaHCO_3$ and extracting with EtOAc to afford pure D-aminoluciferin whose ^{1}H-NMR spectrum is shown in figure 3.13.

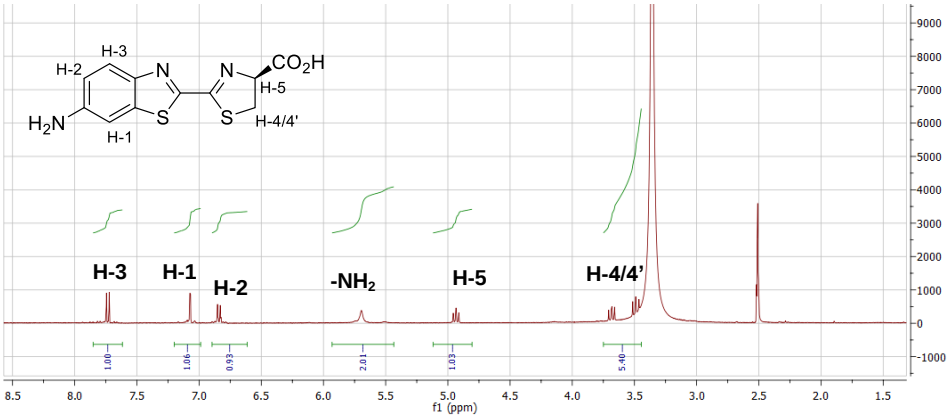

Figure 3.13. ^{1}H-NMR spectrum of D-aminoluciferin **3.1** in DMSO

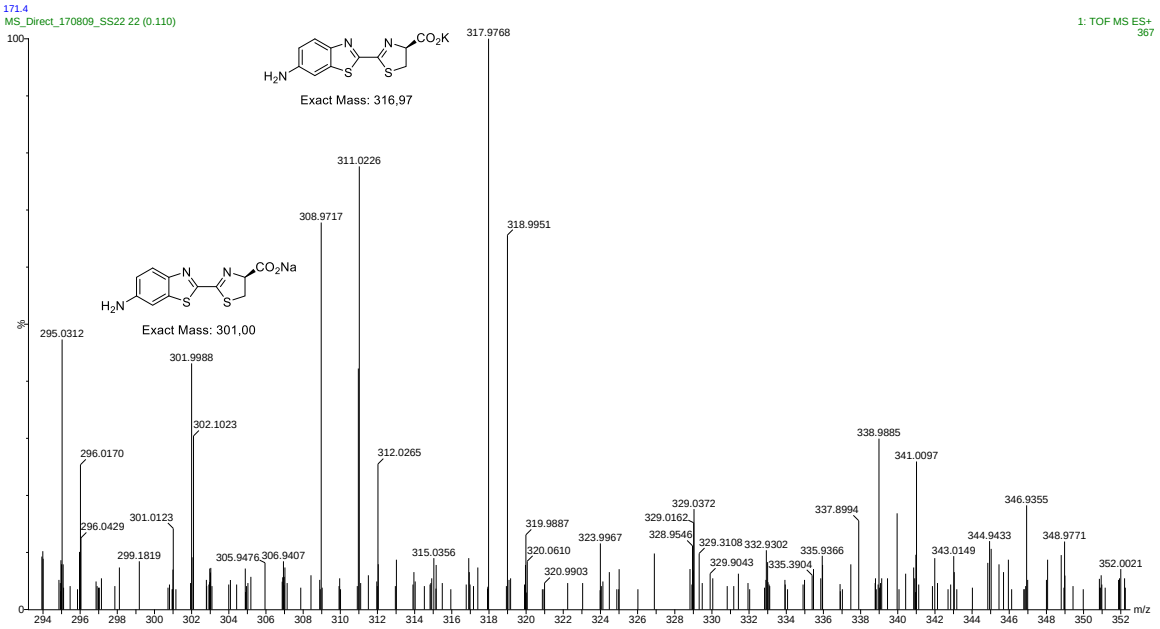

Figure 3.14. HRMS trace of D-aminoluciferin

Further support for the successful synthesis of D-aminoluciferin was provided by the ^{13}C-NMR which displayed the expected 11 signals and the mass spectrum which displayed a mass ion at *m/z* 317.9768 corresponding to [M+K] (calculated 317.9768). D-aminoluciferin was produced in an overall yield of 20 % using the modified Prescher et al sequence utilised in the prior D-luciferin synthesis.

Prescher et al Improved Syntheses; scalable but not general

As previously stated, the low overall yield was largely as a result of the low yielding C-S coupling reaction. McCutcheon and Prescher et al have since developed an improved scalable one-pot method that does not make use of a Pd-catalysed C-S coupling reaction (discussed in Chapter 2).[17] However, the reaction reportedly does not allow for the cyclisation of anilides containing electron withdrawing substituents and therefore could not be made use of as an alternative synthetic strategy for D-aminoluciferin synthesis.

These findings suggest that the development of a more general route that negates the use of traditional C-S oxidative couplings would indeed be of interest and should be further explored.

Bioluminescent Evaluation of D-aminoluciferin

The synthesised D-aminoluciferin was evaluated for bioluminescence using purified luciferase in the same manner that D-luciferin was evaluated in the preceding Chapter.

The synthesised D-aminoluciferin was reacted with luciferase and the resultant luminescence measured. The results from the assay are highlighted in figure 3.15.

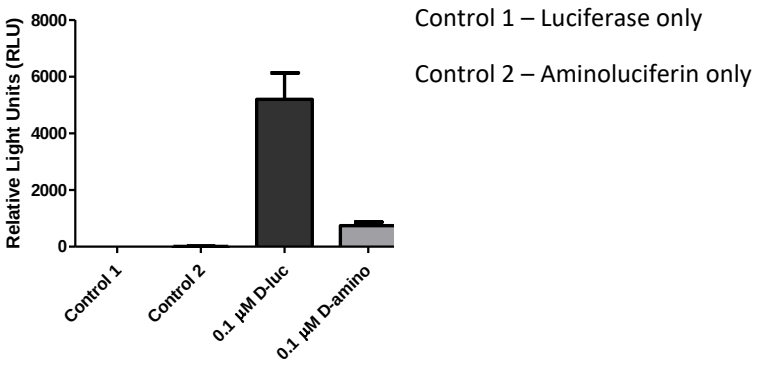

Figure 3.15. Bioluminescence emission of D-luciferin and D-aminoluciferin. The RLU were determined 1 min post-enzyme addition and were recorded in triplicate and are represented as the mean ± SEM

Control 1 contained only 90 µL of 10 nm luciferase in its enzyme buffer and control 2 contained 90 µL of 0.1 µM D-aminoluciferin in substrate buffer. In both instances the resultant luminescence recorded was negligible. However, a strong luminescent response was observed upon injecting 30 µL of 10 nm luciferase in luciferase enzyme buffer to 60 µL of 0.1 µM D-luciferin and 0.1 µM D-aminoluciferin. As expected the light emission intensity observed for the natural D-luciferin was found to be 5-fold higher relative to that of D-aminoluciferin and, as previously discussed, is not due to lower binding affinity, but rather as a result of the reaction's lower light emitting efficiency.

Since D-aminoluciferin had a reportedly longer wavelength of emission, it was also necessary to record its observed λ_{max} to ensure that it corresponds to the λ_{max} previously reported. This was done using a fluorimeter which records the emission wavelength of light emitted in the D-aminoluciferin/ luciferase reaction. Normally fluorimeters are used to measure fluorescence emission in response to excitation. However, in the case of bioluminescence emission spectra, the excitation slits required to irradiate a particular sample are sealed off, and the resultant luminescence is recorded in the absence of an excitation signal. This was done for D-aminoluciferin as well as D-luciferin as a reference.

To record the emission spectrum, purified luciferase in enzyme buffer was rapidly injected into a cuvette containing D-aminoluciferin in substrate buffer to a final enzyme concentration of 100 nM and a final substrate concentration of 10 µM. The peak emission (measured from 200 to 800 nm) was recorded and the resultant bioluminescence emission spectrum of D-aminoluciferin, along with D-luciferin for reference is shown in figure 3.16. Peak bioluminescence emission for D-aminoluciferin was observed at 595 nm while peak emission for D-luciferin at 550 nm. The observed λ_{max} for both D-aminoluciferin and D-luciferin were found to be in good agreement with those previously reported and further confirms the successful preparation of the amino analogue.

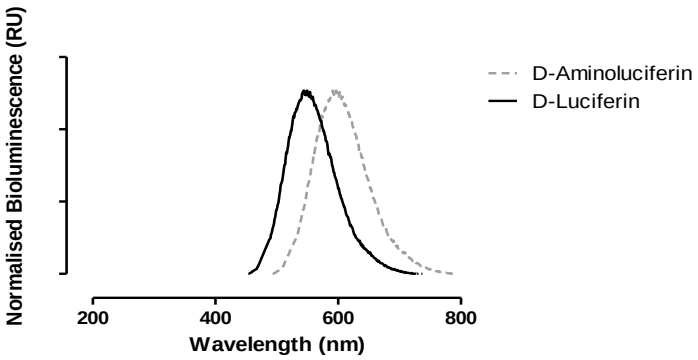

Figure 3.16. Bioluminescence emission spectrum of D-luciferin and D-aminoluciferin in pH 7.4 Tris buffer

Summary: D-luciferin and D-aminoluciferin, what next?

The synthesis of D-aminoluciferin was achieved in six steps with a 20 % overall yield. Again, the metal mediated cyclisation to form the benzothiazole was limiting and an alternative methodology for forming the benzothiazole from the thioanilide would be advantageous. In terms of its luminescent properties, the synthesised D-aminoluciferin was found to be luminescent active when treated with luciferase and hence, pure D-aminoluciferin had been successfully prepared and was now primed for use as a luminescent standard.

With both the 6'-hydroxy and 6'-amino luciferins in hand, focus was shifted to two main goals; the first being the potential preparation of a 6'-thio analogue of D-luciferin, of which there was surprisingly not a reported synthesis or bioluminescent data. The premise for this undertaking concerned the previously noted knowledge gap in directly linking luminescence and sulfur-related redox chemistry. Of course, there were other reasons for attempting to synthesise 6'-thio derivatives of D-luciferin, all of which are described in the relevant Chapters.

The second goal concerned the consistently low yielding C-S oxidative coupling employed in the D-luciferin and D-aminoluciferin syntheses. Prescher et al had already demonstrated that the overall D-luciferin synthesis could be improved using their latest scalable one-pot methodology, which avoided the use of the palladium mediated intramolecular C-S coupling oxidative coupling reaction. However, that methodology was exclusive to the D-luciferin synthesis and could not be used to construct D-aminoluciferin.

After some deliberation, it was predicted that both the low yielding intramolecular C-S oxidative coupling and the Prescher et al scalable one-pot method could be improved, so that the low yielding C-S coupling would be higher yielding and that the Prescher et al scalable method could be applied to D-aminoluciferin synthesis. Moreover, it was predicted that both these improvements would be brought about by the same chemistry, namely *ortho*-bromination.

References

1. Walter, K.; Schutt, C., Methods of enzymatic analysis. *New York: Academic* **1974,** *2*, 856-864.
2. Kaskova, Z. M.; Tsarkova, A. S.; Yampolsky, I. V., 1001 lights: luciferins, luciferases, their mechanisms of action and applications in chemical analysis, biology and medicine. *Chemical Society Reviews* **2016,** *45* (21), 6048-6077.
3. Li, J.; Chen, L.; Du, L.; Li, M., Cage the firefly luciferin!–a strategy for developing bioluminescent probes. *Chemical Society reviews* **2013,** *42* (2), 662-676.
4. Meroni, G.; Rajabi, M.; Santaniello, E., D-Luciferin, derivatives and analogues: synthesis and in vitro/in vivo luciferase-catalyzed bioluminescent activity. *Arkivoc* **2009,** *1*, 265-288.
5. White, E. H.; Wörther, H.; Seliger, H. H.; McElroy, W. D., Amino Analogs of Firefly Luciferin and Biological Activity Thereof1. *Journal of the American Chemical Society* **1966,** *88* (9), 2015-2019.
6. Shinde, R.; Perkins, J.; Contag, C. H., Luciferin derivatives for enhanced in vitro and in vivo bioluminescence assays. *Biochemistry* **2006,** *45* (37), 11103-11112.
7. Denburg, J. L.; Lee, R. T.; McElroy, W., Substrate-binding properties of firefly luciferase: I. Luciferin-binding site. *Archives of biochemistry and biophysics* **1969,** *134* (2), 381-394.
8. Reddy, G. R.; Thompson, W. C.; Miller, S. C., Robust light emission from cyclic alkylaminoluciferin substrates for firefly luciferase. *Journal of the American Chemical Society* **2010,** *132* (39), 13586-13587.
9. Wu, W.; Su, J.; Tang, C.; Bai, H.; Ma, Z.; Zhang, T.; Yuan, Z.; Li, Z.; Zhou, W.; Zhang, H., cybLuc: an effective aminoluciferin derivative for deep bioluminescence imaging. *Analytical chemistry* **2017,** *89* (9), 4808-4816.
10. Biserni, A.; Roncoroni, C.; Kirkland, T.; Klaubert, D.; Maggi, A.; Ciana, P., A novel tool to study apoptosis in living mice. AACR: 2010.
11. Hickson, J.; Ackler, S.; Klaubert, D.; Bouska, J.; Ellis, P.; Foster, K.; Oleksijew, A.; Rodriguez, L.; Schlessinger, S.; Wang, B., Noninvasive molecular imaging of apoptosis in vivo using a modified firefly luciferase substrate, Z-DEVD-aminoluciferin. *Cell Death & Differentiation* **2010,** *17* (6), 1003-1010.

12. Mofford, D. M.; Adams Jr, S. T.; Reddy, G. K. K.; Reddy, G. R.; Miller, S. C., Luciferin amides enable in vivo bioluminescence detection of endogenous fatty acid amide hydrolase activity. *Journal of the American Chemical Society* **2015,** *137* (27), 8684-8687.
13. Porterfield, W. B.; Jones, K. A.; McCutcheon, D. C.; Prescher, J. A., A "Caged" Luciferin for Imaging Cell–Cell Contacts. *Journal of the American Chemical Society* **2015,** *137* (27), 8656-8659.
14. Li, J.; Chen, L.; Wu, W.; Zhang, W.; Ma, Z.; Cheng, Y.; Du, L.; Li, M., Discovery of bioluminogenic probes for aminopeptidase N imaging. *Analytical chemistry* **2014,** *86* (5), 2747-2751.
15. Miyoshi, N.; Ishii, H.; Nagano, H.; Haraguchi, N.; Dewi, D. L.; Kano, Y.; Nishikawa, S.; Tanemura, M.; Mimori, K.; Tanaka, F., Reprogramming of mouse and human cells to pluripotency using mature microRNAs. *Cell stem cell* **2011,** *8* (6), 633-638.
16. Gryshuk, A. L.; Perkins, J.; LaTour, J. V., Methods and systems for synthesis of a D-aminoluciferin precursor and related compounds. Google Patents: 2013.
17. McCutcheon, D. C.; Porterfield, W. B.; Prescher, J. A., Rapid and scalable assembly of firefly luciferase substrates. *Organic & Biomolecular Chemistry* **2015,** *13* (7), 2117-2121.
18. English, R. F.; Rakitin, O. A.; Rees, C. W.; Vlasova, O. G., Conversion of imino-1, 2, 3- into 2-cyanobenzothiazoles, cyanoimidoyl chlorides and diatomic sulfur. *Journal of Chemical Society, Perkin Transactions 1* **1997,** (3), 201-206.
19. Besson, T.; Dozias, M.-J.; Guillard, J.; Rees, C. W., New route to 2-cyanobenzothiazoles via N-arylimino-1, 2, 3-dithiazoles. *Journal of the Chemical Society, Perkin Transactions* **1998,** (23), 3925-3926.
20. Bénéteau, V.; Besson, T.; Rees, C. W., Rapid synthesis of 2-cyanobenzothiazoles from N-aryliminodithiazoles under microwave irradiation. *Synthetic communications* **1997,** *27* (13), 2275-2280.

Chapter 4

Improved Syntheses of 2-Cyanobenzothiazoles

Abstract

Bioluminescence imaging with luciferase–luciferin pairs are popular methods of visualising biological processes in vivo. Unfortunately, most luciferins are difficult to access and remain prohibitively expensive for some imaging applications. The most cited methods of luciferin preparation were found to be generally low yielding and made use of relatively toxic reagents. This chapter concerns the development of scalable and efficient syntheses of C6-substituted 2-cyanobenzothiazoles, precursors to bioluminescent substrates. The proposed methodologies employ easily prepared and inexpensive *ortho*-brominated anilines as starting materials. These anilines are subsequently converted to thioanilides and thereafter cyclised using base-mediated intra-molecular cyclisation reactions to generate the desired 2-cyanobenzothiazoles. Additionally, it is demonstrated that the syntheses of 6-substituted 2-cyanobenzothiazoles can be achieved in one-pot by the stepwise addition of reagents and in the absence of palladium and copper catalysts. It is further demonstrated that these reactions, unlike their metal-based equivalents, are more scalable, have better functional group tolerability and are relatively greener.

Chapter 4

Improved Syntheses of 2-Cyanobenzothiazoles

Introduction

One of the factors limiting the use of D-luciferin based imaging is associated with the cost of commercial D-luciferin. This has been attributed to the difficulty in synthesising the 2-cyanobenzothiazole ring, which forms the D-luciferin core. Thus, an efficient, economical and convenient method for the construction of highly functionalised 2-cyanobenzothiazoles is of interest. Previously, the synthesis of D-luciferin involved a metal mediated C-S cross-coupling reaction to generate the benzothiazole motif. It was previously noted that the palladium, copper co-catalysed cross-coupling reaction was limiting and consistently afforded the benzothiazole in low yield. Furthermore, the metal mediated methodology did not allow for the preparation of C6-halogenated 2-cyanobenzothiazoles and hence motivated an investigation into alternative cyclisation strategies.

Limitations and Shortcomings of Existing Methodologies and Sequences

The syntheses of benzothiazoles in the context of D-luciferin preparation has been limited to two general strategies highlighted in scheme 4.1. The original sequence used by White et al in the first synthesis of D-luciferin involved forming a C2-carboxybenzothiazole derivative from the oxidative cyclisation of a thioanilide. The oxidative cyclisation was metal mediated and generally produced the C2-carboxybenzothiazole in low yield and, in addition, the C6-carboxybenzothiazole had to be further chemically transformed to afford the desired 2-cyanobenzothiazole.[1] A few different routes have been reported since but almost all of them make use of the same general strategy to generate a 2-carboxybenzothiazole derivative that requires further modification to afford the 2-cyano functionality.[2] Prescher et al improved on the original sequence by employing a methodology developed by Rolf Appel and refined by Reese et al.[3]

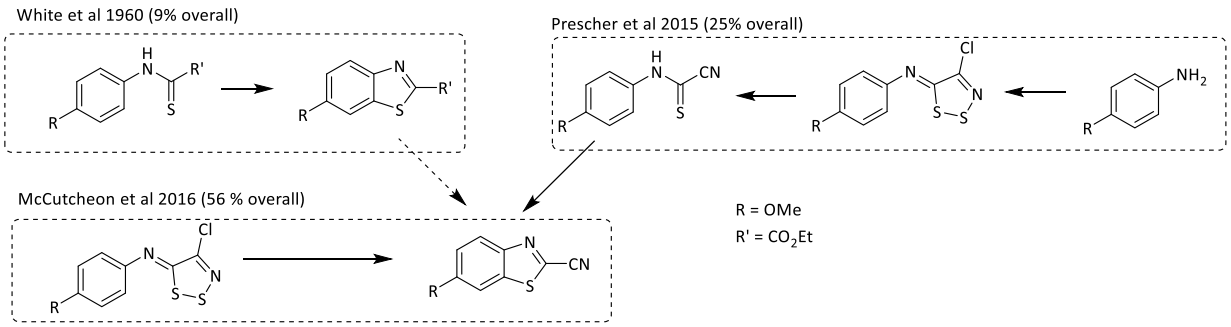

Scheme 4.1. Previous syntheses of the 6-substituted 2-cyanobenzothiazole core

This method involved fragmenting *N*-aryldithiazolimines to afford cyanoformanilides which directly produced 2-cyanobenzothiazoles when cyclised. The cyclisation step however, is equally low yielding and makes use of palladium(II) and copper(I) catalysts. McCutcheon and Prescher et al then further refined that sequence and recently reported a condensed and improved methodology which completely negated the use of metal catalysts for the cyclisation, instead employing a thermolytic cleavage cyclisation reaction.[4] In this way, they were able to report the successful synthesis of a 2-cyanobenzothiazole from an aniline in two steps, with a 50 % overall yield of D-luciferin (one of the highest recorded to date). Similarly, the aim of this study was to move away from the low yielding C-S oxidative couplings and develop an improved and unique cyclisation strategy.

Metal-mediated C-S bond formation

Having confirmed from previous syntheses that the intramolecular C-S bond forming reaction was indeed limiting, potential improvements and alternative reactions were then investigated. The first option considered was to increase the reactivity of the carbon involved in the coupling reaction by substituting it with a bromine, since palladium insertion occurs more readily between the C-Br bond relative to the C-H equivalent, hence improving the overall reaction. This was already demonstrated in a report on the synthesis of 2-substituted-benzothiazoles by palladium-catalysed intramolecular cyclisation of *o*-bromo-phenylthioureas, where yields from various substituted anilides ranged between 68-100 % using a $Pd_2(dba)_3$/monophosphine catalytic system .[5] This *o*-brominated reaction was reported to be an improvement on the unsubstituted system, where palladium activation occurs on a less reactive C-H and yields ranged from 3-78 % while also strictly requiring a copper co-catalyst (Figure 4.1).[6] The bromine allowed for a relatively milder cyclisation, occurring at 80 °C compared to the 120-150 °C in the unsubstituted case and reportedly allowed for copper(I) mediated cyclisation under reflux in DME, in the absence of palladium.[7]

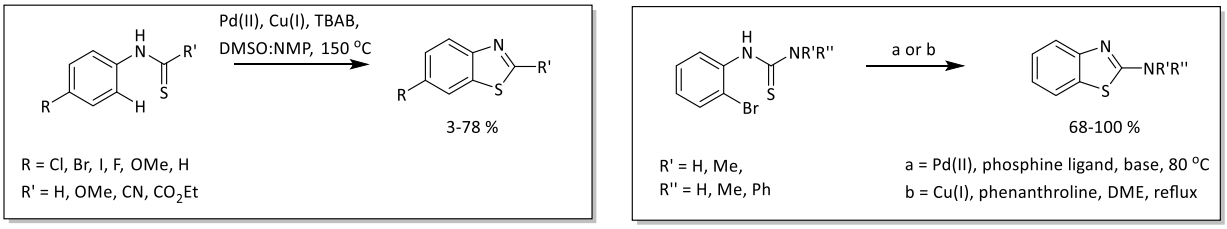

Figure 4.1. Palladium mediated intramolecular C-S cross-coupling reactions.

What was also exciting was that the *o*-bromo intramolecular cyclisation was not previously used to construct 2-cyanobenzothiazoles and thus further prompted the investigation. However, the improved brominated method was still by nature an oxidative coupling and, therefore, meant that it probably was not scalable and that it still maintained a relatively prohibitive cost associated with the palladium catalysts and/or palladium/copper ligands. Accordingly, it was decided that other potential

modes of cyclisation would also be investigated, like the thermolytic electrocyclic cyclisation developed by Charles W. Reese and employed by McCutcheon et al in their scalable luciferin synthesis.

Thermolytic cyclisation of *N*-aryliminodithiazoles for 2-cyanobenzothiazole synthesis

When Prescher et al first synthesised D-luciferin starting from an *N*-aryliminodithiazole formed from Appel's salt they opted to not use the reaction in its original form, instead employing a stepwise approach where the *N*-aryliminodithiazole was fragmented first, and then cyclised using an oxidative coupling reaction. The original transformation is shown in scheme 4.2 which involved heating the *N*-aryliminodithiazole (neat or in solvent) to afford the corresponding 2-cyanobenzothiazole and cyanoimdoyl chloride.[8-10]

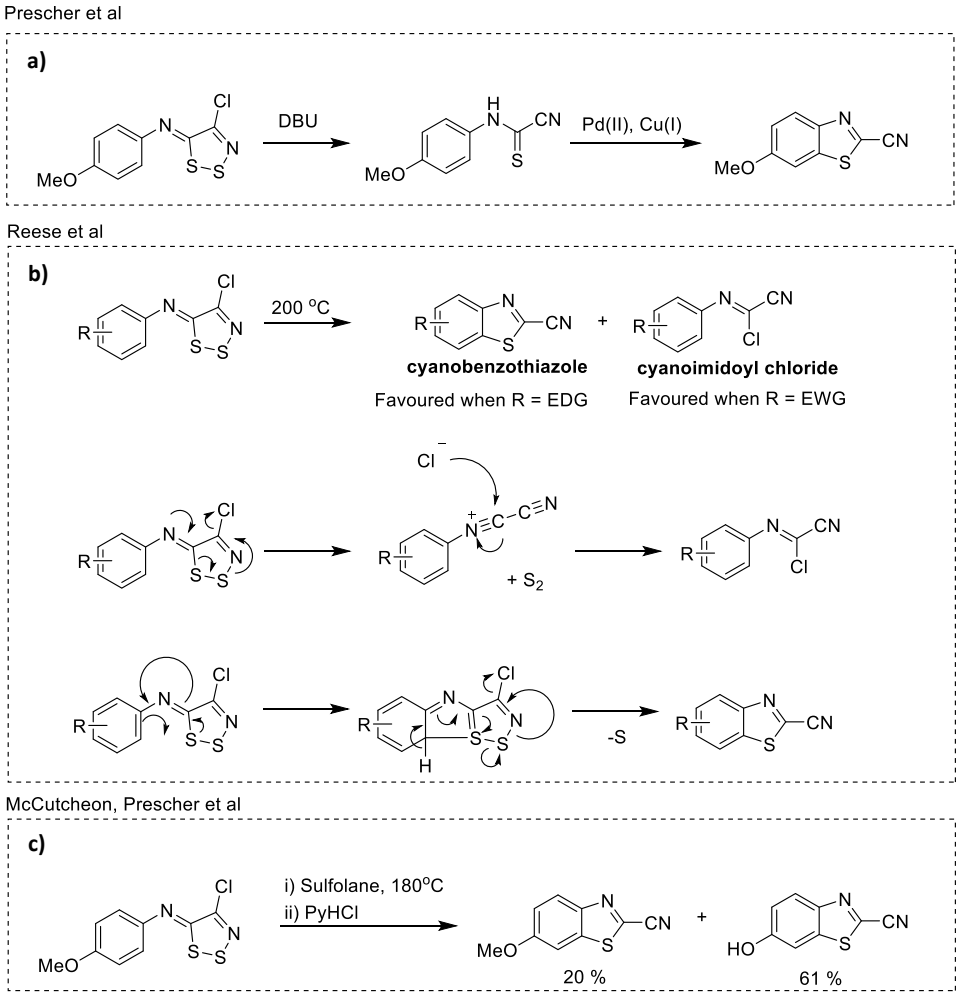

Scheme 4.2. a) The use of a cyanoformanilide in an oxidative cross-coupling reaction employed by Prescher et al to prepare 2-cyanobenzothiazoles, b) the proposed mechanism for the thermolytic electrocyclic fragmentation cyclisation reactions of *N*-aryliminodithiazoles that directly produce 2-cyanobenzothiazoles and c) the use of sulfolane by McCutcheon and Prescher et al to promote the selective formation of the benzothiazole from the thermolytic reaction.

The Reese reaction was reported as an electrocyclic fragmentation cyclisation that produced predominantly the imidoyl chloride but could be pushed to form more of the 2-cyanobenzothiazole by having more electron donating groups on the ring. McCutcheon, Prescher and co-workers later reverted to the original reaction and found that they could produce the 2-cyanobenzothiazole in good yield (80 %), presumably without forming any of the imidoyl chloride, by heating the *N*-aryliminodithiazole in sulfolane (Scheme 4.2). This suggested that sulfolane played an important role in the selectivity of the reaction since Reese et al originally reported a lower yield (60 %) for the same reaction in toluene.[9] Of course, despite the relatively good yields, the methodology still has many limitations, arguably the biggest drawback is its lack of generality. For example, D-aminoluciferin cannot be efficiently accessed from this reaction since its precursor, 4-nitro-*N*-aryliminodithiazole, produces predominantly the imidoyl chloride as opposed to the 2-cyanobenzothiazole (60 and 9 %, respectively) from the thermolysis.[10] With this in mind, it was theorised that *ortho*-bromination of the starting aniline might promote benzothiazole formation and would therefore allow for the reaction to be applied to more electron deficient systems. In fact, this had already been demonstrated to be true in a study where *o*-bromo-*N*-aryliminodithiazoles with electron withdrawing groups on the ring were heated to exclusively afford the corresponding benzothiazole (Scheme 4.3).[10]

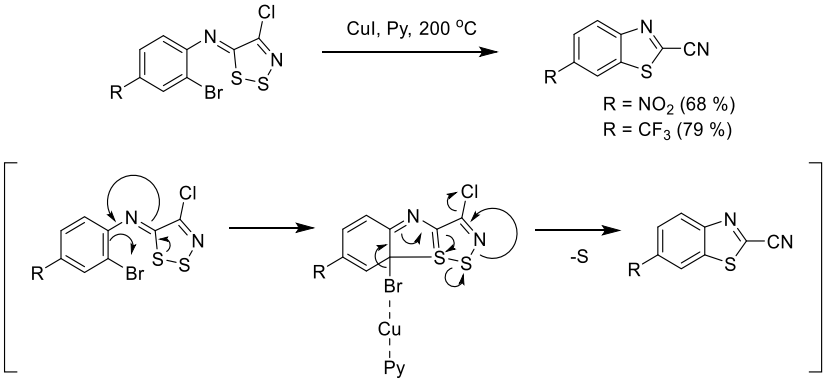

Scheme 4.3. Proposed Cu assisted electrocyclisation and fragmentation process

It was therefore decided to further investigate whether this particular reaction could be used in the context of a luciferin synthesis and to confirm if indeed *o*-bromination would improve the overall reaction sequence. In addition to improving the thermolysis (Scheme 4.3) and oxidative coupling reactions (Scheme 4.1), it was also of interest to explore whether or not it was possible to completely shift the mechanistic mode of cyclisation, away from oxidative coupling and electrocyclic reactions, through *ortho*-bromo introduction.

O-Bromination reportedly shifts mechanism of cyclisation

From previous work done in the Jardine research group and others,[11] it was known that benzothiazoles could also be accessed from the mild base-mediated cyclisation of *ortho*-bromothioanilides. Unlike the oxidative coupling and electrocyclisation process, these reactions were reported to proceed via an S_N2Ar type mechanism (Scheme 4.4).[12-13]

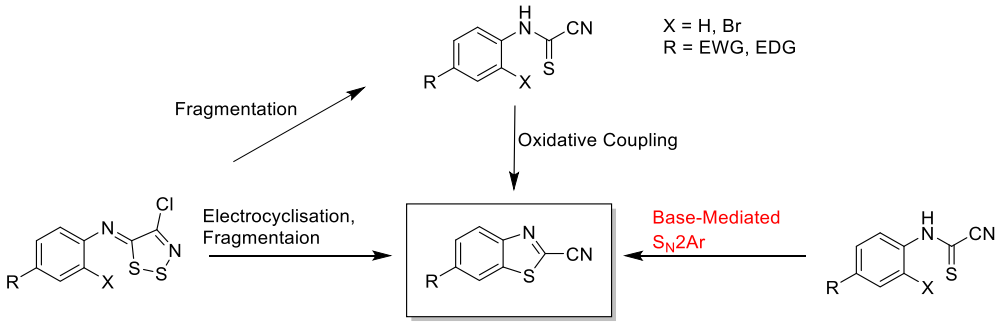

Scheme 4.4. Benzothiazole forming reactions of thioanilides

What this meant practically was that *o*-bromothioanilides that react under C-S coupling or electrocyclisation conditions to afford a benzothiazole could also simply be reacted with a relatively mild base such as NaOMe to afford the same product via a different mode of cyclisation.[12, 14-15] This is important because the mechanism dictates functional group tolerability and hence determines which luciferins can or cannot be accessed.

Aims and Objectives

The aim was to improve on known methods of luciferin syntheses by employing reactions previously not used in the context of luciferin synthesis and evaluating them against the known reactions. More specifically, it was to probe the effects of *o*-bromo functionalisation of thioanilides on their reactivity in the electrocyclisation reaction as well as to evaluate the base-mediated cyclisation as an alternative cyclisation mode.

The objectives were thus;

i) The evaluation of the effects *o*-bromination of thioanilides on previously used, low yielding intra-molecular C-S cross-coupling reactions.

ii) The evaluation of the effects of *o*-bromination on the thermolytic electrocyclisation reaction.

iii) An investigation into whether *ortho*-brominated cyanothioformanilides could be cyclised using a mild base, such as NaOMe, and if cyclisation was indeed possible, an investigation into the use of a single base to both fragment and cyclise *N*-aryliminodithiazoles, thus allowing for the one-pot preparation of 2-cyanobenzothiazoles from *N*-aryliminodithiazoles.

Controlled Monobromination of Activated Arenes

Selective monobromination of *p*-anisidine was necessary for the proposed investigation. However, Selective monobromination of activated arenes via electrophilic aromatic substitution (S_EAr) is a known synthetic challenge due to the increased reactivity of such aromatic compounds. Several common brominating reagents generally afford an inseparable mixture of the mono- and di-brominated products, as well as starting material.[16-17]

Monobromination through conventional S_EAr becomes increasingly difficult in cases where the aromatic substrates are highly activated and thus more nucleophilic. There are many reports of the bromination of such activated compounds resulting in di- or tri-brominated products, although some control was reportedly observed when the brominations were carried out at low temperatures, typically between 0 and 5 ^oC.[18-19] The investigation into an improved and unique luciferin synthesis met its first challenge here, since *o*-brominated *p*-substituted activated anilines were required to start the synthesis. Unexpectedly, there was not much in literature on the controlled monobromination of 1,4-substituted activated anilines. In fact, the general procedure for brominating activated anilines seems to follow from the conversion of the amino group to its corresponding acetamide. The acetamide is less electron donating than the amine moiety due to delocalisation of electrons from the benzene ring into the acetyl group. Thereafter, monobromination is carried out on the isolated acetamide. Then in a separate step, the acetamide is hydrolysed to afford the mono-brominated aniline. Since the aim was to improve on the previous synthesis of D-luciferin, including acetylation/deacetylation steps would be counterproductive. To this end, an investigation into the use of sodium perborate and potassium bromide for monobrominating activated anilines was undertaken.

Sodium perborate is a relatively mild, safe, and cheap oxidant, and its use in the monobromination of 1,4-substituted deactivated anilines has been reported.[16] It was therefore envisioned that perborate method could also be used to brominate *p*-anisidine, by the slow addition of the electrophilic bromine solution to the activated aniline at low temperature.

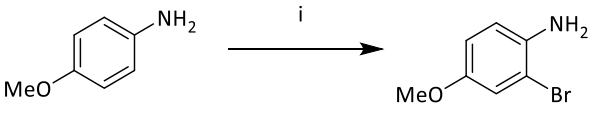

Scheme 4.5. Reagents and conditions: i)) $NaBO_3.H_2O$ / KBr / CH_3COOH / rt / 24 h

As reference, *p*-anisidine, potassium bromide and sodium perborate were suspended in acetic acid and allowed to stir at room temperature for 11 h, in accordance with the original method. TLC analysis of the reaction revealed incomplete conversion of starting material after 11 h.[16] TLC analysis also

indicated the formation of multiple products, most likely due to the lack of selectivity. The same reaction was then repeated at 0-5 °C. TLC analysis here indicated the formation of two major products (similar in R_f), originally believed to be the mono, and di-brominated products, which proved difficult to separate by silica chromatography. The ^{1}H-NMR spectrum of the crude mixture was complex but showed two dominant aromatic splitting patterns, as shown in figure 4.2.

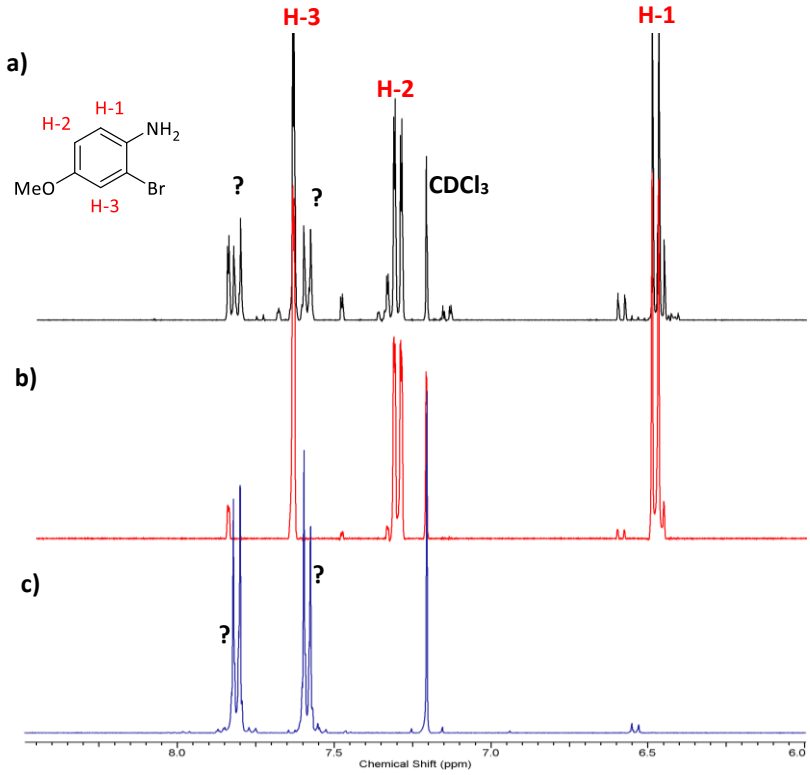

Figure 4.2. ^{1}H-NMR spectra of a) the crude mixture from the bromination reaction, b) the isolated mono-brominated product, and c) an unknown 1,4-substitued product, all in $CDCl_3$

The expected 1,2,4-splitting pattern was observed, in which the three signals seemingly integrated for one proton each. In addition to this, a second set of doublets (J = 9.0 Hz) was observed, which possibly corresponded to a separate 1,4-substituted ring. This proved to be a good initial result because the 1,2,4-splitting pattern was indeed expected for a mono-brominated product. However, the accompanying dd resonance was not expected, in fact what was expected was a single aromatic resonance corresponding to the di-brominated product. It was possible that the dd signal was due to unreacted starting material, but TLC studies had already suggested otherwise. Furthermore, the observed proton resonances were significantly more deshielded than the starting material. This suggested that some chemistry had possibly occurred at the amine moiety, resulting in a shift in the aromatic resonances. In an effort to isolate the unknown product, the reaction was repeated without the addition of KBr, and it was found that the starting material had converted into a slightly more non-polar product, as evidenced by TLC. The ^{1}H-NMR spectrum of the crude product displayed the same

dd signals previously observed. A possible explanation for this was that the amino group was being oxidised by the sodium perborate, to an azo or azoxy complex, previously reported to form under similar conditions.[16, 20-23] This particular reaction had been reported previously, wherein the amine of *p*-anisidine was oxidised to a nitro group, in the presence of sodium perborate at 55 °C. In this case however, it was not the nitro analogue that was being isolated, but instead, the azoxy intermediate, which forms at room temperature. This was supported by melting point analysis, where it was demonstrated that the presumed azoxy material had a melting point of 160 °C, which was comparable to the literature melting point recorded at 155-158 °C. In addition, the determined melting point was also much lower than that of the starting material *p*-anisidine, which had a melting point of 274-278 °C. Further support for the formation of the azoxy complex was found in IR and NMR analysis, where data for the synthesized material was found to be comparable to that previously reported.

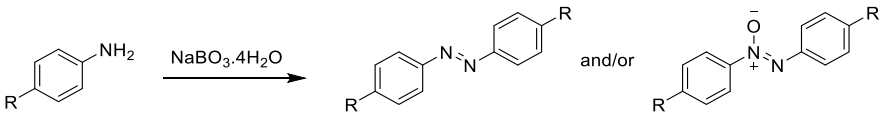

Scheme 4.6. Perborate mediated oxidation of anilines to azo and azoxy complexes

While perborate mediated oxidation of the amine moiety was of course very interesting, there was in fact no use for the resultant azoxy complex, and hence its formation during the bromination reaction was undesired. For this reason, sodium perborate and potassium bromide were stirred in acetic acid to generate the required electrophilic bromine perborate complex. That solution was then added dropwise to a stirring suspension of aniline in acetic acid, maintained below 5 °C. The reaction progress was monitored by TLC. This method resulted in mono-bromination almost exclusively. Furthermore, the generality of this procedure was demonstrated in the attempted mono-bromination of various other anilines that were to be used in the synthesis of D-luciferin 6'-analogues. Table 4.1 shows the results from the mono-bromination method.

Table 4.1. Controlled monobromination of activated arenes

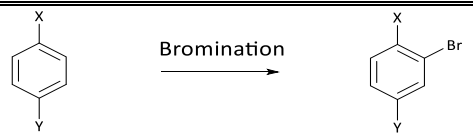

	X	Y	Major Product	Yield, %	m.p. °C (lit m.p.)
1	NH_2	OMe	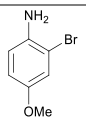	92	Oil (N/A)
2	NH_2	I	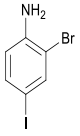	78	70-71 (75-76)[9]
3	NH_2	F	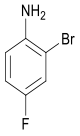	81	38-40 (41)[1]
4	NH_2	SH	Disulfide* 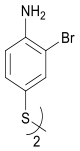	77	138-140
5	CH_3	SH	Disulfide* 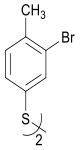	64	48-50

* Thiol oxidation takes priority to give the disulfide, followed by mono-bromination. Brominated products were characterised by ^{1}H-NMR spectroscopy, melting points and LRMS and the products from the bromination reactions were used in the synthesis of C6-substituted 2-cyanobenzothiazoles. Based on average isolated yields

The results concluded that monobromination of activated anilines were possible with sodium perborate/potassium bromide and that conversion of activated anilines to their corresponding anilides prior to bromination was, in fact, not always necessary. In addition, amino and thiol functionalities could also be oxidised under the same conditions required for bromination, which may be useful since it allows for multiple functional group transformations to be achieved in one synthetic step. The mono-bromination of activated anilines demonstrates the subtleties associated with the order in which reagents are added and the synthetic chemist's practical control over functional group transformations. Much like the reactions of epoxides, where the order of addition of acid and nucleophile dictates the distribution of products (regio- and stereoisomers). So too, does the order of

addition of $NaBO_3$ and KBr allow control over the distribution of N/S-oxidation and bromination products. In theory, this reaction could allow for the selective production of *o*-brominated nitro systems from 1,4-substituted anilines. Where the amino functionality is used to direct bromination and, upon heating, is oxidised to produce the corresponding *o*-bromo-nitrobenzene, perfect for S_NAr. Alternatively, oxidation could precede bromination, in which case *m*-bromo-nitrobenzene could be generated. The versatility of this reactions was kept in mind in subsequent syntheses. The products from the bromination reactions were then used to evaluate various methods of cyanobenzothiazole preparation, all of which were aimed at developing improved syntheses of luciferins.

C-S Oxidative coupling of *o*-brominated thioanilides

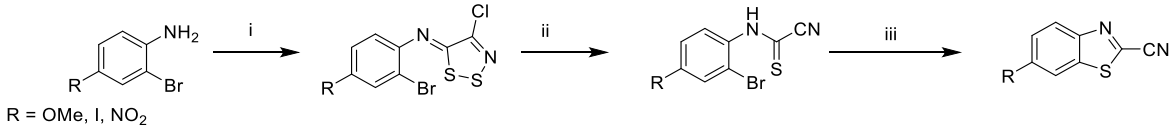

Scheme 4.7. Reagents and conditions: i) Appel's salt / DCM / Py / rt / 4 h, ii) DBU / DCM / 5 ^oC / 1 h, iii) $PdCl_2$ / CuI / TBAB / DMSO:co-solvent (1:1) / 120 ^oC / 4 h

With the *o*-bromoanilines in hand, it was decided to first evaluate the effects of the bromine on the previously described low yielding oxidative coupling. The precursors for the C-S coupling were prepared using methods detailed earlier, involving the condensation of *o*-bromoanilines to *N*-aryliminodithiazoles which were subsequently fragmented to afford the corresponding cyanoformanilide.[3] The cyclisation was attempted using three different anilines and the result are summarised in table 4.2.

Table 4.2. Yields from intramolecular C-S cross coupling reaction

R	Yield from o-bromo-thioanilide[a]	Yield from o-bromothioanilide[b]	Yield from unsubstituted thioanilide
OMe	23	25	25
I	21	21	3
NO_2	13	20	8

*Based on average isolated yields: a) co-solvent = DMF and b) co-solvent = NMP

Contrary to what was expected, *o*-bromination had very little effect on the yield, with generally low yields observed across all analogues. This suggests that it was perhaps the combination of reagents used in the reaction that were not optimised and that alternate catalysts, choice of base and even catalyst loading should have been explored. One of the more interesting discoveries from these reactions was that a small amount (<5 %) of 2-cyanobenzothiazole product was being formed in the

DBU mediated fragmentation step, observed by TLC analysis and ^{1}H-NMR spectroscopy. This was later demonstrated to be as a result of nucleophilic substitution of the resultant thiolate with bromine. It was also demonstrated that the 2-cyanobenzothiazole product was not formed in any isolatable quantity when the starting *o*-bromothioanilide was heated in the absence of the coupling reagents. This suggested that only *N*-aryliminodithiazoles could cyclise in this manner.

Electrocyclisation of *o*-brominated *N*-aryliminodithiazoles

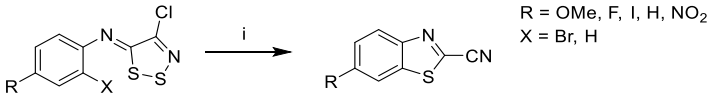

Scheme 4.8. Reagents and conditions: CuI / Py / 160 ^{o}C / 1 h

The same precursors were subsequently used in a thermolytic electrocyclisation reaction, where the *o*-bromo-*N*-aryliminodithiazoles were heated both neat and in solvent to afford the corresponding 2-cyanobenzothiazoles. The electrocyclic reaction was expected to be superior to the preceding C-S oxidative coupling in terms of scalability and cost, since intra-molecular cyclisation could be achieved by simply heating the *N*-aryliminodithiazole neat. The resultant yields from these reactions are summarised in table 4.3.

Table 4.3. Yields from electrocyclisation fragmentation reaction of *o*-bromo-*N*-aryliminodithiazoles

	***o*-bromo-*N*-arylimine**					***N*-arylimine**
R	**120 °C neat**	**120 °C, DMF**	**120 °C, Py**	**120 °C, CuI, Py**	**160 °C, CuI, Py**	**120 °C DMF**
OMe	58	59	60	63	84	60
I	3	-	70	70	74	19
F	75	80	52	85	80	30
H	35	-	45	40	67	23
NO_2	41	58	32	65	68	9

*Based on average isolated yields

In all cases, it appeared that the *o*-brominated precursors were afforded in higher yields when compared to the unsubstituted *N*-arylimininodithiazoles. What was striking was the increase in yield observed for EWG's such as the nitro and fluoro analogues, when comparing unsubstituted and *o*-bromo-*N*-aryliminodithiazoles. In the McCutcheon/Prescher et al synthesis that involved thermolysis of the unsubstituted *N*-arylamine, D-aminoluciferin could not be efficiently accessed using this route. With *o*-bromination however, the same method can now be applied in aminoluciferin synthesis.

Furthermore, it was also apparent that the CuI and Py directly promoted the formation of the benzothiazole product, since yields were generally increased by their addition. There were cases however where CuI/Py addition had little/no effect on the observed yield. Overall, the electrocyclisation fragmentation of *o*-bromo-*N*-aryliminodithiazoles proved to be quite effective and generally applicable in luciferin synthesis.

Metal-free base-mediated cyclisation

The electrocyclisation reaction was clearly superior to the C-S coupling reactions under the conditions reported, but its use was limited to the cyclisation of *N*-aryliminodithiazoles formed exclusively from the condensation of anilines and Appel's salt. Appel's salt is of course a notoriously toxic reagent that is produced from sulfur monochloride and chloroacetonitrile.[24] It was predicted that a base-mediated S_N2Ar like cyclisation could be used to cyclise all thioanilides irrespective of ring constituents. The base mediated method involved reacting a thioanilide with NaOMe to generate the thiolate anion which undergoes an intra-molecular nucleophilic substitution to afford the corresponding benzothiazole.[12] The benzothiazoles were formed in good-excellent yields under the conditions shown in scheme 4.9.

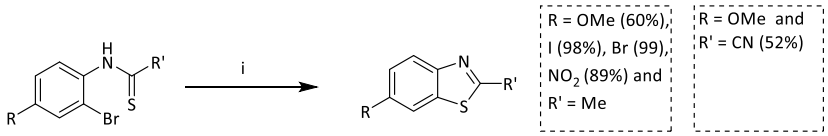

Scheme 4.9. Reagents and conditions: i) NaOMe / NMP / 150 °C / 2 h

Interestingly, the same reaction in the absence of base did not produce any of the corresponding benzothiazoles which suggests that thiolate formation is indeed key and that weaker bases will have no effect on promoting product formation.

One pot, Metal-free base-mediated cyclisation from *N*-aryliminodithiazoles

In the previous fragmentation of *o*-bromo-*N*-aryliminodithiazoles, the consistent formation of a small amount (<1-5 %) of unsubstituted 2-cyanobenzothiazole was noted along with the expected fragmentation product. It was predicted that the benzothiazole was being formed from the DBU generated thiolate nucleophilic substitution of the bromine. As a result of this, a one-pot base mediated fragmentation cyclisation reaction was developed. Using previously prepared *o*-mono-brominated anilines, subsequent imine formation, fragmentation, and cyclisation was attempted in one-pot. The initial reaction involved stirring the *o*-brominated-*p*-anisidine in DCM at room temperature and to that suspension was added a slight excess of Appel's salt. After conversion of the starting material to the imine, monitored by TLC, the reaction was cooled to 0 °C and DBU was added

dropwise over 30 minutes. The reaction was then allowed to warm to room temperature and stirred for an additional 3 hours. The crude reaction mixture was concentrated *in vacuo* and purified through a short pad of silica, eluting with hexanes to afford the benzothiazole product in good yield (60-67 %). The ^{1}H-NMR spectrum of the product matched that of the previously synthesised benzothiazole scaffold formed from the low yielding C-S metal mediated cross-coupling reaction. The melting point of the product, which was in good agreement with the reported literature value (129-131 °C, lit. 129-131 °C), further supported the success of the one-pot reaction.

Improved alternate routes to luciferins

Based on all the exploratory synthetic work concerning the development of an improved and unique luciferin synthesis; two relatively short, scalable and arguably cheaper sequences toward luciferin substrates were produced.

1) Route A; DBU cyclisation using *o*-bromo-*N*-aryliminodithiazoles
2) Route B; NaOMe cyclisation of *o*-bromoanilides

The first route, shown in scheme 4.10, makes use of the previously described one-pot DBU mediated fragmentation cyclisation. The sequence starts with the monobromination of a *p*-substituted aniline which is subsequently converted into an *N*-aryliminodithiazole and thereafter its corresponding cyanobenzothiazole, by the slow addition of DBU. Lastly, the 2-cyanobenzothiazole is reacted with D-Cys to afford a luciferin. The condensed synthesis of the benzothiazole scaffold greatly improved the overall synthesis of D-luciferin by decreasing the number of individual synthetic steps, increasing the overall yield (from 9 to 49 %), and eliminating the need for metal catalysts.

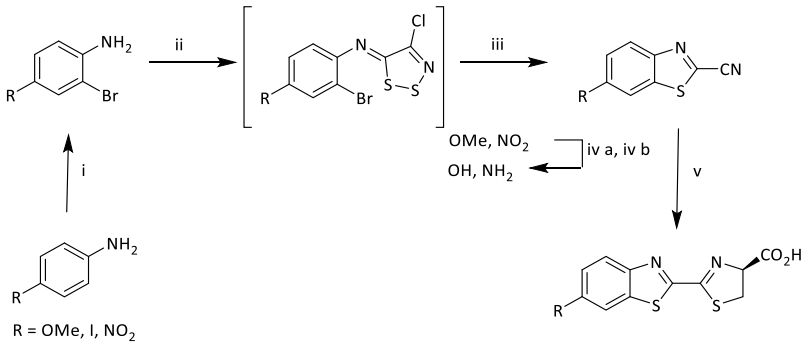

Scheme 4.10. Reagents and conditions: i) $NaBO_3$ / KBr / AcOH / rt / 16 h, (R = OMe, 71%; R= I, 89%; R = NO_2, 99%), ii) Appel's salt / DCM / 1-2 h, (90-98%), iii) DBU / DCM / 5 °C, 3-4 h, (60-63%), iv a) PyHCl / DMF / 150 °C / 1 h, (99%), iv b) Zn / NH_4Cl / MeOH / rt / 20 min, (99%), v) D-Cys / K_2CO_3 / MeOH or CH_3CN / rt / 20 min, (99%)

Furthermore, this sequence, unlike the one-pot method demonstrated by McCutcheon et al, can be used to prepare D-aminoluciferin since the *o*-bromination allows for improved cyclisation in cases

where R=EWG (Scheme 4.10). One disadvantage, as mentioned in the preceding section, is the use of Appel's salt and excessive amounts of DBU. In light of this, a sequence that still used a base-mediated cyclisation but not the Appel's salt was investigated. Here, a sequence that resembles the natural product synthesis by White et al was employed, characterised by C2-modification post-benzothiazole formation. The sequence is shown in scheme 4.11 and involved forming 6-iodo-2-methylbenzothiazole from an *o*-bromoaniline. The C2-methyl was then converted to a C2-nitrile over two steps to afford the corresponding cyanobenzothiazole. The 6-iodo-benzothiazole could then be converted to various other functional groups and then to the corresponding luciferins. The 6-iodo functionality was targeted because the starting aniline (4-iodoaniline) was relatively cheap and readily available.

It should be noted that the synthesis of the C6-iodo 2-cyanobenzothiazole was also attempted using the Prescher et al Appel's salt method. The results from that attempt suggested that an alternative cyclisation method, which did not employ an intramolecular C-S coupling reaction, would be necessary to construct an iodinated 2-cyanobenzothiazole, since the coupling reaction also resulted in the loss of the iodo functional group.

This iodo functionality was particularly appealing because the Prescher et al method made use of different anilines as starting materials, depending on which luciferin was being targeted. For example, if D-luciferin was being synthesised, *p*-anisidine would be used in the first step, whereas if the target was D-aminoluciferin, *p*-nitroaniline would be used instead. With the iodo functionality both luciferins, as well as others, could potentially be accessed from the 2-cyano-6-iodobenzothiazole formed from 4-iodoaniline **4.1**.

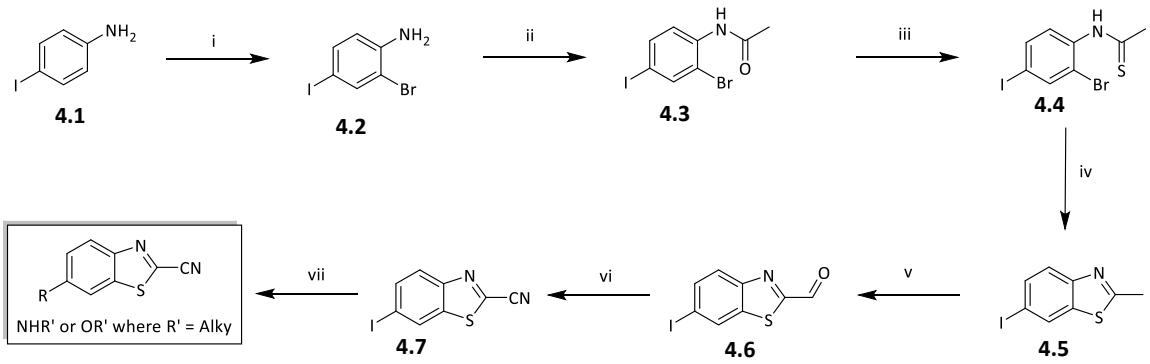

Scheme 4.11. Reagents and conditions: i) $NaBO_3.H_2O$ / KBr / CH_3COOH / rt / 24 h, ii) Ac_2O / Py / 100 °C / 2 h, iii) Lawesson's reagent / toluene / 7 h / 100 °C, iv) NaOMe / NMP / 150 °C / 2 h, v) SeO_2 / dioxane / 150 °C / 4 h, vi) NH_3OHCl / NEt_3 / Phthalic anhydride / rt / 2 h

In this sequence, *p*-iodoaniline **4.1** was ortho-brominated using a solution of sodium perborate and KBr in acetic acid. The resultant 2-bromo-4-iodoaniline **4.2** was then acetylated in acetic anhydride and pyridine to afford the acetamide **4.3**. Subsequent thionylation of **4.3** afforded the thioacetamide

4.4, and sodium methoxide mediated cyclisation of **4.4** afforded the benzothiazole **4.5**. Further modification at C2 generated the aldehyde **4.6** and then the nitrile **4.7**.

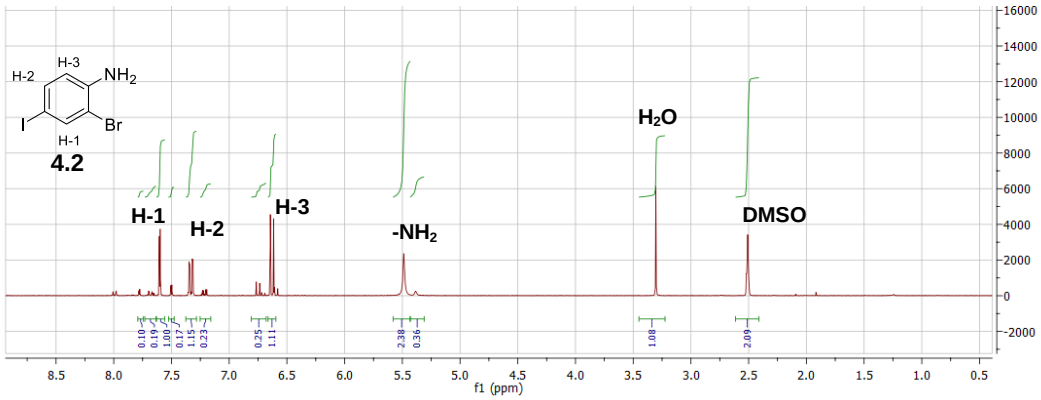

Figure 4.3. ^{1}H-NMR spectrum of **4.2** in DMSO

The products from the bromination and acetylation reactions were characterised by their melting points and by ^{1}H-NMR spectroscopy, further characterisation was not necessary since these were commonly prepared compounds. The ^{1}H-NMR spectrum of the brominated product **4.2** displayed the correct three aromatic protons, as well as a broad singlet arising from its amine protons. Both the spectrum and the broad melting point indicated that the product also contained trace impurities. These impurities were not dealt with immediately; instead, the impurities were carried over to the thionylation step, since column chromatography is generally used in this reaction to remove the thionylation product from the Lawesson's reagent by-product. The ^{1}H-NMR spectra of the acetamide **4.3** and the thioacetamide **4.4** are shown in figure 4.4. It should be noted that there were still smaller signals in the ^{1}H- and ^{13}C-NMR of the acetamides (**4.3**, **4.4**) that persisted even after repeated purification. These smaller resonances were most likely due to conformational isomers of the compounds involving the restricted rotation of the nitrogen-phenyl bond.

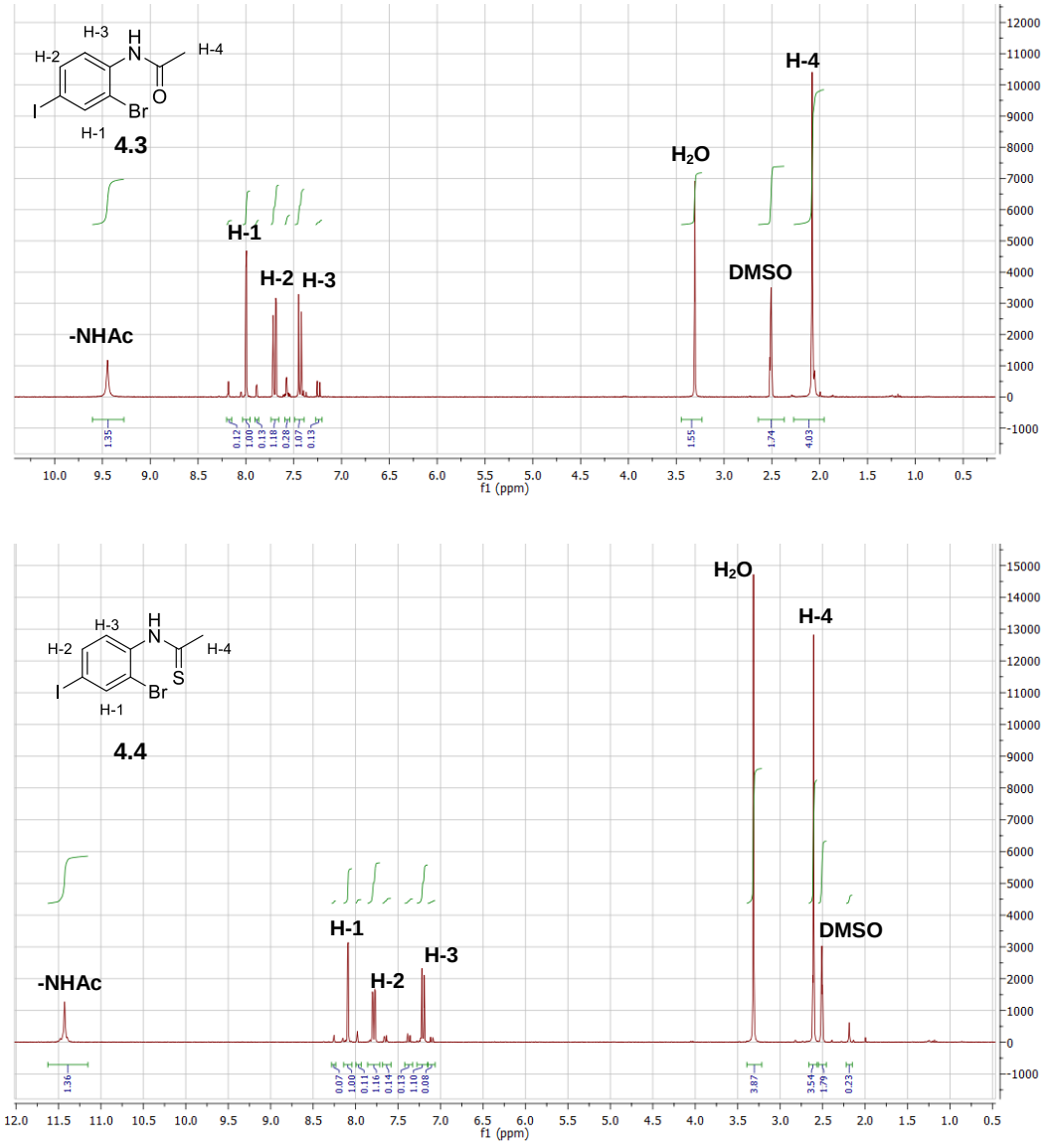

Figure 4.4. ^{1}H-NMR spectra of **4.3** and **4.4** in DMSO

Of note in the ^{1}H-NMR spectrum of **4.3** is the absence of the amine resonance, formerly observed in the precursor, and the presence of two signals at 2.59 and 11.45 ppm which are diagnostic for the acetamide functionality. In the ^{1}H-spectrum of **4.4** the diagnostic acetamide proton resonances are conserved, but have shifted significantly when compared to the starting material (NHAc shifted from 9.48 to 11.47 ppm), confirming successful thionylation.

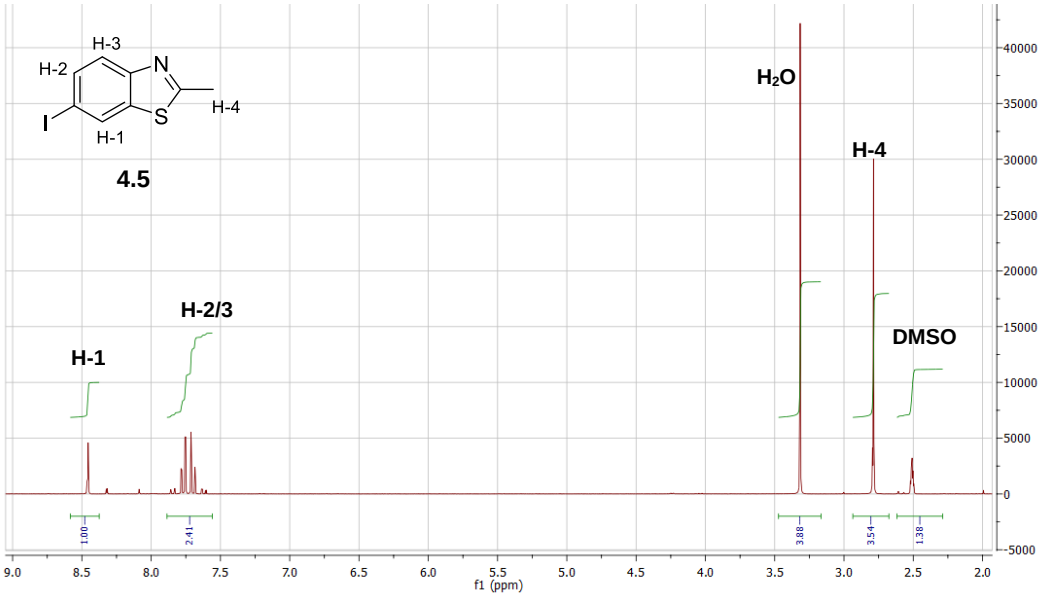

Figure 4.5. ^{1}H-NMR spectrum of **4.5** in DMSO

The thioacetamide **4.4** was then reacted with sodium methoxide in NMP at 150 °C to afford the cyclised product **4.5** in good yield. Interestingly, the mechanism by which the reaction proceeds has not yet conclusively been established. What is certain is that the role of the sodium methoxide is to form the thioenolate from the thioacetamide. The thioenolate then displaces the bromine to form the cyclised product **4.5**. What is ambiguous is the process of how the thioenolate goes about displacing the bromine. Normally, a reaction like this would be considered S_NAr, since it proceeds via the thioenolate. However, the system lacked an EWG group ortho/para to the bromine capable of stabilizing the resultant negative charge in the Meisenheimer intermediate and, therefore, a typical S_NAr mechanism seemed unlikely. Scheme 4.12 shows two possible mechanisms for the substitution. The first is the concerted S_N2Ar mechanism and the second is the, rarer, stepwise S_N1Ar.

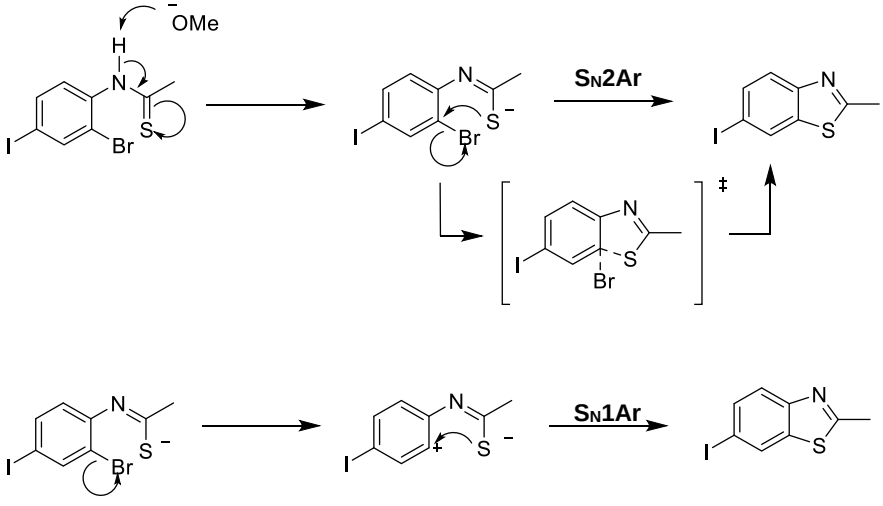

Scheme 4.12. Proposed mechanisms of nucleophilic aromatic substitution

With the C2-methylbenzothiazole in place, a selenium dioxide oxidation was employed to generate the desired aldehyde (Scheme 4.13). Selenium dioxide has been used extensively in the oxidation of allylic carbons,[25-27] and its use in the oxidation of the C2-methyl of a 2-methylbenzothiazole was reported, thus making it an ideal choice for the preparation of the aldehyde. However, complete consumption of the starting material afforded predominantly the acid and, because of this, it was decided to terminate the reaction before the starting material could be fully consumed and the aldehyde converted to acid. The shortening of the prescribed reaction time resulted in the isolation of an inseparable mixture (by column chromatography) of the starting material **4.5** and the aldehyde **4.6**.

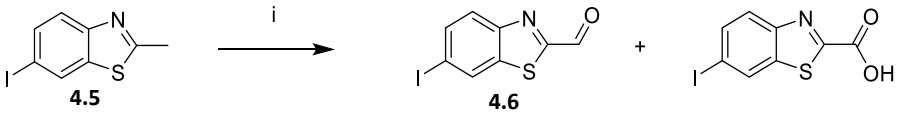

Scheme 4.13: Reagents and conditions: i) SeO_2 / H_2O / dioxane / 150 °C / 4 h (15% **4.6**)

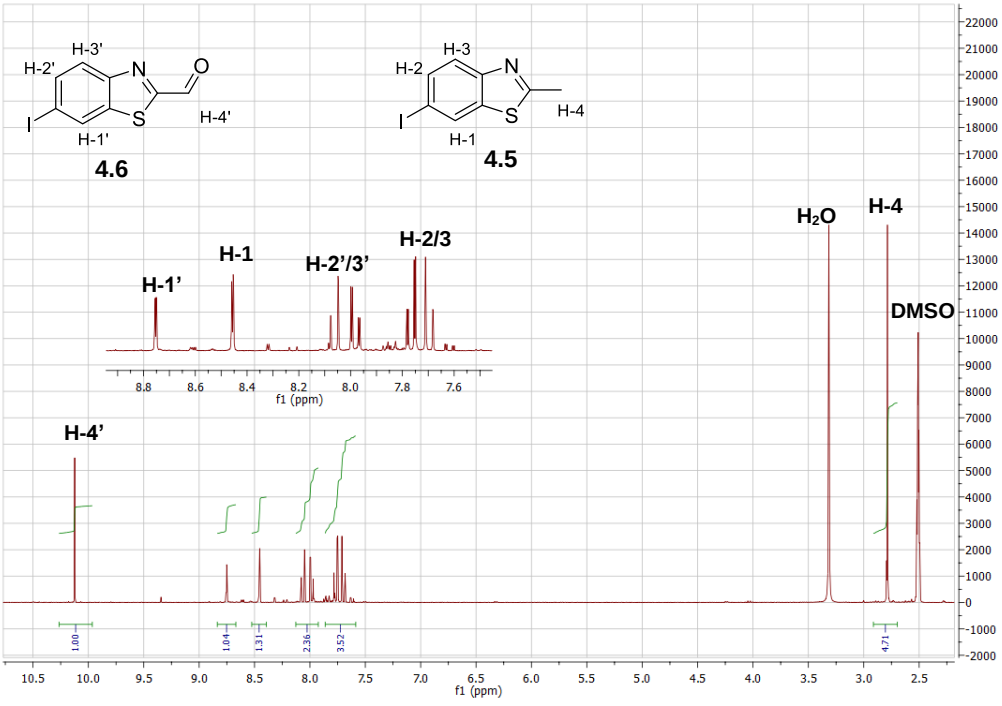

Figure 4.6. ^{1}H-NMR spectrum of **4.5** and **4.6** in DMSO

The ^{1}H-NMR spectrum clearly supported the formation of the aldehyde, however, it proved difficult to remove the residual starting material. Fortunately, the starting material **4.5** was predicted to be quite unreactive and proved to be so in the subsequent reaction, allowing a mixture of **4.5** and **4.6** to be used to form the nitrile. For the conversion of the aldehyde to the nitrile, a one-pot hydroxylamine

condensation and dehydration was employed.[28] The conversion involved reacting the aldehyde **4.6** (containing residual **4.5**) with hydroxylamine hydrochloride to form an oxime **4.9** which then reacted with phthalic anhydride to form an imidoyl or oxime ester **4.10** that underwent an elimination to form **4.7**, as demonstrated in scheme 4.14.

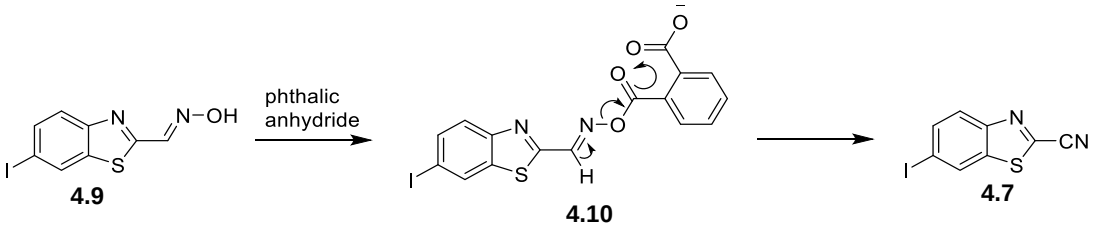

Scheme 4.14. Proposed mechanism for nitrile formation

The ^{1}H-NMR of the pure starting materials and crude reaction mixture after two hours is shown in figure 4.7, which demonstrates the absence of the aldehyde proton in the crude reaction mixture, two hours post-phthalic anhydride addition.

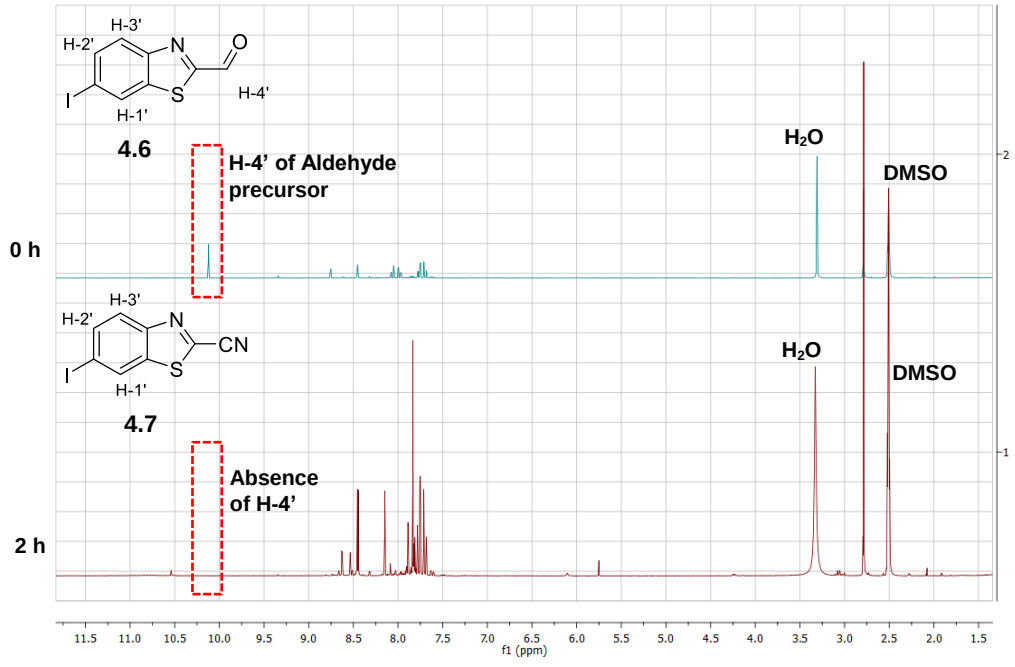

Figure 4.7. ^{1}H-NMR spectra showing the conversion of **4.6** to **4.7** in DMSO

The 2-cyano-6-iodobenzothiazole was purified using silica column chromatography in order remove the unreacted phthalic anhydride from the product. The ^{1}H-NMR spectrum is shown in figure 4.9, where all the expected resonances were observed. In addition, the infrared spectrum of **5.7** displayed a weak band at 2250 cm^{-1} which supported the presence of the nitrile functionality (figure 4.8) and the ^{13}C-NMR displayed the expected eight resonances, further supporting its successful preparation.

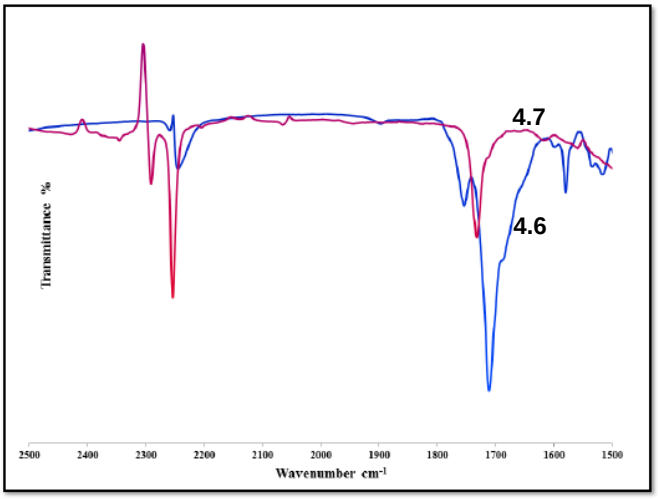

Figure 4.8. IR spectra of the aldehyde **4.6** and the nitrile product **4.7**

As a result of the low yielding oxidation step (15 %), the 2-cyano-6-iodobenzothiazole was unfortunately prepared in a low overall yield of 6-8 %. Attempts at improving the yield on the oxidation reaction were unsuccessful and generally resulted in increased production of the carboxylic acid. Despite the low overall yield, the iodo-functionality was still quite interesting since it could potentially be used to rapidly prepare 6'-analogues of D-luciferin.

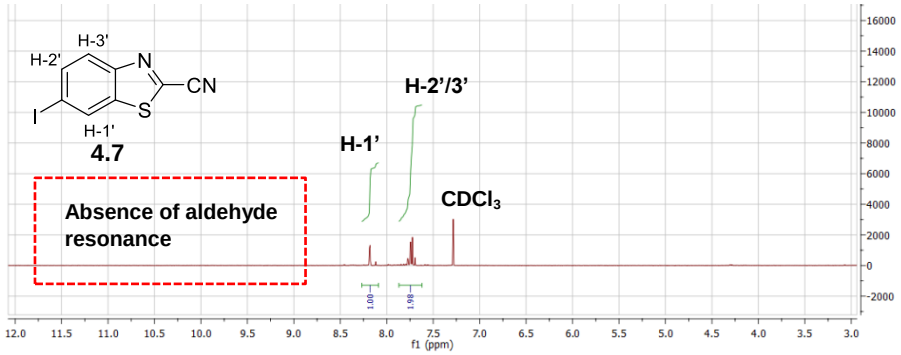

Figure 4.9. ^{1}H-NMR spectrum of purified **4.7** in $CDCl_3$

The iodo functionality was expected to be a very good handle to introduce other functional groups through substitution reactions. This made the iodo-benzothiazole a particularly important compound since it could potentially be considered a common intermediate for D-luciferin, aminoluciferin, and might further allow for the facile preparation of structurally related 6'-luciferin analogues.

Bioluminescence of 6'-halogenated luciferins

The 2-cyano-6-iodobenzothiazole was reacted with D-Cys to produce a 6'-iodo derivative of D-luciferin. The derivative's bioluminescence was evaluated, alongside other 6'-analogues formed from the previously prepared C6-substituted 2-cyanobenzothiazoles, using purified *Ppy* luc according to the method described in the preceding chapters (Chapters 2-3). It was already known from previous work reported by White et al that derivatives of D-luciferin that had been fluorinated on the benzothiazole ring were found to be inactive in the bioluminescent reaction with luciferase. This was due to the halogen's electron withdrawing effects and indeed, this was also demonstrated when the iodo-derivative was evaluated for bioluminescence. In addition to the 6'-iodo analogue, 6'-nitro, 6'-methoxy and unsubstituted luciferins were also evaluated for the bioluminescent reaction, but none were found to emit significant bioluminescence when compared to D-luciferin under the same conditions (Figure 4.10).

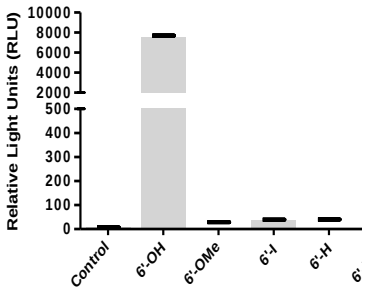

Control – 10 nM Luciferase in the absence of a luciferin

Figure 4.10. Bioluminescence emission of 0.1 µM D-luciferin and related 6'-analogues of D-luciferin, when treated with 10 nM luciferase. The RLU were determined 1 min post-enzyme addition and were recorded in triplicate and are represented as the mean ± SEM.

These results suggested that only the electron donating free hydroxyl and amine could produce significant bioluminescence in the presence of O_2, ATP and Mg^{2+} and luciferase. In addition, these results also eluded to the potential of a 6'-thiol analogue which, based on the observed bioluminescence for the different 6'-functionalities, was predicted to be bioluminescent.

The common intermediate; could the C6-iodo 2-cyanobenzothiazole allow access to C6-OH, C6-NH_2 and the unreported C6-SH 2-cyanobenzothiazole

In the preceding chapter, two project milestones were identified; one of which concerned developing a shorter and improved synthesis of C6-substituted 2-cyanobenzothiazoles through *o*-bromination. This chapter then demonstrated how *o*-bromination resulted in the condensed one-pot metal-free synthesis of the benzothiazole scaffold, which ultimately improved the overall synthesis of D-luciferin and D-aminoluciferin, by decreasing the number of individual synthetic steps and increasing the

overall yield (from 9 to 49 % and 25 to 54 % for D-luciferin and D-aminoluciferin, respectively). In addition to the improved method, a potentially interesting C6-iodinated 2-cyanobenzothiazole was prepared, which was thought to be a good common intermediate for 6'-analogues of D-luciferin.

At this point, it seemed that the synthetic development work had, in fact, laid the groundwork for the facile preparation of new D-luciferin 6'-analogues. At the time, all known bioluminescent 6'-derivitives of D-luciferin were based on 6'-amino analogues. Since the bioluminescence associated with both the hydroxyl and amino groups were relatively well reported, attention was turned to preparing the first 6'-thio analogue of D-luciferin, whose luminescent properties and potential applications were still unexplored.

First attempt at C6-iodo substitution

It was proposed that the C6-iodobenzothiazole be reacted in the presence of various nucleophilic coupling partners to evaluate whether or not it could be successfully converted to a C6-hydroxy, amino or thiol derivative under standard C-S palladium mediated coupling conditions (Scheme 4.15).

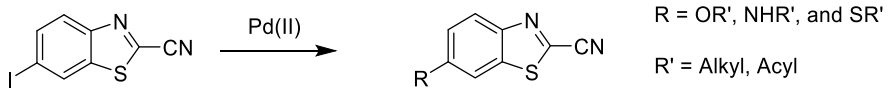

Scheme 4.15. Proposed conversion of 2-cyano-6-iodobenzothiazole to O, N, S-substituted benzothiazoles

Interestingly, Miller et al reported that a palladium-mediated coupling reaction, although not reported for the 2-cyano-6-iodobenzothiazole, could be used to construct 6-amino derivatives from the bromo and fluoro-precursors.[29] This was an encouraging result as it reinforced the usefulness of the 6-halogenated 2-cyanobenzothiazoles. It should be noted however, that this publication was released only after the iodo-benzothiazole work highlighted here was completed. Miller et al went on to further demonstrate the generality of the C6-fluoro 2-cyanobenzothiazole by preparing the first published examples of C6-sulfur 2-cyanobenzothiazoles, via an S_NAr reaction. Miller et al reported two sulfide analogues but did not report the free thiol, which further warranted its synthesis.

Miller et al synthesis of 6-substituted 2-cyanobenzothiazoles; challenges associated with aryl-halide substitutions

In the 2017 publication, a library of D-luciferin C6-analogues were prepared from 2-cyano-6-fluorobenzothiazole.[29] It was reported that the fluoro-precursor exclusively underwent S_NAr type reactions to afford the corresponding benzothiazoles (Scheme 4.16), whereas the bromo-derivative could not react in this way and, instead, had to be reacted under standard Buchwald-Hartwig amination conditions to afford the same products. Miller et al also commented on the reactivity of

the nitrile moiety to which they attributed their low yielding substitutions. As mentioned previously, Miller et al (via the 2-cyano-6-fluorobenzothiazole) made a very significant contribution to the plethora of 6'-luciferin analogues, however, what noticeably remained to be seen was the free thiol.

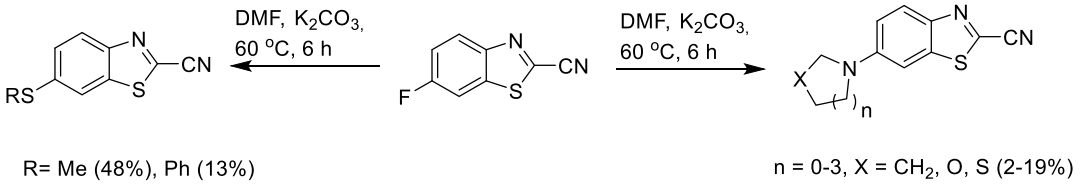

Scheme 4.16. Miller et al method of preparing 6'-analogues of D-luciferin

Miller et al also commented on the bioluminescent activity of the sulfides, which were found to not be bioluminescent active. This could of course have been predicted based on the reactivity of the hydroxyl parent, where the free hydroxyl is bioluminescent active while the *O*-alkylated/arylated derivatives are not. Presumably, Miller et al was not able to produce the free thiol because the sulfides were not amenable to alkyl/aryl deprotection to provide the free thiol.

Towards D-thioluciferin

Since the value of a 6'-thiol analogue of D-luciferin was becoming increasingly apparent, it was decided to first try and form the C6-thio 2-cyanobenzothiazole from the C6-iodo precursor. This was proposed to be done via reacting the 6-iodobenzothiazole with potassium thioacetate, thioacetic acid or thiourea, under standard Pd-coupling conditions. The pursuit of the C6 -thio analogue of D-luciferin follows in Chapter 5.

In conclusion

In the previous syntheses of D-luciferin and D-aminoluciferin, the 2-cyanobenzothiazole forming palladium-mediated cyclisation, a reaction common to both luciferin syntheses, was found to be limiting and was the main contributor to the poor overall yields. A number of different methods were attempted to increase the efficacy of the palladium C-S coupling reaction. Ultimately, *ortho*-bromination of the starting anilide lead to a successful cyclisation and afforded the cyclised products in generally improved yields (54-85 % relative to 9-25 %) and was demonstrated to have better functional group tolerability with respect to the C6-substituent. An unrelated route involving a C6-iodo functional group on the benzothiazole was also explored as an alternative intermediate, which unlocked new possibilities for method improvement. The iodo functionality was however incompatible with the previously reported palladium chemistry and was better suited for *ortho*-brominated reactions.

References

1. White, E. H.; McCapra, F.; Field, G. F.; McElroy, W. D., The structure and synthesis of firefly luciferin. *Journal of the American Chemical Society* **1961,** *83* (10), 2402-2403.
2. Seto, S.; Ogura, K.; Nishiyama, Y., A convenient synthetic method of 2-carbamoyl-6-methoxybenzothiazole, one of intermediates for the synthesis of firefly luciferin. *Bulletin of the Chemical Society of Japan* **1963,** *36* (3), 331-333.
3. McCutcheon, D. C.; Paley, M. A.; Steinhardt, R. C.; Prescher, J. A., Expedient synthesis of electronically modified luciferins for bioluminescence imaging. *Journal of the American Chemical Society* **2012,** *134* (18), 7604-7607.
4. McCutcheon, D. C.; Porterfield, W. B.; Prescher, J. A., Rapid and scalable assembly of firefly luciferase substrates. *Organic & Biomolecular Chemistry* **2015,** *13* (7), 2117-2121.
5. Benedí, C.; Bravo, F.; Uriz, P.; Fernández, E.; Claver, C.; Castillón, S., Synthesis of 2-substituted-benzothiazoles by palladium-catalyzed intramolecular cyclization of o-bromophenylthioureas and o-bromophenylthioamides. *Tetrahedron letters* **2003,** *44* (32), 6073-6077.
6. Inamoto, K.; Hasegawa, C.; Hiroya, K.; Doi, T., Palladium-catalyzed synthesis of 2-substituted benzothiazoles via a C− H functionalization/intramolecular C− S bond formation process. *Organic letters* **2008,** *10* (22), 5147-5150.
7. Evindar, G.; Batey, R. A., Parallel synthesis of a library of benzoxazoles and benzothiazoles using ligand-accelerated copper-catalyzed cyclizations of ortho-halobenzanilides. *The Journal of organic chemistry* **2006,** *71* (5), 1802-1808.
8. English, R. F.; Rakitin, O. A.; Rees, C. W.; Vlasova, O. G., Conversion of imino-1, 2, 3-dithiazoles into 2-cyanobenzothiazoles, cyanoimidoyl chlorides and diatomic sulfur. *Journal of the Chemical Society, Perkin Transactions 1* **1997,** (3), 201-206.
9. Bénéteau, V.; Besson, T.; Rees, C. W., Rapid synthesis of 2-cyanobenzothiazoles from N-aryliminodithiazoles under microwave irradiation. *Synthetic communications* **1997,** *27* (13), 2275-2280.
10. Besson, T.; Dozias, M.-J.; Guillard, J.; Rees, C. W., New route to 2-cyanobenzothiazoles via N-arylimino-1, 2, 3-dithiazoles. *Journal of the Chemical Society, Perkin Transactions 1* **1998,** (23), 3925-3926.
11. Feng, E.; Huang, H.; Zhou, Y.; Ye, D.; Jiang, H.; Liu, H., Metal-Free Synthesis of 2-Substituted (N, O, C) Benzothiazoles via an Intramolecular C− S Bond Formation. *Journal of combinatorial chemistry* **2010,** *12* (4), 422-429.
12. Spitulnik, M. J., A new general synthesis of 2-methylbenzothiazoles. *Synthesis* **1976,** *1976* (11), 730-731.

13. Bunce, R. A.; Nago, T.; Sonobe, N.; Slaughter, L. M., Benzo-fused heterocycles and carbocycles by intramolecular SNAr and tandem SN2-SNAr reactions. *Journal of Heterocyclic Chemistry* **2008,** *45* (2), 551-557.
14. Karlsson, H. J.; Lincoln, P.; Westman, G., Synthesis and DNA binding studies of a new asymmetric cyanine dye binding in the minor groove of [poly (dA-dT)] 2. *Bioorganic & medicinal chemistry* **2003,** *11* (6), 1035-1040.
15. Karlsson, H. J.; Eriksson, M.; Perzon, E.; Åkerman, B.; Lincoln, P.; Westman, G., Groove-binding unsymmetrical cyanine dyes for staining of DNA: syntheses and characterization of the DNA-binding. *Nucleic acids research* **2003,** *31* (21), 6227-6234.
16. Roche, D.; Prasad, K.; Repic, O.; Blacklock, T. J., Mild and regioselective oxidative bromination of anilines using potassium bromide and sodium perborate. *Tetrahedron letters* **2000,** *41* (13), 2083-2085.
17. Cossy, J.; Poitevin, C.; Pardo, D. G.; Peglion, J. L., An Easy and Efficient Access to 2-Bromo-4-methoxyaniline. *Synthetic communications* **1997,** *27* (20), 3525-3527.
18. Ando, W.; Tsumaki, H., Synthetic Application of Aminosilanes: Selective Bromination of Anilines via Reaction of Anilinosilanes with N-Bromosuccinimide. *Synthesis* **1982,** *1982* (04), 263-264.
19. Cossy, J.; Poitevin, C.; Pardo, D. G.; Peglion, J., An Easy and Efficient Access to 2-Bromo-4-methoxyaniline. *Synthetic communications* **1997,** *27* (20), 3525-3527.
20. McKillop, A.; Sanderson, W. R., Sodium perborate and sodium percarbonate: cheap, safe and versatile oxidising agents for organic synthesis. *Tetrahedron* **1995,** *51* (22), 6145-6166.
21. Mehta, S. M.; Vakilwala, M. V., Sodium Perborate as a Reagent in Organic Chemistry. I. Preparation of Azo-Compounds. *Journal of the American Chemical Society* **1952,** *74* (2), 563-564.
22. Huestis, L., Sodium perborate oxidation of an aromatic amine. *Journal of chemical education* **1977,** *54* (5), 327.
23. McKillop, A.; Tarbin, J. A., Sodium perborate-a cheap and effective reagent for the oxidation of anilines and sulphides. *Tetrahedron Letters* **1983,** *24* (14), 1505-1508.
24. Cuadro, A. M.; Alvarez-Buila, J., 4, 5-Dichloro-1, 2, 3-dithiazolium chloride (Appel's Salt): Reactions with N-nucleophiles. *Tetrahedron* **1994,** *50* (33), 10037-10046.
25. Umbreit, M.; Sharpless, K., Allylic oxidation of olefins by catalytic and stoichiometric selenium dioxide with tert-butyl hydroperoxide. *Journal of the American Chemical Society* **1977,** *99* (16), 5526-5528.
26. Rabjohn, N., Selenium dioxide oxidation. *Organic Reactions* **1949**.

27. Ito, K.; Nakajima, K., Selenium dioxide oxidation of alkylcoumarins and related methyl-substituted heteroaromatics. *Journal of heterocyclic chemistry* **1988,** *25* (2), 511-515.

28. Wang, E.-C.; Lin, G.-J., A new one pot method for the conversion of aldehydes into nitriles using hydroxyamine and phthalic anhydride. *Tetrahedron letters* **1998,** *39* (23), 4047-4050.

29. Sharma, D. K.; Adams Jr, S. T.; Liebmann, K. L.; Miller, S. C., Rapid Access to a Broad Range of 6'-Substituted Firefly Luciferin Analogues Reveals Surprising Emitters and Inhibitors. *Organic letters* **2017,** *19* (21), 5836-5839.

Chapter 5

Synthesis and Evaluation of D-Thioluciferin Bioluminescence

Abstract

D-Luciferin is the light emitting molecule responsible for the bioluminescence observed in the American Firefly *Photinus pyralis*. Modifications to the natural substrate have resulted in new luminogenic substrates with often improved properties that have been exploited in the development of sensitive luciferin-based probes for in vivo imaging. Most of these probes however, are based on the release of either natural D-luciferin or a 6'-amino analogue thereof. This has limited D-luciferin based applications, particularly in terms of linking bioluminescence and sulfur biology. To date, there are only a few reported examples of bioluminescent probes used in cellular redox imaging and, as previously mentioned, all known D-luciferin bioluminescent technologies are derived from either D-luciferin or it's amino analogue. In an effort to provide a new functional luciferin analogue, a 6'-thiol derivative was investigated.

Herein, a relatively short synthetic route toward the 6'-thiol analogue of D-luciferin is reported. The synthetic route is based on a thiol-protecting group strategy, which allowed for the rapid preparation the 6'-thiol analogue, aptly named D-thioluciferin. D-Thioluciferin was successfully synthesised over five steps (34 % yield) using a thioacrylate protecting group strategy, where the new luminogenic substrate displayed a lower K_m (0.1 µM relative to the 8 µM of D-luciferin) and a more red-shifted maximum emission (λ_{max} 600 nm compared to the 557 nm of D-luciferin), but with a much lower luminescent output relative to D-luciferin. Overall, it was found to be a promising alternative to existing luminogenic technologies.

Chapter 5

Synthesis and Evaluation of D-Thioluciferin Bioluminescence

Introduction

When White first synthesised D-luciferin, he ushered in the era of bioluminescence assays and bioluminescence imaging (BLI). His subsequent work involved changing the 6'-hydroxyl of D-luciferin to an amine, to birth D-aminoluciferin. Similarly, D-aminoluciferin's arrival was accompanied by an exponential increase in the development of luciferin-based assays where the amine moiety was used as a link to construct probes based on amide hydrolysis. Since then, many different derivatives have been prepared by various research groups in an effort to yield new bioluminogenic substrates and probes that may be applied in bioimaging. However, all of the derivatives are based on modifications of either the natural (6'-hydroxy) D-luciferin or D-aminoluciferin, limiting their utility to *O* and *N*-linked chemistry.

In Chapter 4, it was proposed that a 6'-thio analogue of D-luciferin would be of interest since its preparation would allow for the evaluation of the effects of replacing the 6'-oxygen with sulfur. The effects of replacing the 6'-oxygen with nitrogen on the bioluminescent reaction have already been demonstrated and these results, coupled with the bioluminescence data from a 6'-thio analogue, could provide further insight into how the 6'-heteroatom of D-luciferin effects the photobiology. In addition, if the thiol were prepared and was found to be bioluminescent, then it would undoubtedly pave the way for the generation of novel bioluminescent probes, which may find application in areas where D-luciferin and D-aminoluciferin could not easily be applied.

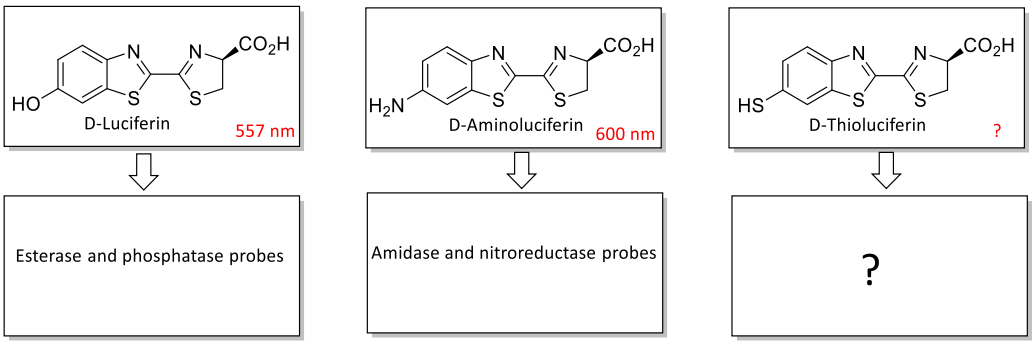

Figure 5.1. Structures of D-luciferin, D-aminoluciferin and D-thioluciferin and select examples of luciferin-based applications

Replacing oxygen with nitrogen and sulfur

The heteroatom substitution induced changes in the photophysical properties of many well-known chromophores have been investigated to both better understand the photophysics and, to allow for improved or novel applications. In publications concerning fluorescent chalcogenxanthylium dyes, it was demonstrated that replacement of the oxygen by a sulfur heteroatom resulted in the increase in the fluorescence emission maxima (Figure 5.2), this was reportedly due to a decrease in oscillator strength of the $S_o - S_1$ transition as a result of having replaced the oxygen with a heavier atom, potentially via the heavy-atom effect.[1-2] The heavy-atom effect is the enhancement of the rate of a spin-forbidden process by the presence relatively heavy atom, which is either part of, or external to, the excited molecular entity.[3]

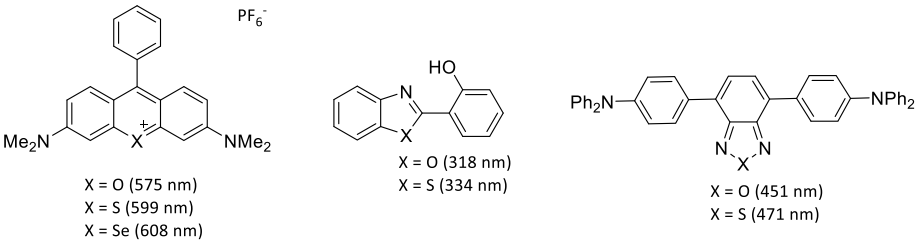

Figure 5.2 Examples of fluorescent compounds demonstrating the effects of heteroatom substitution on the fluorescence emission maxima

In addition to empirical investigations, a number of TD-DFT studies have also looked into the effects of the heteroatom substitution on the photophysical properties of heteroaromatic fluorescent molecules, of which some examples are shown (Figure 5.2).[4-5] These studies found that, in general, a more red-shifted fluorescence emission maxima was observed when replacing oxygen with sulfur and, that the shift in emission maxima was related to a decrease in the energy difference between the excited and ground state energy levels. It is of course already well known that the highest molecular orbitals (HOMOs) and lowest unoccupied orbitals (LUMOs) of the ground and excited state energy levels are important, not only to the spectral properties of the compound, but also to its reactivity.

These same energy differences that govern the fluorescence emission maxima are also responsible for the observed bioluminescence emission maxima in bioluminescent reactions. The results from these fluorescent investigations are therefore also relevant to bioluminescence, since the effects of heteroatom substitution on the relative energies of the excited and ground state would be the same, while the source of energy resulting in excitation is different. Thus, it was predicted that D-thioluciferin, if found to be luminescent active, would display more-red shifted luminescence emission maxima, when compared to D-luciferin.

Aims and Objectives

The aim was to synthesise a 6'-thio analogue of D-luciferin and to evaluate its bioluminescence. If the analogue did retain luminescent activity, it would be further evaluated to determine the effects of the thiol on the wavelength of maximum emission and K_m for purified *Ppy* luc (expressed from *E. coli*). In addition, the fluorescence properties of D-thioluciferin were also to be explored, along with the effects of thiol oxidation on its luminescent activity.

The specific objectives were thus:

i) The synthesis and characterisation of D-thioluciferin using standard analytical and spectroscopic techniques.

ii) The evaluation of D-thioluciferin bioluminescence using purified luciferase expressed from *E. coli* (including the determination of its λ_{max}, K_m, burst Kinetics profile and emission half-life).

iii) The evaluation of D-thioluciferin sulfide and disulfide bioluminescence using purified luciferase expressed from *E. coli*

iv) The evaluation of D-thioluciferin fluorescence.

Retrosynthesis of D-Thioluciferin

2-Cyano-6-iodobenzothiazole was identified as a key intermediate for D-thioluciferin synthesis, where the iodo-functionality would act as a surrogate group that would later allow access to the thiol moiety. However, the synthesis of D-thioluciferin would first be attempted via methodologies formerly used in the synthesis of D-luciferin and D-aminoluciferin by Prescher et al. The synthesis would aim to utilise 2-cyano-6-iodobenzothiazole as a key intermediate, where its preparation would involve the condensation, fragmentation and cyclisation of Appel's salt and 4-iodoaniline (Scheme 5.1, Route A).

It was already demonstrated (in Chapter 4) that the 2-cyano-6-iodobenzothiazole intermediate could be accessed using an alternate approach from the benzothiazole carboxaldehyde precursor (Scheme 5.1, Route B). While this route did allow for the successful preparation of 2-cyano-6-iodobenzothiazole, it afforded the product in a low 6-8 % yield. It was therefore of interest to evaluate the Prescher method of benzothiazole preparation for comparison and, in doing so, perhaps demonstrate how *o*-bromination could be used to improve the overall synthesis of this new luciferin.

From the 2-cyano-6-iodobenzothiazole, the thiol functionality would be accessed using reported aryl-iodide coupling reactions. A general scheme outlining the two possible disconnections is shown in scheme 5.1.

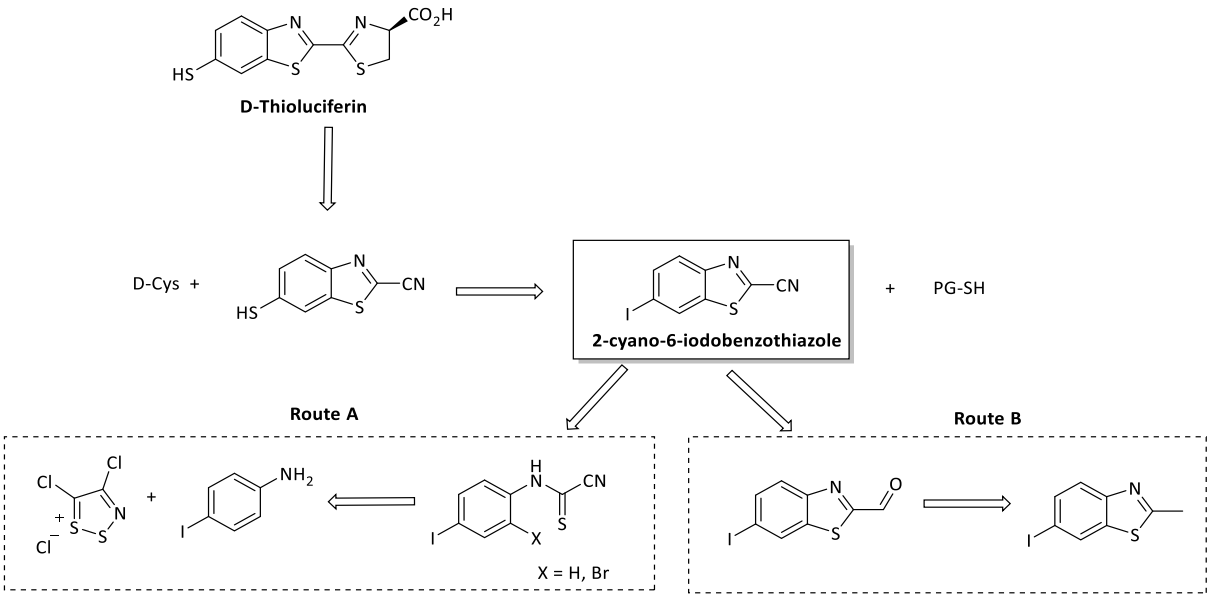

Scheme 5.1. Retrosynthesis of D-thioluciferin

Synthesis of D-Thioluciferin

Iodo-Surrogate Strategy (Route A)

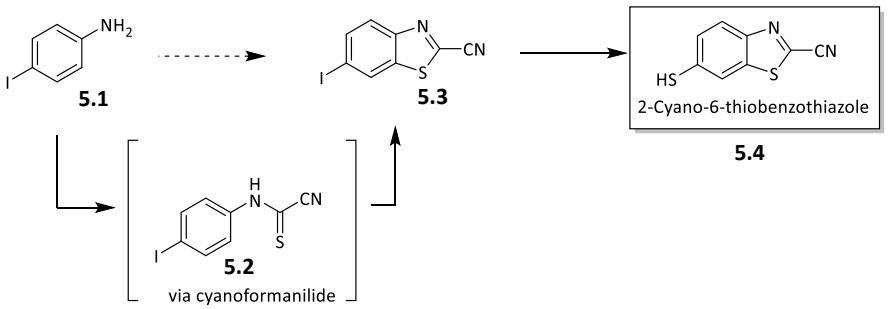

Scheme 5.2. Proposed synthesis of 2-cyano-6-thiobenzothiazole **5.4** from 2-cyano-6-iodobenzothiaole **5.3**

The conversions of aryl-iodides to aryl-thiols are well documented.[6] Typically, the reactions are carried out at high temperatures (100-150 °C), in polar aprotic solvents, in the presence of a palladium(II) and/or copper(I) catalysts and a nucleophilic source of sulfur. Thus, the iodo precursor **5.3** was prepared with the intention that it could be transformed into the desired aryl-thiol. The synthesis of the iodobenzothiazole started from the reaction of the *p*-iodoaniline with previously prepared Appel's salt to afford a dithiazolimine, which was further fragmented to afford the cyanoformanilide **5.2**. The isolated dithiazolimine and the fragmented product **5.2** were characterised by NMR and IR spectroscopy, as well as LRMS.

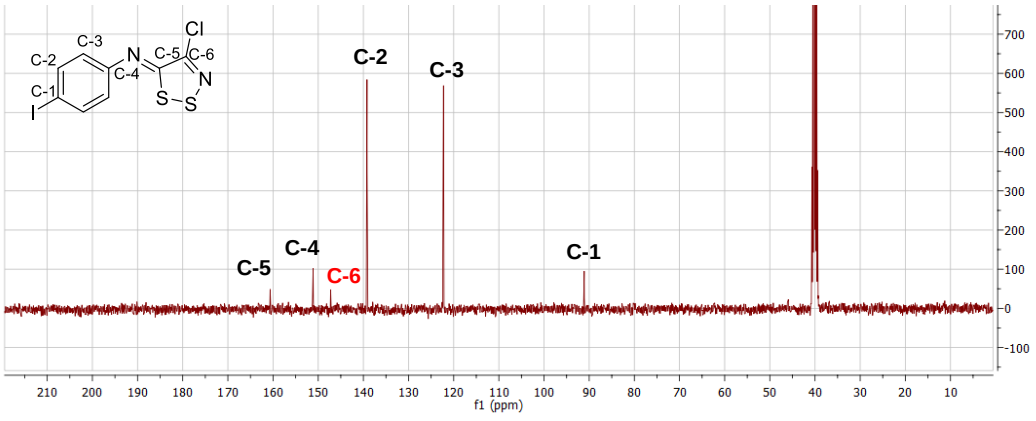

Figure 5.3. ^{13}C-NMR spectrum of dithiazolimine in DMSO

The ^{1}H-NMR spectrum of the dithiazolimine displayed the doublet of doublets expected of a 1,4-substituted phenyl ring and the ^{13}C-NMR spectrum displayed the correct six carbon resonances.

The ^{13}C-NMR spectrum of the fragmented iodo-nitrocyanoformamide **5.2** in DMSO is shown in figure 5.4. The spectrum displayed a conspicuous resonance at 114.7 ppm due to the carbon of the nitrile

(note C-6 in figures 5.3 and 5.4). A similar signal was observed in the ^{13}C-NMR spectra of the methoxy and nitro analogues. A clear doubling of all the NMR resonances were also observed in the spectra, this was most likely either due to the interconversion of **5.2** between its tautomeric (thione-thiol) forms or the existence of rotamers, previously observed in D-luciferin and D-aminoluciferin syntheses.

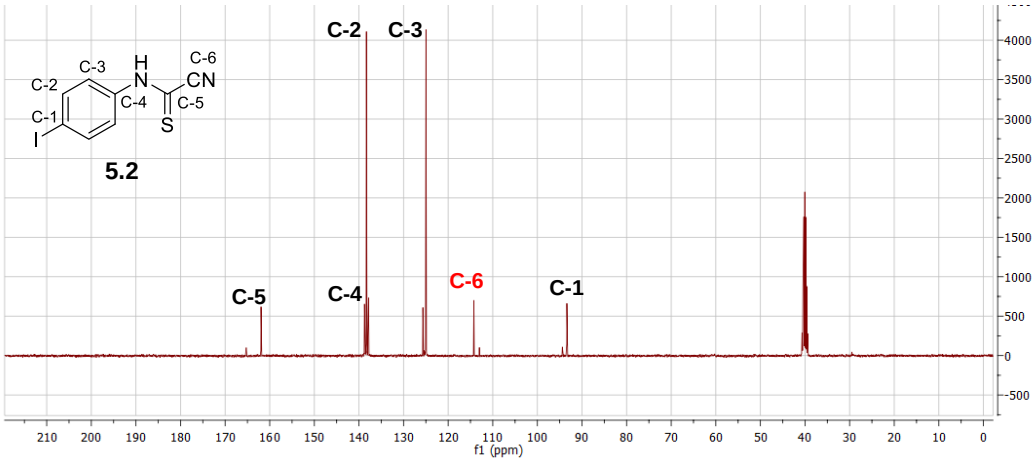

Figure 5.4. ^{13}C-NMR spectrum of **5.2** in DMSO

With the iodo-nitrocyanoformamide **5.2** successfully prepared, an intra-molecular C-S cross-coupling reaction was attempted to form the benzothiazole (Scheme 5.3). Initially, there were concerns that the iodo would be reactive under the cross-coupling conditions which could result in the unwanted formation of inter-molecular cross-coupling products. However, Hrobàrik et al had already demonstrated an oxidative coupling on a similar system where the correct, cyclised product was predominantly formed and isolated in moderate yield (60 %).[7]

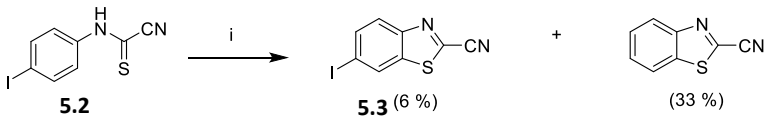

Scheme 5.3. Reagents and conditions: i) $PdCl_2$ / CuI / TBAB / DMF:DMSO (1:1) / 120 °C / 4 h

The reaction was thus carried out and TLC analysis revealed the formation of two non-polar products. The compounds were isolated by standard silica chromatography and the structures determined by spectroscopic and analytical techniques. The less polar product isolated was unsubstituted 2-cyanobenzothiazole, based on LCMS and NMR spectroscopy, and was also the major product formed from the reaction (33 %). The other product was the desired 2-cyano-6-iodobenzothiazole **5.3** which was isolated in very low yield (6 %). The remaining material (61 %) was highly water soluble and could not be effectively isolated from the aqueous phase, presumably because the nitrile moiety had been hydrolysed.

The formation of the unsubstituted benzothiazole was surprising but also very interesting since Hrobàrik did not make mention of such unwanted side reactions. In addition, the substitution of the C6-iodo group with hydrogen necessitates a hydride source which was difficult to rationalise from the reagents used. It once again become apparent at this point that the oxidative C-S cross-coupling reaction was perhaps not the best methodology for benzothiazole synthesis, since poor yields were generally observed in the different luciferin syntheses and, it was particularly limiting with regards to the iodo-precursor where a generally poor yield was made worse because of the formation of the unsubstituted 2-cyanobenzothiazole. Nevertheless, enough material of the 2-cyano-6-iodobenzothiazole was obtained for characterisation and its ^{1}H-NMR spectrum is shown in figure 5.5.

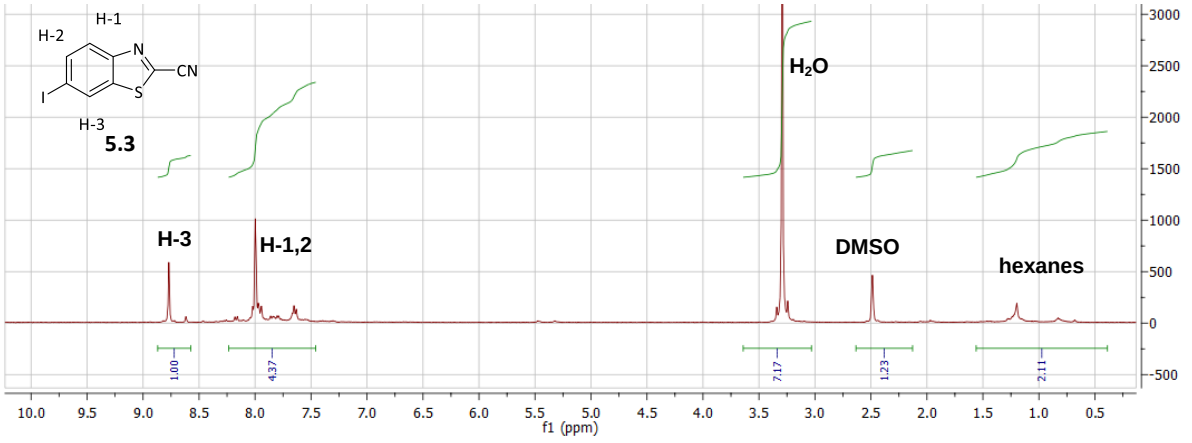

Figure 5.5. ^{1}H-NMR spectrum of 2-cyano-6-iodobenzothiazole **5.3** in DMSO

The ^{1}H-NMR spectrum alone could not be used as conclusive evidence for the successful synthesis of the cyanobenzothiazole **5.3**. The spectrum displayed a singlet integrating for one proton and another set of signals integrating for roughly four protons, that could support the presence of a C6-substituted benzothiazole. The IR spectrum of **5.3** revealed a weak peak at 2200 cm^{-1}, corresponding to the nitrile C-N stretch, further supporting the formation of **5.3**. The mass spectrum, unfortunately, did not display a mass ion peak corresponding to the molecular weight of **5.3** and could therefore not confirm that the cyclisation was successful. It did however display a mass ion peak corresponding to the molecular weight of the unsubstituted benzothiazole (M^{+}-I). Although the sequence did not conclusively produce the desired 6-iodo-2-cyanobenzothiazole, it did produce some interesting results with regards to the influence of C6-substitution on the cyclisation reaction.

Since the Prescher et al method did not efficiently nor conclusively allow access to the 6-iodo-2-cyanobenzothiazole, it provided the perfect opportunity to apply the recently developed one pot, metal-free base-mediated cyclisation (Scheme 5.4).

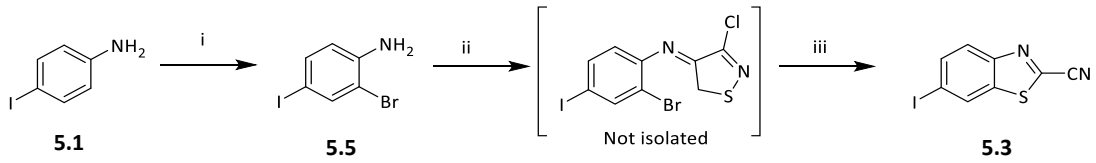

Scheme 5.4. one pot, metal-free base-mediated cyclisation from *o*-bromoaniline; reagents and conditions: i) $NaBO_3$ / KBr / AcOH / rt / 16 h, 78 % ii) Appel's salt / DCM / 3 h, iii) DBU / DCM / 5 ^oC / 3-4 h, 67 %

2-Cyano-6-iodobenzothiazole was afforded in a good yield of 67 %, using the one-pot metal free method, starting from 2-bromo-4-iodoanilne **5.5**. The reaction proved to be superior to both the Prescher et al reaction (6 % of **5.3**), as well as the SN_2Ar sequence described in Chapter 4 (8 %). The iodobenzothiazole was then reacted under standard coupling conditions in an attempt to produce the thiobenzothiazole **5.4** (Scheme 5.5).

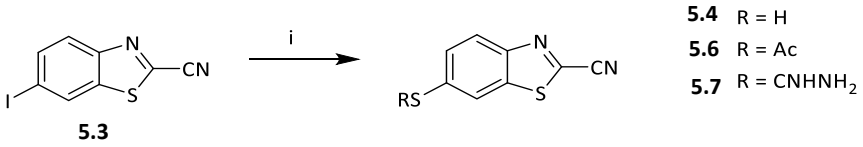

Scheme 5.5. Reagents and conditions: R = H; i) CuI / Sulfur powder / K_2CO_3 / DMF / 90 ^oC / $NaBH_4$, R = Ac; i) $Pd(OAc)_2$ / KSAc / DPPF / NaOtBu / dioxane / 100 ^oC or Pd_2dba_3 / KSAc / DPPF / DIPEA / toluene / reflux and, R = $CHNNH_2$; i) CuI / thiourea / PEG / K_2CO_3 / 100 ^oC[6, 8]

Various reported methods for the conversion of aryl-iodides to thiols and thioesters were attempted but none afforded the C6-thio derivative. This was presumably due to the reactivity of the C2-nitrile functionality, which may have reacted with the sulfur reagents in a manner similar to its reaction with D-Cys. The argument that the C6-nitrile was responsible for preventing the formation the thiobenzothiazoles **5.4**, **5.6**, and **5.7** was later supported by Miller et al, who noted that the reactivity of the C2-nitrile moiety was indeed a challenge in C6-halide substitution.[9]

For the time being, the 2-cyano-6-iodobenzothiazole surrogate strategy was abandoned and focus was shifted to other potential methodologies.

Diazotization Strategy

Following on the unsuccessful attempted C6-iodo substitution, an alternative surrogate group was considered. Diazotization was attempted using previously prepared 6-amino-2-cyanobenzothiaozole, shown in scheme 5.6. The amine was reacted with sodium nitrite in concentrated HCl to produce the diazonium salt that was then reacted with potassium thioacetate and thiourea in separate reactions. Both reactions proceeded similarly and in both instances the products formed from the reaction could not be extracted from water, presumably because the nitrile had been hydrolysed to the acid.

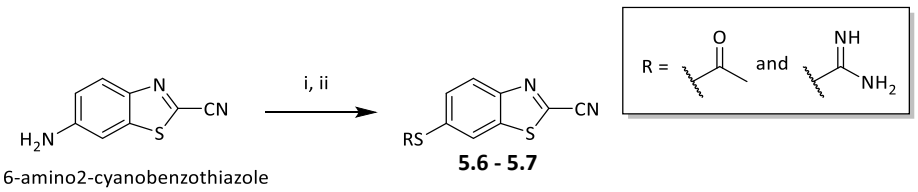

Scheme 5.6. Diazotization of 6-amino-2-cyanobenzothiazole. Reagents and conditions: i) $NaNO_2$ / $HCl_{conc.}$ / -5 °C / 40 min, ii) KSAc or Thiourea / 30 min

_S_-Protection Strategy

Since attempts at introducing the thiol functionality via the iodo and amino surrogate groups failed, its preparation was next attempted with the sulfur functionality in place, pre-benzothiazole formation. Thus, the synthesis of D-thioluciferin was tried using a protected sulfur starting material and the Appel's salt methodologies employed in the preparation of D-luciferin and D-aminoluciferin. The proposed synthesis of thioluciferin is shown in scheme 5.7. In the syntheses of D-luciferin and D-aminoluciferin, the nucleophilic C6'-hydroxyl and C6'-amine functionalities were introduced as protected/masked groups and liberated only after cyanobenzothiazole formation, by *O*-methyl deprotection and nitro reduction, respectively. Similarly, in the synthesis of D-thioluciferin a protecting group strategy using triphenylmethyl chloride (trityl chloride) was proposed. This was chosen on the basis of the starting material that was available, *p*-aminothiophenol **5.8**, which would require a protecting group that would selectively protect the thiol in the presence of the amine. There are a number of reported methods for such chemoselective reactions, most of which exploit the basicity of the amine to achieve the desired selectivity.[10-11] Practically, this means that the thiol is protected in acidic media, wherein the amine is protonated to form the less nucleophilic ammonium salt. In addition to being selective, the trityl group was chosen because it was predicted to be relatively stable in mildly basic reaction conditions and could easily be removed by treatment with trifluoracetic acid.

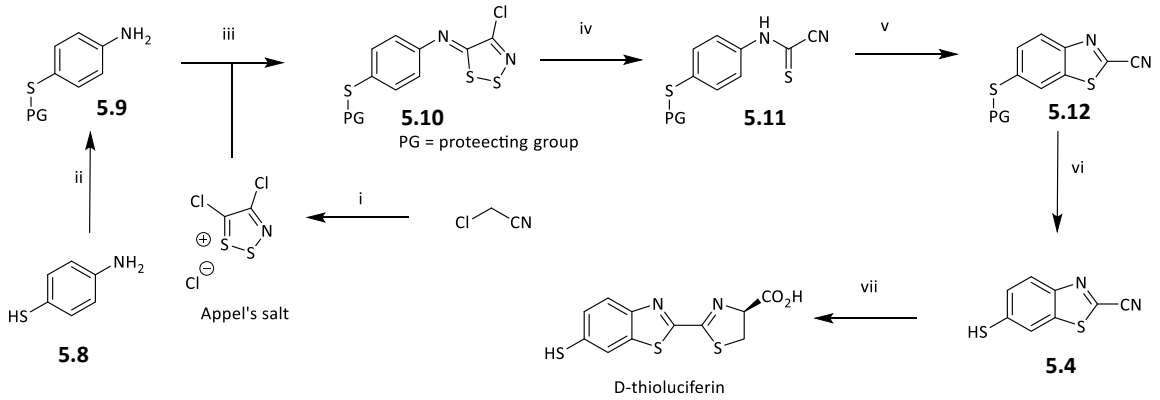

Scheme 5.7. Proposed synthesis of D-thioluciferin. Reagents and conditions: i) S_2Cl_2 / DCM / rt, ii) PG addition, iii) Appel's salt / DCM / Py / rt, iv) DBU / DCM / 5 °C, v) $PdCl_2$ / CuI / TBAB / DMF:DMSO (1:1) / 120 °C, vi) TFA / DCM / rt, vii) D-Cys / K_2CO_3 / MeOH:H_2O (7:3) / rt

To form the *S*-protected aniline, an *S*-trityl group was introduced. The S-trityl was however not stable to chromatography and all attempts at isolating the protected thiol made it increasingly clear that the *S*-tritylated aminothiophenol was indeed not stable, and that perhaps an alternive protecting group should be considered. The chemoselective acetylation of aminothiophenol was thereafter attempted using a mixture of acetic acid and acetic anhydride. Here, the amine reacted almost exclusively despite literature reporting otherwise.[10] This method was thus also abandoned.

Homodisulfide Protecting Group Strategy

As a result of the failed previous attempts at *S*-protection, a somewhat unrelated strategy involving the protection of the thiol as a disulfide was pursued. This strategy was appealing because it too exploited differences in the chemical reactivity between the thiol and amino functionalities, in that the free thiol could easily be oxidised to the symmetrical disulfide (Scheme 5.8).

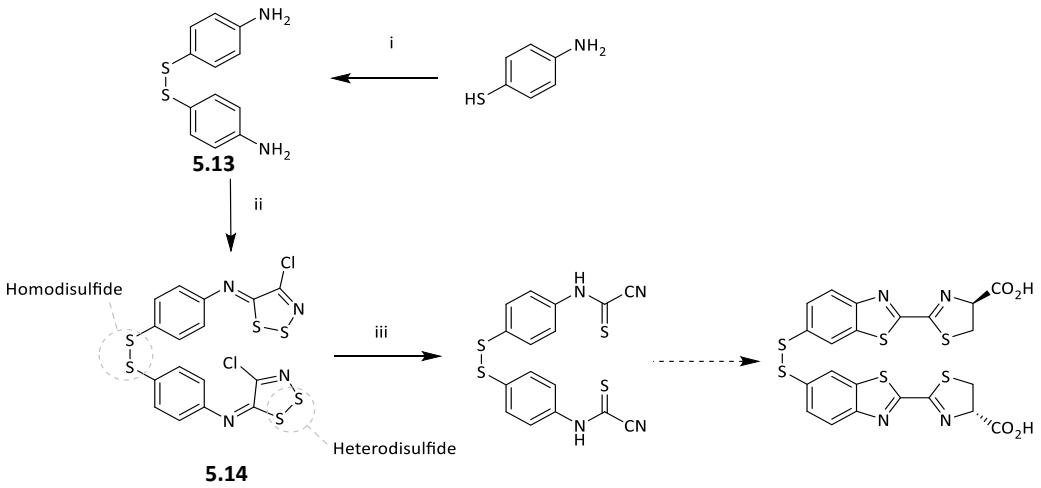

Scheme 5.8. Proposed synthesis of D-thioluciferin disulfide. Reagents and conditions: i) $NaBO_3$ / AcOH / H_2O / rt / 48 h, (98%) or i) I_2 / DMSO:$CHCl_3$ (1:1)/ rt / 4 h (93%), ii) Appel's Salt / DCM / Py / rt / 4h, (68%) iii) DBU / DCM / 5 °C / 1 h

To achieve the desired oxidation, *p*-aminothiophenol was stirred in a solution of $NaBO_3$, acetic acid and water to generate the disulfide **5.13**. The structure of the disulfide **5.13** was confirmed by ^{1}H- and ^{13}C-NMR spectroscopy, and was further supported by mass spectrometry in which a mass ion peak corresponding to the calculated molecular weight of **5.13** was observed. The disulfide was then reacted with Appel's salt afford the corresponding dithioazolimine **5.14** in good yield (68 %). The subsequent base mediated fragmentation proved to be very problematic, possibly due to the large excess of DBU used (6 eq), and/or chemoselectivity issues arising from having two distinct disulfide moieties within the molecule, namely; the hetero-disulfide of the dithiazolimine and the homo-aryldisulfide.[12] A publication on the DBU-Mediated cleavage of aryl- and heteroaryl disulfides demonstrated that DBU, in addition to fragmenting the dithiazolimines, could also reduce aryl-disulfides (Scheme 5.9). Interestingly, that publication was the first to report DBU as a nucleophile in the direct cleavage of aryl-disulfides and, to date, remains one of only a few literature examples demonstrating the lesser known thiophilic character of DBU.

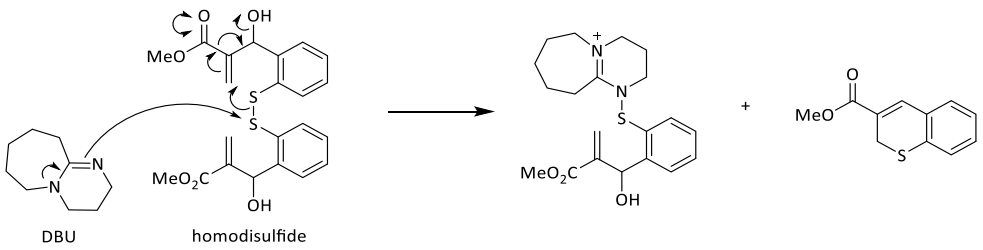

Scheme 5.9. Example of a DBU mediated cleavage of aryl-homodisulfides[12]

LCMS of the crude reaction mixture of the DBU mediated fragmentation of **5.14** did not display a mass ion peak corresponding to the molecular weight of the fragmented product, and various attempts at isolating defined products were unsuccessful. Ultimately, the homo-disulfide thiol protecting strategy was also abandoned.

Synthesis of D-thioluciferin vinyl sulfide via a thioacrylate protecting group

Most of the challenges that manifested in the previously described attempted syntheses of D-thioluciferin were largely due to the incompatibility of the employed synthetic methodologies with the free thiol, protected thiol, and/or disulfide in various reactions. The free thiol was too reactive in the presence of Appel's salt and could not be used directly, acid sensitive protecting groups (such as trityl) were not tolerated and the acylated thiol (or thioester) could not be selectively formed in the presence of the free amine. Furthermore, the same reaction that forms the benzothiazole from thioamides also generates benzothiofuran from thioesters. A surrogate group such as the C6'-iodo proved challenging to prepare as well and the disulfide strategy also presented issues concerning chemoselectivity in the fragmentation reaction, requiring a much larger excess of DBU and was therefore abandoned. The sulfides were generally not considered an option since harsh conditions would have been required to free the thiol. However, vinyl sulfides in the form of thioacrylates are reported to be readily reactive in the presence of *S*-nucleophiles and were therefore of interest, even though their use as protecting groups had not been reported.[13-14]

Interestingly, the idea of using a thioacrylate as a protected thiol to synthesise thioluciferin came about from the design of a thiol/thiolate sensing probe (discussed in more detail in Chapter 6). Scheme 5.10 shows the proposed mechanism of D-thioluciferin release in response to a reactive thiolate. The irreversible release of the less reactive aryl thiol (in this case D-thioluciferin) would be driven by the greater nucleophilicity of the incoming thiolate which forms a relatively more stable thioacrylate when compared to D-thioluciferin.

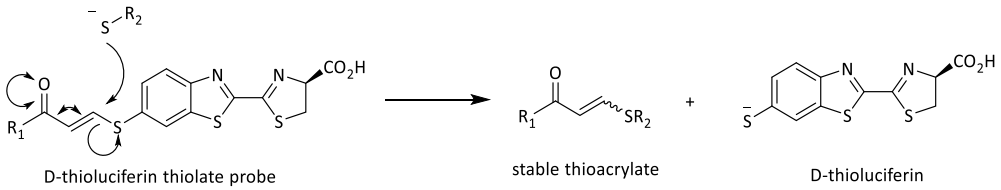

Scheme 5.10. D-Thioluciferin probe and the proposed mechanism for thiolate mediated release of D-thioluciferin

This meant that the thioacrylate could be prepared from *p*-aminothiophenol which could then be converted to D-thioluciferin and released upon reaction of the vinyl sulfide moiety with an alkyl

thiolate. Furthermore, it was hypothesised that D-Cys could be used to simultaneously both form and release D-thioluciferin. The synthesis involved the formation of the vinyl-sulfide functionality (thioacrylate) using the well-known thiol-yne (also known as the "thio-click") reaction. The reaction normally involves an alkyne and an aryl- or alkyl-thiol reacted in the presence of a radical initiator in cases where the -yne moiety is not directly conjugated to a carbonyl. For this reaction, *p*-aminothiophenol was reacted with propiolic acid to form a vinyl sulfide **5.16**, where the free amine would later be used to construct the rest of the luciferin molecule, scheme 5.11.

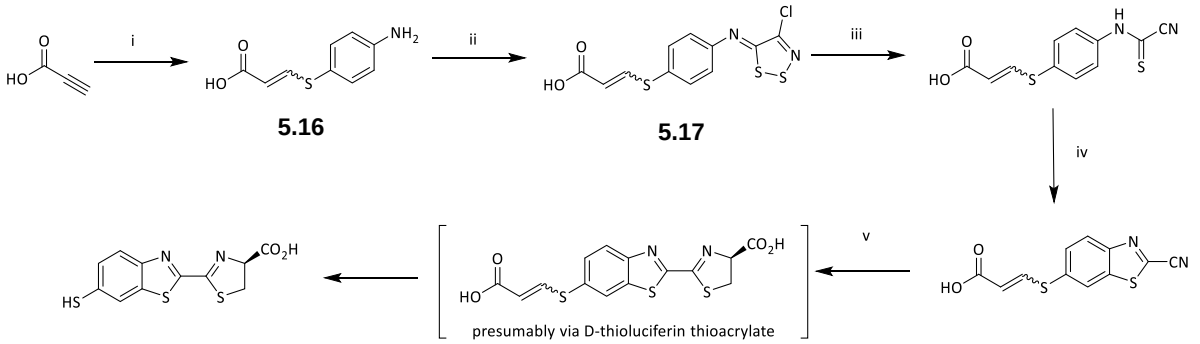

Scheme 5.11. Reagents and conditions: i) *p*-Aminothiophenol / DMF / rt / 24 h, (30%), ii) Appel's salt / DCM / Py / rt / 3 h, (99%), iii) DBU / DCM / 5 °C / 30 min, iv) $PdCl_2$ / CuI / TBAB / DMSO / 120 °C / 4 h, v) D-Cys / K_2CO_3 / DMSO:H_2O (2:1) / rt / 20 min

It should be noted that the sequence starts off with the doubly nucleophilic *p*-aminothiophenol instead of *p*-nitrothiopenol or *N*-protected thiophenol. This is because the free thiol is a relatively soft nucleophile when compared to the amine and it was therefore predicted to be more reactive toward the alkyne. This assumption was proven to be correct as none of the vinyl amine was formed from the reaction of *p*-aminothiophenol and propiolic acid, as evidenced by ^{1}H-NMR analysis.

TLC analysis of the reaction revealed two new products observed as two distinct spots that were very close in R_f and significantly more polar than the starting amine. This was thought to be the cis and trans isomers resulting from addition to the alkyne. TLC analysis also showed significant conversion of the starting aminothiophenol to its oxidised disulfide, even under inert conditions. This was observed as the most polar spot and lead to the use of silica chromatography for the purification of the thioacrylate **5.16**. The thioacrylate was easily separated from the disulfide but the cis and trans isomers were not separable. The purified products were characterised by ^{1}H-NMR spectroscopy which showed that the cis:trans ratio was approximately 4:1. To avoid working with a mixture of isomers, the reaction was repeated at 0 and 100 °C. the ^{1}H-NMR spectra of the products isolated from these reactions are shown in figure 5.6.

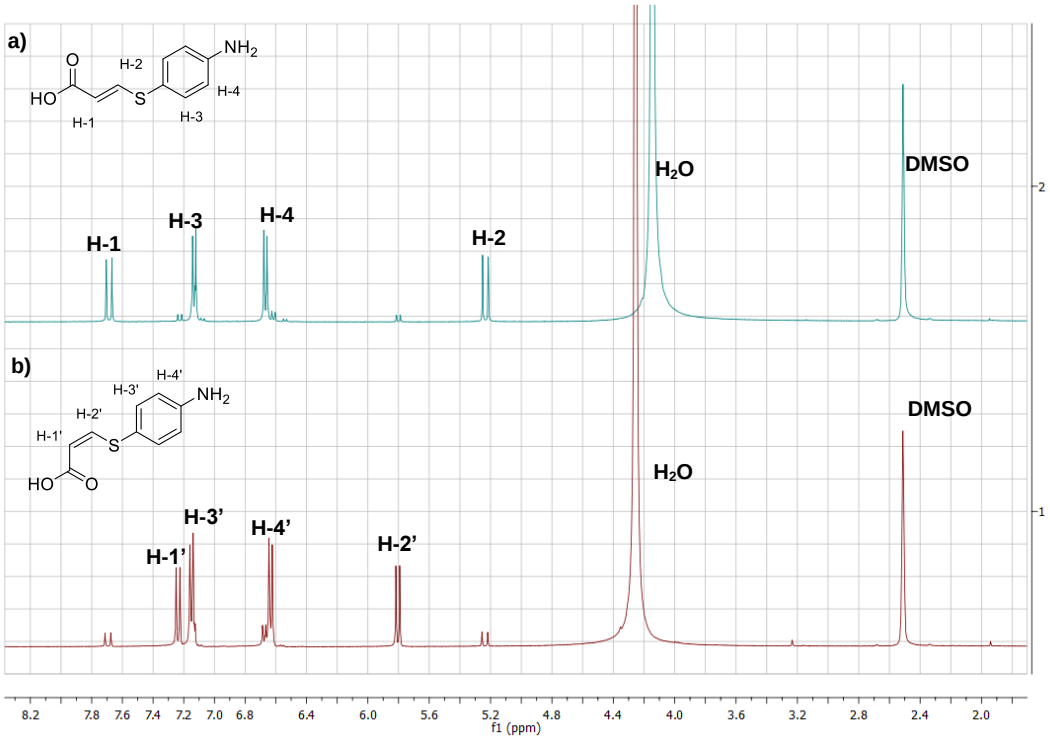

Figure 5.6. ^{1}H-NMR spectra in DMSO (D_2O wash) of mixtures of cis and trans thioacrylate **5.16** isolated from reactions performed at a) 100 °C and b) 0 °C.

At 0 °C less than 10 % of the trans isomer was observed and at 100 °C less than 5 % of the cis isomer was observed, by ^{1}H-NMR spectroscopy, where the cis and trans isomers were distinguishable by their J values for protons H-1/2 (cis *J* = 10.0 Hz, trans *J* = 14.8 Hz). These products corresponded to what was expected for a reaction under typical kinetic/thermodynamic control, where the more stable trans-isomer was favoured at increased temperatures, while the faster formed but less stable cis-isomer is predominately isolated at lower temperature.

Ultimately, neither pure cis nor trans was achieved from temperature control and thus a mixture of isomers were carried over to the next step. The next reaction in the sequence involved using the free amine of the thioacrylate to form an *N*-aryl-iminodithiazole that could be fragmented and cyclised to afford the terminal 2-cyanobenzothiazole. This was done by reacting the amine with an excess of Appel's salt in DMF at room temperature. Again, there was the possibility of Appel's salt reacting with the carboxylate of the vinyl sulfide, but that process has already proven to be reversible, unlike the formation of the imine. The product was isolated as mixture of cis and trans isomers (*E*:*Z* ratio conserved) and the ^{1}H- and ^{13}C-NMR spectra are shown below.

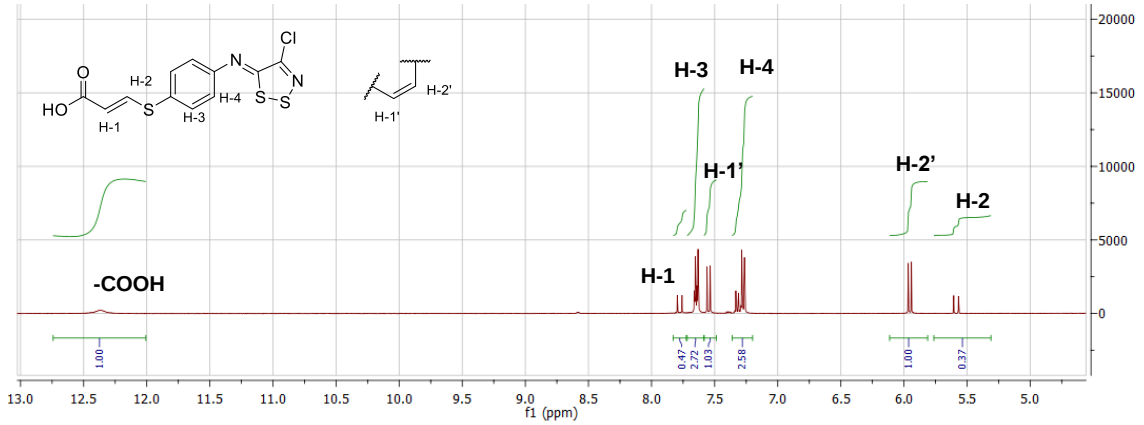

Figure 5.7. ^{1}H-NMR spectrum of **5.17** in DMSO

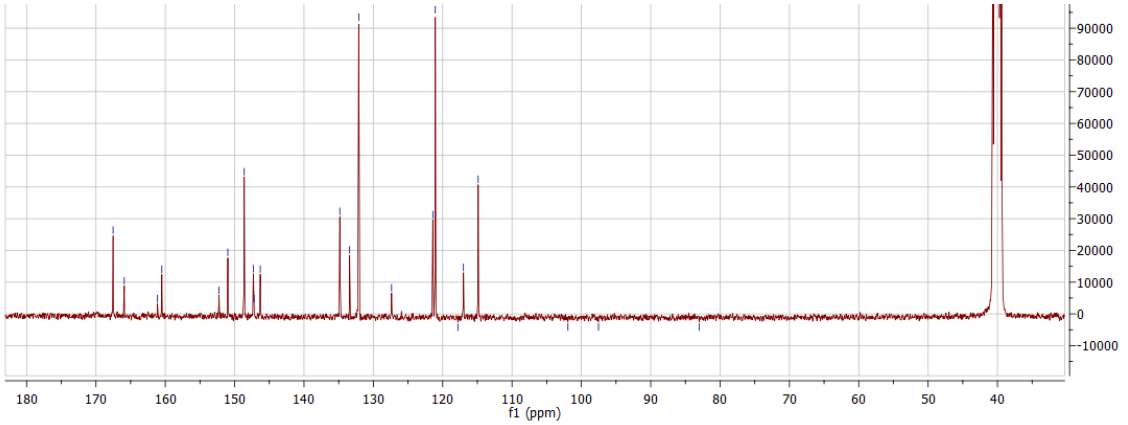

Figure 5.8. ^{13}C-NMR spectrum of **5.17** in DMSO

The ^{1}H-NMR spectrum of **5.17** showed all the expected proton signals, a significant downfield shift in the aromatic protons H-3/4 were also observed relative to the starting material, reasoned to be due to the conversion of the donating amine group to the lesser donating imine functionality. The ^{13}C-NMR spectrum which displayed the expected 18 resonances (9 for each *E* and *Z* isomer), along with a molecular ion peak in the mass spectrum, further supported the successful preparation of the dithiazolimine product. The fragmentation of the diathiazolimine **5.17** was then carried out by slow addition of DBU. Unexpectedly, the fragmented product was highly water soluble and, as a result, could not be easily separated from the polar DBU salts and DBU-thiolane by-product. For this reason, the sequence was attempted again, but this time using a benzyl ester instead of the free acid.

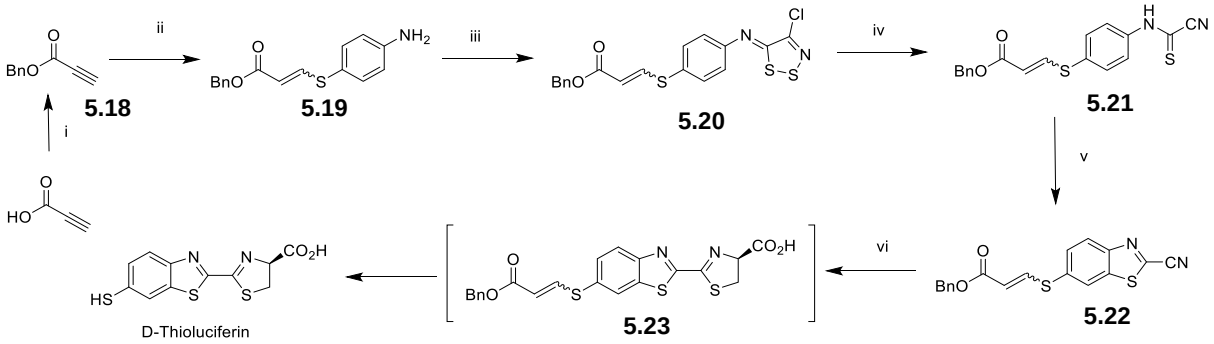

Scheme 5.12. Reagents and conditions: i) BnBr / Cs_2CO_3 / DMF / 0 °C / 2 h, (99%), ii) *p*-aminothiophenol / DMF / rt / 24 h, (39%), iii) Appel's salt / DCM / Py / rt / 3 h, (99%), iv) DBU / DMSO / 5 °C / 30 min, (61%), v) $PdCl_2$ / CuI / TBAB / DMSO / 120 °C / 4 h, (62%), vi) D-Cys / K_2CO_3 / DMSO:H_2O (2:1) / rt / 20 min, (98%)

To ensure that a more hydrophobic product would be produced by DBU fragmentation, the benzyl ester of propiolic acid was prepared. The benzylation was achieved by reacting the carboxylate with benzyl bromide at 0 °C. The ^{1}H-NMR spectrum is shown in figure 5.9 and displayed the correct three expected signals. The ester was then reacted in the same way as the acid to afford the vinyl sulfide.

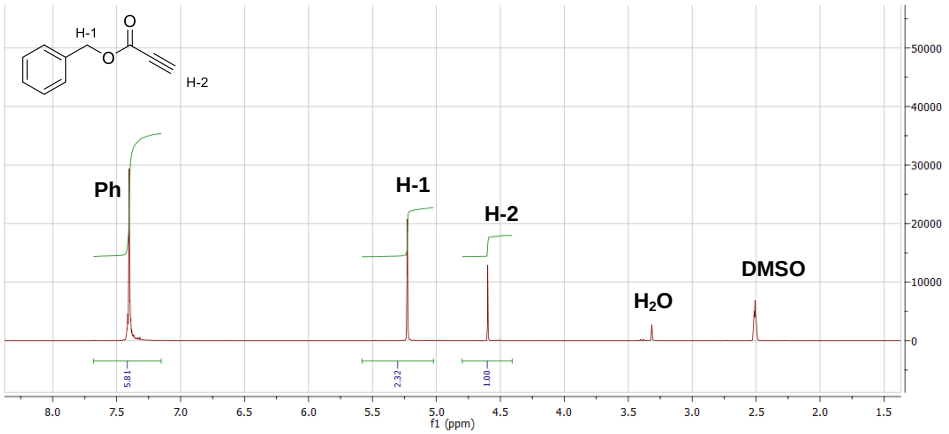

Figure 5.9. ^{1}H-NMR spectrum of benzyl propiolate **5.18** in DMSO

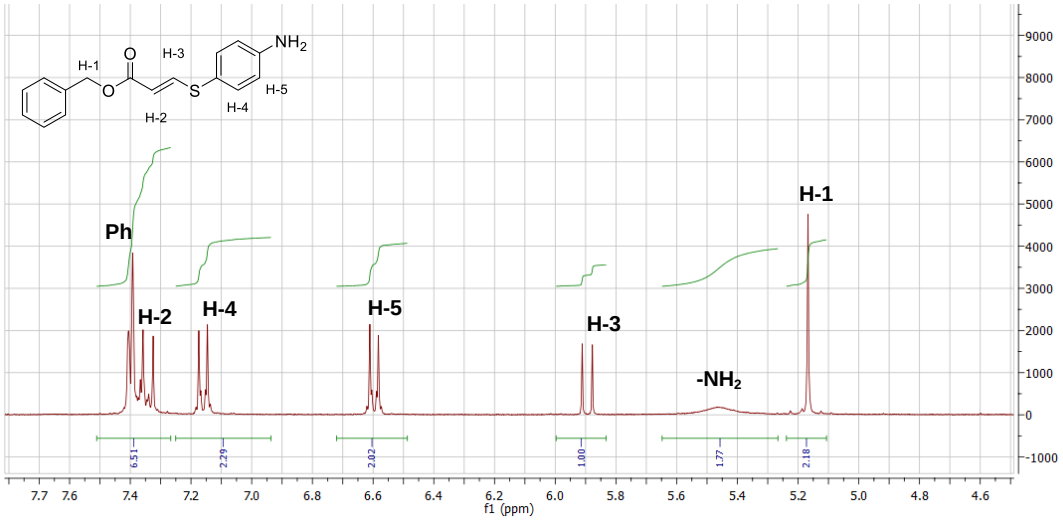

Figure 5.10. ^{1}H-NMR spectrum of the benzyl thioacrylate **5.19** in DMSO

The propiolate ester was allowed to stir with *p*-aminothiophenol in DMF at rt for 24 h. The reaction was monitored by TLC analysis which revealed total consumption of *p*-aminothiophenol. Interestingly, only one of the two possible isomers was formed as revealed by TLC analysis which was subsequently confirmed by NMR spectroscopy. TLC analysis once again showed conversion of aminothiophenol to the more polar disulfide which lead to the use of chromatography for purification. The ^{1}H-NMR spectrum of the benzyl thioacrylate is shown in figure 5.10. The spectrum displayed all the expected proton resonances, confirming that only the trans isomer was formed from the reaction with the ester, based on the coupling constants for the alkenyl protons (H-3/2, J = 15.0 Hz). The steric bulk of the benzyl moiety may have had a directing effect in the formation of the thioacrylate since a mixture of isomers were produced under the same conditions but in the absence of the benzyl. The reaction was also repeated at increased temperature (100 °C) to lessen reaction time. This however, yielded an unexpected result whereby the free amine also reacted with the propiolate ester to form a vinyl amine, observed as a non-polar spot by TLC. The vinyl sulfide-vinylamine product was isolated and fully characterised. Subsequent reactions were then maintained at 25 °C and 24 h, to ensure the formation of only one product. Gratifyingly, this result meant that the next reaction could be attempted using one analytically pure isomer. The dithiazole was then formed from the reaction of the free amine with Appel's salt. The reaction was monitored by TLC which confirmed the formation of a new, relatively non-polar product.

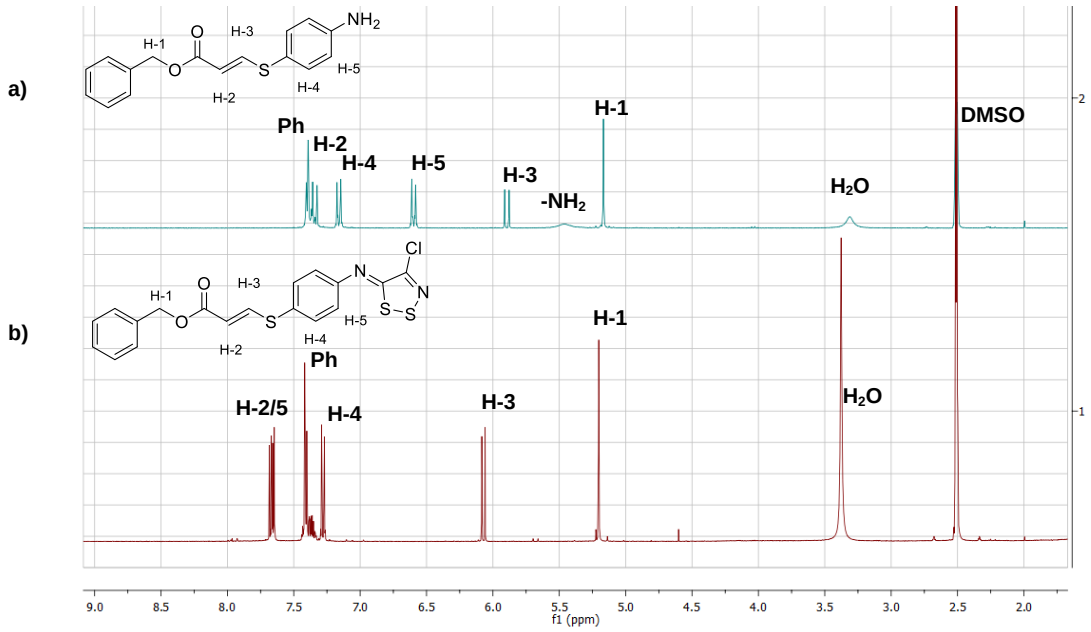

Figure 5.11. ^{1}H-NMR spectra of a) benzyl thioacrylate **5.19** and b) its Appel's salt adduct **5.20** in DMSO

The ^{1}H-NMR spectrum of the benzyl thioacrylate dithiazolimine is shown in figure 5.11. The formation of the dithiazole was supported by the ^{1}H- and ^{13}C- NMR spectra. Most obvious in the ^{1}H-NMR spectrum was the downfield shift of the aromatic protons H-4/5 due to the conversion of the amine to an imine, which was further supported by the absence of the amine resonance at 5.5 ppm, previously observed in the starting material. A reduction in the coupling constant for H-3 (from J = 15.0 to 13.5 Hz) could suggest that complete isomerisation of the double bond had occurred, however the corresponding stereoisomer would have been needed to confirm this and, overall, this was thought to be unlikely. The ^{13}C-NMR spectrum (figure 5.12) further supported the formation of the dithiazole since two more carbon resonances were observed in the spectrum of the product relative to the starting material.

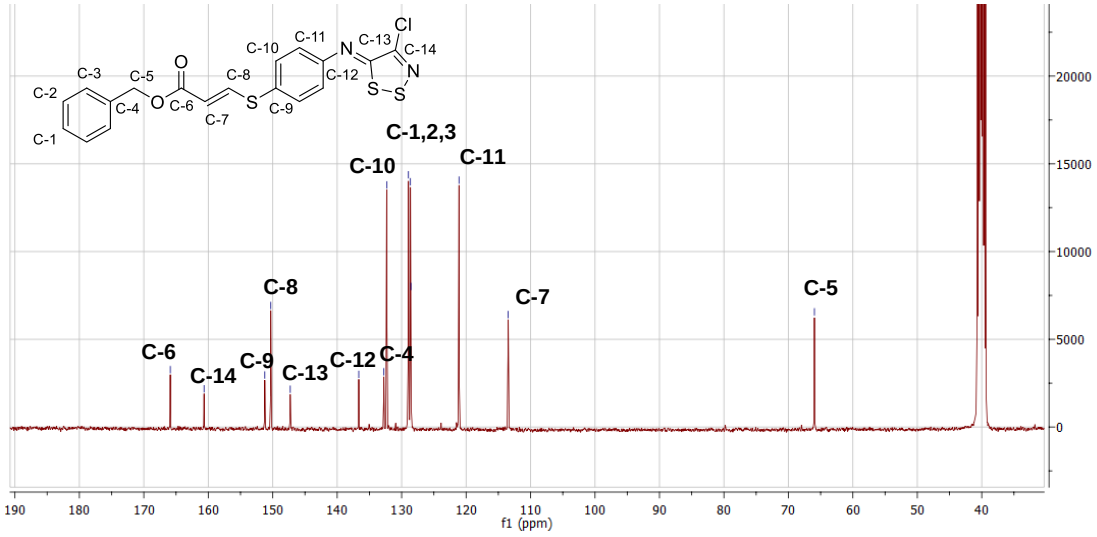

Figure 5.12. ^{13}C-NMR spectrum of the benzyl thioacrylate Appel's salt adduct **5.20** in DMSO

The ^{13}C-NMR displayed the correct 14 resonances expected for the adduct with diagnostic signals observed at 147.3 and 160.7 ppm for the dithiazolimine carbons (C-13, 14). Further support for the successful installation of the dithiazolimine was provided in the mass spectrum, figure 5.13, where a molecular ion peak corresponding to [M+H] at *m/z* 420.9890 was observed.

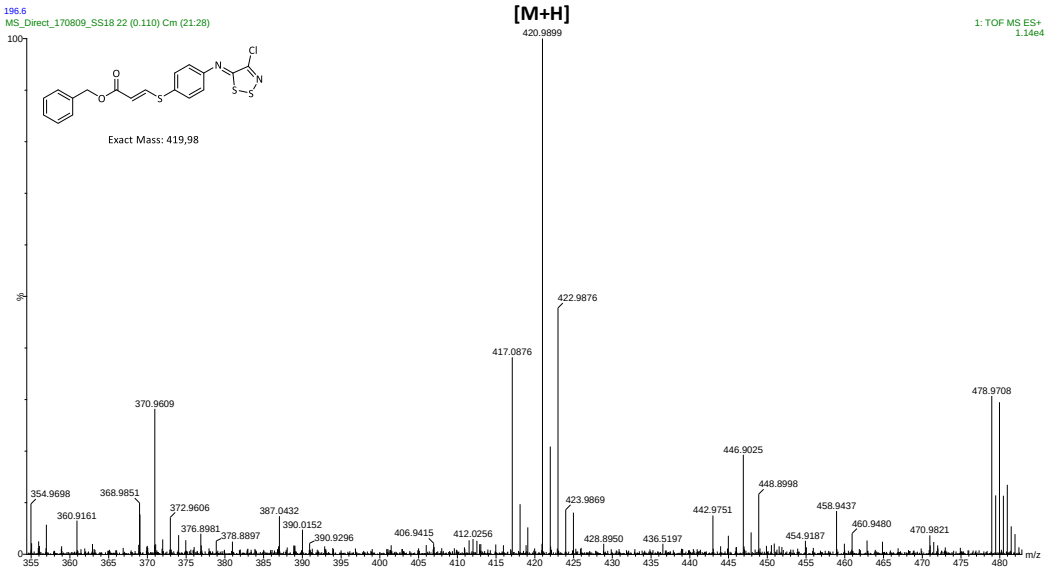

Figure 5.13. HRMS of the benzyl thioacrylate Appel's salt adduct **5.20**

The adduct **5.20** was then subjected to DBU mediated dithiazole fragmentation to afford the cyanoformanilide **5.21** required for cyclisation. The fragmentation was achieved without any complications and the product was isolated in relatively good yield (67 %). The ^{1}H-NMR spectrum of the fragmented product is shown in figure 5.14. The spectrum displayed all the expected signals with the key thioamide resonance observed as a broad, highly deshielded singlet integrating for one proton at 13.52 ppm. Interestingly, a major reduction in the coupling constant for signal H-3 was observed (from *J* = 13.5 Hz in the dithiazole precursor, to *J* = 8.6 Hz in the fragmented product **5.21**). This reduction meant that isomerization about the double bond had occurred, rearranging the compound from its starting trans geometry to the cis geometry shown in figure 5.14. This can be rationalized through the role of the DBU, which through a Michael addition and subsequent elimination results in the inversion of double bond geometry.

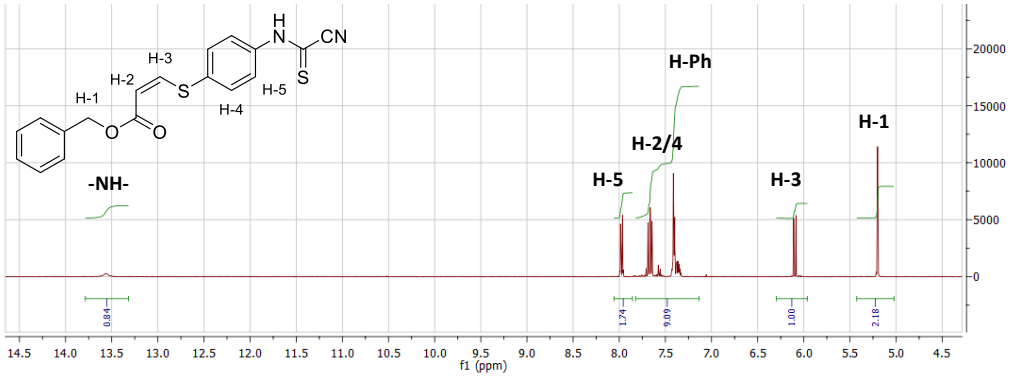

Figure 5.14. ^{1}H-NMR spectrum of the fragmented product **5.21** in DMSO

The thioamide was then cyclised using the previously described intramolecular C-S cross-coupling reaction to afford the 2-cyanobenzothiazole thioacrylate. The product was isolated and characterised by spectroscopic and analytical techniques and the ^{1}H-NMR spectrum is shown below (Figure 5.15). The benzothiazole ring protons were clearly displayed (H-4,5,6) which was indicative of a successful cyclisation. Furthermore, the mass spectrum displayed molecular ion peaks corresponding to [M+2H] at *m/z* 354.9664 and [M+2H+Na] at *m/z* at 378.0146 and the IR spectrum displayed a weak band at 2182 cm^{-1} supporting the conservation of the C2-nitrile. The material was then used in the next reaction to produce D-thioluciferin, even though NMR spectroscopy and EA data suggested that some organic impurities were present, observed in the aromatic region of the ^{1}H-NMR spectrum of figure 5.15. This was done because the reaction that affords D-thioluciferin involved an acid-base extraction were organic impurities would later be dealt with.

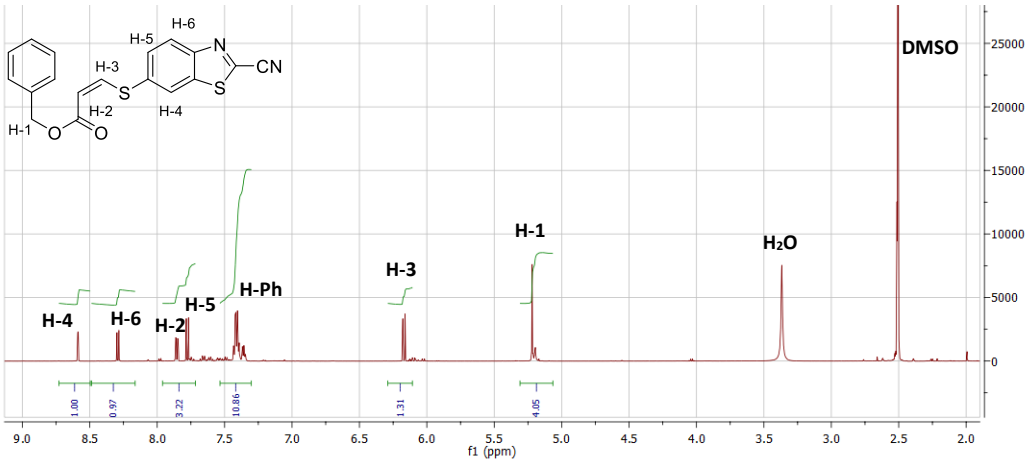

Figure 5.15. ^{1}H-NMR spectrum of 2-cyanobenzothiazole benzyl thioacrylate **5.22** in DMSO

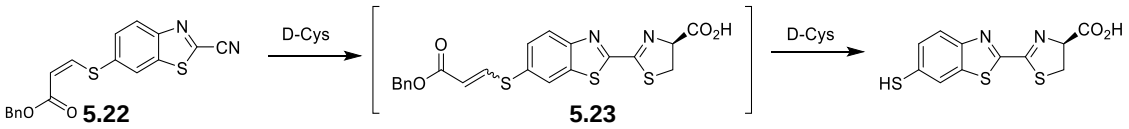

Scheme 5.13. D-Cys mediated formation and release of D-thioluciferin

The proposed reaction sequence for the synthesis of D-thioluciferin from the 2-cyanobenzothiazole precursor is shown in scheme 5.13. Two equivalents of D-Cys were reacted in the presence of potassium carbonate with the cyanobenzothiazole precursor to afford D-thioluciferin. Scheme 5.13 shows that the first equivalent of D-Cys reacts with the cyanobenzothiazole to form D-thioluciferin thioacrylate, after which D-Cys substitutes the vinyl sulfide to release D-thioluciferin. It was in fact not known prior to performing the reaction whether D-Cys cyclisation would occur first, followed by elimination or vice versa, or whether both reactions would occur simultaneously under the standard reaction conditions. The order that the reaction proceeds in was eventually investigated since it was important to consider for D-thioluciferin thioacrylate application (discussed later). After the reaction was completed, as evidenced by TLC, an acid-base extraction was employed to isolate pure D-thioluciferin. The ^{1}H-NMR spectrum of D-thioluciferin is shown in figure 5.16. With the removal of the thioacrylate, the expected five proton resonances were observed. Of note in figure 5.16 is the α-proton H-8, observed as a triplet integrating for one proton. The α-carboxyproton is a key signal in supporting successful D-luciferin synthesis, since the α-carboxyproton of free D-Cys is normally observed at 4.25 ppm, while the cyclised D-Cys dithiazole α-proton is observed much further downfield in the ^{1}H-NMR spectrum (5.40, 4.93 and 5.46 ppm for D-luciferin, D-aminoluciferin and D-thioluciferin, respectively).

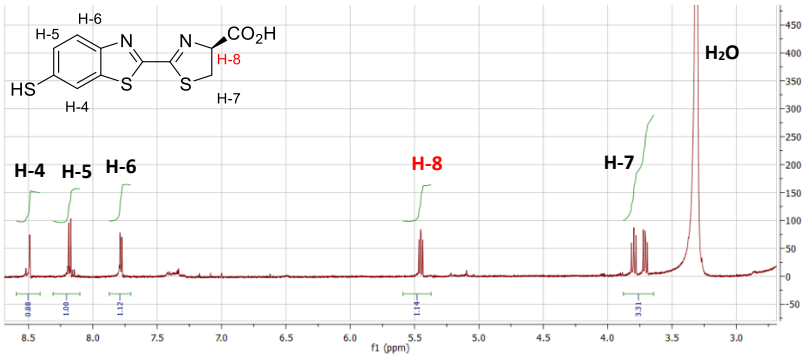

Figure 5.16. ^{1}H-NMR spectrum of D-thioluciferin in DMSO

Additional support for the successful synthesis of D-thioluciferin was found in the ^{13}C-NMR spectrum, where an expected total of 11 carbon resonances were observed and in the mass spectrum where molecular ion peaks at m/z 319.0002 and 294.9907 corresponding to [M+Na] and [M+H] were displayed (Figure 5.17).

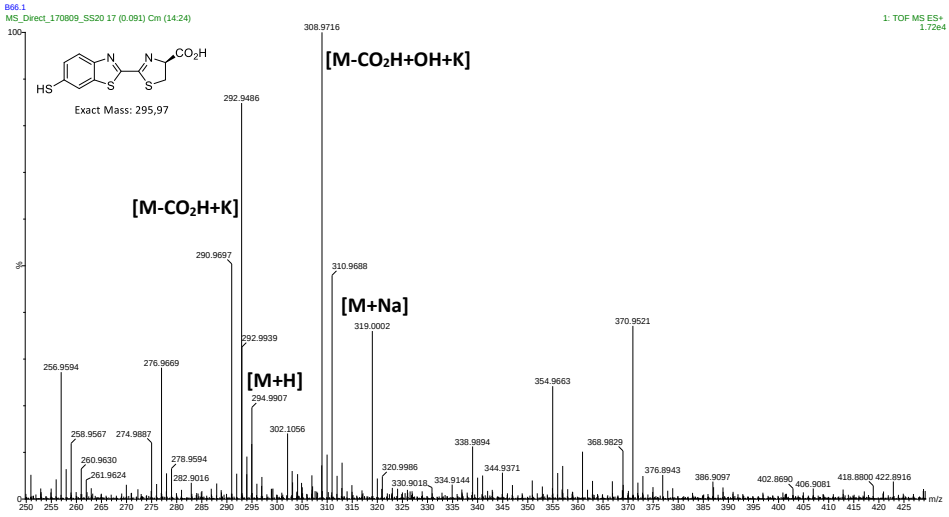

Figure 5.17. HRMS of D-thioluciferin

The optical purity of thioluciferin was also measured using chiral HPLC where a major peak was observed in the HPLC chromatogram (82-89 % *ee*, by HPLC using a Diacel Chiracel OD column, eluting with hexane:*i*-propanol 7:3). This suggested the stereochemistry of D-Cys had largely been conserved and that a small degree of racemisation had occurred during the formation of D-thioluciferin. The optical rotation of the synthesised material was also recorded for reference ($[\alpha]_{D}^{20}$obs: -11°, DMF, c = 1). After confirming its structure and assessing optical purity, focus was shifted to the mechanism by which D-thioluciferin release proceeds. The reaction of the cyanobenzothiazole thioacrylate was repeated using one equivalent of D-Cys. TLC analysis of the organic extracts from the reaction revealed multiple products and the subsequent NMR experiments further supported that there was no or very little selectivity in the reactivity of D-Cys toward the nitrile and vinyl sulfide. The reaction was then repeated at 0 °C and this time, it reacted almost exclusively at the C2-nitrile to form the D-thioluciferin thioacrylate. The ^{1}H-NMR spectrum of the adduct is shown in figure 5.18 where all the previously described thioluciferin resonances were displayed, along with the signals from the acrylate. The thioluciferin thioacrylate was also subjected to LCMS where a molecular ion peak corresponding to its molecular weight was observed. The isolated adduct was then reacted again with D-Cys and potassium carbonate to afford D-thioluciferin. Of course, at this point it was no longer necessary to use D-Cys specifically to deprotect D-thioluciferin and hence a number of reactive thiolates were evaluated for D-thioluciferin deprotection. The effect of the different thiols on the rate of deprotection is discussed later (Chapter 6) in the context of thiolate sensing.

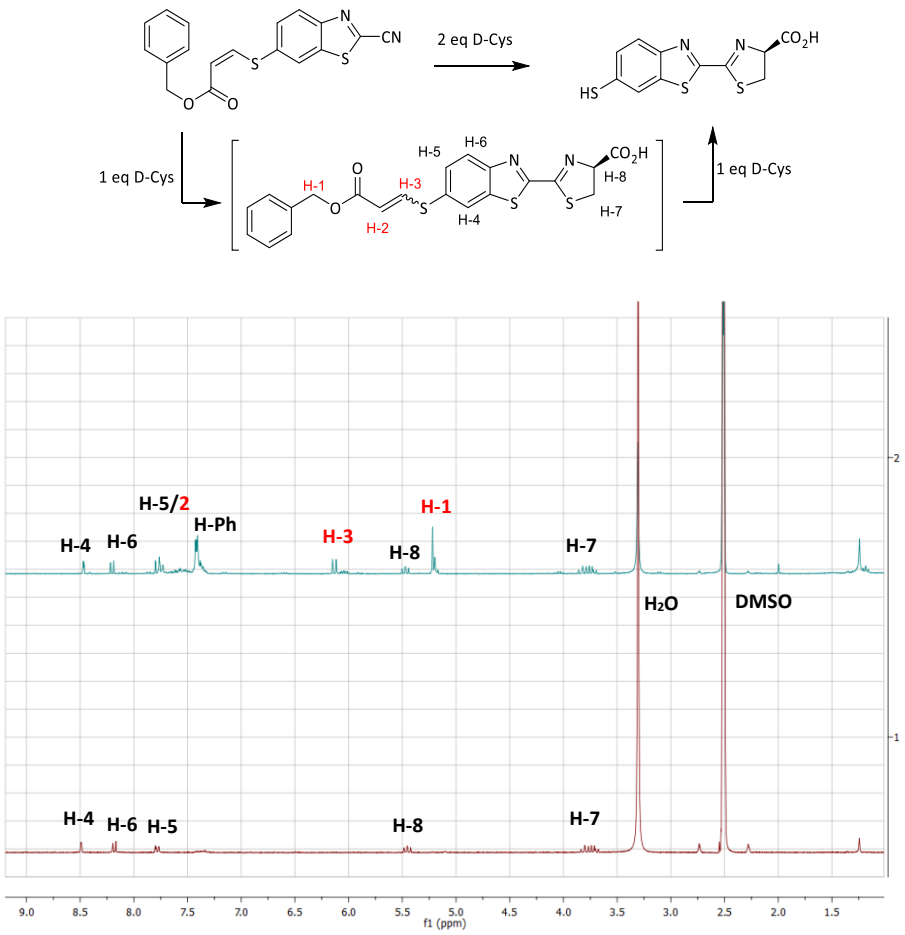

Figure 5.18. ^{1}HNMR spectra of D-thioluciferin and D-thiolucifeirn thioacrylate in DMSO

Improvements to the D-thioluciferin synthesis

It should be noted that improved methods of cyanobenzothiazole preparation were attempted but proved unsuccessful. The previously described method of monobromination was employed to prepare a disulfide protected mono-brominated aminothiophenol, scheme 5.14 **a**. However, both the Appel's salt reaction and the subsequent base mediated fragmentation proved to be very problematic, possibly due to the large excesses of Appel's salt and DBU used (6 eq) in the attempted transformations. Thus, the improved cyclisation could not be carried out. Monobromination of the sulfide was also attempted, scheme 5.14 **b**, but instead resulted in the loss of the thioacrylate functionality, based on ^{1}H-NMR analyses of the reaction.

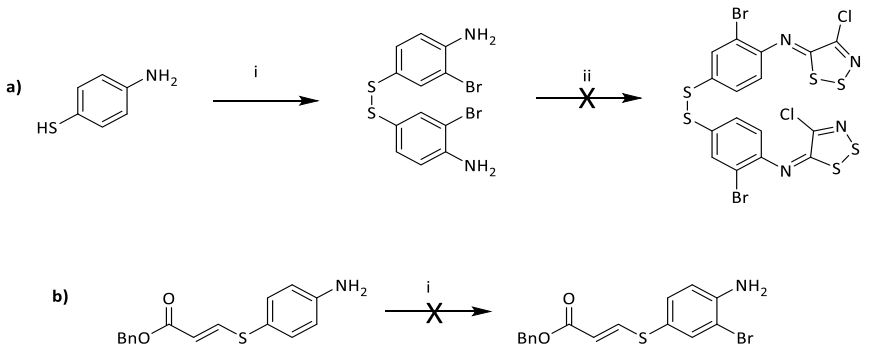

Scheme 5.14. Reagents and conditions; a) i) $NaBO_3$ / KBr / AcOH / rt / 16 h, 75 %, ii) Appel's salt / DCM / 3 h, b) i) $NaBO_3$ / KBr / AcOH / rt / 16 h

As a result, a relatively low overall yield was observed in the D-thioluciferin synthesis, however, studies concerning the conversion of the 2-cyano-6-iodobenzothiazole analogue to a C6-thiol is ongoing. Nevertheless, the results from the investigation into D-thioluciferin synthesis indicated that D-thioluciferin could be prepared rapidly, albeit in a modest yield, from the described thioacrylate protecting group strategy, and so all that remained was to confirm its luminescent activity or lack thereof.

Bioluminescent Evaluation of D-Thioluciferin

D-Thioluciferin

Based on previous work concerning synthetic luciferins and related derivatives it was predicted that the 6'-thio analogue of D-luciferin would be bioluminescent active and that it would display a more red-shifted maximum wavelength of emission, similar to that observed for aminoluciferin. In addition, the more oxidised disulfide of D-thioluciferin was expected to be non-luminescent active (provided its chemical reactivity was not different from the hydroxy-parent) and that could therefore allow for bioluminescence to be coupled to disulfide reduction. It was of course surprising that a thiol analogue had not yet been reported despite its obvious potential applications. Disulfide reduction/oxidation, particularly in the context of cellular redox homeostasis, is an important biomarker for stress and the ability to monitor induced stress is generally important.[15-16] It was therefore a goal of this study to not only evaluate the bioluminescence of D-thioluciferin, but also its oxidised disulfides, scheme 5.15.

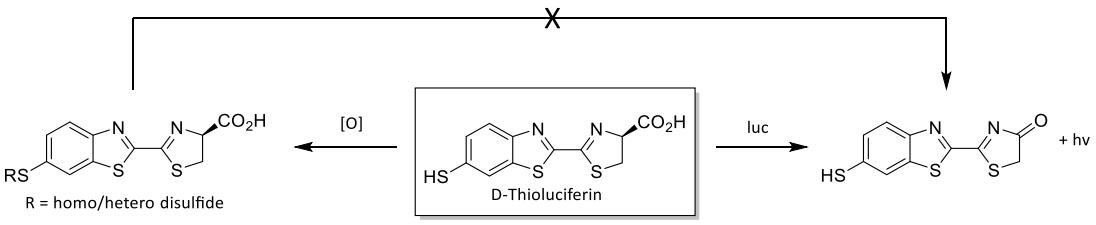

Scheme 5.15. Structure of D-thioluciferin and its disulfide

Sulfur and Biology

Sulfur provides a range of chemical reactivity and provides a degree of structural flexibility in biology and its biological incorporation is believed to have evolved directly for protein folding and to regulate three-dimensional structure.[17] As a result of this, much of biological function is supported by sulfur, hence technologies that potentially enable the monitoring of sulfur related chemistries are constantly being explored. The thiol handle of D-thioluciferin is very appealing in this regard, since it can directly link luminescence to sulfur biology. At this point, it is important to reiterate that for the effective application of D-thioluciferin based probes, two criteria must be met; the first, D-thioluciferin must retain luminescent activity and the second, modifications to the thiol-functionality of D-thioluciferin should result in a loss of luminescent activity.

.

Purified Luciferase Assay:

D-Thioluciferin was reacted with luciferase and the resultant luminescence measured in RLU using a Luminoskan Ascent luminescence plate reader. The luciferase enzyme was prepared as a standard 10 nM solution in enzyme buffer where luciferase lyophilized powder was dissolved in previously prepared luciferase enzyme buffer (20 mM Tris [pH 7.4], 0.1 mM EDTA, 1 mM DTT, and 0.8 mg/mL BSA). Luminescence assays were initiated by adding 30 µL of luciferase in luciferase enzyme buffer to 60 µL of D-thioluciferin in substrate buffer (20 mM Tris [pH 7.4], 0.1 mM EDTA, 8 mM $MgSO_4$, and 4 mM ATP) in a white 96-well plate. The final concentration of D-thioluciferin was varied from 0.1 µM to 3.56 µM, 10 µM and 100 µM. Bioluminescence was recorded one minute after enzyme addition and the results are shown in figure 5.19.

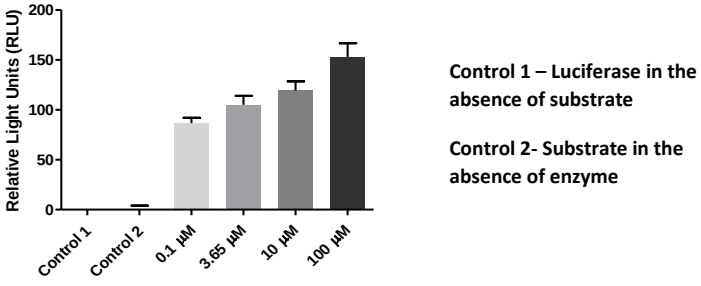

Figure 5.19. Graph of luciferase luminescence at a final enzyme concentration of 10 nM, at varying D-thioluciferin concentrations 1 min after enzyme addition. The assays were performed in triplicate and are represented as the mean ± SEM.

The results from the luminescence assay showed that D-thioluciferin was indeed luminescent active under the standard conditions previously used to demonstrate D-amino and D-luciferin luminescence. Control 1 contained a 10 nM Luciferase solution in enzyme buffer, and Control 2 comprised of 0.1 µM D-thioluciferin in substrate buffer to which a "blank" solution (enzyme buffer not containing luciferase) was added. No significant luminescence was detected from either control. However, when the blank solution was exchanged for the 10 nM luciferase containing solution, a significant light output was observed. Moreover, increased light output was observed for increasing concentrations of D-thioluciferin, further supporting thioluciferin luminescent activity. After confirming luminescent activity, D-thioluciferin was then treated with luciferase to determine its bioluminescence emission spectrum and wavelength of maximum emission.

Bioluminescence Emission spectrum:

Purified luciferase in enzyme buffer was rapidly injected into a cuvette containing D-thioluciferin in substrate buffer to a final enzyme concentration of 100 nM and a final substrate concentration of 10 µM. The peak emission (measured from 200 to 800 nm) was recorded using a Varian Carry Eclipse Fluorimeter. The bioluminescence emission spectrum of D-thioluciferin, along with D-luciferin and D-aminoluciferin for reference, is shown in figure 5.20. Peak bioluminescence emission for D-thioluciferin was observed at 599 nm while peak emission for D-luciferin and D-aminolucifeirn were observed at their respective maxima of 550 and 595 nm, respectively. The longer λ_{max} for D-thioluciferin relative to D-luciferin was expected both because of empirical trends as well as from TD-DFT studies.

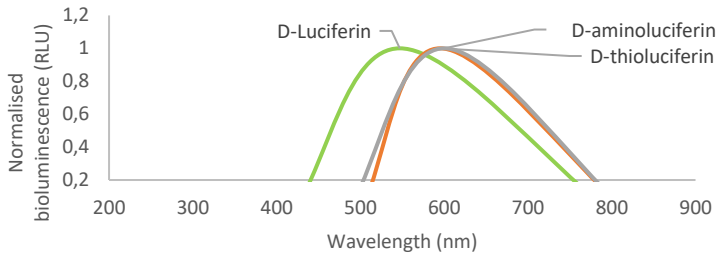

Figure 5.20. Bioluminescence spectrum for 10 nM luciferase with 0.1 µM D-thioluciferin, D-luciferin and D-aminoluciferin

Burst Kinetics profile of D-thioluciferin:

As previously discussed, when purified firefly luciferase is treated with D-luciferin or aminoluciferin, a high initial rate of light emission (burst) was observed in the first few seconds, which was then followed by a substantial decrease in the rate of sustained light output. It has been reported that this effect is more pronounced for D-aminoluciferin and related analogues, than for D-luciferin under the same conditions.[18] The kinetic profile for D-thioluciferin was shown to follow this trend (Figure 5.21).

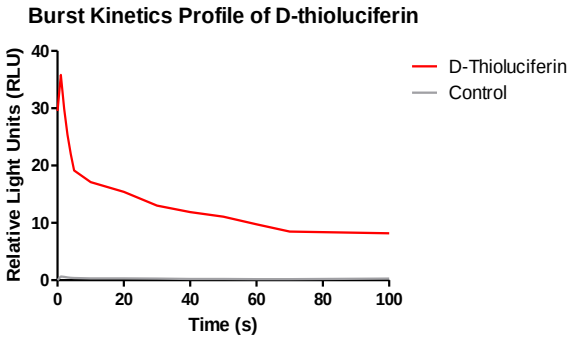

Figure 5.21. Burst kinetics profile of purified luciferase treated with 100 µM D-thioluciferin.

However, relative to D-luciferin treated with the same luciferase, the initial rate of photon flux was much higher, and subsequent decay to a steady light output occurred more rapidly. Despite the faster rates observed in D-thioluciferin, it generally appeared to achieve constant light about 1 min post-enzyme addition, which was the same for D-luciferin. The over-all emission however was greatly reduced for D-thioluciferin relative to D-luciferin although it should be noted that previous analogues, such as aminoluciferins, also have greatly reduced emission 1 minute after substrate addition (consistent with product inhibition as the primary factor limiting the light emission in vitro).[19-20] This means that D-luciferin is superior in terms of luminescent output when treated with purified luciferase. D-thioluciferin does however still offer advantages in terms of its chemical reactivity, where it can form reducible disulfides for measuring redox potentials. However, the requirement for application in redox sensing is that the oxidised thioluciferins should be non-luminescent active and/or inhibitors of luminescence, while the reduced free thiol is luminescent. Thus, an investigation into the luminescent properties of sulfides and disulfides was warranted.

Luciferase bioluminescence upon treatment with various substrates:

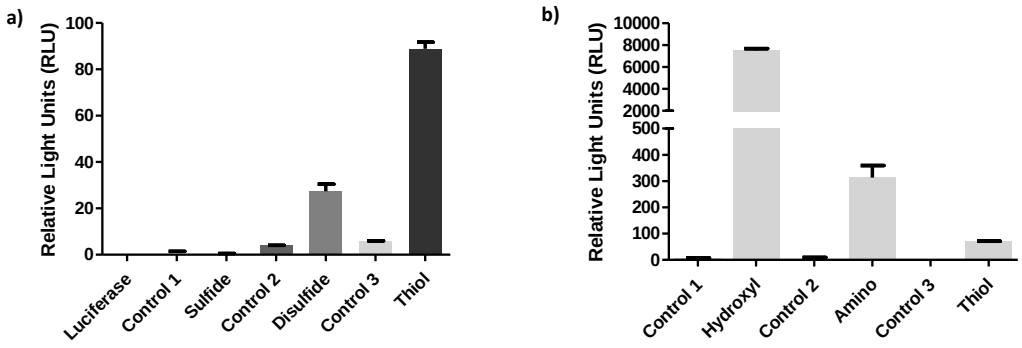

Figure 5.22. a) Luminescence output of 0.1 µM of protected D-thioluciferin thioacrylate, D-thioluciferin disulfide, and D-thioluciferin and b) relative luminescence of the core luciferins at 0.1 µM substrate concentration and at a final luciferase concentration of 10 nM. The RLU were determined in triplicate and are represented as the mean ± SEM

Figure 5.22 shows the luminescence output for D-thioluciferin, its protected thioacrylate **4.23** (i.e sulfide) and disulfide. From graph **a** it can be seen that neither pure luciferase in enzyme buffer nor pure thioacrylate (control 1) in substrate buffer emitted light. It can also be seen that when a 0.1 µM thioacrylate solution was treated with luciferase in enzyme buffer (thioacrylate labelled bar, figure 5.22a), the luminescence output remained negligible. This reinforced that the thioacrylate of D-thioluciferin was not luminescent active, and perhaps by extension that all sulfides of D-thioluciferin are luminescent inactive, as is the case with D-luciferin and its 6'-*O*-alkyl analogues. Control 2 contained only D-thioluciferin disulfide and control 3 only D-thioluciferin, both in substrate buffer at

a final concentration of 0.1 µM. In both cases, in the absence of luciferase, a small degree of luminescence was detected. The luminescence increased significantly when D-thioluciferin and its disulfide were treated with luciferase to a final enzyme concentration of 10 nM. What was interesting was that the disulfide treated with luciferase had a much higher luminescence output than its control (control 2) when compared to the sulfide and its corresponding control (control 1), since both were predicted to be non-luminescent active. This was most likely due to the reduction of non-luminescent D-thioluciferin disulfide to the luminescent-active free thiol by reducing agents in the enzyme buffer, namely DTT. This was confirmed by experiments later discussed in the context of D-thioluciferin applications. It should be noted that the assay could not be done in the absence of DTT since it is a crucial component of the enzyme buffer solution and, in addition, the same results were observed when DTT was replaced with tris(2-carboxyethyl)phosphine (TCEP), an alternative reductant.

With either DTT or TCEP, the free thiol displayed five times more luminescence than the disulfide, again a promising result for future redox based applications. Of concern was the relatively low light output generated by D-thioluciferin when compared to natural D-luciferin. D-luciferin was found to emit light at 100 times the intensity of D-thioluciferin while D-aminoluciferin had an emission 10 times more intense than that of the thio-analogue (but still far less than D-luciferin, figure 5.22). This is commonly observed when bioluminescence of new analogues are compared to D-luciferin with the wild-type enzyme and often relate to the quantum yield. Such an example is shown in figure 5.23, where the luminescence of a new 6'-amino analogue of D-luciferin, CycLuc7, is compared to D-luciferin. With the WT enzyme D-luciferin emits light at 100 times greater intensity than CycLuc7.[18-19] This suggested that the new analogues have to be used at higher concentrations to achieve the same relative light output as D-luciferin. This limitation is now being overcome by luciferase screening, where luciferase mutants are evaluated for increased luminescence with non-natural substrates and a similar screening performed with D-thioluciferin could be envisioned in the near future.

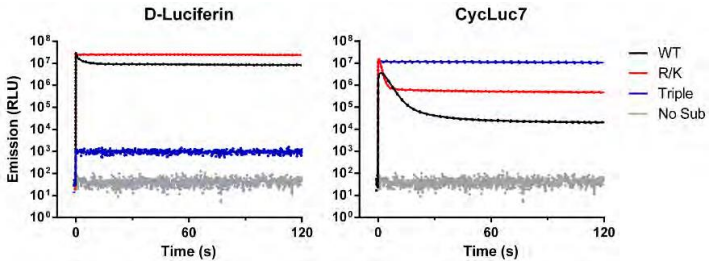

Figure 5.23. Bioluminescence of D-luciferin and CycLuc7 treated with purified WT and mutant luciferases reported by Mofford et al.[18]

Relative rates of luminescence:

In most D-luciferin purified enzyme assays, luminescence is quantitated one-minute post enzyme addition. This is to maximise reproducibility and consistency by ensuring that luminescence is read at a point where minimal fluctuation in light emission over time is observed. This is significantly different for a number of in vivo assays (luciferin administered intraperitoneally or subcutaneously) where peak luminescence was observed between 10 and 20 minutes after injection, followed by a gradual decay in light emission.[21] Unfortunately for D-luciferin, the relatively consistent light output was in fact not so and decayed at fairly consistent rate post peak emission. D-Thioluciferin was evaluated in this respect and was found to generate a more stable light output (post luminescence burst) and had a longer luminescence half-life than both D-luciferin and D-aminoluciferin. This was confirmed by kinetic experiments where the luminescence resulting from the addition of luciferase (10 nM in enzyme buffer) to substrate (0.1 μM in substrate buffer) was recorded over a 20 min period. The rate in reduction of bioluminescence was then calculated after 1 , 5 and 20 minutes (Table 5.1).

Table 5.1. Relative rates of reduction in luminescence

	Rate 1 min post-peak emission	**Rate 5 min post-addition**	**Rate 20 minutes post addition**
D-Luciferin	-	9.300 ± 0.9815	0.3400 ± 0.05773
D-Aminoluciferin	-	1.216 ± 0.1305	0.1510 ± 0.007506
D-thioluciferin	4.929 ± 0.1584	0.006700 ± 0.003753	0.002200 ± 0.00000001377

*Rates are measured for 15 seconds post-specified times and reported in RLU/s

It was noted that compared to D-luciferin and aminoluciferin, D-thioluciferin had a relatively slower rate of luminescence decay. This is advantageous since a slower rate of decay would mean that the luminescent output over time fluctuates much less over the given time-period. The slower rate is desirable for consistency and reproducibility between experiments and also implies that D-thioluciferin will have a longer half-life of emission since its rate of decay is generally slower.

Absorbance and Fluorescence Properties:

In addition to its bioluminescence properties, the fluorescent properties of D-thioluciferin were also explored. The absorbance spectrum of a DMSO solution of D-thioluciferin was obtained using a UV-Vis spectrophotometer where absorbance maxima were observed at 200, 320 and 410 nm. A fluorometer was then used to determine fluorescence emission and excitation maxima (at a final concentration of 1 mg/mL in the appropriate solvent).

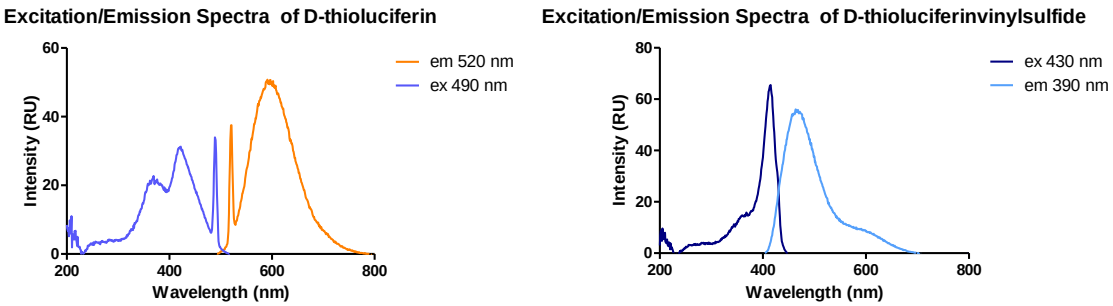

Figure 5.24. Excitation/Emission spectra of D-thioluciferin in DMSO

Generally, absorbance/excitation was measured between 380-430 nm and emission was observed between 500-600 nm, depending on the wavelength of excitation. At an excitation of 520 nm a strong emission response with a maximum at 600 nm was observed (Figure 5.24). Furthermore, the sulfide of D-thioluciferin, unlike free D-thioluciferin, did not emit a strong fluorescence signal at 600 nm when irradiated at 520 nm. This meant that the conversion of the sulfide to the free thiol could potentially be monitored using fluorescence as well as bioluminescence. The emission maxima of D-thioluciferin and its sulfide are shown in figure 5.25.

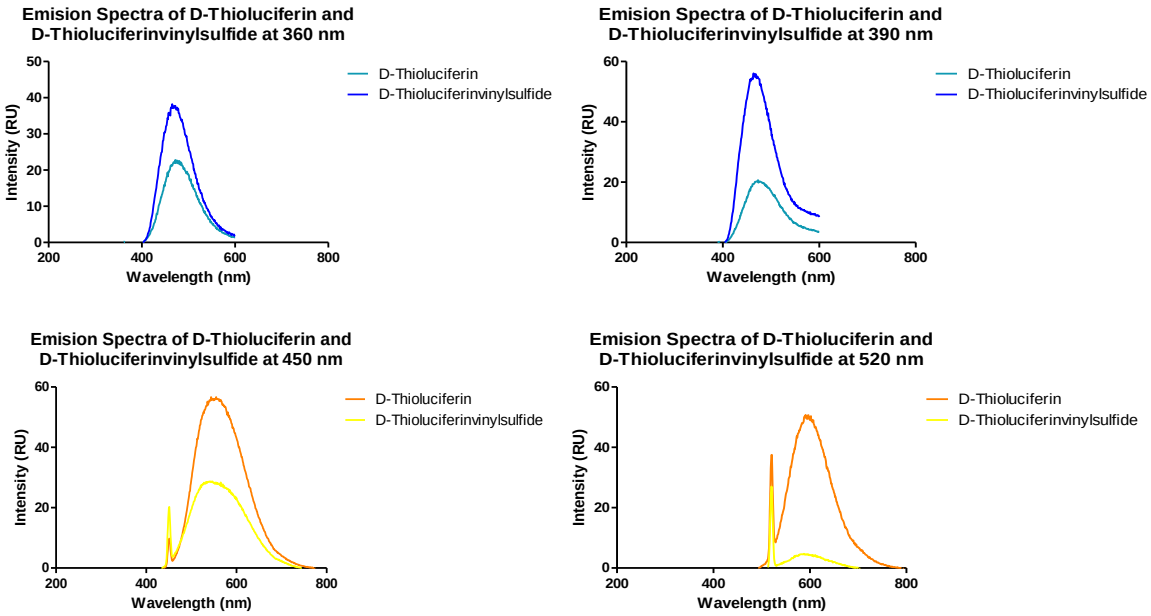

Figure 5.25. Emission spectra for D-thioluciferin and D-thioluciferin thioacrylate irradiated at varying wavelengths

When irradiating at D-thioluciferin's maximum absorbance, corresponding to lower wavelengths (360-380 nm), an emission maximum at around 500 nm is observed. The emission at 500 nm is useful in that it is much more red-shifted relative to the excitation wavelength, whereas at longer wavelengths of excitation the difference between excitation and emission is smaller. This trend was in agreement

with that previously observed for other luciferins where the bioluminescence maxima is always more red-shifted that its corresponding fluorescence signal at the excitation wavelength corresponding to its absorbance maximum.[18]

Enzyme Kinetics:

New luciferins are often evaluated by assessing the affinity of luciferase for the new substrate. For single substrate reactions Michaelis-Menten kinetics are employed to determine enzyme affinity. It must however be noted that while Michaelis-Menten kinetics is generally employed in luciferin analogue evaluation, many high affinity substrates do not fit this analysis well.

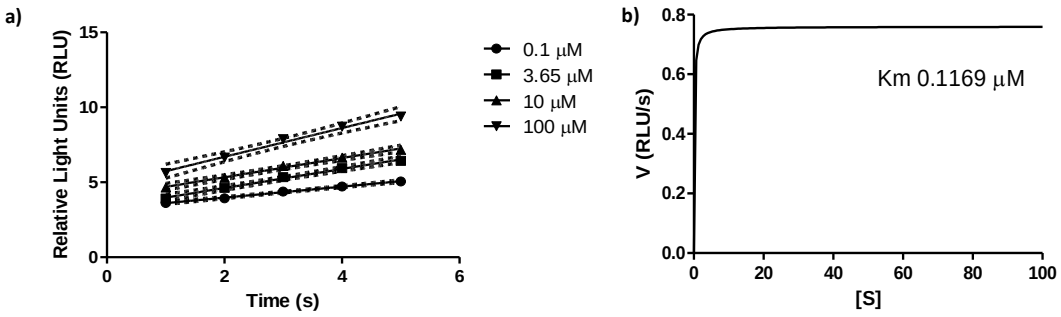

Figure 5.26. Michaelis-Menten kinetics of D-thioluciferin. The assays were performed in triplicate and represented as the mean and each curve was fit to the Michaelis–Menten equation by nonlinear regression (GraphPad 5.0) to determine apparent K_m and Vmax values

Using a plot of initial rates, the apparent K_m of D-thioluciferin was calculated, and as reference; D-luciferin and D-aminoluciferin. As predicted, D-thioluciferin displayed the expected increase in rate of emission with increasing concentration (Figure 5.26). The apparent K_m was calculated at 0.1169 μM, which was in the same order as that previously calculated for D-aminoluciferin (0.62 μM) and related analogues. The K_m was surprisingly much lower than that of the native substrate, D-luciferin (8.3 μM), despite the lower emission intensity (this again suggests that the D-thioluciferin/luciferase light emitting reaction may have a lower quantum yield), however, The lower K_m indicates that less substrate is required by the enzyme to become saturated and it will thus reach its maximum velocity faster because of the lower K_m (This however does not affect the greater light output observed for D-luciferin). Recently, Mofford et al reported that lower K_m values, coupled with increased lipophilicity, can improve imaging in the brain which is a known challenge with current luciferin technologies.[22] The lower K_m of D-thioluciferin and its potential to form more non-polar disulfides may be useful in this regard.

Summary

Table 5.2 highlights some of D-thioluciferin's luminescence properties with amino- and D-luciferin as reference. D-Thioluciferin was found to have a longer bioluminescence wavelength of emission when treated with purified WT luc, expressed and purified from *E. coli*. D-Thioluciferin also displayed a much lower K_m relative to D-aminoluciferin and D-luciferin. D-luciferin was found to have a K_m = ~8 µM and is therefore unlikely to reach saturating conditions when used in live cells and organisms (where a K_m of <1 µM is required).[23] In this regard, D-thioluciferin (K_m ~0.1 µM) may prove advantageous since less of it is required to saturate the enzyme.

Table 5.2. Comparison of luciferin luminescent properties

	D-Luciferin	**D-Aminoluciferin**	**D-Thioluciferin**
λ_{max}	553 nm	597 nm	599 nm
λ_{max} (lit.)	551 nm	594 nm	-
V_{max}	57 $\pm$ 13 RLU/s	13 + 2.2 RLU/s	0.7597 $\pm$ 0.1071 RLU/s
V_{max} (lit.)	1626 $\pm$ 24 photons/min[24] 1.027 ± 0.036 x 10^{-5} RLU/s[25]	169 $\pm$ 2.6 photons/min[24]	-
K_m (App.)	8.3 $\pm$ 0.5 µM	0.39 $\pm$ 0.08 µM	0.1169 $\pm$ 0.01163 µM
K_m (lit.)	9.15 ± 1.32 µM[25-26] 16 ± 1 µM[24] 14.8 ± 1.9 µM[25] 7 µM[27]	0.62 $\pm$ 0.05 µM[24]	-
Fluorescence emission maxima	-	-	500 nm
Fluorescence emission maxima (lit.)	528 nm[18]	517 nm[18]	-

The longer wavelength and lower K_m are indeed promising properties, and if it is found that D-thioluciferin has improved bio-distribution relative to known luciferins, then it will surely be a serious contender for one of the more superior bioluminogenic analogues of D-luciferin.

References

1. Ohulchanskyy, T. Y.; Donnelly, D. J.; Detty, M. R.; Prasad, P. N., Heteroatom substitution induced changes in excited-state photophysics and singlet oxygen generation in chalcogenoxanthylium dyes: Effect of sulfur and selenium substitutions. *The Journal of Physical Chemistry B* **2004,** *108* (25), 8668-8672.
2. Detty, M. R.; Prasad, P. N.; Donnelly, D. J.; Ohulchanskyy, T.; Gibson, S. L.; Hilf, R., Synthesis, properties, and photodynamic properties in vitro of heavy-chalcogen analogues of tetramethylrosamine. *Bioorganic & Medicinal Chemistry* **2004,** *12* (10), 2537-2544.
3. Solov'ev, K. N.; Borisevich, E. A., Intramolecular heavy-atom effect in the photophysics of organic molecules. *Physics-Uspekhi* **2005,** *48* (3), 231-253.
4. Hu, B.; Yao, C.; Wang, Q.; Zhang, H.; Yu, J., CH 2, NH, and O heteroatom substitution effects on the electronic, optical, and charge transport properties of a 2, 1, 3-benzothiadiazole-based derivative: Insights from theory. *Science China Chemistry* **2012,** *55* (7), 1364-1369.
5. Manojai, N.; Daengngern, R.; Kerdpol, K.; Ngaojampa, C.; Kungwan, N., Heteroatom effect on photophysical properties of 2-(2′-hydroxyphenyl)benzimidazole and its derivatives as fluorescent dyes: A TD-DFT study. *Journal of Luminescence* **2017,** *188*, 275-282.
6. Jiang, Y.; Qin, Y.; Xie, S.; Zhang, X.; Dong, J.; Ma, D., A general and efficient approach to aryl thiols: CuI-catalyzed coupling of aryl iodides with sulfur and subsequent reduction. *Organic letters* **2009,** *11* (22), 5250-5253.
7. Hrobárik, P.; Hrobáriková, V.; Sigmundová, I.; Zahradník, P.; Fakis, M.; Polyzos, I.; Persephonis, P., Benzothiazoles with tunable electron-withdrawing strength and reverse polarity: a route to triphenylamine-based chromophores with enhanced two-photon absorption. *The Journal of organic chemistry* **2011,** *76* (21), 8726-8736.
8. Benedí, C.; Bravo, F.; Uriz, P.; Fernández, E.; Claver, C.; Castillón, S., Synthesis of 2-substituted-benzothiazoles by palladium-catalyzed intramolecular cyclization of o-bromophenylthioureas and o-bromophenylthioamides. *Tetrahedron letters* **2003,** *44* (32), 6073-6077.
9. Sharma, D. K.; Adams Jr, S. T.; Liebmann, K. L.; Miller, S. C., Rapid Access to a Broad Range of 6′-Substituted Firefly Luciferin Analogues Reveals Surprising Emitters and Inhibitors. *Organic letters* **2017,** *19* (21), 5836-5839.
10. Firouzabadi, H., Phosphourus, Sulfur and Silicon and the Related Elements, 2003, 178, 1027.(b) H. Firouzabadi, N. Iranpoor and R. Heydari. *Synth. Commun* **2003,** *33*, 703.
11. Paquette, L. A., *Handbook of Reagents for Organic Synthesis: Sulfur-Containing Reagents*. John Wiley & Sons: 2013.

12. Nyoni, D.; Lobb, K. A.; Kaye, P. T.; Caira, M. R., DBU-Mediated cleavage of aryl-and heteroaryl disulfides. *Arkivoc* **2012,** *6*, 245-252.
13. Nair, D. P.; Podgórski, M.; Chatani, S.; Gong, T.; Xi, W.; Fenoli, C. R.; Bowman, C. N., The thiol-Michael addition click reaction: a powerful and widely used tool in materials chemistry. *Chemistry of Materials* **2013,** *26* (1), 724-744.
14. Chan, J. W.; Hoyle, C. E.; Lowe, A. B.; Bowman, M., Nucleophile-initiated thiol-michael reactions: effect of organocatalyst, thiol, and ene. *Macromolecules* **2010,** *43* (15), 6381-6388.
15. Mittler, R., Oxidative stress, antioxidants and stress tolerance. *Trends in plant science* **2002,** *7* (9), 405-410.
16. Sies, H., Hydroperoxides and thiol oxidants in the study of oxidative stress in intact cells and organs. *Oxidative stress* **1985**, 73-90.
17. Go, Y.-M.; Chandler, J. D.; Jones, D. P., The cysteine proteome. *Free Radical Biology and Medicine* **2015,** *84*, 227-245.
18. Mofford, D. M.; Reddy, G. R.; Miller, S. C., Aminoluciferins extend firefly luciferase bioluminescence into the near-infrared and can be preferred substrates over D-luciferin. *Journal of the American Chemical Society* **2014,** *136* (38), 13277-13282.
19. Reddy, G. R.; Thompson, W. C.; Miller, S. C., Robust light emission from cyclic alkylaminoluciferin substrates for firefly luciferase. *Journal of the American Chemical Society* **2010,** *132* (39), 13586-13587.
20. Woodroofe, C. C.; Meisenheimer, P. L.; Klaubert, D. H.; Kovic, Y.; Rosenberg, J. C.; Behney, C. .; Southworth, T. L.; Branchini, B. R., Novel heterocyclic analogues of firefly luciferin. *Biochemistry* **2012,** *51* (49), 9807-9813.
21. Inoue, Y.; Kiryu, S.; Watanabe, M.; Tojo, A.; Ohtomo, K., Timing of imaging after D-luciferin injection affects the longitudinal assessment of tumor growth using in vivo bioluminescence imaging. *Journal of Biomedical Imaging* **2010,** *2010*, 8.
22. Mofford, D. M.; Adams Jr, S. T.; Reddy, G. K. K.; Reddy, G. R.; Miller, S. C., Luciferin amides enable in vivo bioluminescence detection of endogenous fatty acid amide hydrolase activity. *Journal of the American Chemical Society* **2015,** *137* (27), 8684-8687.
23. Adams, S. T.; Miller, S. C., Beyond D-luciferin: expanding the scope of bioluminescence imaging in vivo. *Current opinion in chemical biology* **2014,** *21*, 112-120.
24. Shinde, R.; Perkins, J.; Contag, C. H., Luciferin derivatives for enhanced in vitro and in vivo bioluminescence assays. *Biochemistry* **2006,** *45* (37), 11103-11112.

25. da Silva, L. P.; da Silva, J. C. E., Kinetics of inhibition of firefly luciferase by dehydroluciferyl-coenzyme A, dehydroluciferin and L-luciferin. *Photochemical & Photobiological Sciences* **2011,** *10* (6), 1039-1045.

26. Seliger, H. H.; McElroy, W. D., Spectral emission and quantum yield of firefly bioluminescence. *Archives of biochemistry and biophysics* **1960,** *88* (1), 136-141.

27. Harwood, K. R.; Mofford, D. M.; Reddy, G. R.; Miller, S. C., Identification of mutant firefly luciferases that efficiently utilize aminoluciferins. *Chemistry & biology* **2011,** *18* (12), 1649-1657.

Chapter 6

Low Molecular Weight Thiols and Glutathione Reductase

Abstract

Biological low molecular weight thiols (LMWTs) are involved in many different biochemical processes. Most organisms make use of varying strategies which involve LMWTs to regulate cellular protein and free thiol reduction/oxidation. These biological LMWTs and their associated enzymes have been reported to be upregulated as a result of oxidative stress. One such enzyme is glutathione reductase (GSR), which is reported to be significantly upregulated in response to various chemical stresses. Herein, it is demonstrated how a modified luciferin can be applied in the monitoring of glutathione reductase activity and, by extension, how it can be applied to imaging cellular oxidative stress. The technology described in this chapter centres around bioluminescence that results from disulfide reduction. A mixed disulfide of D-thioluciferin and the LMWT glutathione (GSH) was prepared, where the disulfide was demonstrated to be non-bioluminescent. When the disulfide was reduced by GSR, it afforded the detectable bioluminescent substrate, D-thioluciferin. The bioluminescent emission varied significantly depending on the amounts of disulfide substrate and GSR enzyme present. The thioluciferin-GSH hetero-disulfides was found to be a relatively good substrate for GSR (K_m of 0.89 mM relative to 0.51 mM for glutathione disulfide, GSSG) and, further to that, the hetero -disulfide demonstrated a good correlation between its resulting luminescence signal and disulfide reduction, upon treatment with luciferase at increasing concentrations of GSR in a physiological buffer. Furthermore, GSR activity was monitored over time using the luciferin technology and the data obtained was found to be comparable to commonly used colorimetric GSR assays, where induced changes in GSR activity are observed as fluctuations in sample absorbance at 340 nm as a result of NADP oxidation by the GSR enzyme. These initial studies reported here lay the groundwork for further exploration of D-thioluciferin applications.

Chapter 6

Low Molecular Weight Thiols and Glutathione Reductase

An introduction to biological low molecular weight thiols (LMWTs)

Sulfur and Biology

The many exceptional properties of the thiol functionality, such as its pK_a, nucleophilicity, metal ion affinity, unique bonding characteristics, and redox properties make it a versatile functionality for metabolic processes.[1-2] The thiol functionality present in organic compounds infer versatility and reactivity, it therefore comes as no surprise that many biochemical processes essential for normal cell functioning involve thiol-containing compounds.[3] The unique chemistry of the thiol group is partially attributed to the many oxidation states of sulfur. Sulfur can exist in either its free thiol form, or in more oxidised forms, with each having different properties and reactivity. Sulfur can also act as either an electron donor or an electron acceptor, making the thiol moiety one of the most interesting functional groups, capable of partaking in a wide range of chemical or biochemical reactions.[1, 3] The thiol functionality allows for metal binding in which the sulfur atom acts as a soft base. These sulfur-metal interactions are essential for cellular function and research involving such interactions are well documented.[4-6] In addition, thiols are also involved in cellular molecular recognition processes, electron transport, protein folding, signal transduction, and thiol-based redox homeostasis.[6-8]

Low Molecular Weight Thiols

Biological thiols are found in the form of non-protein low molecular weight thiols (LMWTs) and larger protein thiols. Of the many antioxidants found in the human body, LMWTs constitute the major and most abundant form of antioxidant.[3] LMWTs play their role in cellular defense by reacting with reactive oxygen species (ROS) and, consequently, abnormal levels of native cellular thiols have been noted in various medical disorders including chronic renal failure, stroke, diabetes mellitus, alcoholic cirrhosis, to name a few.[3, 9-10] Thus, technologies that enable the quantitation and evaluation of cellular thiol fluctuations and related enzymes are of great interest.

The thiol functionality present in cellular thiol-containing compounds are known to be a central and adaptable site for the biochemical processes required for normal cell function.[1] Most organisms contain a multitude of LMWTs which are involved in varying biochemical processes. As previously mentioned, one of the characteristics of LMWTs, and thiols in general, is that they are readily oxidised in the presence of oxygen and heavy metals. Consequently, the oxidation states of sulfur-containing

cellular components are highly regulated in order to maintain normal cellular functions. The sensitivity of the thiol functionality to oxidation has been known to differ significantly depending on the type of thiol and its molecular structure.[11]

The oxidation of thiols may also directly result in the production of reactive oxygen species (ROS) as co-products that can be highly toxic to cells.[1] Thus, most organisms make use of varying strategies to minimise the occurrence of undesired thiol oxidation and to mitigate its consequences.[12] The use of small molecule thiols to buffer redox metabolism is a key strategy in regulating the redox environment of cells. The response of a cell to chemical stress often involves changes in the intracellular thiol content. Apart from their role in thiol-based redox homeostasis, LMWTs are also generally consumed in reactions that protect the cell as they remove harmful compounds, and are consequently replaced through either the reduction of disulfides or *de novo* synthesis.[6] In some cases, changes in the intracellular LMW thiol content has even been used as a biomarker of cell toxicity and stress.[13] It is therefore no surprise that research concerning the antioxidant role of LMWTs have become more important in health and disease. The major groups of non-protein LMWTs include cysteine-based compounds and histidine-based compounds. Figure 6.1 displays the structures of select examples of LMWTs which include; glutathione (GSH) **6.1**, trypanothione (TSH) **6.2**, bacillithiol (BSH) **6.3**, mycothiol (MSH) **6.4** and coenzyme A (CoASH) **6.5**. The histidine-based compounds include ergothioneine (ESH) **6.6**, and the ovothiols (OSH); ovothiol A (OSH_A) **6.7**, ovothiol B (OSH_B) **6.8**, and ovothiol C (OSH_C) **6.9**. All these reported thiols are important for normal function/survival and, in general, play a role in redox homeostasis.

Most eukaryotes make use of GSH **6.1** to regulate cellular redox homeostasis. TSH **6.2** is a natural derivative of GSH, containing two molecules of GSH which are covalently linked via a spermidine linker.[14-15] Both TSH and GSH play a role in the defence against oxidative stress, TSH however, unlike GSH, is found in parasitic protozoa, trypanosomes, known to cause sleeping sickness.[15] BSH **6.3** and MSH **6.4** also play the same defensive role and are both considered to be substitutes for GSH in certain organisms, gram positive bacteria in particular. *Mycobacterium tuberculosi*s for example, lack the redox protective molecule GSH and instead produce cysteine based MSH **6.4** and histidine based ESH **6.6** as their principal LMWTs.[16] In most organisms, CoASH **6.5** plays an important role in fatty acid metabolism. The ovothiols **6.7**-**6.9** are also highly reducing antioxidant thiohistidine derivatives found in various organisms.[17-19]

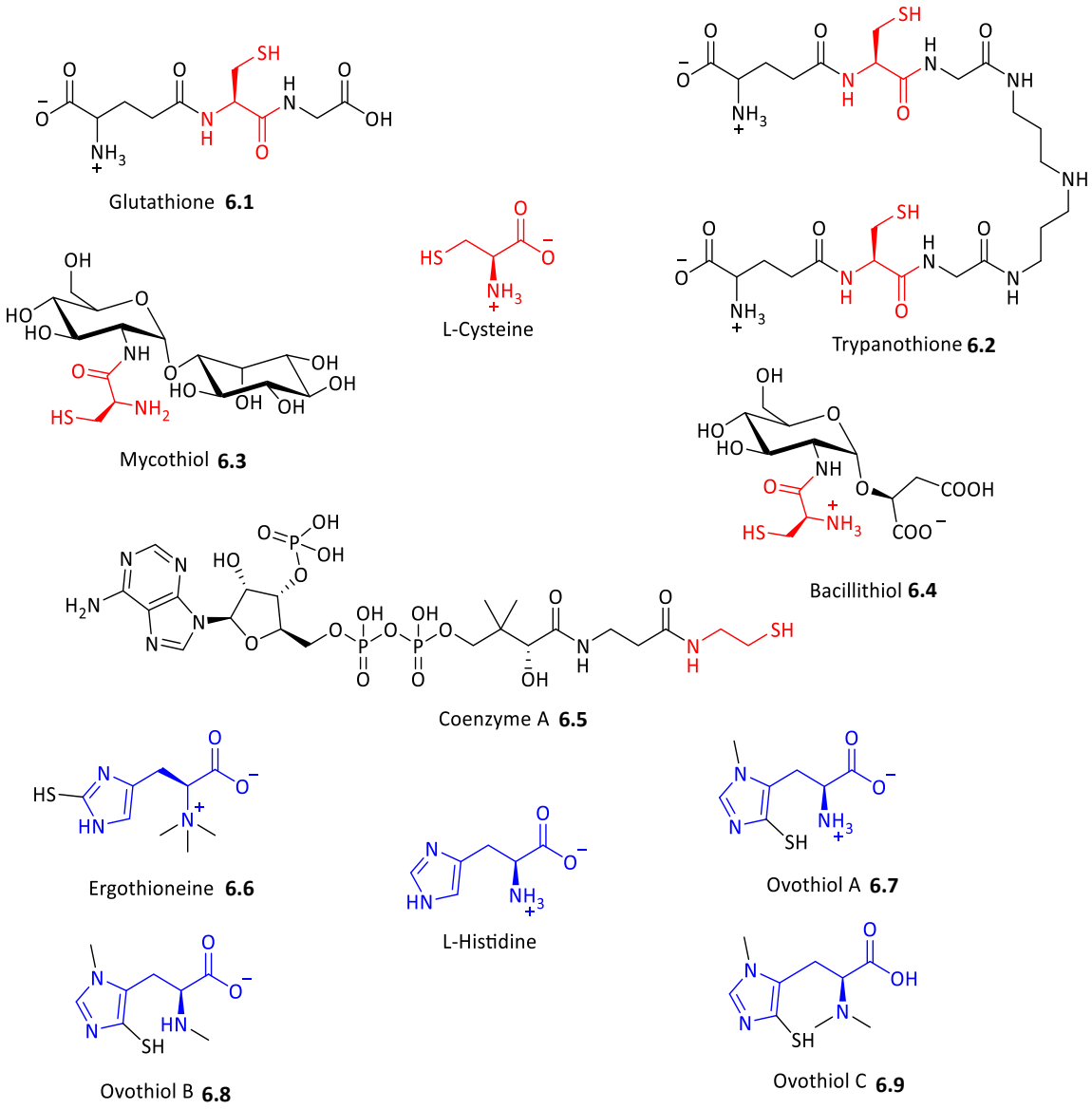

Figure 6.1. Select examples of LMWTs, including; L-Cysteine, GSH **6.1**, TSH **6.2**, BSH **6.3**, MSH **6.4**, CoASH **6.5** and L-Histidine, ESH **6.6**, OSH_A **6.7**, OSH_B **6.8**, and OSH_C **6.9**

Most living organisms contain high concentrations of one or more of the aforementioned LMWTs, which act as redox buffers to protect cells and cellular machinery against a variety of reactive chemical species.[20] The concentration and free thiol/disulfide ratios of these different LMWTs influence the redox potential of the intracellular reducing environment that is essential for metabolic processes and stress signaling.[20] Changes in cellular LMWT content are closely associated with increased oxidative stress and it is for that reason that technologies that enable LMWT quantitation have become so important. This can either be done by monitoring the thiol directly or monitoring the activity of related enzymes.

Glutathione

Humans and eukaryotes in general, make use of GSH to regulate cellular redox homeostasis and this particular thiol will form the focus of this Chapter. GSH is the major and most abundant antioxidant in humans (recorded at a cellular concentration of around 5 mM in animal cells).[14] The structure of GSH is shown in Scheme 6.1, GSH is a tripeptide formed from a gamma peptide linkage between its constituent glutamate and cysteinylglycine residues. GSH prevents damage to cellular components caused by ROS through reductive disulfide exchanges. It was mentioned previously that thiols are exceptionally susceptible to oxidation. This makes them ideal reducing agents, and for that reason, a thiol such GSH is maintained at relatively high cellular concentrations. GSH reacts with potentially harmful oxidising species and forms glutathione disulfide (GSSG) in the process (Scheme 6.1). In the blood plasma of humans, around 15 % of GSH is found in the disulfide form GSSG. The ratio of GSH to GSSG within cells can be used as a measure of oxidative stress and new technologies that could potentially allow for the monitoring of this ratio are constantly being investigated.[21-22]

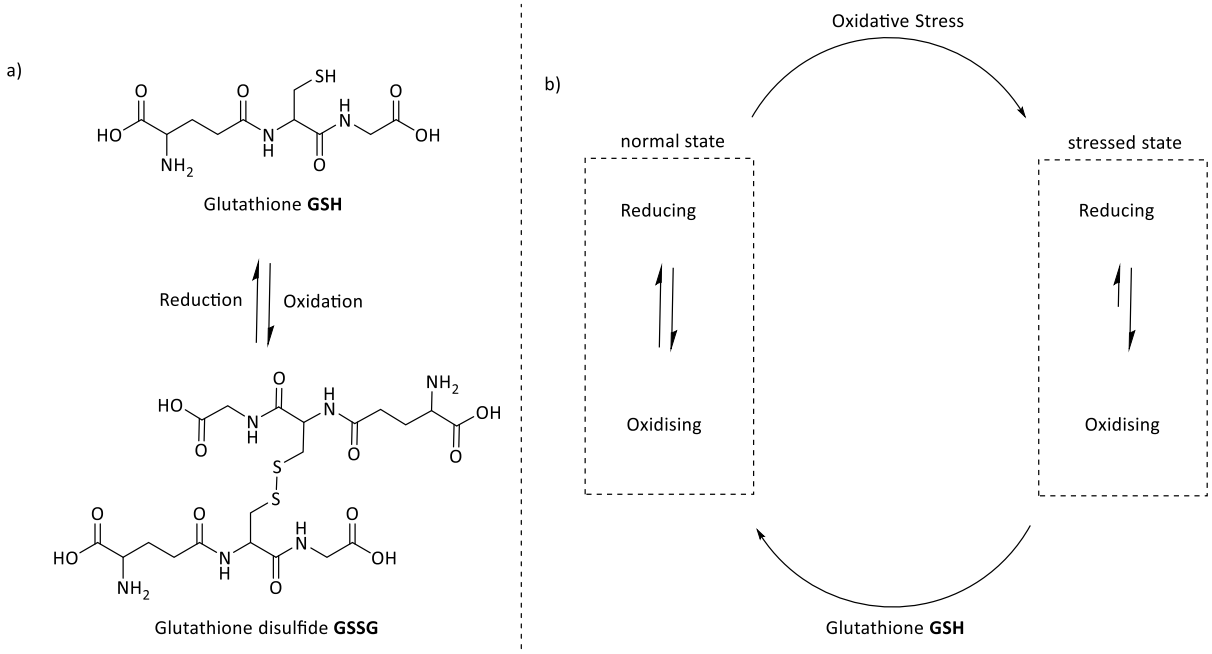

Scheme 6.1. a) The cellular oxidation/reduction reaction of GSH/GSSG, where GSH is converted to GSSG by oxidants and GSSG is reduced, predominantly via an NADPH dependant reduction, to reform GSH. The levels of GSH and GSSG are generally conserved but fluctuations as a result of increased oxidative stress is commonly observed, b) demonstrates the idealised shifting of the redox equilibrium in response to oxidative stress or increased GSH.

In addition to its well-established roles in cellular redox homeostasis, GSH is also known to function directly and/or indirectly in many other important biological phenomena, including the synthesis of proteins and DNA, transport, enzyme activity, metabolism, and protection of cells.[23-24] GSH is also a

co-enzyme in various enzymatic reactions where it conjugates with foreign compounds (e.g. drugs) and results in their effective metabolism. Interestingly, GSH levels are strongly associated with its transport out of cells, where inhibition of such transporters results in drastic decreases in blood plasma GSH concentrations.[7] The relatively high concentrations of GSH is however not purely attributed to its role as an antioxidant. Instead, its high concentrations presumably speak to its role as a storage and transport form of cysteine.[25]

REDOX reactions of GSH and GSSG

Glutathione Oxidation

Biologically, GSH is readily converted to GSSG in presence of oxygen and specific oxidising enzymes whose distributions vary quite significantly depending on their locality.[26] Initially, the biochemical conversion of GSH was purely attributed to the activity of a GSH oxidase enzyme. Such oxidase activity was found, to varying degrees, in the homogenate of different tissue, including kidney, epididymis, jejunum, choroid plexus.[14] It was also discovered quite early on that not all GSH oxidations are controlled by GSH oxidase. In addition to the enzyme mediated oxidation, GSH is also non-enzymatically oxidised via disulfide exchange reactions between GSH and cysteinyl-bis-glycine, or between GSH and any mixed disulfide for that matter. These types of oxidations were inhibited by EDTA and are thus considered to be mechanistically mediated by metal ions.[14] It is probably worth noting that the spontaneous oxidation of other biological thiols, such as cysteinylglycine and cysteine is more rapid than that of GSH, which may further support its role as a storage compound. The rates of oxidation for GSH and its two precursors are as follows; cysteinylglycine > cysteine > GSH.

Glutathione Peroxidase

The biochemical conversion of GSH to GSSG is also achieved through the consumption of H_2O_2. The reduction of H_2O_2 by GSH is catalysed by the enzyme GSH peroxidase (Scheme 6.2). This enzyme is present in various tissue and catalyses the reduction of H_2O_2 by GSH to produce GSSG and, by extension, NADPH.

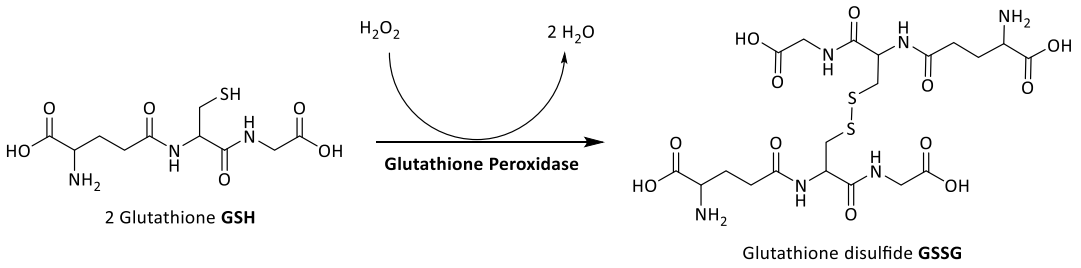

Scheme 6.2. GSH peroxidase catalysed reduction of H_2O_2

This cycle constitutes the major pathway of H_2O_2 metabolism in cells and allows for the regulation of H_2O_2 concentrations. Thus, it protects the membrane lipids and various other cellular components against oxidation.

Glutathione Reductase

Glutathione reductase (GSR) is a widely distributed flavoprotein, which catalyses the NADPH mediated reduction of GSSG to GSH. The biochemical reduction is essentially irreversible and accounts for the very high GSH:GSSG ratios found in cells (0.9:0.1).[27] Early studies suggested that the enzyme could exclusively catalyse the reduction of GSSG and mixed disulfides formed from GSH and γ-glutamylcysteine, and the mixed disulfide formed from GSH and coenzyme A.[27] However, it has since been demonstrated that most mixed disulfides of GSH are suitable substrates for GSH reductase and, in some cases, are even better substrates than native GSSG. GSH reductase contains a cysteine residue that undergoes reduction and oxidation during the catalytic cycle and makes use of NADPH as the reducing agent (Scheme 6.3).

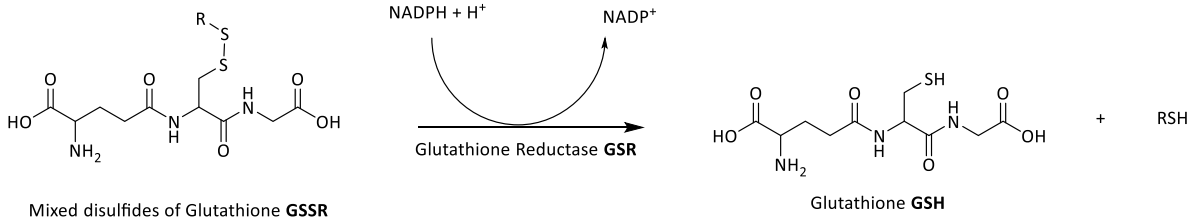

Scheme 6.3. GSR catalysed reduction of GSSR to GSH

Because of the great importance of these enzymes in regulating redox states and maintaining the GSH:GSSG ratios, many technologies have been developed that allow for quantitating and monitoring GSR, as well as GSH peroxidase activity. Generally, these technologies involve the use of GSH mixed disulfides, formed from GSH and alkyl/aryl thiols that can easily be detected when in the free thiol form. Similarly, it was an aim of this project to prepare a complementary bioluminescent technology from the conjugation of D-thioluciferin and GSH. The design of the probe that would couple bioluminescence and GSR activity was based on a direct disulfide linkage between D-thioluciferin and GSH (Scheme 6.4).

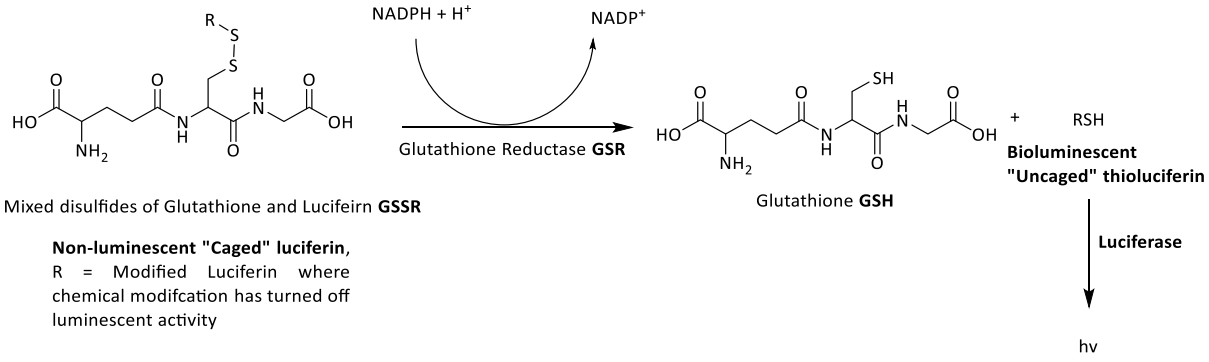

Scheme 6.4. Luciferin-GSH conjugate for monitoring GSR activity and redox flux

Of course, for the technology to be successful, it was necessary for the disulfide to be non-bioluminescent while also being a substrate for GSR. Based on the exploratory work discussed in Chapter 5, the Thioluciferin-GSH disulfide was predicted to not be a suitable substrate for luciferase and, therefore, the mixed disulfide would not be bioluminescent active. In addition, it was also predicted that the disulfide would be a substrate for GSR, since the GSR mediated reduction of various GSH mixed disulfides had been reported.[28]

The thioluciferin-GSH conjugate would then be introduced into a sample lysate, cell line, or organism and, depending on the redox state and GSR concentration, some of the conjugate (or probe) would be reduced by GSR and potentially other reducing agents to release free D-thioluciferin, which in the presence of luciferase would produce a quantifiable luminescent signal which would then be used as a reference for a particular redox state.

A redox state is a term used very loosely in relation to cellular oxidative stress. It is used as a general term referring to relative changes that are not well defined or quantitated.[29] Initially it was envisioned that changes in GSR activity, and resultant changes in the GSH:GSSG ratio would be used as a proxy for redox state since many studies show that certain pathophysiological conditions result in a decrease in the free GSH:GSSG ratio.[3, 9] Thus, in samples or areas that have increased or decreased oxidative stress, corresponding increased or decreased bioluminescence would be observed due to probe reduction. The significance of such technologies have already been established, but to further emphasise this, a select few examples demonstrating how protein thiol concentrations and redox imbalances relate to various diseases and disorders have been highlighted, as well as a number of GSR monitoring technologies.

Thiol status in various disorders

LMWTs in Tuberculosis

Parasitic protozoa and bacteria are responsible for a number of diseases and it is well documented that LMWTs are integral for the detoxification of reactive chemical species used by the host in defense against infection. In response to infection from such parasitic protozoa or bacteria, a host organism often uses a myriad of strategies to defend against the parasite. One such strategy is the use of reactive oxygen species (ROS) such as superoxide, hydrogen peroxide and hydroxyl radicals generated by their metabolism as a component of the host antimicrobial response.[30] ROS damage membrane fatty acids, proteins, and DNA. However, LMWTs and their associated proteins help protect these pathogens against oxidative damage. By controlling their local redox environments, pathogenic bacteria and protozoa can limit unwanted oxidation of cellular components essential for survival. Thus, LMWTs and their associated redox enzymes are not only of interest for monitoring disease progression/regression but are also potential drug targets for drug development.

Not only do these pathogenic organisms withstand the barrage of oxidative radicals by the immune system, they do so using several antioxidant and detoxification systems to cope with the hosts' immune response. An example of an organism that exploits this protective mechanism is Tuberculosis.

Tuberculosis (TB) is an infectious disease caused by the pathogenic gram positive bacterium, *Mycobacterium tuberculosis*(M. *tb*).[31] TB remains one of the most wide spread diseases, with an estimated 9 million people infected annually[32] and is one of the leading causes of mortality in developing countries. It is believed that the success of M. *tb* is largely attributed to its ability to persist in host tissue.[33] One of the factors contributing to M. *tb* persistence is its use of the LMWT, mycothiol (MSH), which is involved in the protection of M. *tb* from toxic oxidants and antibiotics.[12] Studies showed that MSH has significant antioxidant activity as well as the ability to detoxify a variety of toxic compounds. As a result, MSH is able to contribute to the protection of M. *tb* from inactivation by the host during infections and thus influences M. *tb* resistance to anti-tuberculosis drugs.[12] In the host, increased oxidative tension is observed in areas affected by the pathogen, which translates to a local upregulated GSR concentration and a decreased GSH:GSSG ratio. Technologies that are responsive to changes in the oxidative state of blood plasma and cells allows for drugs to be evaluated in ways other than measuring their toxicity.[34]

LMWTs in Malaria

Malaria is yet another chronic infectious disease where the major, and most fatal form is caused by the protist, *Plasmodium falciparum* (P. *falciparum*). As was the case with M. *tb*, P. *falciparum* also makes use of LMWTs to protect against the oxidants produced by the host in response to infection, which may also play a role in malarial drug resistance. The principal LMWT in the malaria parasite is GSH. Studies show that inhibition of enzymes which regulate GSH allows cells to remain in an increased oxidative stressed state and consequently aids in killing the malarial parasite.[35-36] Here, the differences in GSH and GSR activity could be used to measure the effects of drugs on the malarial parasite. A number of optical imaging strategies have since been developed in an attempt to exploit these differences.[37]

LMWTs in kidney disease and diabetes

Studies show there is a well-defined relationship between thiol redox status and kidney disease.[9] This correlation between chronic renal failure and the presence of oxidative stress has been shown to result in decreased levels of free plasma thiols.[38-39] This again provides an application opportunity for a disulfide-based sensing tool such as the GSH-luciferin conjugate. There have also been reports indicating decreased plasma thiol levels in patients suffering from type 2 diabetes mellitus. Similarly, this relationship could potentially be used as a basis to support diagnoses of diabetes and/or other diseases.[40-41]

LMWTs in Cancer

There are many reports that suggest that cancer cells exhibit increased oxidative stress due to ROS, primarily because of oncogenic stimulation and increased metabolic activity. The escalated ROS generation in cancer cells serves as an endogenous source of DNA-damaging agents that promote genetic instability and development of drug resistance.[42-43] These conditions allow for cancer cells to be easily distinguishable from normal cells via technologies that evaluate the degree of oxidative stress. However, direct detection of ROS and other free radicals is often difficult because of their greater reactivity. Thus, oxidative damage is generally analysed by measuring secondary products such as lipid peroxidation and related ROS regulating enzymes. A common method for measuring changes in ROS is by measure of antioxidant activity. The cellular levels of ROS are controlled not only by LMWTs but also antioxidant enzymes. The antioxidant enzymes, superoxide dismutases (SODs), play critical roles in scavenging superoxide and there are many commercially available assays that measure SOD activity which can be used as measure for oxidative stress in a variety of samples, including; serum, plasma, cells, tissues and erythrocyte lysates.[44-45] In addition to the antioxidant enzymes,

glutathione processing enzyme levels were also shown to be significantly different between cancer and normal cells.

Reduced GSH and oxidised GSSG, GSR and glutathione S-transferase (GST) activities in 38 tumoral lung tissues and 17 normal lung tissues were determined to obtain a comprehensive profile of the lung glutathione and glutathione processing enzymes in cancer. These enzyme levels in tumoral tissues were found to be significantly higher than those in normal tissues. Reduced glutathione levels were found to be higher in normal tissues than those in tumoral tissues.[46] Diagnostic technologies that exploit such differences are becoming increasingly popular, particularly in pre-clinical studies were a variety of assays are employed to gather biological data. It was therefore an aim of this study to enable similar investigations using D-thioluciferin and, as previously outlined, couple D-thioluciferin bioluminescence to the GSH/GSSG redox reaction and the GSR enzyme.

GSR and Cellular Redox Potential Sensing

There are many ways of measuring GSH and GSR activity, including colorimetric, fluorescent and bioluminescent assays. A popular assay kit for quantitating GSH and GST activity is commercially available from Promega. The GSH-Glo™ Glutathione Assay is a luminescence-based assay designed specifically for detecting and quantifying GSH. The assay is based on the conversion of a luciferin derivative, Luc-NT, into D-luciferin in the presence of glutathione, catalysed by GST. The signal generated in a coupled reaction with luciferase is proportional to the amount of glutathione present in the sample. Luminescence is generated in less than one hour and the assay reportedly generates a stable luminescent signal and is easily adaptable to multiwell formats such as 96- and 384-well plates. Cells can be grown, treated, lysed and assayed for GSH changes in the same plate. This assay was also used to detect and quantify GSH in various other biological samples, a scheme providing an overview of the assay is shown below (Scheme 6.5).

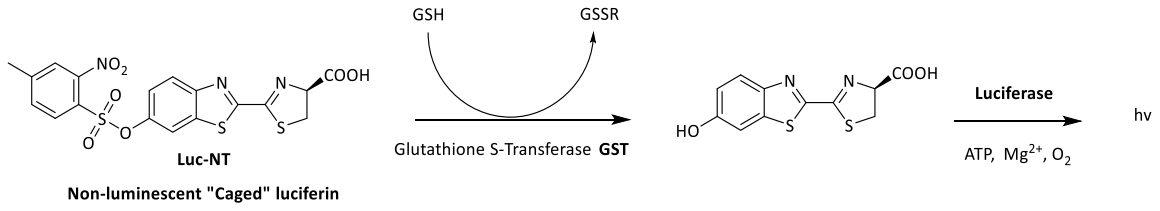

Scheme 6.5. Promega Luc-NT probe for quantitively measuring GSH and oxidised GSSG in samples

There are very few examples of D-luciferin based technologies such as GSH-Glo, where D-luciferin had been directly coupled to GSH and/or GSR. The GSH system is undoubtedly governed by its thiol functionality and, since examples of bioluminescent thiol containing luciferins were limited, it was not

possible to directly link a luciferin to GSH via a disulfide linkage. There are however examples of luciferin linkers containing a disulfide moiety. The D-luciferin molecule has been coupled to various molecules of interest and sometimes the coupling is done indirectly through what is referred to as a spacer or linker moiety. In one publication, D-luciferin was a coupled to a membrane bound transporter protein via an alkyl linker.[47] The linker, which contained a disulfide moiety that was susceptible to disulfide reduction, was attached to D-luciferin via its C6-hydroxyl (Scheme 6.6).

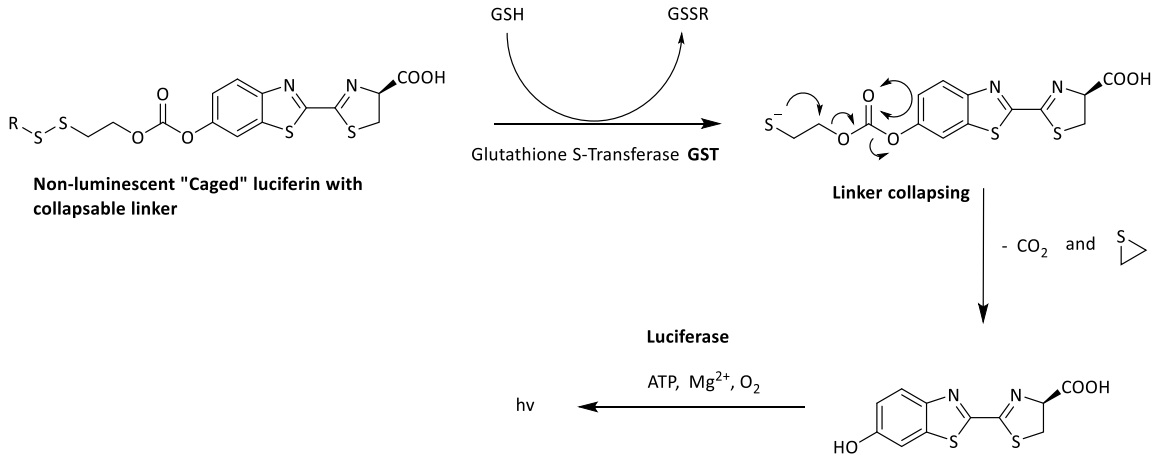

Scheme 6.6. Example of D-luciferin collapsible linker technology

Although these molecules contained disulfides, their application focused on cell uptake rather than redox sensing. A publication dealing with the design, synthesis, and evaluation of conjugates of arginine-rich transporters and luciferin reported that the release of D-luciferin was observed only after entry into cells that were stably transfected with luciferase.[47] The conjugates provided a method to assay uptake and release of free luciferin as a function of variations in the R functionality. The linker in this case was only required since a direct disulfide linkage could not be formed between D-luciferin and the peptide of interest. In contrast, a thio-analogue such as D-thioluciferin may be able to achieve a similar result without having to make use of a linker molecule.

Aims and Objectives

The primary aim concerned coupling bioluminescence to GSH redox to enable the quantitation of GSH and GSSG as well as to enable the monitoring of GSR and GSH peroxidase activity, of relevance in evaluating the degree and effects of oxidative stress. Based on previous work concerning synthetic luciferins and related derivatives, it was already well established that the 6'-thio analogue of D-luciferin was luminescent active and that it resulted in a more red-shifted maximum wavelength of emission, similar to that observed for aminoluciferin. In addition, the more homo disulfide of D-thioluciferin was non-luminescent active which formed the premise for the proposed luminescence-coupled GSR mediated reduction assay (Scheme 6.7).

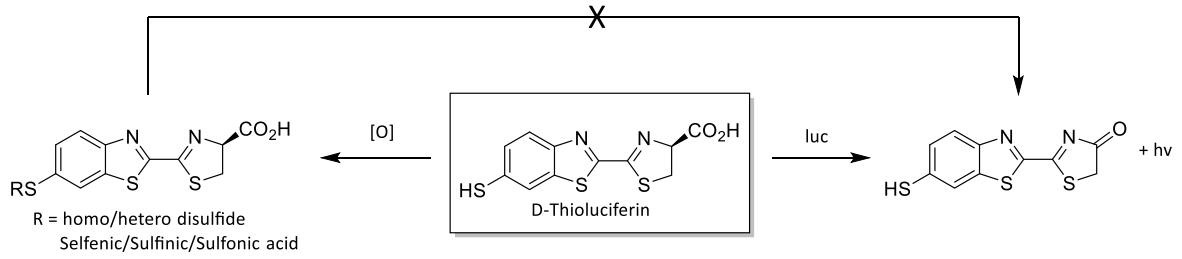

Scheme 6.7. D-Thioluciferin luminescence

It was demonstrated in Chapter 5 that D-thioluciferin bioluminescence was 'turned off' after it had been oxidised to its homodisulfide, which was of course a promising result for intended GSR activity monitoring. This meant that the mixed disulfides formed from D-thioluciferin would likely behave in the same way and could therefore be used to measure GSR activity, provided of course that the thioluciferin disulfides were substrates for GSR. Thus, the thioluciferin disulfides would have to be separately evaluated as substrates for both GSR and luciferase in order to successfully measure GSR activity in samples using bioluminescence.

Scheme 6.8. demonstrates the potential use of a D-thioluciferin disulfide in the monitoring of cellular redox potentials. In cells, the local redox potential varies as a result of many and often interrelated factors. Oxidative stress, which results from increased cellular oxidants, causes a shift in the redox potential equilibrium which in turn would affect the ratio of the thiol/disulfide forms of D-thioluciferin thus resulting in differences in observed luminescence for the stressed cells relative to normal cells.

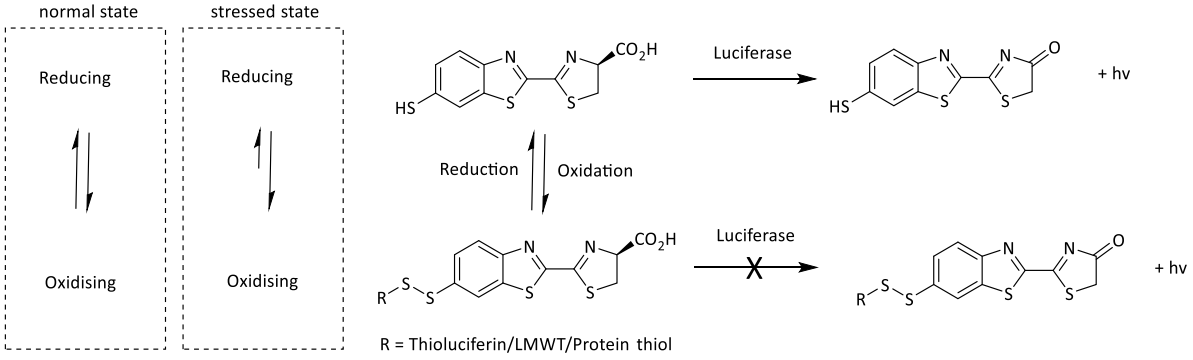

Scheme 6.8. D-Thioluciferin luminescence coupled to redox equilibrium

To lay the groundwork for D-thioluciferin redox sensing applications, D-thioluciferin bioluminescence would first be evaluated in the presence of GSR, GSH and GSSG. This chapter focused on the evaluation of the thioluciferin-GSH disulfide as a substrate of GSR and whether changes in GSR activity could be evaluated using the D-thioluciferin-disulfide.

The specific objectives were thus:

i) The synthesis and characterisation of a thioluciferin-GSH disulfide probe

ii) The evaluation of mixed disulfide bioluminescence using purified luciferase assays

iii) The evaluation of the prepared disulfide probe as a substrate for GSR and subsequent quantitation of GSR activity using the disulfide probe

iv) The evaluation of D-thioluciferin-GSH probes compared to known GSR assays

Synthesis and Evaluation of Luciferin-Based Probes

One of the most common methods for monitoring GSR activity in samples is a colorimetric assay that monitors the oxidation of NADPH to $NADP^+$ by the GSR enzyme. The assay involves monitoring GSR activity via a change in absorbance at 340 nm over time. Generally, a decrease in absorbance is observed over time as a result of NADPH consumption/oxidation upon GSR mediated GSSG reduction. To couple luminescence to GSR activity, modified disulfide substrates were prepared, in the hope that GSR would reduce the substrates and, in doing so, release a detectable bioluminescent analyte. The bioluminescent signal could then be used in addition, or as an alternative to NADPH monitoring. One of the disadvantages of monitoring GSR by NADPH reduction concerns potential interference from compounds that also absorb in same region. To this end, GSSG, D-thioluciferin disulfide and GSH-luciferin disulfide were prepared. The GSSG was prepared as a standard and means of comparison against the newly prepared thioluciferin-GSH disulfide.

GSR probe preparation

Synthesis of homo-disulfides

It has been demonstrated that various mixed disulfides of GSH can be reduced by GSR in the presence of NADPH. To evaluate the thioluciferin-GSH disulfide, a GSSG standard was first prepared from the perborate mediated oxidation of GSH. The homo-disulfide of D-thioluciferin was prepared similarly. Scheme 6.9 shows the preparation of the GSR substrates.

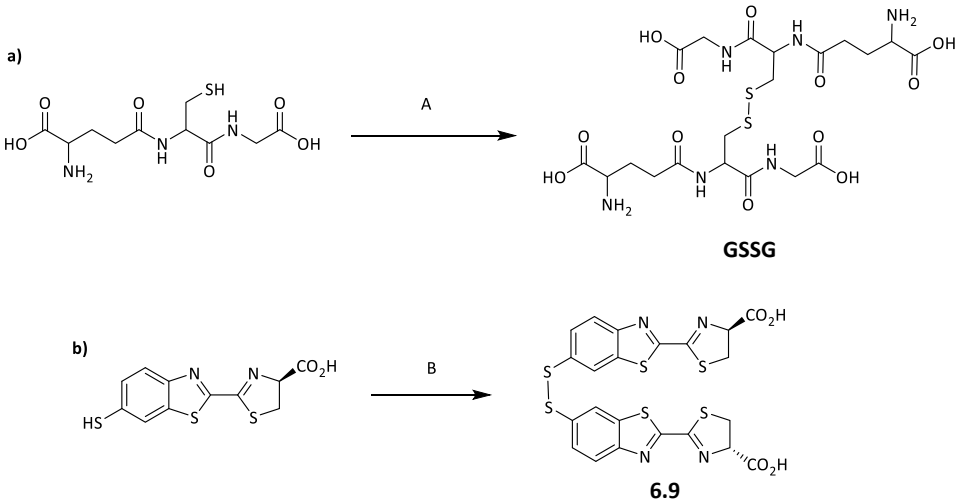

Scheme 6.9. Synthesis of GSR homo-disulfide substrates, reagents and conditions; A) $NaBO_3$ / CH_3COOH / H_2O / rt / 48 h (88 %), B) I_2 / $CHCl_3$ / DSMO / 0 °C / 1 h (99 %)

The homo-disulfides of GSH was achieved using a perborate oxidation reaction, while the homo-disulfide of D-thioluciferin was prepared using an I_2 mediated oxidation. The I_2 oxidation was used

instead of perborate because of isolation challanges experienced when attempting to oxidise D-thioluciferin using an aqueous solution of sodium perborate. Nevertheless, both compounds were isolated in exceptional yields (>90 %) and were characterized using standard techniques. The disulfide of D-thioluciferin, like its free thiol, was unstable to storage (as revealed by TLC analysis) and was prepared strictly before use. The mixed disulfides proved more challenging to prepare and required the synthesis of an intermediate sulfide transfer reagent.

Synthesis of GSH hetero-disulfide

Mixed disulfides of GSH were prepared using aldrithiol mixed disulfide methodology. There are relatively few methods available to form unsymmetrical disuflides, and the aldrithiol method was chosen for two reasons, the first being that it has previously been used to prepare mixed disulfides of GSH and the second being that the thiopyridine formed from the substitution can be used to monitor disulfide reduction as it absorbs strongly at 430 nm. The GSH mixed disulfide was formed by reacting GSH and 2,2'-aldrithiol **6.10** to form an activated mixed disulfide **6.11**. The disulfide **6.11** was subsequently reacted with D-thioluciferin to produce a GSH-luciferin mixed disulfide **6.12**, the GSR probe.

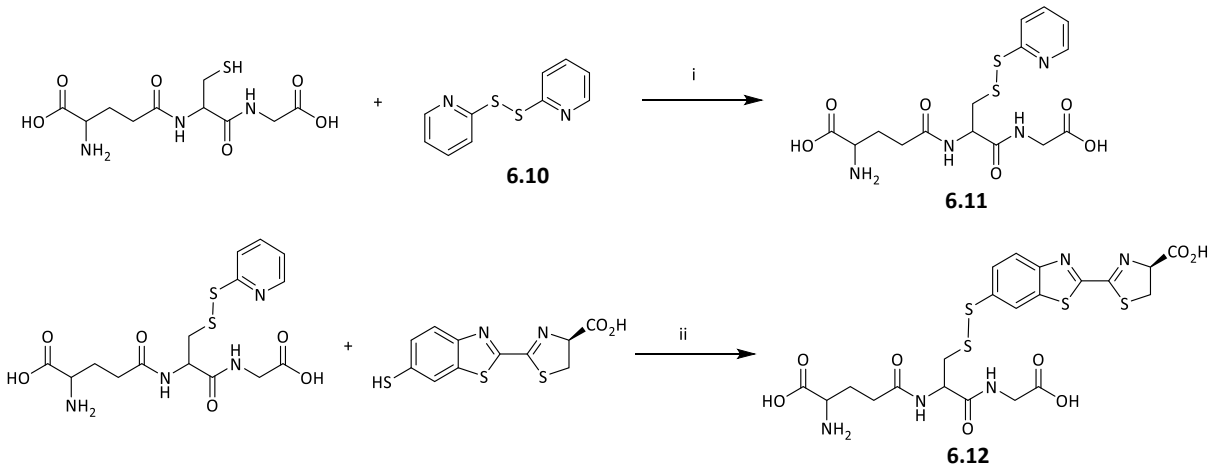

Scheme 6.10. Synthesis of GSR hetero-disulfide substrates. Reagents and conditions: i) DCM / MeOH / rt / 2 h (99 %), ii) H_2O / MeOH / CH_3COOH / rt / 20 min (86 %)

The disulfides were characterised by standard techniques and were evaluated alongside the GSSG standard and D-thioluciferin homo-disulfide for their affinity for the GSR enzyme.

GSR Assays

NADPH/GSR Assay

As a reference, the affinity of GSSG for GSR was measured using spectrophotometry and measuring the change in absorbance of NADPH with time. Test samples were prepared by dissolving GSSG in a previously prepared phosphate buffer containing NADPH. The solution was then incubated, after which the absorbance was recorded at 340 nm until a steady reading was observed. After a constant absorbance reading was achieved, the GSR enzyme was then rapidly injected into the solution and the change in absorbance at 340 nm was measured over a 30 min period. The results from the GSSG/GSR assay are shown in figure 6.2. The Rate of GSSG reduction clearly decreased with increasing substrate concentration. This was due to the increase in the amount of NADPH consumed in the GSR mediated reduction of GSSG. The rates observed were then plotted against their associated concentrations to determine the substrate affinity using Michaelis-Menten kinetics. The observed K_m was 0.024 mM and was of the same order as reported K_m values for GSSG (0.061 mM-0.51 mM).[48-49]

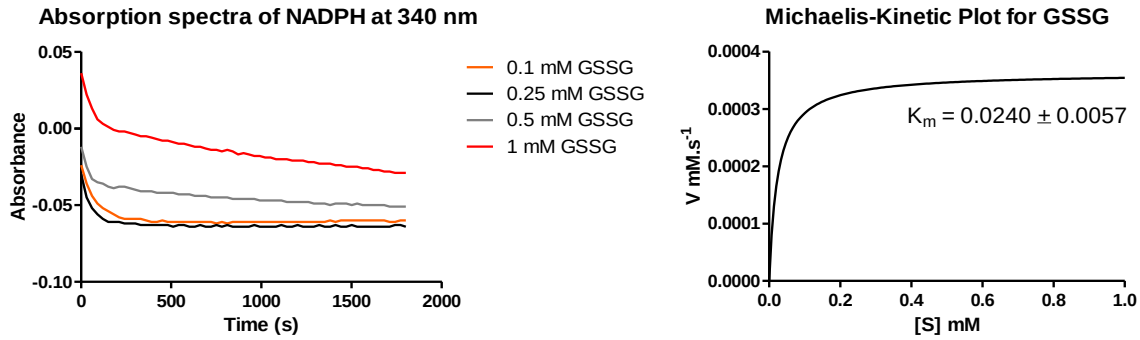

Figure 6.2. a) Change in absorbance associated with NADPH oxidation measured at 340 nm and b) resultant Michaelis-Menten plot

Next the thiopyridine-GSH disulfide was evaluated as a substrate. Here, the same process was repeated as that used for GSSG evaluation, except that instead of recording NADPH reduction at 340 nm, an increase in 2-thiopyridine at 340 nm was measured. The release of 2-thiopyridine would result in a net increase in absorbance over time since thiopyridine has a much higher extinction co-efficient at 340 nm than NADPH (7060 and 0.00622 $M^{-1}cm^{-1}$, respectively).[50] Figure 6.3 displays the absorption spectra of thiopyridine, where a strong absorbance maximum is observed at 340 nm.

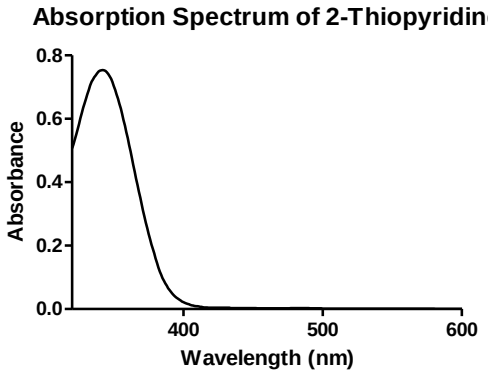

Figure 6.3. Absorption spectrum of 2-thiopyridine

The change in absorbance for the reduction of the thiopyridine-GSH disulfide is shown in figure 6.4, where an initial linear increase in absorbance is observed over time. The different rates observed at varying concentrations of the GSH-thiopyridine substrate were used, as before, to determine the affinity of the enzyme for the substrate. The K_m for the non-natural GSH-thiopyridine disulfide was calculated at 0.1696 mM, which was in the same order as that previously calculated for the native substrates. As expected, GSSG was a better substrate for GSR, however the GSH-Aldrithiol disulfide was still an interesting molecule since it could be used to better monitor GSR activity at 340 nm.

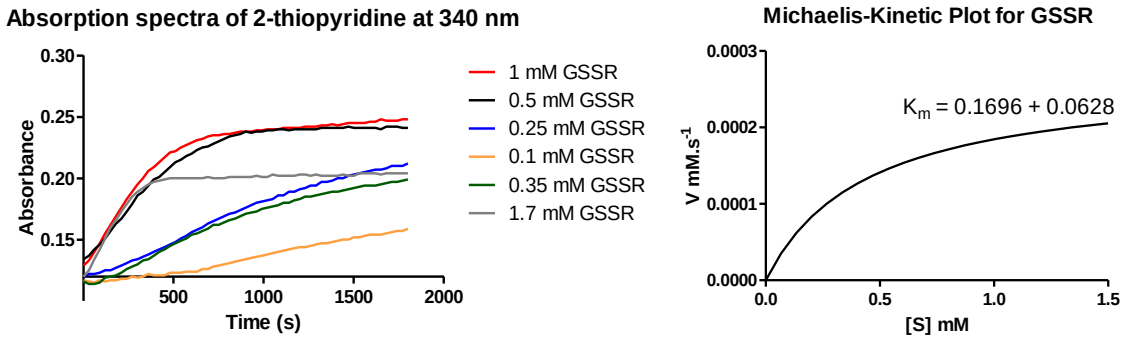

Figure 6.4. a) Change in absorbance associated with NADPH oxidation measured at 340 nm and b) resultant Michaelis-Menten plot. R = 2-thiopyridine

The D-thioluciferin GSH disulfide was then evaluated. The evaluation was done using both colorimetric and bioluminescent readings so as to demonstrate that the disulfide was indeed a substrate for GSR and that the rate of reduction was comparable to GSSG. The absorbance maxima of D-thioluciferin were previously reported (Chapter 5) and based on that, an absorbance of 360 nm was used to measure thioluciferin-GSH reduction. An increase in absorbance over time as well as concentration dependant increases in observed rates clearly demonstrated that the thioluciferin-GSH disulfide was indeed a substrate for GSH reductase.

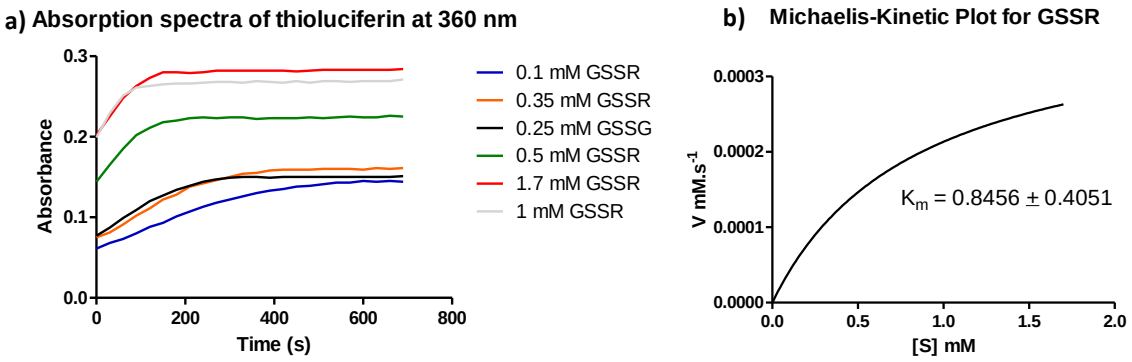

Figure 6.5. a) Change in absorbance associated with NADPH oxidation measured at 360 nm and b) resultant Michaelis-Menten plot. R = thioluciferin

Furthermore, the observed K_m was of the same order as those previously calculated for natural disulfides (0.85 mM and 0.51 mM for the thioluciferin-GSH and GSSG disulfides, respectively). The relatively good affinity and response meant that D-thioluciferin had potential for GSR monitoring. What was needed was to further evaluate whether or not the thioluciferin-GSH could be coupled to the light producing luciferase reaction and whether the bioluminescent emission would afford similar rates and K_m as those observed using the calorimetric assay. Scheme 6.1 shows the intended reaction pathway for the thioluciferin-GSH disulfide.

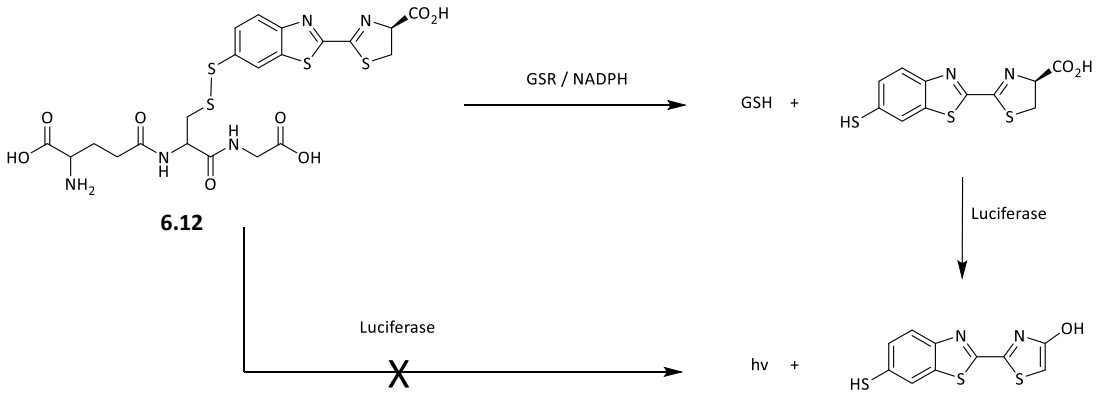

Scheme 6.11. GSR-luciferase coupled bioluminescence

Prior to evaluating the thioluciferin-GSH disulfide **6.12** for GSR monitoring activity, the lack of bioluminescent activity had to be confirmed. Figure 6.6 shows the luminescence output for D-thioluciferin, its homo-disulfide and the thioluciferin-GSH hetero-disulfide **6.12**. Figure 6.6 shows that pure **6.12** in substrate buffer emitted no light. It is also demonstrated that when a 0.1 µM solution of **6.12** was treated with luciferase in enzyme buffer a much lower emission intensity was observed relative to a 0.1 µM solution of D-thioluciferin treated with luciferase, supporting that the disulfide is not a substrate for the light emitting reaction.

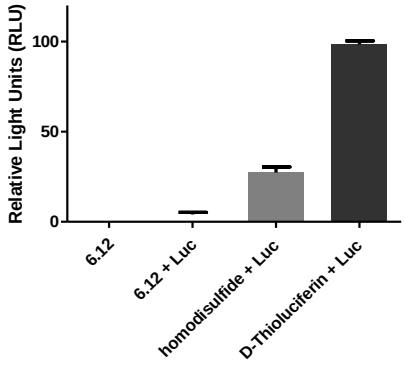

Figure 6.6. Bioluminescence output of 0.1 µM D-thioluciferin, D-thioluciferin homo-disulfide, and thioluciferin-GSH disulfide. The RLU were determined in triplicate and are represented as the mean ± SEM

The homodisulfide of D-thioluciferin when treated with luciferase had a much higher luminescence output than the D-thioluciferin, and the luminescence that was observed for the homodisulfide was assumed to be as a result of DTT mediated reduction of the disulfide in solution, as discussed in Chapter 5. Interestingly, in the case of the thioluciferin-GSH disulfide, no significant luminescence was observed. This could suggest that DTT is in fact not responsible for the bioluminescence observed when the homodisulfide was treated luciferase, however further studies would be required to confirm this. After assessing the bioluminescence of the disulfide **6.12**, it was next evaluated for the GSR monitoring assay.

The bioluminescence resulting from the GSR mediated reduction of thioluciferin-GSH disulfide **6.12** was recorded by pre-treating the samples with the luciferase enzyme prior to GSR addition. The reaction was then monitored using a luminescence plate reader and the resultant data is shown in figure 6.7.

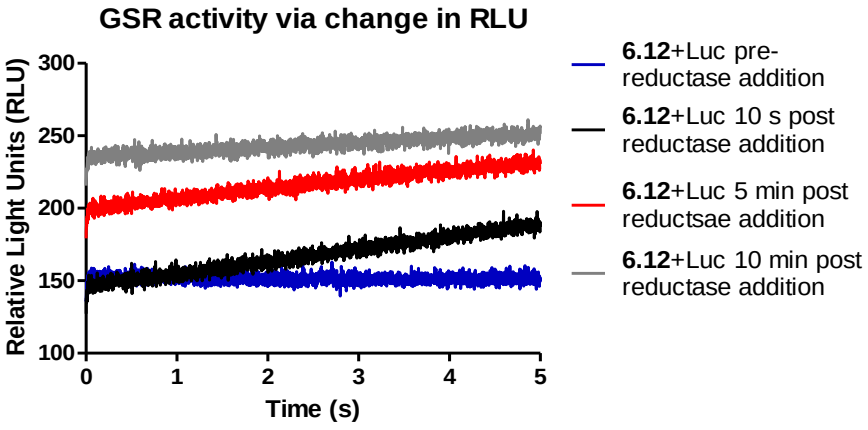

Figure 6.7. Bioluminescence emission of 0.1 mM D-thioluciferin-GSH disulfide **6.12** treated with both 10 nM luciferase in luc enzyme buffer and 0.5 unit/mL GSR in GSR buffer

A clear increase in the bioluminescence emission intensity was observed for the disulfide **6.12** upon treatment with GSR. This was a promising result since it meant that GSR addition clearly promoted a stronger bioluminescence emission and could therefore be used as a measure for GSR activity. What was also interesting was that the homodisulfide of D-thioluciferin was found to not be substrate for GSR as a significant change in absorbance was not observed at 340 and 360 nm upon treatment with GSR. This suggests that only the thioluciferin-GSH mixed disulfide can be used for the monitoring of GSR. It should be noted that a significant baseline emission was also observed prior to GSR addition, which meant that the thioluciferin-GSH disulfide itself was producing some luminescence while in solution with luciferase. This was not expected since a previous study, where the hetero disulfide **6.12** was incubated with luciferase in the absence of GSR, did not produce any luminescence. That reaction was however carried out using a less concentrated solution of the disulfide compared to the GSR coupled assay (0.1 µM in the purified protein assay relative to 0.1 mM in the GSR coupled assay). The reason why the GSR coupled reaction was not done at a concentration where the luminescence of the disulfide **6.12** was previously tested was so that a better comparison could be made between the bioluminescent and colorimetric assays. The concentration of the disulfide was therefore maintained at millimolar levels during the assay since the previous GSSG and GSH-aldrithiol assays were carried out in this range. Despite the significant baseline luminescence, the effects of GSR addition on the emission intensity was still clearly demonstrated. As a precautionary measure, the baseline was also observed over twenty minutes where a relatively stable luminescence reading was recorded. After twenty minutes the baseline reading started to decrease over time which may suggest that the GSR coupled bioluminescence assay might be challenged where extended periods of GSR monitoring is required.

Another method of monitoring GSR activity is by measuring free GSH, either indirectly via enzymes such GST or directly using GSH responsive detectable molecules. There are many examples of thiol sensing molecules and the importance of the selective detection of thiols using reaction-based probes and sensors in basic research and in disease diagnosis have already been highlighted. The disulfide probe allowed for directly coupling GSR reduction to D-thioluciferin bioluminescence, could the thiol functionality of D-thioluciferin also be exploited to quantify GSH directly?

Thioacrylate Thiolate Sensing

Previously prepared D-thioluciferin thioacrylate was predicted to be reactive in the presence of GSH in the same way that it reacted with D-Cys to afford free D-thioluciferin, scheme 6.12.

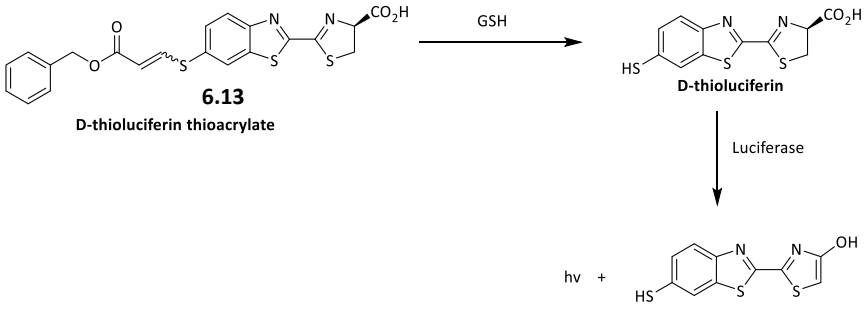

Scheme 6.12. Proposed reaction pathway of D-thioluciferin thioacrylate

Preliminary studies were conducted to evaluate the potential thiol sensing applications, which involved a spectrophotometric analysis of the reaction. First, the rate of thiolate deprotection of the thioacrylate **6.13** was monitored via the change in absorbance at 360 nm upon addition of various thiolates. Unfortunately, a clear and linear increase in the absorbance over time was not observed when the thioacrylate was treated with various thiols/thiolates, including; potassium thioacetate (KSAc), Cys and GSH (Figure 6.8). What was discovered instead was that the thioacrylate in solution, prior to treatment with GSH, Cys and KSAc did not produce a steady baseline reading in solutions of water, water:DMSO (0.8:0.2) and water:CH_3CN (0.7:0.3).

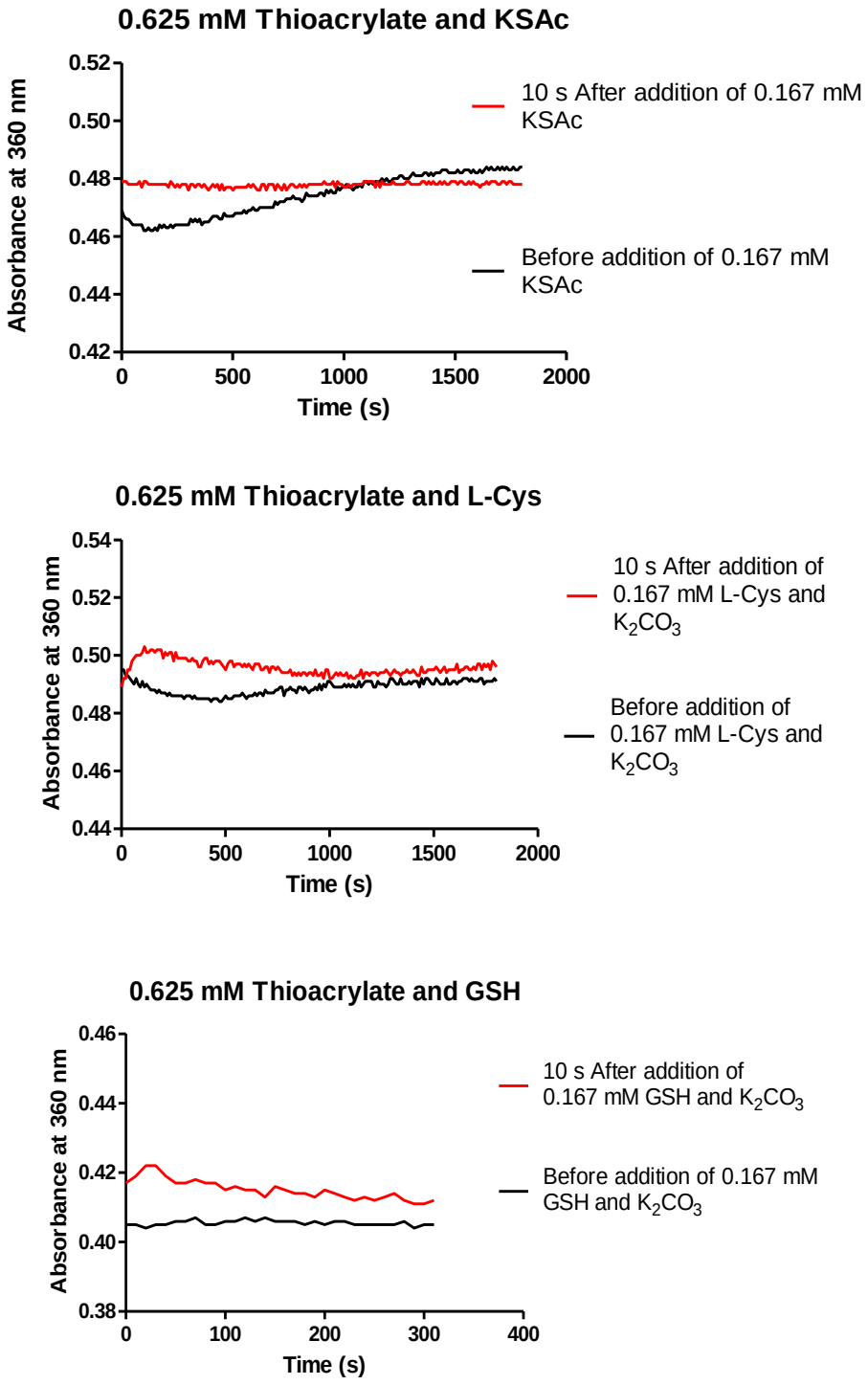

Figure 6.8. Thiolate release studies of D-thioluciferin thioacrylate **6.13**

The fluctuating baseline readings were thought to be related to the solubility of **6.13** in the water:DMSO/CH_3CN solutions. Thus, different ratios of the organic and aqueous solvents were tested but proved to have little effect on achieving a steady pre-assay reading. Thiolate addition was thus only initiated after an eventual steady reading was recorded for at least 1 min prior to the addition.

After addition of the thiolate to the thioacrylate, an increase in absorbance (approximately 0.2 unit increase) across all samples was observed. The rate at which the absorbance increased could however not be determined, presumably because the reaction had gone to completion before the post-thiol(ate) addition readings were recorded. The thiolate sensing of the D-thioluciferin thioacrylate was not further explored in this context but did provide some interesting results for future endeavours.

Summary and Conclusions

GSH detection using the thioacrylate of D-thioluciferin could provide a useful means for quantifying thiolates in solution, however, the stability of the thioacrylate may prove to be an issue, especially since the D-thioluciferin component is known to be quite unstable, particularly in basic and acidic media.

The luciferase-GSR coupled assay demonstrated that the D-thioluciferin thiol functionality has the potential to be coupled to GSR monitoring and perhaps redox reactions in general. The disulfide was demonstrated to be a suitable substrate for GSR and, moreover, it was demonstrated that GSR activity could be determined using thioluciferin bioluminescence, in the same way that GSR activity was determined using the absorbance of NADPH at 340 nm. Further investigations relating to the differences in limits of detection between the colorimetric and bioluminescent assays should still be explored, since the sensitivity of bioluminescence assays are known to be greater than their non-bioluminescent counterparts. It is well established that monitoring the change in NADPH absorbance to provide a measure of GSR activity is extremely limited in terms of in vivo and cell-extract based applications. These limitations might be overcome through the use of a D-thioluciferin bioluminescence assay alternative, whose bioluminescence signal is easily distinguishable and is not affected by the presence of other biological components.

Based on these preliminary studies, there is strong evidence that the D-thioluciferin molecule could prove useful in LMWT and GSR monitoring.

References

1. Fahey, R. C., Novel thiols of prokaryotes. *Annual Reviews in Microbiology* **2001,** *55* (1), 333-356.
2. Kinsella, J. E.; Whitehead, D. M., Proteins in whey: chemical, physical, and functional properties. *Adv.Food Nutr.Res* **1989,** *33* (3), 437-438.
3. Mungli, P.; Shetty, M. S.; Tilak, P.; Anwar, N., Total thiols: Biomedical importance and their alteration in various disorders. *Online journal of health and allied sciences* **2009,** *8* (2).
4. O'Halloran, T. V.; Culotta, V. C., Metallochaperones, an intracellular shuttle service for metal ions. *Journal of Biological Chemistry* **2000,** *275* (33), 25057-25060.
5. Rosenzweig, A. C., Metallochaperones: bind and deliver. *Chemistry & biology* **2002,** *9* (6), 673-677.
6. Dickinson, D. A.; Forman, H. J., Cellular glutathione and thiols metabolism. *Biochemical pharmacology* **2002,** *64* (5), 1019-1026.
7. Fernandez-Checa, J. C.; Kaplowitz, N., Hepatic mitochondrial glutathione: transport and role in disease and toxicity. *Toxicology and applied pharmacology* **2005,** *204* (3), 263-273.
8. Hartman, P. E., [32] Ergothioneine as antioxidant. *Methods in enzymology* **1990,** *186*, 310-318.
9. Oberg, B. P.; McMenamin, E.; Lucas, F. L.; McMonagle, E.; Morrow, J.; Ikizler, T. A.; Himmelfarb, J., Increased prevalence of oxidant stress and inflammation in patients with moderate to severe chronic kidney disease. *Kidney international* **2004,** *65* (3), 1009-1016.
10. Andersson, A.; Hultberg, B.; Lindgren, A., Redox status of plasma homocysteine and other plasma thiols in stroke patients. *Atherosclerosis* **2000,** *151* (2), 535-539.
11. Ziegler, D. M., Role of reversible oxidation-reduction of enzyme thiols-disulfides in metabolic regulation. *Annual Review of Biochemistry* **1985,** *54* (1), 305-329.
12. Buchmeier, N. A.; Newton, G. L.; Koledin, T.; Fahey, R. C., Association of mycothiol with protection of Mycobacterium tuberculosis from toxic oxidants and antibiotics. *Molecular microbiology* **2003,** *47* (6), 1723-1732.
13. Sies, H.; De Groot, H., Role of reactive oxygen species in cell toxicity. *Toxicology letters* **1992,** *64*, 547-551.
14. Meister, A.; Anderson, M. E., Glutathione. *Annual Review of Biochemistry* **1983,** *52* (1), 711-760.
15. Stich, A.; Abel, P. M.; Krishna, S., Human African trypanosomiasis. *BMJ: British Medical Journal* **2002,** *325* (7357), 203.

16. Khonde, P. L.; Jardine, A., Improved synthesis of the super antioxidant, ergothioneine, and its biosynthetic pathway intermediates. *Organic & biomolecular chemistry* **2015,** *13* (5), 1415-1419.
17. Hand, C. E.; Taylor, N. J.; Honek, J. F., Ab initio studies of the properties of intracellular thiols ergothioneine and ovothiol. *Bioorganic & medicinal chemistry letters* **2005,** *15* (5), 1357-1360.
18. Ariyanayagam, M. R.; Fairlamb, A. H., Ovothiol and trypanothione as antioxidants in trypanosomatids. *Molecular and biochemical parasitology* **2001,** *115* (2), 189-198.
19. Turner, E.; Hager, L. J.; Shapiro, B. M., Ovothiol replaces glutathione peroxidase as a hydrogen peroxide scavenger in sea urchin eggs. *Science* **1988,** *242* (4880), 939-941.
20. Van Laer, K.; Hamilton, C. J.; Messens, J., Low-Molecular-Weight Thiols in Thiol–Disulfide Exchange. *Antioxidants & redox signaling* **2013,** *18* (13), 1642-1653.
21. Owen, J. B.; Butterfield, D. A., Measurement of oxidized/reduced glutathione ratio. In *Protein Misfolding and Cellular Stress in Disease and Aging*, Springer: 2010; pp 269-277.
22. Morier-Teissier, E.; Mestdagh, N.; Bernier, J.-L.; Henichart, J.-P., Reduced and oxidized glutathione ratio in tumor cells: comparison of two measurement methods using HPLC and electrochemical detection. *Journal of Liquid Chromatography & Related Technologies* **1993,** *16* (3), 573-596.
23. Ketterer, B., The role of nonenzymatic reactions of glutathione in xenobiotic metabolism. *Drug metabolism reviews* **1982,** *13* (1), 161-187.
24. Forman, H. J.; Zhang, H.; Rinna, A., Glutathione: overview of its protective roles, measurement, and biosynthesis. *Molecular aspects of medicine* **2009,** *30* (1), 1-12.
25. Hanigan, M. H.; Ricketts, W. A., Extracellular glutathione is a source of cysteine for cells that express. gamma.-glutamyl transpeptidase. *Biochemistry* **1993,** *32* (24), 6302-6306.
26. Ames, S. R.; Elvehjem, C., Enzymatic oxidation of glutathione. *Journal of Biological Chemistry* **1945,** *159* (2), 549-562.
27. Carlberg, I.; Mannervik, B., [59] Glutathione reductase. In *Methods in enzymology*, Elsevier: 1985; Vol. 113, pp 484-490.
28. Carlberg, I.; Mannervik, B., [59] Glutathione reductase. *Methods in enzymology* **1985,** *113*, 484-490.
29. Schafer, F. Q.; Buettner, G. R., Redox environment of the cell as viewed through the redox state of the glutathione disulfide/glutathione couple. *Free Radical Biology and Medicine* **2001,** *30* (11), 1191-1212.
30. Bogdan, C., Nitric oxide and the immune response. *Nature immunology* **2001,** *2* (10), 907.

31. Raviglione, M. C.; Snider Jr, D. E.; Kochi, A., Global epidemiology of tuberculosis. *JAMA: the journal of the American Medical Association* **1995,** *273* (3), 220-226.

32. Dye, C.; Williams, B. G., The population dynamics and control of tuberculosis. *Science (New York, N.Y.)* **2010,** *328* (5980), 856-861.

33. Gomez, J. E.; McKinney, J. D., < i> M. tuberculosis</i> persistence, latency, and drug tolerance. *Tuberculosis* **2004,** *84* (1), 29-44.

34. Shuhendler, A. J.; Pu, K.; Cui, L.; Uetrecht, J. P.; Rao, J., Real-time imaging of oxidative and nitrosative stress in the liver of live animals for drug-toxicity testing. *Nature biotechnology* **2014,** *32* (4), 373.

35. McClendon, S. L., Attempt to Synthesize the (S) Enantiomer of a Glutathione Analog to be an Inhibitor of Glutathione Reductase. **2013**.

36. Şentürk, M.; Talaz, O.; Ekinci, D.; Çavdar, H.; Küfrevioğlu, Ö. İ., In vitro inhibition of human erythrocyte glutathione reductase by some new organic nitrates. *Bioorganic & medicinal chemistry letters* **2009,** *19* (13), 3661-3663.

37. Cho, S.; Kim, S.; Kim, Y.; Park, Y., Optical imaging techniques for the study of malaria. *Trends in biotechnology* **2012,** *30* (2), 71-79.

38. Galle, J., Oxidative stress in chronic renal failure. *Nephrology Dialysis Transplantation* **2001,** *16* (11), 2135-2137.

39. Hasselwander, O.; Young, I. S., Oxidative stress in chronic renal failure. *Free radical research* **1998,** *29* (1), 1-11.

40. Dursun, E.; Timur, M.; Dursun, B.; Süleymanlar, G.; Ozben, T., Protein oxidation in Type 2 diabetic patients on hemodialysis. *Journal of diabetes and its complications* **2005,** *19* (3), 142-146.

41. Pasaoglu, H.; Sancak, B.; Bukan, N., Lipid peroxidation and resistance to oxidation in patients with type 2 diabetes mellitus. *The Tohoku journal of experimental medicine* **2004,** *203* (3), 211-218.

42. Toyokuni, S.; Okamoto, K.; Yodoi, J.; Hiai, H., Persistent oxidative stress in cancer. *FEBS letters* **1995,** *358* (1), 1-3.

43. Pelicano, H.; Carney, D.; Huang, P., ROS stress in cancer cells and therapeutic implications. *Resistance Updates* **2004,** *7* (2), 97-110.

44. Oberley, L. W.; Spitz, D. R., [61] Assay of superoxide dismutase activity in tumor tissue. In *Methods in enzymology*, Elsevier: 1984; Vol. 105, pp 457-464.

45. Sun, Y.; Oberley, L. W.; Li, Y., A simple method for clinical assay of superoxide dismutase. *Clinical chemistry* **1988,** *34* (3), 497-500.

46. Saydam, N.; Kirb, A.; Demir, Ö.; Hazan, E.; Oto, Ö.; Saydam, O.; Güner, G., Determination of glutathione, glutathione reductase, glutathione peroxidase and glutathione S-transferase levels in human lung cancer tissues. *Cancer letters* **1997,** *119* (1), 13-19.

47. Jones, L. R.; Goun, E. A.; Shinde, R.; Rothbard, J. B.; Contag, C. H.; Wender, P. A., Releasable Luciferin− Transporter Conjugates: Tools for the Real-Time Analysis of Cellular Uptake and Release. *Journal of the American Chemical Society* **2006,** *128* (20), 6526-6527.

48. Gaullier, J.; Lafontant, P.; Valla, A.; Bazin, M.; Giraud, M.; Santus, R., Glutathione Peroxidase and Glutathione Reductase Activities toward Glutathione-Derived Antioxidants. *Biochemical and biophysical research communications* **1994,** *203* (3), 1668-1674.

49. Mavis, R. D.; Stellwagen, E., Purification and subunit structure of glutathione reductase from bakers' yeast. *Journal of Biological Chemistry* **1968,** *243* (4), 809-814.

50. Augustinsson, K.-B.; Eriksson, H., The effects of two disulphides on cholinesterase activity in the spectrophotometric assay. *Biochemical Journal* **1974,** *139* (1), 123-127.

Chapter 7

Conclusions and Future Work

Conclusions

D-luciferin and the non-natural C6-amino analogue, D-aminoluciferin, were successfully prepared in overall yields of 12 % and 20 %, respectively. Their spectroscopic and relative bioluminescent properties were found to be in good agreement with previously reported data.

In both instances, the 2-cyanobenzothiazole scaffold was identified as a key intermediate for luciferin preparation. The C2-nitrile moiety of the benzothiazole scaffold was used to construct the thiazole carboxylic acid component of D-luciferin upon reaction of the nitrile with D-Cys. This particular reaction was highly efficient and produced the resultant luciferin quantitively. As a result of the high yield and generally good stereospecificity, most reported synthesis of D-luciferin and related analogues make use of a key 2-cyanobenzothiazole intermediate. However, these syntheses, despite their common target, differ significantly in how the 2-cyanobenzothiazole scaffold is prepared. For most reported syntheses, the 2-cyanobenzothiazole is formed in poor yield and over multiple functionalisation steps.

For the synthesis of D-luciferin and D-aminoluciferin, the 2-cyanobenzothiazole forming palladium-mediated cyclisation, a reaction common to both luciferin syntheses, was found to be limiting and was the main contributor to the poor overall yields. Since both these compounds were highly sought after for various bioluminescence applications, an investigation into further optimising as well exploring other methods of preparation was undertaken. A number of different methods were attempted to increase the efficacy of the palladium C-S coupling reaction. These included, among others, exploring the use of different palladium catalysts, reverting to a classical thermolytic electrocyclisation reaction, and exploring the effects of *ortho*-bromination on the thioanilide cyclisation. Ultimately, *ortho*-bromination of the starting anilide lead to a successful cyclisation and afforded the cyclised products in generally improved yields (60-85 %) and was demonstrated to have better functional group tolerability with respect to the C6-substituent. An unrelated route involving a C6-iodo functional group on the benzothiazole was also explored as an alternative intermediate, which unlocked new possibilities for method improvement.

After reaction optimisation and method development, attention was turned to the preparation of new C6-analogues of D-luciferin. With both the 6'-hydroxy and 6'-amino luciferins in hand, the obvious target became a 6'-thio analogue. Synthesis of the thio-analogue proved challenging, but it was eventually prepared using a synthetic route based on a thiol-protecting group strategy. The thio-analogue, D-thioluciferin, was successfully synthesised over six steps (34 % yield) using an unconventional thioacrylate protecting group. The new luminogenic substrate displayed a lower K_m (0.1 µM relative to the 8 µM of D-luciferin) and a more red-shifted maximum emission (λ_{max} 600 nm compared to the 557 nm of D-luciferin), but with a much lower luminescent output (100-fold less) relative to D-luciferin.

After preparing and evaluating the bioluminescence of the novel C6-thio analogue, its thiol functionality was exploited to produce a disulfide probe/sensor for GSR activity. First, a mixed disulfide of D-thioluciferin and GSH was prepared and evaluated as a substrate for the enzyme luciferase, since it was important that the disulfide probe be non-luminescent active until reduced. The results from that study demonstrated that the disulfide was indeed non-bioluminescent in the presence of the luciferase enzyme. Thereafter, the disulfide was shown to be a relatively good substrate for GSR (K_m of 0.85 mM relative to a K_m of 0.51 mM for GSSG) which meant that D-thioluciferin bioluminescence could indeed be coupled to GSR monitoring. A bioluminescence assay of GSR activity was then carried out and was shown to be a viable method of GSR monitoring.

In addition to monitoring GSR activity, D-thioluciferin was also evaluated for thiol/thiolate sensing. The protected thioacrylate was shown to react with thiols in basic media to produce D-thioluciferin.

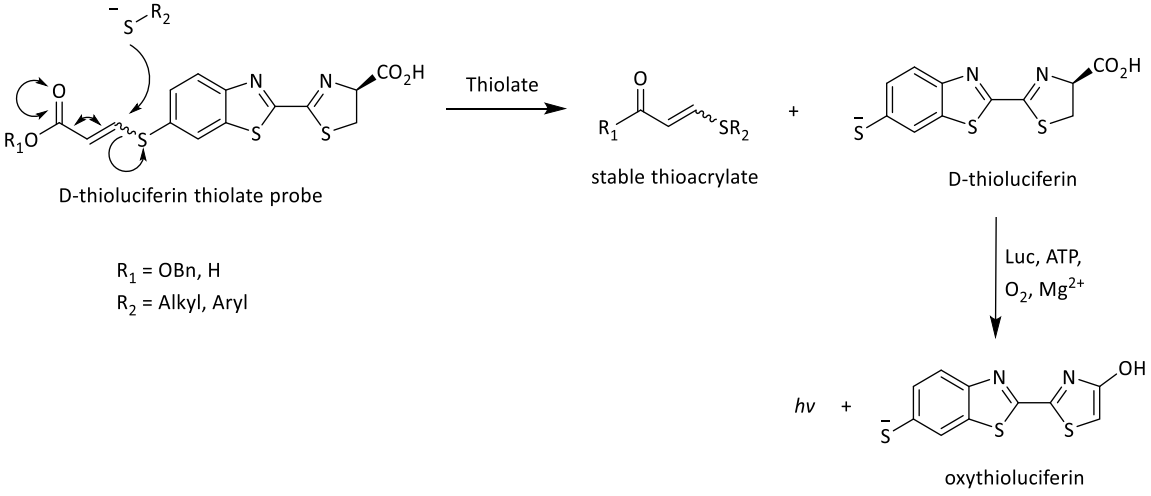

Scheme 7.1. Mechanism of thiolate-mediated D-thioluciferin release

However, the rate at which the reaction occurred was relatively fast and did not allow for differentiation of various thiols/thiolates based on their relative reaction rates. Despite this, the acrylate is still an exciting prospect for thiol sensing and should be explored further.

Future Work

After D-aminoluciferin was introduced to the research community, an exponential increase in luciferin application-based research was observed. This was, in part, due to the C6-amino handle that D-aminoluciferin provided. The thiol functionality should be viewed similarly, as it too provides a unique chemical handle that might allow D-thioluciferin to be applied in areas relatively untouched by its bioluminescent predecessors. This relates specifically to the monitoring of biological thiols and their processing enzymes.

The groundwork for such applications have been explored here but still does not cover any in vivo testing of the thio-analogues. The cellular uptake, localisation, distribution and stability in biological media should be further explored. It has already been demonstrated here how the oxidation state of the C6-thiol moiety of D-thioluciferin governs the molecule's ability to produce light with the luciferase enzyme. What should be explored next is whether the thiol functionality is responsive to changes in redox states within cells and whether those changes can be observed through bioluminescence.

In cells, abnormal changes in redox equilibria or cellular redox potentials are observed as a result of increased oxidative stress, which in turn affect biological free thiol/disulfide ratios. These changes in redox states are often directly linked to certain diseases and it would be interesting to evaluate whether such redox state changes could be observed using the thioluciferin molecule.

As an example, this could be done by evaluating differences in bioluminescence emission between a luciferase expressing cancer cell line and a healthy luciferase expressing cell line. Another potential study could involve plant stress monitoring. The thioluciferin-GSH probe could be tested in the evaluation of the degree of stress induced by dehydration in luciferase expressing plants. Where dehydrated plants are treated with the thioluciferin-GSH probe alongside plants that have not been dehydrated to evaluate differences in their cellular redox states based on observed differences in bioluminescence. Such differences in bioluminescence could then be used as part of a measure of how well plants cope with dehydration and hence as a method of screening for drought resistance among mutant plants.

Future work concerning LMWTs and their conjugation to the D-thioluciferin molecule should also be considered. Other LMWT mixed disulfides of D-thioluciferin should be explored for potential

reductase monitoring, for example, a thioluciferin-MSH disulfide could in theory be used to monitor mycothione reductase activity, just as how the thioluciferin-GSH conjugate was used to measure GSR activity. MSH is of course a LMWT found in M. *tb* and is, in part, responsible for the protection of M. *tb* from oxidants. Studies show that MSH and mycothione reductase are upregulated in response to oxidative stress. Their concentration and activity could therefore be used for bioluminescence imaging and as a measure of drug efficacy.

In terms of the synthesis of the luciferin molecules, there are a number of investigations that should be undertaken to further improve the one-pot metal free DBU methodology. The priority would probably be to replace DBU with another base that could be more easily removed from the reaction mixture, while still retaining the ability to fragment and cyclise the dithiazole. The excessive amounts of DBU required for the transformation is definitely one of the biggest disadvantages of the method. There are publications that report on the use of phosphine reagents that are able to fragment dithiazoles, however, based on the mechanism, they most likely would not be able to bring about cyclisation at room temperature. It might therefore be of interest to explore the joint use of both an amidine base and a phosphine additive or, alternatively, a reagent that has both a basic nitrogen and phosphine functionality. Another interesting approach could be to immobilize a recyclable amidine base onto a solid support for a simpler purification.

Recently, there have been far more publications concerning the applications and bioluminescent properties of D-luciferin derivatives than publications relating to improved methods of luciferin preparation. However, both are required for sustainable D-luciferin research within a chemistry/chemical biology context.

Thus, improvements in both the synthesis and properties of these very important research molecules should and will continue to be investigated.

Chapter 8

Experimental Procedures

General procedures

All reactions were carried out in oven-dried glassware under an inert nitrogen atmosphere, unless otherwise stated. Reagents were obtained from commercial sources (Sigma–Aldrich, Merck) and used as received unless otherwise stated. Solvents were evaporated under reduced pressure at 40 °C using a Buchi Rotavapor, unless otherwise stated. Reaction temperatures were achieved with heat/silicone oil (for > 25 ^{o}C), ice/NH_4Cl salt (for 0 °C), and acetone/liquid nitrogen (< -20 °C). Aqueous solutions were prepared using distilled water. All reactions were monitored by TLC using aluminium-backed Merck silica-gel 60 F254 plates, and compounds were visualised on TLC under a UV-lamp and/or were sprayed with a 2.5 % solution of *p*-anisaldehyde in a mixture of sulfuric acid and ethanol (1:10 v/v), iodine vapour, or ceric ammonium sulfate solution and then heated using a 1600 W heat gun. Normal phase column chromatography was carried out using silica-gel (Fluka Silica Gel 60, 40-63 microns) and compounds eluted with the appropriate solvent mixtures. Reverse phase chromatography was effected by using a Biotage KP-C-18-HS and compounds were eluted with millipore water and AR methanol (gradient from water to a mixture of water/MeOH), unless otherwise stated. All compounds were dried under vacuum before yields were determined and spectroscopic analyses performed. Purity was determined using an analytical Agilant HPLC 1260 equipped with an Agilent infinity diode array detector (DAD) 1260 UV-Vis detector, with an absorption wavelength range of 210 - 640 nm. The compounds were eluted using a mixture of 10 mM NH_4OAc/H_2O and 10 mM NH_4OAc/MeOH at a flow rate of 0.9 mL.min^{-1} (10 % NH_4OAc/MeOH between 0 and 1 min, 10 - 95 % NH_4OAc/MeOH between 1 and 3 min, 95 % NH_4OAc/MeOH between 3 and 5 min).

Nuclear Magnetic Resonance (NMR) spectra (^{1}H and ^{13}C) were recorded on either a Bruker XR400 MHz spectrometer (^{1}H at 400.0 MHz and ^{13}C at 100.6 MHz), Varian Mercury XR400 MHz spectrometer (^{1}H at 400.0 MHz and ^{13}C at 100.6 MHz), a Varian Mercury XR300 MHz spectrometer (^{1}H at 300.1 MHz and ^{13}C at 75 MHz) or a Bruker unity spectrometer (^{1}H at 600 MHz and ^{13}C at 151 MHz) and were carried out in $CDCl_3$, DMSO-d_6 and D_2O as the solvents, unless otherwise stated. Chemical shifts (δ) and *J*-coupling values were reported in units of ppm and Hz respectively. Chemical shifts for ^{1}H and ^{13}C were recorded using tetramethylsilane (TMS) as the internal standard. Assignments were confirmed by COSY, APT and HSQC analysis, when required.

Elemental analyses were performed using a Fisons EA 1108 CHNS elemental analyser. Infrared (IR) spectroscopy was performed on a Bruker FT-IR Spectrometer with vibrations measured in units of

cm^{-1}. Melting points were obtained using a Reichert-Jung Thermovar hot stage microscope (HSM) and are uncorrected. Optical rotations were obtained using a Perkin Elmer 141 polarimeter at 20 °C. The concentration *c* refers to g/100 mL. UV-Vis studies were conducted on UV-Vis spectrophotometer Agilent technology Cary 60 and the spectrums were processed using Scan Application version 5.0.0.99. Mass Spectrometry (MS) determinations were carried out using electron impact (EI) on a JOEL GC Matell instrument. LCMS analyses were carried out with a UHPLC Agilent 1290 Infinity Series (Germany), accurate mass spectrometer Agilent 6530 Quadrupole Time Of Flight (QTOF) equipped with an Agilent jet stream ionisation source (positive ionization mode) (ESI+) and column (Eclipse + C18 RRHD 1.8 µm.2.1 X 50, Agilent, Germany). All UV-vis spectra were recorded with a Varian Cary 100 spectrophotometer or a Shimadzu UV 1800 Probe at constant temperature by attachment of the cell chamber to an external water bath. Hellma, Suprasil® quartz cuvettes of 1 and 10 mm pathlength in varied volume capacity were used for all measurements. A Varian Cary Eclipse fluorometer equipped with a regulated temperature cell holder was used to perform all steady-state fluorescence measurements. Hellma, Suprasil® quartz fluorescence cuvettes of 10 mm pathlength and 1.5 mL volume capacity were used for all measurements.

Bioluminescence evaluation using purified protein (luciferase from *Photinus Pyralis*, Sigma-Aldrich) were performed using a Luminoskan Ascent at a final enzyme concentration of 10 nM and final substrate concentrations ranging from 0.1 to 100 µM. Data acquisition and analyses were performed with Ascent Software version 2.6 (detector range 270-670 nm, detecting at 545 nm). Bioluminescence imaging of transgenic luciferase expressing *N. Tabacum* plant leaves were carried out with a 3D-luminometer consisting of a 0.5 square inch CCD camera and a field of view of 12.5 cm (Xenogen IVIS Lumina, Caliper, USA) at an exposure time of 300 s per leaf. Photon or count emission by luciferase expressing leaves was quantified using the Living Image software (Caliper, USA). The GFP assay was selected to negate any luminescence from chloroplasts.

Synthetic procedures

The numbering scheme given for each compound is for assignment purposes only and not necessarily consistent with the IUPAC naming convention.

Synthesis of D-luciferin[1]

4,5-Dichloro-1,2,3-dithiazol-1-ium chloride[2]

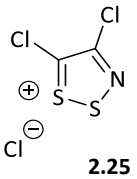

2.25

Sulfur monochloride (13 mL, 158 mmol, 5 eq) was added to a solution of chloroacetonitrile (2 mL, 31.6 mmol, 1 eq) in anhydrous DCM (15 mL) in an oven-dried flask equipped with a gas outlet. Thereafter, the reaction mixture was swirled for a few seconds and then left to stand, without further agitation, for 24 h at room temperature under a nitrogen atmosphere. The resulting brown precipitate that had formed was filtered under vacuum, and washed copiously with DCM (3 x 200 mL) to afford Appel's salt as a green solid (5.30 g, 80 %). **Mp**: 117-130 °C. **MS (ESI+):** *m/z* Calculated for $C_2Cl_3NS_2$ [M+H] 207.8616, found 207.8610.

N-[(5Z)-4-chloro-5H-1,2,3-dithiazol-5-ylidene]-4-methoxyaniline

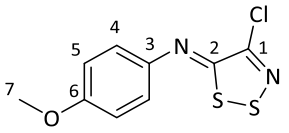

2.22

Appel's salt **1** (3.39 g, 16.3 mmol, 1 eq) and *p*-anisidine (2.00 g, 16.3 mmol, 1 eq) were suspended in anhydrous DCM (30 mL). The resulting mixture was stirred at room temperature under a nitrogen atmosphere for 1 h. Thereafter, anhydrous pyridine (2.62 mL, 32.5 mmol, 2 eq) was slowly added to the suspension and the resulting red brown mixture was allowed to stir for an additional 2 h. The mixture was then concentrated *in vacuo* and purified using silica column chromatography, eluting with hexanes, to afford the dithiazole adduct as a yellow solid (2.72 g, 65 %). **Mp**: 87-88 °C (lit. 89 °C).[3] **^{1}H-NMR (300 MHz, $CDCl_3$)** δ 7.28 (2H, d, *J* = 8.9 Hz, H-4), 6.99 (2H, d, *J* = 8.9 Hz, H-5), 3.85 (3H, s, H-7) ppm. **^{13}C-NMR (100.6 MHz, $CDCl_3$)** δ 158.1 (C-6), 156.9 (C-2), 147.8 (C-1), 143.3 (C-3), 122.1 (C-5), 115.4 (C-4), 55.9 (C-7) ppm. **MS (ESI+):** *m/z* Calculated for $C_9H_7ClN_2OS_2$ [M+H] 258.9766, found 258.9760.

1-[(Cyanocarbothioyl)amino]-4-methoxybenzene

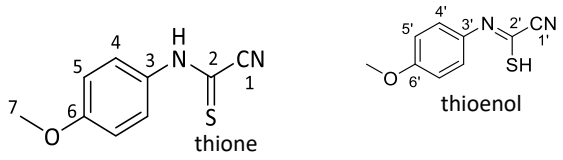

2.23

DBU (1.12 mL, 7.72 mmol, 4 eq) was added dropwise to a 5 °C solution of *N*-[(5Z)-4-chloro-5H-1,2,3-dithiazol-5-ylidene]-4-methoxyaniline **2.22** (0.50 g, 1.93 mmol, 1 eq) in anhydrous DCM (10 mL) under a nitrogen atmosphere. The resulting red brown mixture was stirred and maintained below 5 °C for 30 min, after which it was allowed to warm to room temperature. The reaction mixture was then washed with saturated NH_4Cl_{aq} (3 x 10 mL), H_2O (1 x 10 mL), and brine (1 x 10 mL). The organic phase was dried over Na_2SO_4 and concentrated *in vacuo*. The crude material was purified by column chromatography, eluting with 3:7 EtOAc:Hexane to provide the title compound as a red solid (0.27 g, 73 %). **Mp**: 118-121 °C (lit. 118-119 °C).[4] **Thione; ^{1}H-NMR (400 MHz, $CDCl_3$)** δ 9.79 (1H, br s, -NH-), 7.65 (2H, d, *J* = 8.0 Hz, H-4), 6.87 (2H, m, H-5), 3.76 (3H, s, H-7) ppm. **^{13}C-NMR (100.6 MHz, $CDCl_3$)** δ 160.2 (C-2), 158.7 (C-6), 131.4 (C-3), 124.8 (C-4), 114.6 (C-5), 113.2 (C-1), 55.9 (C-7) ppm. **Thioenol; ^{1}H-NMR (400 MHz, $CDCl_3$)** δ 9.52 (1H, br s, -SH), 7.23 (2H, d, *J* = 8.0 Hz, H-4'), 6.87 (2H, m, H-5), 3.76 (3H, s, H-7) ppm. **^{13}C-NMR (100.6 MHz, $CDCl_3$)** δ 164.9 (C-2'), 159.5 (C-6'), 131.6 (C-3'), 125.5 (C-4'), 122.0 (C-1'), 115.1 (C-5'), 55.9 (C-7) ppm. **MS (ESI+):** *m/z* Calculated for $C_9H_8N_2OS$ [M+H] 193.0435, found 193.0472.

2-Cyano-6-methoxybenzothiazole

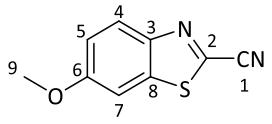

2.8

Palladium chloride (7.00 mg, 0.0350 mmol, 0.1 eq), copper iodide (33.0 mg, 0.174 mmol, 0.5 eq), TBAB (223 mg, 0.694 mmol, 2 eq) and 1-[(cyanocarbothioyl)amino]-4-methoxybenzene **2.23** (100 mg, 0.347 mmol, 1 eq) were suspended in anhydrous 1:1 DMF:DMSO (2 mL). The resultant red brown mixture was placed under an inert nitrogen atmosphere and stirred vigorously at 120 °C for 3 h. The reaction mixture was cooled to room temperature and thereafter diluted with EtOAc (12 mL) and washed with H_2O (4 x 10 mL). The organic layer was then dried over Na_2SO_4, filtered, and concentrated *in vacuo*. The crude material was further purified by column chromatography using 1:9 EtOAc:Hexane to provide the title compound as a pale yellow solid (9.00 mg, 14 %). **Mp**: 126-130 °C (lit. 129-131 °C).[5] **^{1}H-NMR (400 MHz, DMSO)** δ 8.15 (1H, d, *J* = 9.1 Hz, H-4), 7.89 (1H, d, *J* = 2.4 Hz, H-7), 7.33 (1H, dd, *J* =

9.1, 2.4 Hz, H-5), 3.93 (3H, s, H-9) ppm. **^{13}C-NMR (400 MHz, DMSO)** δ 160.4 (C-2), 146.7 (C-6), 138.3 (C-3), 134.1 (C-8), 125.8 (C-7), 119.1 (C-5), 114.1 (C-1), 106.0 (C-4), 56.52 (C-9) ppm. **IR** ν_{max} (NaCl) / cm^{-1}): 2223 (-CN). **MS (ESI+):** *m/z* Calculated for $C_9H_6N_2OS$ [M+H] 191.0279, found 191.0273.

2-Cyano-6-hydroxybenzothiazole

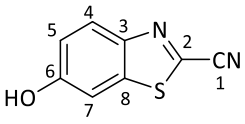

2.9

Pyridine hydrochloride (1.18 g, 10.2 mmol, 10 eq) and 6-methoxy-2-cyanobenzothiazole **2.8** (0.195 g, 1.02 mmol, 1 eq) were combined in a rigorously dried sealed tube, purged and placed under an inert nitrogen atmosphere. The reaction mixture was then stirred at 180 °C for 1 h. The resulting red-brown residue was cooled to room temperature and then dissolved in EtOAc (20 mL) and washed with saturated $NaHCO_3$ (1 x 20 mL), 1M HCl (1 x 10 mL), H_2O (4 x 10 mL), and brine (1 x 10 mL). The organic layer was dried over $MgSO_4$, filtered, and concentrated *in vacuo*. The crude product was purified using column chromatography eluting with 3:7 EtOAc:Hexane to yield 2-cyano-6-hydroxybenzothiazole as a pale yellow solid (0.177 g, 98 %). **Mp**: 202-207 °C (lit. 205-207 °C).[5-6] **^{1}H-NMR (400 MHz, DMSO)** δ 10.51 (1H, br s, -OH), 7.89 (1H, d, *J* = 9.0 Hz, H-4), 7.60 (1H, d, *J* = 2.4 Hz, H-7), 7.19 (1H, dd, *J* = 9.1, 2.4 Hz, H-5) ppm. **^{13}C-NMR (100.6 MHz, $CDCl_3$)** δ 160.4 (C-2), 147.4 (C-6), 139.1 (C-3), 134.0 (C-8), 126.8 (C-7), 119.8 (C-5), 114.4 (C-1), 107.5 (C-4) ppm. **IR** ν_{max} (NaCl) / cm^{-1}): 3430 (-OH), 2259 (-CN). **MS (ESI+):** *m/z* Calculated for $C_8H_4N_2OS$ [M+H] 177.0122, found 177.0117.

D-luciferin

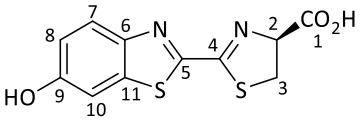

2

D-Cysteine hydrochloride monohydrate (30.0 mg, 0.171 mmol, 1.04 eq) and 2-cyano-6-hydroxy-benzothiazole **2.9** (29.0 mg, 0.163 mmol, 1 eq) were dissolved in 2:1 MeOH:H_2O (1 mL). The resulting solution was allowed to stir at room temperature for 5 min under a nitrogen atmosphere, after which potassium carbonate (23.0 mg, 0.164 mmol 1.01 eq) was added. The resulting bright yellow-green solution was allowed to stir for an additional 20 min, at room temperature, while maintaining the inert atmosphere. Upon consumption of 2-cyano-6-hydroxybenzothiazole, as evidenced by TLC analysis, the methanol was removed *in vacuo* and the remaining aqueous solution cooled to 0 °C and acidified

to pH 3 with 3 M HCl. The aqueous layer was then extracted with EtOAc (5 x 10 mL) and the combined organics were dried over Na_2SO_4, filtered, concentrated *in vacuo* and purified with column chromatography 3:6:1 DCM:EtOAc:MeOH to provide D-luciferin as a pale yellow solid (39.0 mg, 86 %). $[\alpha]_{D\,\text{obs}}^{20}$ = -29°, DMF, c = 1 ($[\alpha]_{D\,\text{lit.}}^{20}$ = -34°, DMF, c = 1).[7] **Mp**: 197-199 °C (lit. 196 °C).[7] **^{1}H-NMR (400 MHz, MeOD)** *δ* 7.93 (1H, d, *J* = 8.9 Hz, H-7), 7.35 (1H, d, *J* = 2.3 Hz, H-10), 7.10 (1H, dd, *J* = 8.9, 2.3 Hz, H-8), 5.40 (1H, app t, *J* = 9.0 Hz, H-2), 3.79 (2H, m, H-3) ppm. **^{13}C-NMR (100.6 MHz, $CDCl_3$)** *δ* 172.1 (C-1), 166.2 (C-4), 157.6 (C-9), 157.1 (C-5), 146.8 (C-6), 137.7 (C-11), 124.5 (C-7), 116.8 (C-10), 105.9 (C-8), 78.2 (C-2), 34.5 (C-3) ppm. **HRMS (ESI+)**: *m/z* Calculated for $C_{11}H_8N_2O_3S_2$ [M+Na] 302.9874, found 302.9868.

Synthesis of D-aminoluciferin[8-9]

N-[(5Z)-4-chloro-5H-1,2,3-dithiazol-5-ylidene]-4-nitroaniline

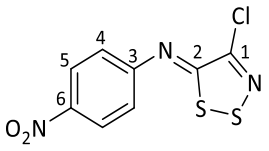

3.20

Appel's salt **2.25** (0.17 g, 0.80 mmol, 1.1 eq) and *p*-nitroaniline (0.10 g, 0.72 mmol, 1 eq) were suspended in anhydrous DCM (2 mL). The resulting mixture was allowed to stir at room temperature under a nitrogen atmosphere for 1.5 h. Thereafter, anhydrous pyridine (0.14 mL, 1.81 mmol, 2.5 eq) was added dropwise to the suspension, and the resulting red brown mixture was allowed to stir for an additional 2 h. The mixture was then concentrated *in vacuo* and purified by column chromatography, eluting with 1:9 EtOAc:hexane, to afford *N*-[(5Z)-4-chloro-5H-1,2,3-dithiazol-5-ylidene]-4-nitroaniline as a yellow solid (0.101 g, 50 %). **Mp**: 161-165 °C (lit. 160 °C).[10] **^{1}H-NMR (400 MHz, DMSO)** δ 8.37 (2H, d, *J* = 12.0 Hz, H-5), 7.42 (2H, d, *J* = 12.0 Hz, H-4) ppm. **^{13}C-NMR (100.6 MHz, DMSO)** δ 162.9 (C-2), 157.5 (C-1), 147.0 (C-6), 145.0 (C-3), 126.5 (C-5), 120.8 (C4) ppm. **MS (ESI+):** *m/z* Calculated for $C_8H_4ClN_3O_2S_2$ [M+H] 273.9511, found 272.9081.

1-[(Cyanocarbothioyl)amino]-4-nitrobenzene

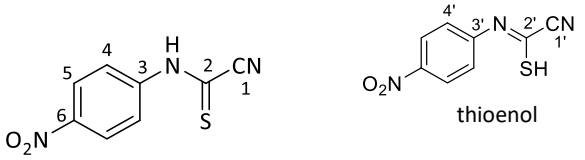

3.12

DBU (0.18 mL, 1.10 mmol, 3 eq) was added dropwise to a 5 °C solution of *N*-[(5Z)-4-chloro-5H-1,2,3-dithiazol-5-ylidene]-4-nitroaniline **3.20** (0.100 g, 0.37 mmol, 1 eq) in anhydrous DCM (1.5 mL) under a nitrogen atmosphere. The resulting red-brown mixture was stirred and maintained below 5 °C for 30 min, it was then allowed to warm to room temperature, after which it was left to stir for a further 30 min, all under a nitrogen atmosphere. The reaction mixture was then washed with saturated NH_4Cl_{aq} (2 x 2 mL), H_2O (1 x 2 mL), and brine (1 x 10 mL). The organic phase was dried over Na_2SO_4 and concentrated *in vacuo*. The crude material was purified by silica gel column chromatography, eluting with 4:6 EtOAc:Hexane to provide the title compound as a red-orange solid (0.270 g, 73 %). **Mp**: 122-130 °C (lit. 128-130 °C).[11] **^{1}H-NMR (400 MHz, $CDCl_3$)** δ 8.35 (2H, d, *J* = 9.3 Hz, H-4), 8.18 (2H, d, *J* = 9.2 Hz, H-5). **^{13}C-NMR (100.6 MHz, DMSO)** δ 163.4 (C-2), 145.6 (C-3), 143.8 (C-6), 125.3 (C-5), 123.6 (C-4), 114.2 (C-1) ppm. **MS (ESI+):** *m/z* Calculated for $C_8H_5N_3O_2S$ [M+H] 208.0180, found 206.9830.

2-Cyano-6-nitrobenzothiazole

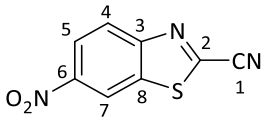

3.13

Palladium chloride (10.0 mg, 0.0590 mmol, 0.1 eq), copper iodide (56.0 mg, 0.295 mmol, 0.5 eq), TBAB (0.380 g, 1.18 mmol, 2 eq), and 1-[(cyanocarbothioyl)amino]-4-nitrobenzene **3.12** (0.123 g, 0.590 mmol, 1 eq) were suspended in anhydrous 1:1 DMF:DMSO (2 mL). The resultant red-brown mixture was placed under an inert nitrogen atmosphere and heated at 120 °C for 3 h. The reaction was then allowed to cool to room temperature, diluted with EtOAc (12 mL) and washed with H_2O (4 x 10 mL). The organic layer was then dried over Na_2SO_4, filtered, and concentrated *in vacuo*. The crude product was purified by column chromatography 1:9 EtOAc:Hexane to provide 2-cyano-6-nitrobenzothiazole as a light yellow solid (25.4 mg, 21 %). **Mp**: 118-119 °C. **^{1}H-NMR (400 MHz, $CDCl_3$)** δ 8.97 (1H, dd, *J* = 2.2, 0.5 Hz, H-7), 8.55 (1H, dd, *J* = 9.6, 1.4 Hz, H-5), 8.42 (1H, dd, *J* = 9.1, 1.4 Hz, H-4) ppm. **^{13}C-NMR (100.6 MHz, $CDCl_3$)** δ 155.3 (C-2), 147.3 (C-6), 141.8 (C-3), 135.6 (C-8), 126.1 (C-5), 123.0 (C-4), 118.6 (C-7), 114.0 (C-1) ppm. **FT-IR** (ATR) ν_{max} / cm^{-1}: 2217 (-CN). **MS (ESI+):** *m/z* Calculated for $C_8H_3N_3O_2S$ [M+H] 206.0024, found 204.9715.

6-Amino-2-cyanobenzothiazole

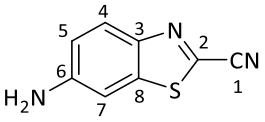

3.7

Method A: 2-Cyano-6-nitrobenzothiazole **3.13** (0.100 g, 0.490 mmol, 1 eq) was dissolved in EtOH (5 mL). $SnCl_2$ (0.322 g, 1.30 mmol, 2.5 eq) was then added and the reaction mixture was heated to 60 °C under a nitrogen atmosphere and allowed to stir for 2 h. The reaction mixture was then cooled to room temperature and poured into chilled water (5 ml and the pH adjusted to pH 7 using $NaHCO_3$. The resulting aqueous solution was extracted with EtOAc (5 x 2 mL), dried over $MgSO_4$ and excess solvent removed *in vacuo*. The crude material was further purified by silica column chromatography 4:6 EtOAc:Hexane to afford the amine as an orange solid (56.0 mg, 65 %).

Method B: 2-Cyano-6-nitrobenzothiazole **3.13** (66.0 mg, 0.323 mmol, 1 eq) and ammonium chloride (170 mg, 3.23 mmol, 10 eq) were suspended in freshly distilled MeOH (3 mL) and allowed to stir for 5 min at room temperature under a nitrogen atmosphere. Thereafter, Zn powder (0.420 g, 6.45 mmol, 20 eq) was added and the resultant reaction was left to stir vigorously for a further 30 min. The reaction mixture was then filtered through Celite and the filtrate reduced *in vacuo*. The residue obtained was purified by silica column chromatography using 1:1 EtOAc:Hexane to afford the title compound as an orange solid (56.2 mg, 99 %). **Mp**: 136-140 °C. **^{1}H-NMR (400 MHz, $CDCl_3$)** δ 7.87 (1H, d, *J* = 8.9 Hz, H-4), 7.13 (1H, d, *J* = 2.0 Hz, H-7), 6.98 (1H, dd, *J* = 9.0, 2.2 Hz, H-5), 6.10 (2H, br s, -NH_2) ppm. **^{13}C-NMR (100.6 MHz, $CDCl_3$)** δ 153.8 (C-2), 143.76 (C-3), 138.9 (C-6), 128.29 (C-8), 125.6 (C-5), 117.9 (C-4), 114.7 (C-1), 102.7 (C-7) ppm. **FT-IR** (ATR) ν_{max} / cm^{-1}: 3684 (-NH_2), 2254 (-CN). **MS (ESI+):** *m/z* Calculated for $C_8H_5N_3S$ [M+H] 176.0282, found 176.0115.

Potassium (S)-2-(6-aminobenzo[d]thiazol-2-yl)-4,5-dihydrothiazole-4-carboxylate

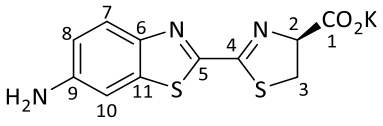

3.1a

D-Cysteine hydrochloride monohydrate (81.2 mg, 0.462 mmol, 1.1 eq) and 6-amino-cyano-benzothiazole **3.7** (71.0 mg, 0.405 mmol, 1 eq) were dissolved in 2:1 MeOH:H_2O (1 mL). The resulting solution was allowed to stir at room temperature for 5 min under a nitrogen atmosphere, after which potassium carbonate (56.5 mg, 0.409 mmol, 1.01 eq) was added. The resulting bright yellow-green solution was allowed to stir for an additional 40 min, while maintaining an inert atmosphere. Upon

consumption of 6-amino-cyanobenzothiazole, as evidenced by TLC analysis, the reaction mixture was diluted with water (4 mL) and washed with EtOAc (1 x 4 mL). The aqueous was then reduced and the resulting precipitate was filtered and washed with cold MeOH (2 x 1 mL). The precipitate was then further purified using reverse phase chromatography eluting with a gradient of 0-90 % MeOH in water to afford D-aminoluciferin potassium salt as a pale yellow solid (0.123 g, 96 %). **$[\alpha]_{D}^{20}$obs**: -14° (H_2O, c = 1). **Mp**: 111-123 °C. **^{1}H-NMR (400 MHz, D_2O)** *δ* 8.32 (1H, d, *J* = 8.8 Hz, H-7), 7.79 (1H, s, H-10), 7.55 (1H, d, *J* = 8.0 Hz, H-8), 5.72 (1H, m, H-2), 3.8-4.2 (2H, m, H-3). **HRMS (ESI+):** *m/z* Calculated for $C_{11}H_9N_3O_2S_2K$ [M+H] 317.9773, found 317.9768.

(S)-2-(6-aminobenzo[d]thiazol-2-yl)-4,5-dihydrothiazole-4-carboxylic acid

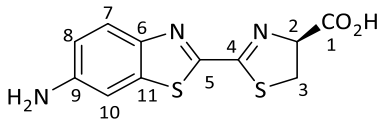

3.1b

D-Aminoluciferin potassium salt **3.1a** (30.0 mg, 0.0950 mmol) was dissolved in water (1 mL). The solution was then cooled to 0 °C and acidified to pH 4 with 1 M HCl. The aqueous solution was then extracted with EtOAc (4 x 1 mL) and the organic extracts were combined, washed with brine (1 x 1 mL), dried over $MgSO_4$, filtered through Celite and concentrated *in vacuo* to afford the acid as a light yellow solid (10.0 mg, 37 %). **^{1}H-NMR (400 MHz, DMSO)** *δ* 7.73 (1H, d, *J* = 8.8 Hz, H-7), 7.07 (1H, d, *J* = 2.2 Hz, H-10), 6.84 (1H, dd, *J* = 8.8, 2.2 Hz, H-8), 5.70 (2H, s, -NH_2), 4.93 (1H, app t, *J* = 8.4 Hz, H-2), 3.68-3.49 (2H, m, H-3) ppm. **^{13}C-NMR (100.6 MHz, DMSO)** *δ* 178.1 (C-1), 163.2 (C-4), 160.5 (C-5), 146.6 (C-6), 144.1 (C-11), 135.9 (C-9), 124.2 (C-7), 114.5 (C-10), 103.9 (C-8), 81.8 (C-2), 34.5 (C-3) ppm. **HRMS (ESI+):** *m/z* Calculated for $C_{11}H_9N_3O_2S_2$ [M+K] 317.9768, found 317.9768.

Synthesis of D-thioluciferin

3-((4-Aminophenyl)thio)acrylic acid

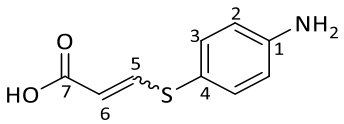

5.16

Propiolic acid (60.0 mg, 0.810 mmol, 1.05 eq) and *p*-aminothiophenol (100 mg, 0.800 mmol, 1 eq) were stirred in anhydrous DMF (1 mL) at room temperature under a nitrogen atmosphere for 24 h. The resulting red-brown solution was diluted with EtOAc (10 mL), washed with brine (4 x 10 mL), dried over $MgSO_4$ and then reduced *in vacuo*. The crude material was then further purified by silica column

chromatography 3:7 EtOAc:Pet. ether to afford the title compound, a pale yellow solid, as a 1:9 mixture of E:Z isomers (47.0 mg, 30 % yield). **Mp**: 113-207 °C. **E-isomer; ^{1}H-NMR (400 MHz, $CDCl_3$)** δ 12.0 (1H, br s, -COOH), 7.67 (1H, d, *J* = 14.8 Hz, H-6), 7.14 (2H, d, *J* = 8.5 Hz, H-3), 6.65 (2H, d, *J* = 8.5 Hz, H-2), 5.95 – 5.39 (2H, br s, $-NH_2$), 5.26 (1H, d, *J* = 14.8 Hz, H-5). **^{13}C-NMR (100.6 MHz, $CDCl_3$)** δ 166.1 (C-7), 150.1 (C-5), 149.6 (C-1), 135.8 (C-4), 115.3 (C-6), 114.8 (C-3), 112.2 (C-2) ppm. **Z-isomer; ^{1}H-NMR (400 MHz, $CDCl_3$)** δ 12.0 (1H, br s, -COOH), 7.26 (1H, d, *J* = 10.0 Hz, H-6), 7.14 (2H, d, *J* = 8.5 Hz, H-3), 6.65 (2H, d, *J* = 8.5 Hz, H-2), 5.95 – 5.39 (2H, br s, $-NH_2$), 5.80 (1H, d, *J* = 10.0 Hz, H-5). **^{13}C-NMR (100.6 MHz, $CDCl_3$)** δ 167.5 (C-7), 153.0 (C-5), 149.9 (C-1), 133.3 (C-4), 120.0 (C-6) 114.9 (C-3), 113.0 (C-2) ppm.

3-((4-(((Z)-4-chloro-5H-1,2,3-dithiazol-5-ylidene)amino)phenyl)thio)acrylic acid

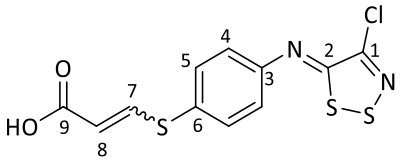

5.17

Appel's salt (0.170 g, 0.850 mmol, 1.5 eq) and a 2:8 E:Z mixture of 3-((4-aminophenyl)thio)acrylic acid **5.16** (0.110 g, 0.560 mmol, 1 eq) were suspended in DCM (4 mL). The resulting suspension was stirred at room temperature under a nitrogen atmosphere for 1 h. Thereafter, anhydrous pyridine (0.09 mL, 1.12 mmol, 2 eq) was slowly added to the suspension, and the resulting mixture was allowed to stir for an additional 2 h. The reaction mixture was then concentrated *in vacuo* and purified by column chromatography, eluting with 3:7 EtOAc:Pet. ether to afford the title compound as a yellow solid with the ratio of geometric isomers conserved (185 mg, 99 % yield). **Mp**: 199-201 °C. **E-isomer; ^{1}H-NMR (400 MHz, $CDCl_3$)** δ 12.36 (1H, br s, -COOH), 7.77 (1H, d, *J* = 15.1 Hz, H-8), 7.65 (2H, d, *J* = 8.6 Hz, H-5), 7.40 – 7.14 (2H, m, H-4), 5.59 (1H, d, *J* = 15.0 Hz, H-7). **^{13}C-NMR (100.6 MHz, $CDCl_3$)** δ 165.92 (C-9), 161.13 (C-1), 152.26 (C-2), 150.98 (C-7), 147.20 (C-6), 134.83 (C-3), 133.42 (C-8), 127.37 (C-5), 121.42 (C-4) ppm. **Z-isomer; ^{1}H NMR (400 MHz, $CDCl_3$)** δ 12.36 (1H, br s, -COOH), 7.65 (2H, d, *J* = 8.6 Hz, H-5), 7.54 (1H, d, *J* = 10.0 Hz, H-8), 7.40 – 7.14 (2H, m, H-4), 5.95 (1H, d, *J* = 9.9 Hz, H-7). **^{13}C-NMR (100.6 MHz, $CDCl_3$)** δ 167.59 (C-9), 160.5 (C-1), 148.62 (C-7), 147.3 (C-2), 146.3 (C-3), 132.1 (C-6), 121.06 (C-8), 117.0 (C-5), 114.47 (C-4) ppm. **MS (ESI+):** *m/z* Calculated for $C_{11}H_7ClN_2O_2S_3$ [M+H] 330.9436, found 330.9430.

3-((4-((Cyanocarbonothioyl)amino)phenyl)thio)acrylic acid

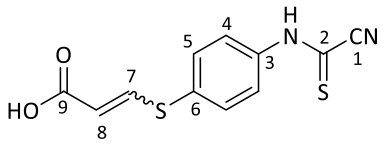

5.17a

Method A: DBU (0.3 mL, 1.80 mmol, 3 eq) was added dropwise to a 5 °C solution of 3-((4-((cyano-carbonothioyl)amino)phenyl)thio)acrylic acid **5.17** (200 mg, 0.600 mmol, 1 eq) in freshly distilled DCM (5 mL) under a nitrogen atmosphere. The resulting red-brown mixture was stirred at 5 °C for 30 min, after which it was allowed to warm to room temperature and left to stir for a further 30 min. The reaction mixture was then washed with saturated ammonium chloride solution (2 x 2 mL), and H_2O (1 x 2 mL). The organic phase was dried over Na_2SO_4 and concentrated *in vacuo*. The crude material was purified by silica gel chromatography, eluting with 1:8.9:0.1 MeOH:EtOAc:TFA to provide the title compound as an orange oil (8.00 mg, < 5 % yield).

Method B: DBU (0.3 mL, 1.80 mmol, 3 eq) was added dropwise, over 30 min, to a solution of 3-((4-((cyanocarbonothioyl)-amino)phenyl)thio)acrylic acid **5.17** (0.200 g, 0.600 mmol, 1 eq) in DMSO (2 mL) at room temperature under a nitrogen atmosphere. The resulting mixture was stirred for 30 min, after which it was allowed to warm to room temperature and left to stir for a further 30 min. The reaction mixture was then diluted with saturated NH_4Cl_{aq} solution (6 mL), and washed with DCM (4 x 2 mL). The aqueous was concentrated under reduced pressure, MeOH (3 mL) was added and the resulting precipitate filtered under vacuum. The filtrate was then reduced *in vacuo* and diluted with additional MeOH (5 mL) resulting in the precipitation of trace NH_4Cl salts. The precipitate was filtered and the filtrate reduced and lyophilised to afford the crude product. The crude material was purified by silica gel chromatography, eluting with 1:8.9:0.1 MeOH:EtOAc:TFA to provide the title compound, a 2:8 mixture E:Z isomers, as a red-orange oil (52.0 mg, 33 % yield). **E-isomer; ^{1}H-NMR (400 MHz, DMSO)** δ 12.38 (1H, br s, -COOH), 9.91 (1H, br s, -NH), 7.42 (1H, d, *J* = 15.0 Hz, H-8), 7.59 (2H, d, *J* = 8.6 Hz, H-5), 7.11 (2H, d, *J* = 8.6 Hz, H-4), 5.50 (1H, d, *J* = 15.0 Hz, H-7). **Z-isomer; ^{1}H NMR (400 MHz, DMSO)** δ 12.38 (1H, br s, -COOH), 9.91 (1H, br s, -NH), 7.65 (2H, d, *J* = 8.6 Hz, H-5), 7.56 (1H, d, *J* = 10.0 Hz, H-8), 7.40 (2H, m, H-4), 4.67 (1H, d, *J* = 10.0 Hz, H-7).

Benzyl propiolate[12]

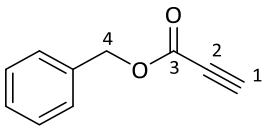

5.18

Cesium carbonate (5.81 g, 17.9 mmol, 3 eq) was suspended in DMF (5 mL) and cooled to 0 °C. The reaction mixture was allowed to stir and propiolic acid (0.44 mL, 7.14 mmol, 1.2 eq) was added dropwise to the stirring cooled suspension. After the addition, the resulting solution was left to stir for a further 20 min, maintained at 0 °C. Benzyl bromide (0.71 mL, 5.95 mmol, 1 eq) was then slowly added and thereafter the reaction was allowed to warm to rt at which point it was left to stir for an additional 10 min. The reaction mixture was then diluted with Et_2O (15 mL) and washed with a saturated brine solution (5 x 10 mL). The organic layer was dried over $MgSO_4$ and reduced *in vacuo* to afford benzyl propiolate as a yellow oil (0.940 g, 99 % yield). **^{1}H-NMR (400 MHz, $CDCl_3$)** δ 7.40 (5H, m, Ar-H), 5.23 (2H, S, H-4), 4.60 (1H, s, H-1) ppm. **^{13}C-NMR (100.6 MHz, $CDCl_3$)** δ 152.3 (C-3), 135.34 (Ar-q), 129.03 (Ar-H), 129.0 (Ar-H), 128.9 (Ar-H), 79.8 (C-2), 78.8 (C-1), 67.96 (C-4) ppm.

Benzyl (E)-3-((4-aminophenyl)thio)acrylate

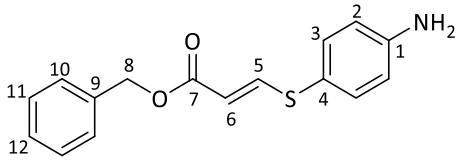

5.19

Propiolic ester **5.18** (0.580 g, 3.63 mmol, 1 eq) and *p*-aminothiophenol (0.450 g, 3.63 mmol, 1 eq) were stirred in anhydrous DMF (2 mL) at room temperature under a nitrogen atmosphere for 24 h. The resulting red-brown solution was diluted with EtOAc (12 mL), washed with brine (4 x 6 mL), dried over $MgSO_4$ and excess solvent reduced *in vacuo*. The crude residue was then subjected to column chromatography eluting with 3:7 EtOAc:Pet. ether and the material obtained was recrystallised to a constant melting point from boiling pet. ether to afford the geometrically pure product **5.19** as a brown solid (0.276 g, 39 %). **Mp**: 118-119 °C. **^{1}H-NMR (300 MHz, $CDCl_3$)** δ 7.36 (5H, m, H-10 – 12), 7.32 (1H, d, *J* = 14.8 Hz, H-6), 7.14 (2H, d, *J* = 8.5 Hz, H-3), 6.60 (2H, d, *J* = 8.5 Hz, H-2), 5.89 (1H, d, *J* = 14.8. Hz, H-5), 5.47 (2H, br s, -NH_2), 5.13 (2H, s, H-8) ppm. **^{13}C-NMR (100.6 MHz, $CDCl_3$)** δ 165.8 (C-7), 154.6 (C-6), 149.9 (C-1), 136.8 (C-5), 133.4 (C-3), 128.9 (C-10), 128.5 (C-11), 128.4 (C-12), 119.4 (C-9), 115.0 (C-2), 111.5 (C-5), 65.6 (C-8) ppm. **MS (ESI+):** *m/z* Calculated for $C_{16}H_{15}NO_2S$ [M+H] 286.0901, found 286.0889.

Benzyl (E)-3-((4-(((Z)-4-chloro-5H-1,2,3-dithiazol-5-ylidene)amino)phenyl)thio)acrylate

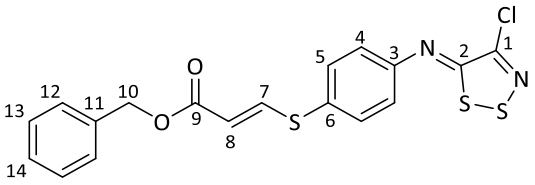

5.20

Appel's salt (0.220 g, 1.08 mmol, 2 eq) and benzyl (E)-3-((4-aminophenyl)thio)acrylate **5.19** (0.150 g, 0.540 mmol, 1 eq) were dissolved in DMF (4 mL). The resulting solution was stirred at room temperature under a nitrogen atmosphere for 1 h. Thereafter, anhydrous pyridine (0.05 mL, 1.08 mmol, 2 eq) was slowly added to the solution, after which it was left to stir for an additional 2 h. The mixture was then concentrated *in vacuo* and purified by silica column chromatography, eluting with 1:9 EtOAc:Pet. ether, to afford the title compound as a bright yellow solid (0.225 g, 99 %). **Mp**: 130-152 °C. **^{1}H-NMR (300 MHz, DMSO)** δ 7.66 (3H, m, H-8,5), 7.41 (5H, m, H-12,13,14), 7.28 (2H, d, *J* = 8.5 Hz, H-4), 6.07 (1H, d, *J* = 13.3 Hz, H-7), 5.20 (2H, s, H-10). **^{13}C-NMR (100.6 MHz, DMSO)** δ 165.8 (C-9), 160.6 (C-2), 151.2 (C-1), 150.3 (C-7), 147.2 (C-3), 136.6 (C-6), 132.7 (C-11), 132.3 (C-5), 128.9 (C-13), 128.6 (C-14), 128.5 (C-12), 121.1 (C-4), 113.4 (C-8), 65.9 (C-10). **MS (ESI+):** *m/z* Calculated for $C_{18}H_{13}ClN_2O_2S_3$ [M+H] 420.9905, found 420.9899.

Benzyl (E)-3-((4-((cyanocarbonothioyl)amino)phenyl)thio)acrylate

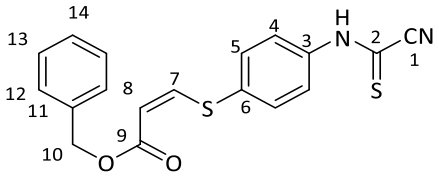

5.21

DBU (0.13 mL, 0.854 mmol, 3 eq) was added, dropwise over 30 min, to a solution of (E)-3-((4-(((Z)-4-chloro-5H-1,2,3-dithiazol-5-ylidene)amino)phenyl)thio)acrylate **5.20** (0.120 g, 0.285 mmol, 1 eq) in anhydrous DMSO (2 mL) at room temperature under a nitrogen atmosphere. The resulting red-brown mixture was stirred for 40 min, after which it was diluted with EtOAc (12 mL). The reaction mixture was then washed with a saturated NH_4Cl_{aq} solution (3 x 6 mL) and H_2O (1 x 10 mL). The organic phase was dried over Na_2SO_4 and concentrated *in vacuo*. The crude material was purified by silica gel column chromatography, eluting with 2:8 EtOAc:Hexane, to provide the title compound as a red solid (48.0 mg, 61 %). **Mp**: 96-97 °C. **^{1}H-NMR (400 MHz, DMSO)** δ 13.56 (1H, br s, -NH), 7.98 (2H, d, *J* = 8.9 Hz, H-5), 7.67 (3H, app dd, *J* = 9.5, 7.7 Hz, H-8,4), 7.41 (5H, m, H-12,13,14), 6.10 (1H, d, *J* = 8.6 Hz, H-7), 5.20 (2H, s, H-10). **^{13}C-NMR (100.6 MHz, DMSO)** δ 165.8 (C-9), 161.8 (C-2), 149.2 (C-7), 137.9 (C-3), 136.6 (C-6), 134.7 (C-11), 130.9 (C-5), 131.3 (C-12), 128.6 (C-13), 128.5 (C-14), 123.8 (C-4), 114.2

(C-1), 113.9 (C-8), 66.0 (C-10). **MS (ESI+):** *m/z* Calculated for $C_{18}H_{14}N_2O_2S_2$ [M+H] 355.0574, found 355.0580.

Benzyl (E)-3-((2-cyanobenzo[d]thiazol-6-yl)thio)acrylate

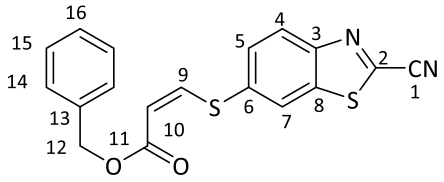

5.22

Palladium chloride (4.00 mg, 0.020 mmol, 0.1 eq), copper iodide (19.0 mg, 0.099 mmol, 0.5 eq), TBAB (0.127 g, 0.394 mmol, 2 eq) and (E)-3-((4-(((Z)-4-chloro-5H-1,2,3-dithiazol-5-ylidene)amino)-phenyl)thio)acrylate **5.21** (70.0 mg, 0.197 mmol, 1 eq) were suspended in anhydrous DMSO (1 mL). The resultant orange-red mixture was placed under a nitrogen atmosphere and stirred at 120 °C for 4 h. The reaction mixture was then diluted with EtOAc (6 mL) and washed with a saturated brine solution (4 x 2 mL). The organic layer was then dried over Na_2SO_4, filtered, and concentrated *in vacuo*. The crude product was purified by column chromatography 3:7 EtOAc:Hexane to provide the 2-cyanobenzothiazole as a yellow solid (0.0430 g, 62 %). **Mp**: 113-120 °C. **^{1}H-NMR (400 MHz, DMSO)** δ 8.59 (1H, d, *J* = 1.9 Hz, H-7), 8.29 (1H, d, *J* = 8.7 Hz, H-4), 7.85 (1H, dd, *J* = 8.7, 1.9 Hz, H-5), 7.78 (1H, d, *J* = 10.0 Hz, H-10), 7.41 (5H, m, H-14,15,16), 6.17 (1H, d, *J* = 10.0 Hz, H-9), 5.22 (2H, s, H-12). **^{13}C-NMR (100.6 MHz, DMSO)** δ 165.9 (C-11), 151.4 (C-2), 148.6 (C-9), 138.4 (C-3), 137.0 (C-8), 136.8 (C-6), 136.5 (C-13), 130.1 (C-7), 128.9 (C-14), 128.6 (C-15), 128.6 (C-16), 125.6 (C-5), 124.3 (C-4), 114.5 (C-10), 113.7 (C-1), 66.1 (C-12). **FT-IR** (ATR) ν_{max} / cm^{-1}:1686 (C=C), 1735 (C=O), 2226 (-CN). **MS (ESI+):** *m/z* Calculated for $C_{18}H_{12}N_2O_2S_2$ [M+H] 353.0418, found 353.0542.

(S,E)-2-(6-((3-(benzyloxy)-3-oxoprop-1-en-1-yl)thio)benzo[d]thiazol-2-yl)-4,5-dihydrothiazole-4-carboxylic acid

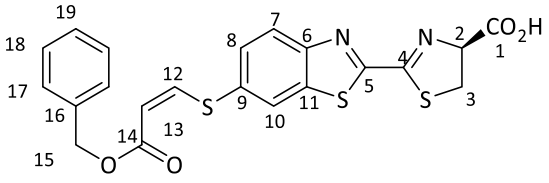

5.23

To a stirring solution of benzyl (E)-3-((2-cyanobenzo[d]thiazol-6-yl)thio)acrylate **5.22** (4.00 mg, 0.0110 mmol, 1 eq) in DMSO (0.4 mL) at room temperature under a nitrogen atmosphere was added D-Cysteine (2.00 mg, 0.0110 mmol, 1 eq) in H_2O (0.6 mL). The solution was left to stir for 5 min, cooled

to 0 °C, and then potassium carbonate (15.0 mg, 0.0110, 1 eq) was added. The reaction mixture was then left to stir a further 10 min after which the pH was adjusted to pH 3 using 3 M HCl, all whilst maintaining a reaction temperature of 0 °C. The solution was then allowed to warm to room temperature and diluted with EtOAc (2 mL) and washed with H_2O (4 x 1mL). The organic layer was then dried over $MgSO_4$, filtered and evaporated under reduced pressure at 35 °C to afford a red oil. The crude material was further purified using silica column chromatography, eluting with 1:9 MeOH:DCM to afford the title compound as a red oil (5.00 mg, 99 %). **^{1}H-NMR (300 MHz, DMSO)** δ 8.47 (1H, d, *J* = 1.9 Hz, H-10), 8.20 (1H, d, *J* = 8.6 Hz, H-7), 7.76 (2H, m, H-8,13), 7.40 (5H, m, H-19,18,17), 6.13 (1H, d, *J* = 10.1 Hz, H-12), 5.47 (1H, dd, *J* = 9.7, 8.5 Hz, H-2), 5.22 (2H, s, H-15), 3.77 (2H, m, H-3). **MS (ESI+):** *m/z* Calculated for $C_{21}H_{16}N_2O_4S_3$ [M+H] 457.0350, found 457.0341.

(S)-2-(6-mercaptobenzo[d]thiazol-2-yl)-4,5-dihydrothiazole-4-carboxylic acid

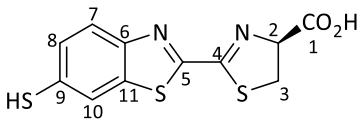

5

D-Cysteine hydrochloride monohydrate (15.0 mg, 0.0790 mmol, 2.01 eq) and benzyl (E)-3-((2-cyanobenzo[*d*]thiazol-6-yl)thio)acrylate **5.22** (14.0 mg, 0.0397 mmol, 1 eq) were suspended in DMSO (0.4 mL) at room temperature under a nitrogen atmosphere. Potassium carbonate (35.0 mg, 0.119 mmol, 3 eq) dissolved in water (0.4 mL) was then added to the mixture, and the resulting bright orange solution was stirred under an inert atmosphere for a further 10 min. Upon consumption of benzyl (E)-3-((2-cyanobenzo[d]thiazol-6-yl)thio)acrylate, as evidenced by TLC analysis, the methanol was removed *in vacuo* and the remaining aqueous solution acidified to pH 3 with 3 M HCl. The aqueous was then extracted with EtOAc (5 x 1 mL). The combined organics were dried over $NaSO_4$, filtered, concentrated *in vacuo* and purified with column chromatography 1:8.9:0.1 MeOH:DCM:TFA to provide D-thioluciferin **5** as a pale yellow solid (11.0 mg, 99 %). The *ee* was determined to be 93:7, by HPLC using a Diacel Chiracel OD column (hexane:*i*-Pr 7:3): flow rate: 1 mL/min: τ_{major} = 8.24 min. **$[\alpha]^{20}_{D\,obs}$**: -11°, DMF, c = 1. **Mp**: 89-90 °C. **^{1}H-NMR (400 MHz, DMSO)** δ 8.49 (1H, s, H-10), 8.18 (1H, dd, *J* = 8.7, 0.5 Hz, H-7), 7.78 (1H, dd, *J* = 8.7, 2.0 Hz, H-8), 5.45 (1H, dd, *J* = 9.8, 8.3 Hz, H-2), 3.75 (2H, m, H-3) ppm. **^{13}C-NMR (100.6 MHz, DMSO** *δ* 177.5 (C-1), 166.3 (C-4), 163.2 (C-11), 155.4 (C-5), 150.5 (C-6), 130.0 (C-9), 125.5 (C-7), 123.0 (C-10), 121.9 (C-8), 82.1 (C-2), 34.5 (C-3) ppm. **HRMS (ESI+):** *m/z* Calculated for $C_{11}H_8N_2O_2S_3$ [M+Na] 318.9645, found 319.0000.

Metal-free, base mediated synthesis of 2-cyanobenzothiazoles

***2-Bromo-4-methoxyaniline*[32-43]**

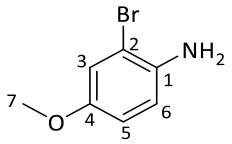

4.1a

KBr (0.320 g, 2.65 mmol, 1.2 eq) and $NaBO_3$ (0.371 g, 2.51 mmol, 1.1 eq) were suspended and left to stir in acetic acid (4 mL) at room temperature for 15 min. The resulting solution was added dropwise to a stirring suspension of *p*-anisidine (0.500 g, 2.28 mmol, 1.0 eq) in acetic acid (4 mL) at 0 °C. The reaction mixture was maintained at 0 °C throughout the addition. Thereafter, it was allowed to warm to room temperature and stirred for an additional 11 h. The reaction was quenched by the addition of chilled water (50 mL). The aqueous phase was then extracted with EtOAc (4 x 10 mL), the combined organic extracts were dried over $MgSO_4$, filtered, and the solvent reduced *in vacuo* to afford 2-bromo-4-methoxyaniline as brown oil that was used without further purification (0.480 g, 71 %). **^{1}H-NMR (400 MHz, $CDCl_3$)** δ 7.56 (1H, d, *J* = 2.0 Hz, H-3), 7.28 (1H, d, *J* = 8.0 Hz, H-6), 7.24 (1H, d, *J* = 8 Hz, H-5), 3.89 (H-7) ppm. **^{13}C-NMR (100.6 MHz, $CDCl_3$)** *δ* 148.4 (C-4), 140.0 (C-1), 119.5 (C-2), 118.4 (Ar-H), 118.3 (Ar-H), 114.1 (Ar-H), 55.8 (C-7) ppm.

2-Bromo-4-nitroaniline

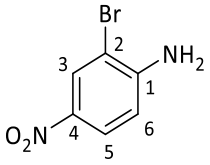

4.1b

KBr (8.00 g, 67.2 mmol, 1.16 eq) and $NaBO_3$ (9.80 g, 63.7 mmol, 1.1 eq) were suspended and left to stir in acetic acid (40 mL) at room temperature for 15 min. The resulting solution was added dropwise to a stirring suspension of *p*-nitroaniline (8.00 g, 57.9 mmol, 1 eq) in acetic acid (10 mL) at 0 °C. The reaction mixture was maintained at 0 °C throughout the addition. Thereafter, it was allowed to warm to room temperature and left to stir overnight. The reaction mixture was poured into chilled water (250 mL) and the resulting precipitate filtered and washed with copious amounts of water to afford 2-bromo-4-nitroaniline as a yellow solid (11.2 g, 89 %). **Mp**: 100-101 °C (Lit. 104 °C).[15] **^{1}H-NMR (400 MHz, $CDCl_3$)** δ 8.31 (1H, s, *J* = 1.9 Hz, H3), 7.56 (1H, dd, *J* = 8.0, 2.0 Hz, H-5), 6.95 (1H, d, *J* = 8 Hz, H-6), 6.21 (2H, br s, -NH_2) ppm. **^{13}C-NMR (100.6 MHz, $CDCl_3$)** *δ* 153.3 (C-1), 142.1 (C-4), 129.5 (C-2), 123.4 (Ar-H), 119.7 (Ar-H), 118.4 (Ar-H) ppm.

1,2-Di-p-tolyldisulfane[16]

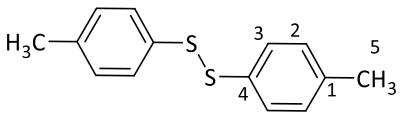

4.1c

p-Tolylthiophenol (0.100 g, 0.805 mol, 1 eq) and $NaBO_3$ (0.190 g, 1.24 mmol, 1.54 eq) were suspended and stirred in a solution of DCM (2 mL) and acetic acid (0.2 mL) at room temperature for 48 h. The reaction was poured into chilled water (40 mL). The aqueous phase was then extracted with DCM (4 x 10 mL), the combined organic extracts were dried over $MgSO_4$, filtered, and the solvent reduced *in vacuo* to afford 4,4'-disulfanediylbis(2-bromoaniline) as a colourless solid (0.177 g, 90 %). **Mp**: 30-42 °C (Lit. 54 °C).[17] **^{1}H-NMR (400 MHz, $CDCl_3$)** δ 7.54 (1H, s, *J* = 9.0 Hz, H-3), 7.21 (1H, d, *J* = 9.0 Hz, H-2), 2.21 (1H, s, H-7) ppm. **^{13}C-NMR (100.6 MHz, $CDCl_3$)** *δ* 142.1 (C-4), 133.3 (C-1), 129.5 (Ar-H), 129.0 (Ar-H), 21.6 (C-5) ppm.

4,4'-Disulfanediylbis(2-bromoaniline)

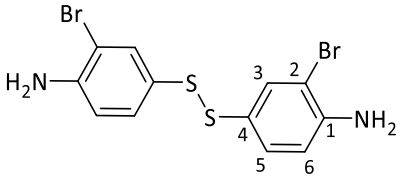

4.1d

p-Aminothiophenol (0.100 g, 0.799 mol, 1 eq) and $NaBO_3$ (0.189 g, 1.23 mmol, 1.54 eq) were suspended and stirred in a solution of DCM (2 mL) and acetic acid (0.2 mL) at room temperature for 48 h. The reaction mixture was then cooled to 0 °C upon complete consumption of the *p*-aminothiophenol, as evidenced by TLC analysis. A suspension of KBr (0.200 g, 1.68 mmol, 2.1 eq) and $NaBO_3$ (0.123 g, 0.799 mmol, 1 eq) in acetic acid (4 mL) was slowly added to the reaction mixture that was maintained at 0 °C throughout the addition. Thereafter, it was allowed to warm to room temperature and left to stir overnight. The reaction was quenched by the addition of chilled water (40 mL). The aqueous phase was then extracted with EtOAc (4 x 10 mL), the combined organic extracts were dried over $MgSO_4$, filtered, and the solvent reduced *in vacuo* to afford 4,4'-disulfanediylbis(2-bromoaniline) as a yellow oil (0.250 g, 77 %). **^{1}H-NMR (300 MHz, CDCl3)** δ 7.52 (1H, s, H-3), 7.28 (1H, d, *J* = 8.0 Hz, H-5), 6.67 (1H, d, *J* = 8.0 Hz, H-6), 4.24 (2H, br s, -NH_2) ppm. **^{13}C-NMR (100.6 MHz, $CDCl_3$)** *δ* 144.4 (C-1), 128.2 (C-4), 130.8 (Ar-H), 129.4 (Ar-H), 118.1 (Ar-H), 117.8 (C-2) ppm. **MS (ESI+):** *m/z* Calculated for $C_{12}H_{10}Br_2N_2S_2$ [M+H] 404.8730, found 405.8802.

(5Z,5'Z)-N,N'-(disulfanediylbis(2-bromo-4,1-phenylene))bis(4-chloro-5H-1,2,3-dithiazol-5-imine)

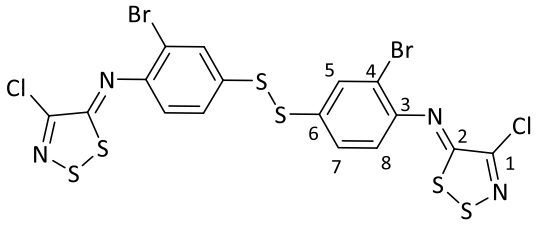

5.14b

Appel's salt (0.875 g, 4.20 mmol, 2.1 eq) and 4,4'-disulfanediylbis(2-bromoaniline) **4.1d** (0.812 g, 2.00 mmol, 1 eq) were dissolved in DMF (6 mL). The resulting solution was stirred at room temperature under a nitrogen atmosphere for 1 h. Thereafter, anhydrous pyridine (0.29 mL, 4.00 mmol, 2 eq) was slowly added to the solution, after which it was left to stir for an additional 2 h. The mixture was then diluted with EtOAc (30 mL), washed with saturated NH_4Cl_{aq} (3 x 10 mL), H_2O (1 x 10 mL), dried over $MgSO_4$, and concentrated *in vacuo*. The crude material was purified by silica column chromatography, eluting with 1:9 EtOAc:Pet. ether, to afford the title compound as a yellow solid (1.16 g, 41 %). **Mp**: 217 °C. **^{1}H-NMR (400 MHz, $CDCl_3$)** δ 7.67 (2H, s, H-5), 7.60 (2H, d, *J* = 8.0 Hz, H-8), 7.07 (2H, d, *J* = 8.0 Hz, H-7) ppm. **^{13}C-NMR (100.6 MHz, $CDCl_3$)** *δ* 157.7 (C-1), 149.2 (C-2), 143.6 (C-3), 136.7 (C-6), 129.7 (Ar-H), 128.8 (Ar-H), 124.3 (Ar-H), 112.5 (C-4) ppm.

4,4'-Disulfanediyldianiline

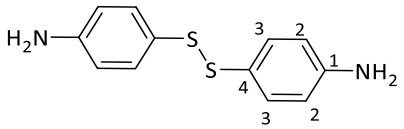

5.13

p-Aminothiophenol (0.100 g, 0.799 mmol, 1 eq) and $NaBO_3$ (0.189 g, 1.23 mmol, 1.54 eq) were suspended and stirred in a solution of DCM (2 mL) and acetic acid (0.2 mL) at room temperature for 48 h. Thereafter, chilled water (40 mL) was added to the reaction mixture. The aqueous phase was then extracted with EtOAc (4 x 10 mL), the combined organic extracts were dried over $MgSO_4$, filtered, and the solvent reduced *in vacuo* to afford 4,4'-disulfanediyldianiline as a yellow oil (0.191 g, 96 %). **^{1}H-NMR (300 MHz, CDCl3)** δ 7.03 (4H, m, H-3), 6.51 (4H, m, H-2), 5.07 (2H, br s, -NH_2), 4.53 (4H, br s, -NH_2) ppm.

(5Z,5'Z)-N,N'-(disulfanediylbis(4,1-phenylene))bis(4-chloro-5H-1,2,3-dithiazol-5-imine)

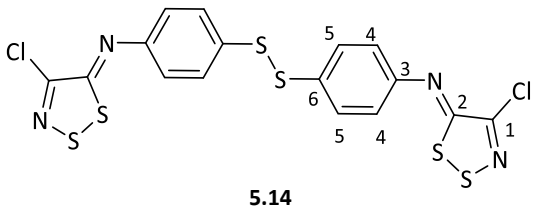

5.14

Appel's salt (0.378 g, 1.268 mmol, 2.1 eq) and 4,4'-disulfanediyldianiline **5.13** (0.150 g, 0.603 mmol, 1 eq) were suspended in DCM (8 mL). The resulting solution was stirred at room temperature under a nitrogen atmosphere for 1 h. Thereafter, anhydrous pyridine (0.10 mL, 1.206 mmol, 2 eq) was slowly added to the solution, after which it was left to stir for an additional 2 h. The mixture was then diluted with EtOAc (30 mL), washed with saturated NH_4Cl_{aq} (3 x 10 mL), H_2O (1 x 10 mL), dried over $MgSO_4$, and concentrated *in vacuo*. The crude material was purified by silica column chromatography, eluting with 1:9 EtOAc:Pet. ether, to afford the title compound as a yellow solid (1.16 g, 41 %). **Mp**: 227-229 °C. **^{1}H-NMR (300 MHz, CDCl3)** δ 7.21 (4H, m, H-5), 6.56 (4H, m, H-4) ppm.

General procedure for the Synthesis of monobrominated para substituted anilines

KBr and $NaBO_3$ were suspended and left to stir in acetic acid at room temperature. The resulting solution was added dropwise to a suspension of the appropriate aniline in acetic acid at 0 °C. The reaction mixture was maintained at 0 °C throughout the addition. Thereafter, it was allowed to warm to room temperature and left to stir overnight. The reaction mixture was poured into chilled water and the resulting precipitate filtered and washed with copious amounts of water to afford the brominated product.

2-Bromo-4-iodoaniline

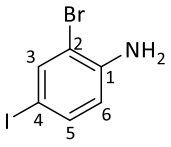

5.5

Following the above outlined procedure, KBr (5.70 g, 48.0 mmol, 1.2 eq) and $NaBO_3$ (7.00 g, 45.0 mmol, 1.1 eq) dissolved in acetic acid (60 mL) was added to *p*-iodoaniline (9.10 g, 42.0 mmol, 1 eq) in acetic acid (1 mL) to obtain 2-bromo-4-iodoaniline as a brown solid (12.40 g, 99 %). **Mp**: 75-76 °C (lit. 75-76 °C).[18] **^{1}H-NMR (400 MHz, $CDCl_3$)** δ 7.67 (1H, d, *J* = 2.0 Hz, H3), 7.34 (1H, dd, *J* = 8.5, 2.0 Hz, H-5), 6.52 (1H, d, *J* = 8.5 Hz, H-6), 4.44 (2H, br s, -NH_2) ppm. **^{13}C-NMR (100.6 MHz, $CDCl_3$)** *δ* 144.1 (C-1), 140.2 (C-4), 137.2 (C-3), 117.5 (Ar-H), 110.2 (Ar-H), 95.2 (C-2) ppm.

2-Bromo-4-fluoroaniline

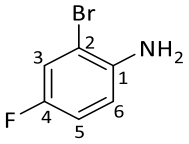

4.1e

Following the above outlined procedure, KBr (3.86 g, 32.4 mmol, 1.2 eq) and $NaBO_3$ (4.57 g, 29.7 mmol, 1.1 eq) dissolved in acetic acid (40 mL) was added to *p*-fluoroaniline (3.00 g, 27.0 mmol, 1.0 eq) in acetic acid (1 mL) to obtain 2-bromo-4-fluoroaniline as a pale yellow solid (5.13 g, 99 %). **Mp**: 39-41 °C (lit. 41 °C).[19] **^{1}H-NMR (400 MHz, $CDCl_3$)** δ 7.23 (1H, dd, *J* = 8.0, 1.5 Hz, H-3), 6.91 (1H, td, *J* = 8.5, 1.2 Hz, H-5), 6.67 (1H, dd, *J* = 7.5, 5.0 Hz, H-6), 5.32 (2H, br s, -NH_2) ppm. **^{13}C-NMR (100.6 MHz, $CDCl_3$)** *δ* 148.9 (C-4), 142.8 (C-1), 121.5 (Ar-H), 210.1 (Ar-H), 118.9 (C-2), 117.7 (C-2) ppm.

General procedure for the metal free synthesis of 6-substituted 2-cyanobenzothiazoles from monobrominated para-substituted anilines

Appel's salt and an aniline were allowed to stir in DCM for 1 h at room temperature under a nitrogen atmosphere. The solution was then cooled to below 5 °C and DBU was added, dropwise over 30 min, to the stirring solution maintained at 5 °C, all under a nitrogen atmosphere. After the addition, the resulting mixture was stirred for 30 min while allowing it to warm to room temperature, after which it was refluxed at 40 °C for 4 h. Upon cooling to rt, EtOAc was added. The reaction mixture was then washed with saturated NH_4Cl_{aq} solution, and H_2O. The organic phase was dried over Na_2SO_4 and concentrated *in vacuo*. The crude material was purified by silica gel chromatography to provide the corresponding benzothiazoles.

2-Cyano-6-methoxybenzothiazole

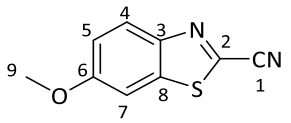

2.8

Following the above outlined procedure, Appel's salt (0.260 g, 1.24 mmol, 1 eq) and 2-bromo-4-methoxyaniline (0.250 g, 1.24 mmol, 1 eq) were combined and reacted with DBU (0.92 mL, 6.19 mmol, 5 eq) to afford 2-cyano-6-methoxybenzothiazole as a pale yellow solid (0.150 g, 64 %). **Mp**: 129-130 °C (lit. 129-131 °C).[5] **^{1}H-NMR (400 MHz, DMSO)** δ 8.15 (1H, d, *J* = 9.1 Hz, H-4), 7.89 (1H, d, *J* = 2.4 Hz, H-7), 7.33 (1H, dd, *J* = 9.1, 2.4 Hz, H-5), 3.93 (3H, s, H-9) ppm. **^{13}C-NMR (400 MHz, DMSO)** δ 160.4 (C-2), 146.7 (C-6), 138.3 (C-3), 134.1 (C-8), 125.8 (C-7), 119.1 (C-5), 114.1 (C-1), 106.0 (C-4), 56.52 (C-9) ppm. **MS (ESI+):** *m/z* Calculated for $C_9H_6N_2OS$ [M+H] 191.0279, found 191.0273.

2-Cyano-6-nitrobenzothiazole

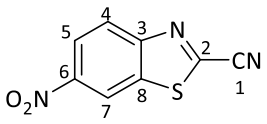

3.13

Following the above outlined procedure, Appel's salt (0.211 g, 1.01 mmol, 1.1 eq) and 2-bromo-4-nitroaniline (0.200 g, 0.921 mmol, 1 eq) were combined and reacted with DBU (0.70 mL, 4.61 mmol, 5 eq) to afford 2-cyano-6-nitrobenzothiazole as an orange solid (0.081 g, 43 %). **Mp**: 118-119 °C. **^{1}H-NMR (400 MHz, $CDCl_3$)** δ 8.97 (1H, dd, *J* = 2.2, 0.5 Hz, H-7), 8.55 (1H, dd, *J* = 9.6, 1.4 Hz, H-5), 8.42 (1H, dd, *J* = 9.1, 1.4 Hz, H-4) ppm. **^{13}C-NMR (100.6 MHz, $CDCl_3$)** δ 155.3 (C-2), 147.3 (C-6), 141.8 (C-3), 135.6 (C-8), 126.1 (C-5), 123.0 (C-4), 118.6 (C-7), 114.0 (C-1) ppm. **MS (ESI+):** *m/z* Calculated for $C_8H_3N_3O_2S$ [M+H] 206.0024, found 204.9715.

2-Cyano-fluorobenzothiazole

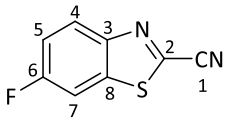

4.2b

Following the above outlined procedure, Appel's salt (0.241 g, 1.16 mmol, 1.1 eq) and 2-bromo-4-fluoroaniline (0.200 g, 1.05 mmol, 1 eq) were combined and reacted with DBU (0.79 mL, 5.26 mmol, 5 eq) to afford 2-cyano-6-fluorobenzothiazole as a yellow solid (0.0870 g, 46 %). **Mp**: 86-87 °C. **^{1}H-NMR (400 MHz, DMSO)** δ 8.04 (1H, dd, *J* = 8.0, 1.5 Hz, H-4), 7.64 (1H, dd, *J* = 7.5, 5.0 Hz, H-7), 7.26 (1H, td, *J* = 8.0, 1.5 Hz, H-5) ppm. **^{13}C-NMR (100.6 MHz, DMSO)** δ 158.5 (C-6), 147.2 (C-3) 136.7 (C-8), 138.1 (Ar-H), 123.8 (Ar-H), 113.8 (Ar-H), 113.2 (C-1), 108.9 (Ar-H) ppm. **FT-IR** (ATR) ν_{max} / cm^{-1}: 2218 (-CN).

2-Cyano-6-iodobenzothiazole

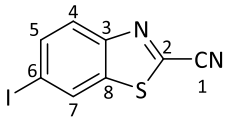

4.7

Following the above outlined procedure, Appel's salt (0.154 g, 0.738 mmol, 1.1 eq) and 2-bromo-4-iodoaniline (0.200 g, 0.671 mmol, 1 eq) were combined and reacted with DBU (0.50 mL, 3.35 mmol, 5 eq) to afford 6-iodo-2-cyanobenzothiazole as pale yellow solid (0.104 g, 54 %). **Mp**: 131-132 °C. **^{1}H-NMR (400 MHz, DMSO)** δ 8.52 (1H, d, *J* = 8.0 Hz, H-4), 7.90 (1H, d, *J* = 2.0 Hz, H-7), 7.43 (1H, dd, *J* = 8.0, 2.1 Hz, H-5) ppm. **^{13}C-NMR (100.6 MHz, DMSO)** δ 150.5 (C-6), 136.7 (C-2), 136.4 (C-1), 133.2

(Ar-q), 131.9 (Ar-q), 123.2 (Ar-q), 113.3 (C-1), 92.1 (C-6) ppm. **FT-IR** (ATR) ν_{max} / cm^{-1}: 2254 (-CN). **MS (ESI+):** *m/z* Calculated for $C_8H_3IN_2S$ [M+H] 286.9139, found 286.9134.

Alternative syntheses of luciferins

p-Iodoaniline

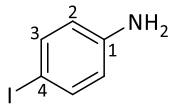

4.1

To a stirring solution of sodium bicarbonate (4.09 g, 48.8 mmol, 1.54 eq) in water (350 mL) was added aniline (3.0 mL, 31.6 mmol, 1.2 eq). The resultant mixture was cooled to 0 °C and iodine (6.32 g, 25.0 mmol, 1 eq) was added in small portions over 3 min intervals under intensive stirring during which the temperature of the reaction mixture was maintained below 15 °C. After the addition of the iodine, the mixture was allowed to warm to room temperature and was left to stir for an additional 40 min. Thereafter, the crude product was collected by centrifugation. The crude product was then recrystallised from pet. ether (30 mL) to afford 4-iodoaniline as a pale yellow solid (4.10 g, 72 %). **Mp**: 57-61 °C (lit. 61-63 °C).[20] **^{1}H-NMR (300 MHz, DMSO)**: δ 7.41 (2H, d, *J* = 8.0 Hz, H-3), 6.47 (1H, d, *J* = 8.0 Hz, H-2), 3.67 (2H, s, -NH_2) ppm. **^{13}C-NMR (100.6 MHz, DMSO)** δ 146.1 (C-1), 138.0 (C-3), 117.2 (C-2), 79.4 (C-4) ppm.

N-(4-iodophenyl)acetamide

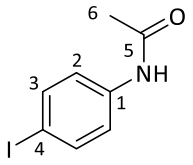

4.1f

p-Iodoaniline **4.1** (5.26 g, 24.0 mmol, 1 eq) and acetic anhydride (2.5 mL, 26.4 mmol, 1.1 eq) were dissolved in pyridine (10 mL). The resultant solution was allowed to stir for 2 h at 100 °C, after which, the solution was left to cool to room temperature. The reaction mixture was then poured into water (35 mL) and the resulting precipitate was collected by filtration and washed with cold water (2 x 30 mL). *N*-(4-Iodophenyl)acetamide was isolated as a white solid (5.92 g, 95 %). **Mp:** 179-182 °C (lit. 180-182 °C).[20] **^{1}H-NMR (400 MHz, DMSO)** δ 9.99 (1H, s, -NH-), 7.61 (2H, d, *J* = 8.0 Hz, H-3), 7.41 (2H, d, *J* = 8.0 Hz, H-2), 2.03 (3H, s, H-6) ppm. **^{13}C-NMR (100.6 MHz, DMSO)** δ 167.8 (C-5) 138.6 (C-1), 136.7 (C-3), 119.1 (C-2), 85.8 (C-4), 23.7 (C-6) ppm.

N-(2-bromo-4-iodophenyl)acetamide

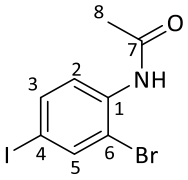

4.3

Method A: KBr (0.320 g, 2.65 mmol, 1.2 eq), $NaBO_3$ (0.320 g, 2.51 mmol, 1.1 eq) and *N*-(4-iodophenyl)acetamide **4.1f** (0.500 g, 1.90 mmol, 1.0 eq) were suspended in acetic acid (6 mL) at room temperature. The resulting mixture was allowed to stir for 24 h at room temperature after which H_2O (30 mL) was added to the reaction mixture. The aqueous phase was then extracted with EtOAc (4 x 10 mL), the combined organic extracts were dried over $MgSO_4$, filtered, and the solvent reduced *in vacuo* to afford *N*-(2-bromo-4-iodophenyl)acetamide as a brown solid (0.480 g, 71 %).

Method B: 4-Iodo-2-bromoaniline **5.5** (3.57 g, 12.0 mmol, 1 eq) and acetic anhydride (1.6 mL, 13.2 mmol, 1.1 eq) were dissolved in pyridine (4 mL). The resultant solution was allowed to stir for 2 h at 100 °C, after which, the reaction mixture was poured into water (50 mL) and the resulting precipitate was collected by filtration and washed with cold water (2 x 10 mL). *N*-(2-Bromo-4-iodophenyl)acetamide was isolated as a brown solid (5.92 g, 99 %). **Mp:** 145-147 °C. **^{1}H-NMR (300 MHz, DMSO)** δ 9.45 (1H, s, -NH-), 8.00 (1H, d, *J* = 2.0 Hz, H-5), 7.77 (1H, dd, *J* = 8.5, 2.0 Hz, H-3), 7.43 (1H, d, *J* = 8.5 Hz, H-2), 2.07 (3H, s, H-8) ppm. **^{13}C-NMR (100.6 MHz, DMSO)** δ 169.0 (C-7), 146.8 (Ar-q), 140.0 (C-1), 137.1 (Ar-H), 134.4 (Ar-H), 133.2 (Ar-H), 128.9 (Ar-q), 23.7 (C-8) ppm.

N-(2-bromo-4-iodophenyl)thioacetamide

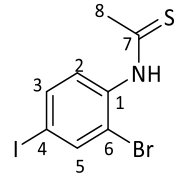

4.4

Method A: To a solution of *N*-(2-bromo-4-iodophenyl)acetamide **4.1** (1.10 g, 4.10 mmol, 1 eq) in DCM (60 mL) at room temperature was added P_2S_5 (1.70 g, 7.70 mmol, 1.9 eq), Al_2O_3 (0.0250 g, 0.250 mmol, 0.06 eq) and elementary sulfur (0.0130 g, 0.410 mmol, 0.1 eq). The reaction mixture was refluxed at 40 °C for 3 h. Once cooled to room temperature, the reaction mixture was poured into water (200 mL) and the aqueous layer extracted with diethyl ether (3 x 50 mL). The combined organic layers were washed with water (3 X 50 mL), brine (100 mL), dried over $MgSO_4$ and the solvent removed under reduced pressure. The crude material was purified using silica column chromatography 1:9 EtOAc:Pet.

ether. The material was further purified by recrystallisation using aqueous EtOH to afford the title compound as a yellow solid (0.430 g, 38 %).

Method B: *N*-(2-Bromo-4-iodophenyl)acetamide (3.53 g, 9.86 mmol, 1 eq) and Lawesson's reagent (2.19 g, 5.43 mmol, 0.55 eq) were dissolved in toluene (35 mL) and allowed to stir for 6 h at 110 °C under a nitrogen atmosphere .Thereafter, the resultant solution was allowed to cool to room temperature and poured into water (600 mL). The aqueous layer was extracted with DCM (3 x 50 mL), the combined extracts were washed with water (3 x 20 mL), brine (50 mL), and dried over $MgSO_4$. Excess solvent was removed under reduced pressure and the resulting residue purified using silica column chromatography, eluting with 1:10 EtOAc:Pet. ether, to afford *N*-(4-iodophenyl)-ethanethioamide as a brown solid that was further purified by recrystallisation using aqueous EtOH (2.95 g, 84 %). **Mp:** 141-144 °C. **^{1}H-NMR (400 MHz, DMSO)** δ11.43 (1H, s, -NH-), 8.09 (1H, d, *J* = 1.9 Hz, H-5), 7.79 (1H, dd, *J* = 8.3, 1.9 Hz, H-3), 7.20 (1H, d, *J* = 8.3 Hz, H-2), 2.61 (3H, s, H-8) ppm. **^{13}C-NMR (100.6 MHz, DMSO)** δ 202.6 (C-7), 140.8 (Ar-H), 138.9 (C-1), 137.5 (Ar-H), 132.2 (Ar-H), 122.4 (C-6), 94.2 (C-4), 33.6 (C-8) ppm.

N-(4-iodophenyl)ethanethioamide

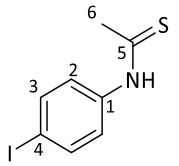

4.1g

A suspension of *N*-(4-iodophenyl)acetamide **4.1f** (1.10 g, 4.20 mmol, 1 eq) and Lawesson's reagent (1.15 g, 2.90 mmol, 0.7 eq) in toluene (20 mL) was heated for 6 h at 110 °C under a nitrogen atmosphere. Thereafter, the resultant solution was left to cool to room temperature and poured into water (200 mL). The aqueous layer was extracted with diethyl ether (3 x 50 mL), the combined extracts washed with water (3 x 50 mL), brine (50 mL), and dried over $MgSO_4$. Excess solvent was removed under reduced pressure and the resulting residue purified using silica column chromatography, eluting with 1:10 EtOAc:Pet. ether, to afford *N*-(4-iodophenyl)ethanethioamide as a brown solid (0.760 g, 94 %); **Mp:** 146-148 °C. **^{1}H-NMR (400 MHz, DMSO)** δ11.58 (1H, s, -NH-), 7.74 (2H, dd, *J* = 8.9, 1.5 Hz, H-3), 7.65 (2H, dd, *J* = 8.8, 1.5 Hz, H-2), 2.59 (3H, s, H-6) ppm. **^{13}C-NMR (100.6 MHz, DMSO)** δ 199.5 (C-5), 139.3 (C-1), 137.1 (C-3), 125.1 (C-2), 90.3 (C-4), 33.6 (C-6) ppm.

6-Iodo-2-methylbenzothiazole

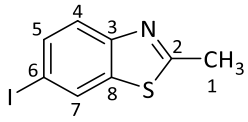

4.5

Method A: *N*-(4-Iodophenyl)ethanethioamide (1.00 g, 3.60 mmol, 1 eq) was dissolved in 30 % $NaOH_{aq}$ (5 mL) and water (5 mL) and allowed to stir at 0 °C for 20 min. The resultant solution was added dropwise, over 4 h, to a stirring solution of $K_3[Fe(CN)_6]$ (4.75 g, 14.5 mmol, 4 eq) in water (2 mL) at 0 °C. The reaction mixture was allowed to warm to room temperature and the resultant precipitate was collected by filtration and washed copiously with water to produce 6-Iodo-methylbenzothiazole as a pale brown solid (0.426 g, 43 %).

Method B: *N*-(2-Bromo-4-iodophenyl)acetamide (0.366 g, 1.03 mmol, 1 eq) and NaOMe (0.0670 g, 1.24 mmol, 1.1 eq) were dissolved and allowed to stir in NMP (2 mL) at 150 °C for 2 hr, after which the NMP was reduced by distillation. The remaining residue was then dissolved in EtOAc (10 mL), washed with brine (3 x 2 mL), water (1 x 2 mL) and the excess solvent reduced *in vacuo* to afford the title compound as a pale orange solid (0.221 g, 78 %). **Mp:** 137-139 °C (lit. 140-141 °C).[21] **^{1}H-NMR (300 MHz, $CDCl_3$)** δ 8.46 (1H, d, *J* = 1.7 Hz, H-7), 7.93-7.48 (2H, m, H-4/5), 2.79 (3H, s, H-1) ppm. **^{13}C-NMR (100.6 MHz, $CDCl_3$)** δ 168.4 (C-2), 152.8 (Ar-q), 138.1 (Ar-H), 135.1 (Ar-q), 130.7 (Ar-H), 124.1 (Ar-H), 89.9 (C-6), 20.1 (C-1) ppm. **MS (ESI+):** *m/z* Calculated for C_8H_6INS [M+H] 275.9343, found 275.9338.

6-Iodobenzothiazole-2-carbaldehyde

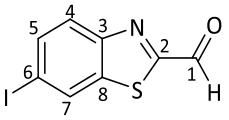

4.6

6-Iodo-2-methylbenzothiazole (0.778 g, 2.83 mmol, 1 eq) and SeO_2 (0.410 g, 3.67 mmol, 1.3 eq) were dissolved in a solution of dioxane (8 mL) and water (0.8 mL) and refluxed at 150 °C for 2 h. The reaction mixture was then cooled to room temperature, filtered through Celite, and the filtrate reduced *in vacuo.* The crude material was subjected to purification by flash chromatography and subsequently recrystallised from hexane to afford 6-iodobenzothiazole-2-carbaldehyde as a red solid (0.123 g, 15 %). **Mp:** 129-131 °C (lit. 133-134 °C).[22] **^{1}H-NMR (400 MHz, DMSO)** δ 10.12 (1H, s, H-1), 8.75 (1H, d, *J* = 1.7 Hz, H-7), 8.04 (2H, m, H-4/5) ppm. **^{13}C-NMR (100.6 MHz, DMSO)** δ 173.7 (C-1), 163.8 (C-2),

152.7 (Ar-q), 147.9 (Ar-q), 135.3 (Ar-H), 130.4 (Ar-H), 125.1 (Ar-H), 90.1 (C-6), ppm. **IR ν_{max} (cm^{-1})** 1732 (C=O, aldehyde)**. MS (ESI+):** *m/z* Calculated for C_8H_4INOS [M+2H] 290.9136, found 290.8680.

2-Cyano-6-iodobenzothiazole

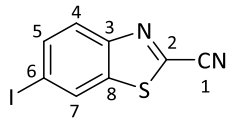

4.7

Method A: Triethylamine (0.10 mL, 0.800 mmol, 1.1 eq) and 6-iodobenzothiazole-2-carbaldehyde (0.200 g, 0.700 mol, 1 eq) was added to a solution of hydroxylamine hydrochloride (0.0600 g, 0.800 mmol, 1.1 eq) in anhydrous acetonitrile (2 mL) under a nitrogen atmosphere. The reaction mixture was allowed to stir for 3 h at room temperature. Thereafter, phthalic anhydride (0.100 g, 0.710 mmol, 1.01 eq) was added the solution refluxed for a further 8 h. The reaction mixture was then allowed to cool to room temperature at which point DCM (3 mL) was added resulting in the formation of a precipitate. The precipitate was filtered and the filtrate washed with 5 % NH_4Cl (4 x 1 mL). The organic layer was dried over $MgSO_4$ and the solvent reduced *in vacuo* to afford 2-cyano-6-benzothiazole as a pale yellow solid (0.170 g, 85 %).

Method B: Palladium chloride (6.00 mg, 0.0350 mmol, 0.1 eq), copper iodide (33.0 mg, 0.174 mmol, 0.5 eq), TBAB (0.224 g, 0.694 mmol, 2 eq), and 1-[(cyanocarbothioyl)amino]-4-iodobenzene (0.100 g, 0.347 mmol, 1 eq) were suspended in anhydrous 1:1 DMF:DMSO (2 mL). The resultant red-brown mixture was placed under an inert nitrogen atmosphere and heated at 120 °C for 4 h. The reaction was diluted with EtOAc (6 mL) and washed with H_2O (4 x 2 mL). The organic layer was then dried over Na_2SO_4, filtered, and concentrated *in vacuo*. The crude product was purified using silica column chromatography using 1:10 EtOAc:hexane to provide 2-cyano-6-iodobenzothiazole as a light yellow solid (7.00 mg, 7 %). **Mp**: 131-132 °C. **^{1}H-NMR (400 MHz, DMSO)** δ 8.52 (1H, d, *J* = 8.0 Hz, H-4), 7.90 (1H, d, *J* = 2.0 Hz, H-7), 7.43 (1H, dd, *J* = 8.0, 2.1 Hz, H-5) ppm. **^{13}C-NMR (100.6 MHz, DMSO)** δ 150.5 (C-6), 136.7 (C-2), 136.4 (C-1), 133.2 (Ar-q), 131.9 (Ar-q), 123.2 (Ar-q), 113.3 (C-1), 92.1 (C-6) ppm. **MS (ESI+):** *m/z* Calculated for $C_8H_3IN_2S$ [M+H] 286.9139, found 286.9134.

N-[(5Z)-4-chloro-5H-1,2,3-dithiazol-5-ylidene]-4-iodoaniline

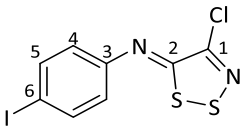

5.2a

Appel's salt (0.523 g, 2.51 mmol, 1.1 eq) and *p*-iodoaniline (0.500 g, 2.28 mmol, 1 eq) were suspended in freshly distilled DCM (3 mL). The resulting mixture was stirred under an inert nitrogen atmosphere at room temperature for 90 min. Thereafter, anhydrous pyridine (0.39 mL, 4.56 mmol, 2 eq) was slowly added to the stirring suspension and the resulting red-brown mixture was allowed to stir for an additional 2 h at room temperature. The mixture was then concentrated *in vacuo* and purified by silica column chromatography, eluting with hexanes, to afford *N*-[(5Z)-4-chloro-5H-1,2,3-dithiazol-5-ylidene]-4-iodoaniline as a yellow solid (0.386 g, 65 %). **Mp**: 90-91 °C. **^{1}H-NMR (400 MHz, $CDCl_3$)** δ 7.83 (2H, d, *J* = 8.0 Hz, H-5), 7.03 (2H, d, *J* = 8.0 Hz, H-4) ppm. **^{13}C-NMR (100.6 MHz, $CDCl_3$)** δ 160.64 (C-1), 151.12 (C-2), 147.25 (C-3), 139.19 (C-5), 122.26 (C-4), 91.09 (C-6) ppm.

1-[(Cyanocarbothioyl)amino]-4-iodobenzene

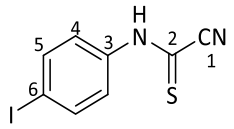

5.2

DBU (0.23 mL, 1.52 mmol, 3 eq) was added dropwise to a 5 °C solution of *N*-[(5Z)-4-chloro-5H-1,2,3-dithiazol-5-ylidene]-4-iodoaniline (0.180 g, 0.510 mmol, 1 eq) in anhydrous DCM (4 mL) under a nitrogen atmosphere. The resulting red-brown mixture was stirred at 5 °C for 30 min, after which it was warmed to room temperature. The reaction mixture was then diluted with DCM (6 mL), washed with saturated NH_4Cl_{aq} (3 x 2 mL), H_2O (1 x 2 mL), and brine (1 x 2 mL). The organic phase was dried over Na_2SO_4 and concentrated *in vacuo*. The crude material was purified by silica gel chromatography, eluting with 1:1 EtOAc:hexane to provide *1-[(cyanocarbothioyl)amino]-4-iodobenzene* as an orange solid (0.100 g, 70 %). **Mp**: 85-86 °C. **^{1}H-NMR (400 MHz, $CDCl_3$)** δ 9.92 (1H, br s, -NH-), , 7.84 (2H, m, H-5), 7.72 (2H, d, *J* = 8.1 Hz, H-4) ppm. **^{13}C-NMR (100.6 MHz, $CDCl_3$)** δ 162.0 (C-2), 138.7 (C-3), 138.3 (C-5), 137.8 (C-4), 114.2 (C-1), 93.3(C-6) ppm.

Synthesis of D-luciferin analogues

General procedure for the preparation of D-luciferin C-6 analogues

D-Cysteine hydrochloride monohydrate (1.05 eq) and the appropriate 2-cyanobenzothiazole (1 eq) were dissolved in either MeOH:H_2O or CH_3CN:H_2O. The solution was allowed to stir at room temperature for 5 min under a nitrogen atmosphere, after which potassium carbonate (1.05 eq) was added. The resulting solution was allowed to stir for an additional 30 min, while maintaining the inert atmosphere. Upon consumption of the 2-cyanobenzothiazole, as evidenced by TLC analysis, the reaction mixture was concentrated under reduced pressure and the remaining aqueous solution cooled to 0 °C and acidified to pH 3 with 3 M HCl. The aqueous was then extracted with EtOAc and the combined organics were dried over Na_2SO_4, filtered, concentrated *in vacuo* and subjected to column chromatography to provide the corresponding luciferin.

(4S)-2-(6-methoxy-1,3-benzothiazol-2-yl)-4,5-dihydro-1,3-thiazole-4-carboxylic acid[6]

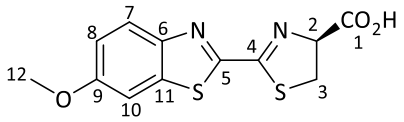

4.11a

Following the above outlined procedure, D-cysteine hydrochloride monohydrate (29.0 mg, 0.166 mmol, 1.05 eq) and 2-cyano-6-methoxybenzothiazole (30.0 mg, 0.158 mmol, 1 eq) were reacted in the presence of potassium carbonate (22.0 mg, 0.166 mmol, 1.05 eq) in 3:1 MeOH:H_2O (1 mL) to afford D-methoxyluciferin as a pale yellow solid (46.0 mg, 99 %). **$[\alpha]_{D}^{20}{}_{obs}$**: -26° (DMF, c = 1). **Mp**: 197-198 °C. **^{1}H-NMR (400 MHz, DMSO)** δ 8.03 (1H, d, *J* = 8.9, H-7), 7.76 (1H, d, *J* = 2.3, H-10), 7.22 (1H, dd, *J* = 8.9, 2.3 Hz, H-8), 5.45 (1H, dd, *J* = 9.7, 8.3 Hz, H-2), 3.79 (3H, s, H-12), 3.72 (2H, m, H-3) ppm. **^{13}C-NMR (100.6 MHz, DMSO)** δ 171.59 (C-1), 164.88 (C-4), 159.29 (C-5), 147.57 (C-9), 137.66 (C-6), 125.19 (C-11), 123.15 (C-8), 117.55 (C-7), 105.22 (C-10), 78.59 (C-2), 56.34 (C-12), 35.20 (C-3). **MS (ESI+):** *m/z* Calculated for $C_{12}H_{10}N_2O_3S_2$ [M+H] 295.0211, found 295.0205.

(4S)-2-(6-iodo-1,3-benzothiazol-2-yl)-4,5-dihydro-1,3-thiazole-4-carboxylic acid

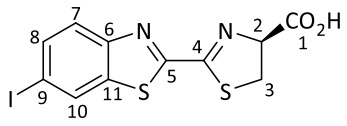

4.11b

Following the above outlined procedure, D-cysteine hydrochloride monohydrate (18.0 mg, 0.105 mmol, 1 eq) and 2-cyano-6-iodobenzothiazole (30.0 g, 0.105 mmol, 1 eq) were reacted in the presence of potassium carbonate (15.0 mg, 0.105 mmol, 1 eq) to afford D-iodoluciferin as an orange solid (41.0 mg, 99 %). **[α]$_{D}^{20}$$_{obs}$**: -11° (DMSO, c = 1). **Mp**: 176-179 °C. **^{1}H-NMR (400 MHz, DMSO)** *δ* 8.51 (1H, d, *J* = 8.0, H-7), 7.93 (1H, d, *J* = 2.3, H-10), 7.45 (1H, dd, *J* = 8.0, 2.0 Hz, H-8), 5.45 (1H, app t, *J* = 9.0 Hz, H-2), 3.70 (2H, m, H-3) ppm. **^{13}C-NMR (100.6 MHz, DMSO)** *δ* 177.59 (C-1), 163.78 (C-4), 159.09 (C-5), 152.51 (C-6), 136.66 (C-11), 131.90 (8), 131.19 (C-10), 123.15 (C-7), 91.29 (C-9), 82.09 (C-2), 34.76 (C-3) ppm.

(4S)-2-(6-nitro-1,3-benzothiazol-2-yl)-4,5-dihydro-1,3-thiazole-4-carboxylic acid

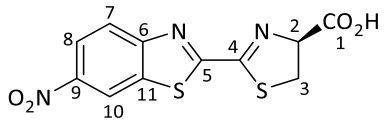

4.11c

Following the above outlined procedure, D-cysteine hydrochloride monohydrate (27.0 mg, 0.154 mmol, 1.05 eq) and 2-cyano-6-nitrobenzothiazole (30.0 mg, 0.146 mmol, 1 eq) were reacted in the presence of potassium carbonate (21.0 mg, 0.154 mmol, 1.05 eq) to afford D-nitroluciferin as a pale yellow solid (45.0 mg, 99 %). **[α]$_{D}^{20}$$_{obs}$**: -19° (DMSO, c = 1). **Mp**: 176-179 °C. **^{1}H-NMR (400 MHz, DMSO)** *δ* 8.64 (1H, d, *J* = 8.5, H-7), 8.30 (1H, d, *J* = 2.0, H-10), 8.07 (1H, dd, *J* = 8.5, 2.0 Hz, H-8), 5.47 (1H, app t, *J* = 9.0, H-2), 3.72 (2H, m, H-3) ppm. **^{13}C-NMR (100.6 MHz, DMSO)** *δ* 177.59 (C-1), 163.78 (C-4), 159.09 (C-5), 152.51 (C-6), 136.66 (C-11), 131.90 (8), 131.19 (C-10), 123.15 (C-7), 91.29 (C-9), 82.09 (C-2), 34.76 (C-3) ppm.

Synthesis of luciferin based probes

2-(Pyridin-2-yldisulfanyl)ethan-1-ol[23]

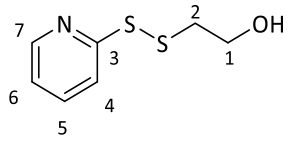

6.10a

Aldrithiol (0.150 g, 0.680 mmol, 2 eq) was dissolved in solution of MeOH (0.75 mL) and glacial acetic acid (0.01 mL). The solution was allowed to stir at room temperature under a nitrogen atmosphere for 5 min after which, mercaptoethanol (0.024 mL, 0.340 mmol, 1 eq) dissolved in MeOH (0.25 mL) was added dropwise over a 30 min period. The solvent was then evaporated under reduced pressure and the crude material purified using silica column chromatography eluting with 1:10 EtOAc:Hexane to afford the title compound as a viscous yellow oil (0.0370 g, 58 %). **^{1}H-NMR (300 MHz, $CDCl_3$)** δ 8.45 (1H, m, H-7), 7.82 (2H, m, H-5,6), 7.24 (1H, m, H-4), 4.99 (1H, t, *J* = 8.3 Hz, -OH), 3.63 (2H, m, H-1), 2.93 (2H, t, *J* = 6.3 Hz, H-2) ppm. **^{13}C-NMR (100.6 MHz, $CDCl_3$)** 159.9 (C-3), 149.6 (C-7), 138.6 (C-6), 122.2 (C-5), 119.8 (C-4), 59.6 (C-1), 41.7 (C-2) ppm.

N5-(1-((carboxymethyl)amino)-1-oxo-3-(pyridin-2-yldisulfanyl)propan-2-yl)glutamine

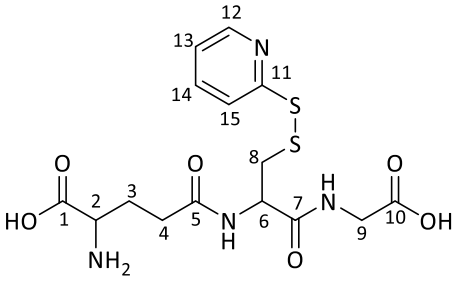

6.11

GSH (0.120 g, 0.103 mmol, 1 eq) dissolved in water (1.5 mL) was added to a stirring solution of aldrithiol (0.360 g, 0.410 mmol, 4 eq) dissolved in glacial acetic acid (0.01 mL) and MeOH (4 mL). The solution was then left to further stir overnight at room temperature, after which the solvent was evaporated and the crude material re-dissolved in distilled water, washed with copious amounts of DCM and then lyophilised to afford the title compound as a white solid (0.0410 g, 96 %). **^{1}H-NMR (300 MHz, DMSO)** δ 8.42 (1H, d, *J* = 4.9 Hz, H-12), 7.87 (2H, m, H-13/14), 7.36 (1H, m, H-15), 4.58 (1H, dd, *J* = 9.5, 4.4 Hz, H-6), 3.88 (2H, s, H-9), 3.75 (1H, m, H-2), 3.22 (2H, m, H-9), 2.25 (4H, m, H-3/4). **^{13}C-NMR (100.6 MHz, DMSO)** δ 178.9 (C-1), 174.6 (C-10), 173.7 (C-5), 172.2 (C-7), 157.7 (C-11), 148.3 (C-12), 139.7 (C-15), 122.6 (C-13), 122.5 (C-14), 53.8 (C-2), 57.2 (C-6), 41.8 (C-8), 39.4 (C-9), 31.3 (C-4), 26.0 (C-3) ppm. **HRMS (ESI+):** *m/z* Calculated for $C_{15}H_{20}N_4O_6S_2$ [M+H] 417.0902, found 417.0892.

Glutathione disulfide

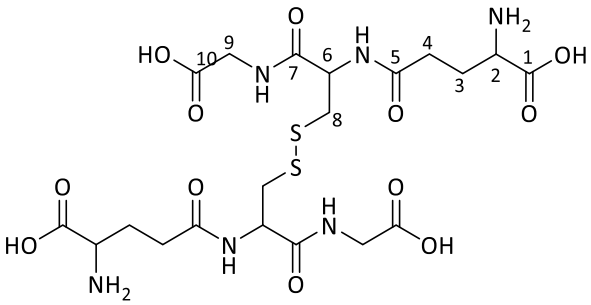

6.11b

Method A: GSH (50.0 mg, 0.0429 mmol, 1 eq) and $NaBO_3$ (10.2 mg, 0.0661 mmol, 1.54 eq) were suspended and stirred in a solution of water (1 mL) and acetic acid (0.01 mL) at room temperature for 72 h. The reaction mixture was then concentrated *in vacuo* and purified using reverse phase chromatography eluting with 9:1 H_2O:MeOH to afford the disulfide as a white powder (26.0 mg, 99 %).

Method B: N5-(1-((carboxymethyl)amino)-1-oxo-3-(pyridin-2-yldisulfanyl)propan-2-yl)glutamine **6.11** (10.0 mg, 0.0249 mmol, 1 eq) and GSH (7.74 mg, 0.0252 mmol, 1.05 eq) were dissolved in water and allowed to stir for 15 min. The resulting yellow solution was washed with DCM (8 x 2 mL) until clear. Thereafter the aqueous was frozen and lyophilised to afford GSSG as a white powder (15.0 mg, 99 %). **Mp**: 30-42 °C (Lit. 54 °C). **^{1}H-NMR (300 MHz, DMSO)** δ 4.58 (1H, dd, *J* = 9.5, 4.4 Hz, H-6), 3.88 (2H, s, H-9), 3.75 (1H, m, H-2), 3.22 (2H, m, H-9), 2.25 (4H, m, H-3,4). **MS (ESI+):** *m/z* Calculated for $C_{15}H_{20}N_4O_6S_2$ [M+2H] 614.6460, found 614.6460.

D-Thioluciferin disulfide

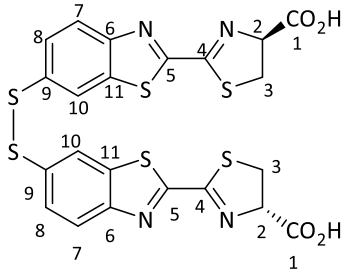

6.11c

D-Thioluciferin (10.0 mg, 0.0337 mmol, 1 eq) and I_2 (1.7 mg, 0.0661 mmol, 0.2 eq) were suspended and stirred in a 1:1 solution of chloroform and DMSO (0.4 mL) at room temperature for 10 min. The reaction mixture was then diluted with EtOAc, (5 mL) and washed with saturated $Na_2S_2O_3$ (2 x 2 mL) and water (1 x 2 mL). The organic layer was then dried over $MgSO_4$ and concentrated *in vacuo* to afford the disulfide as a pale yellow solid (9.7 mg, 99 %). **^{1}H-NMR (400 MHz, DMSO)** δ 8.49 (1H, s, H-10), 8.18

(1H, dd, *J* = 8.7, 0.5 Hz, H-7), 7.78 (1H, dd, *J* = 8.7, 2.0 Hz, H-8), 5.45 (1H, dd, *J* = 9.8, 8.3 Hz, H-2), 3.75 (2H, m, H-3) ppm. **MS (ESI+):** *m/z* Calculated for $C_{22}H_{14}N_4O_4S_6$ [M+H] 591.7472, found 591.7472.

D-Thioluciferin GSH disulfide

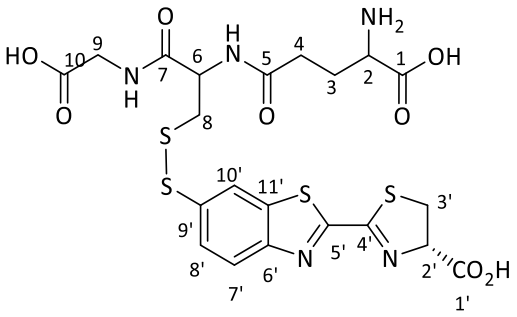

6.12

N5-(1-((carboxymethyl)amino)-1-oxo-3-(pyridin-2-yldisulfanyl)propan-2-yl)glutamine **6.11** (5.0 mg, 0.0125 mmol, 1 eq) and D-thioluciferin (3.7 mg, 0.0125 mmol, 1 eq) were dissolved in a 8:2 solution of water:acetonitrile (1 mL) and allowed to stir for 10 min under a nitrogen atmosphere. The resulting yellow solution was further diluted with additional water (3 mL) and washed with DCM (10 x 2 mL) until clear. Thereafter the remaining aqueous layer was frozen and lyophilised to afford the disulfide as a white powder (4.5 mg, 62 %). **^{1}H-NMR (400 MHz, DMSO)** δ 8.61 (1H, s, H-10'), 8.18 (1H, dd, *J* = 8.7, 0.5 Hz, H-7'), 7.84 (1H, dd, *J* = 8.7, 2.0 Hz, H-8'), 5.50 (1H, dd, *J* = 9.8, 8.3 Hz, H-2'), 4.58 (1H, dd, *J* = 9.5, 4.4 Hz, H-6), 3.88 (2H, s, H-9), 3.60-3.55 (2H, m, H-2/2'), 3.32-3.22 (2H, m, H-9), 2.25 (4H, m, H-3,4) ppm. **^{13}C-NMR (100.6 MHz, DMSO** *δ* 177.8 (C-1'), 175.1 (C-1), 174.9 (C-10), 174.2 (C=O), 174.0 (C=O), 1664 (Ar-q), 166.3 (Ar-q), 155.9 (Ar-q), 151.7 (C-5'), 150.1 (Ar-q), 125.3 (Ar-H), 123.3 (Ar-H), 82.5 (C-2'), 34.3 (C-3') ppm. **MS (ESI+):** *m/z* Calculated for $C_{21}H_{24}N_5O_8S_4$ [M+H+Na] 624.6692, found 624.6692.

Live imaging of luciferase expression

Luciferase expressing *N. Tabacum* plants were received from Dr. Suhail Rafudeen of the Plant Stress Research Unit at the University of Cape Town. The plants were transfected with a previously prepared luciferase coupled stress inducible promotor, *XvSap1*, isolated from *X. viscosa*. Luciferase expression was then induced by subjecting mature *N. Tabacum* plants were subjected to a two week dehydration period, after which leaves were taken from plants for bioluminescence imaging. leaves were individually sprayed and painted with equal amounts of 5 mM D-Luciferin (VivoGlo, Promega Corporation, USA). Luciferase activity was imaged with a 3D-luminometer consisting of a 0.5 square inch CCD camera and a field of view of 12.5 cm (Xenogen IVIS Lumina, Caliper, USA) at an exposure time of 300 s per leaf. Photon or count emission by luciferase expressing leaves was quantified using the Living Image software (Caliper, USA). The GFP assay was selected to negate any luminescence from chloroplasts.

Purified protein luminescence assays

Luminescence assays were initiated by adding 30 µL of purified luciferase in enzyme buffer (20 mM Tris [pH 7.4], 0.1 mM EDTA, 1 mM TCEP, and 0.8 mg/mL BSA) to 30 µL 2x substrate in substrate buffer (20 mM Tris [pH 7.4], 0.1 mM EDTA, 8 mM MgSO4, and 4 mM ATP) in a black 96-well plate (Costar 3915). Imaging was performed one minute after enzyme addition using a Xenogen IVIS-100 at a final enzyme concentration of 10 nM and final substrate concentrations ranging from 0.122 to 250 µM. Data acquisition and analysis was performed with Living Image® software. Data are reported as total flux (p/s) for each ROI corresponding to each well of the 96-well plate.

Bioluminescence emission scans

Purified luciferase in enzyme buffer was rapidly injected into a cuvette containing substrate in substrate buffer to a final enzyme concentration of 100 nM and a final substrate concentration of 10 µM. The emission from 400 to 800 nm was recorded in a SPEX FluoroMax-3 fluorimeter with closed excitation slits 10 s after injection.

Burst kinetics assays

Using a Turner Biosystems 20/20n luminometer, 40 µL of purified luciferase in enzyme injection buffer (20 mM Tris [pH 7.4], 0.1 mM EDTA, 0.625 mM TCEP, and 0.5 mg/mL BSA) was rapidly injected into a clear Eppendorf tube containing 10 µL of substrate in substrate injection buffer (20 mM Tris [pH 7.4], 0.1 mM EDTA, 20 mM MgSO4, and 10 mM ATP) to a final enzyme concentration of 0.2 nM and a final luciferin substrate concentration of 250 µM. Measurements were taken every 0.2 s for 1 s pre-injection and 120 s post-injection. Data acquisition was performed with SIS for 2020n v1.9.0 software.

Data are reported as Relative Light Units (RLU). To correct for the wavelength sensitivity of the PMT in the 20/20n, total flux was also measured using the IVIS-100 as described above with a final enzyme concentration of 10 nM and a final substrate concentration of 250 µM. Data from the IVIS and from the 20/20n at the 60 s time point were normalised to the WT + D-luciferin value. The correction factor of each enzyme/substrate pair was calculated by dividing the normalized IVIS data by the normalised 20/20n data. All 20/20n data were then multiplied by their respective correction factors.

UV-vis Experiments (absorption sectra)

Absorption spectra for D-Luciferin, luciferin-analogues and all precursor 2-cyanobenzothiazoles were recorded with a Cary 60 spectrophotometer, instrument version 2.00. Samples were prepared as a 0.01 mM DMSO solution unless otherwise stated and were scanned from 200 nm to 650 nm at a UV-Vis scan rate of 24000.00 nm/min. Data were analysed using Scan Software Version 5.0.0.999.

Fluorescence Spectrophotometry (excitation emission spectra)

Excitation and emission spectra were recorded on a Varian Cary Eclipse fluorometer equipped with a regulated temperature cell holder and Hellma, Suprasil® quartz fluorescence cuvettes of 10 mm pathlength and 1.5 mL volume capacity. Emission spectra were recorded at an excitation wavelength corresponding to previously recorded absorption maxima. Samples were prepared as a 0.1 mM DMSO solution, unless otherwise stated, and were scanned from 200 nm to 800 nm (Ex. Slit/ Em. Slit 5 nm) at a scan rate of 600.00 nm/mn. Data were analysed using Scan Software Version 1.1.

Purified protein luminescence assays

Luciferase was prepared as a 10 nM solution in enzyme buffer. Luciferase lyophilized powder (luciferase from *Photinus Pyralis*, Sigma-Aldrich) was dissolved in previously prepared luciferase enzyme buffer (20 mM Tris [pH 7.4], 0.1 mM EDTA, 1 mM DTT, and 0.8 mg/mL BSA). D-Luciferin, D-aminoluciferin and D-thioluciferin were prepared as 0.1 µM, 3.56 µM, 10 µM, 100 µM and 1 M solutions in substrate buffer (20 mM Tris [pH 7.4], 0.1 mM EDTA, 8 mM $MgSO_4$, and 4 mM ATP). Luminescence assays were initiated by adding 30 µL of luciferase in luciferase enzyme buffer to 60 µL substrate in substrate buffer in a white 96-well plate (Costar 3915). Imaging was performed one minute after enzyme addition using a Luminoskan Ascent (detector 270 - 670 nm) and data acquisition and analyses were performed with Ascent Software version 2.6. Data are reported as RLU for each ROI corresponding to each well of the 96-well plate.

Purified luciferase inhibition assays

Luciferase was prepared as a 10 nM solution in enzyme buffer. Luciferase lyophilized powder (luciferase from *Photinus Pyralis*, Sigma-Aldrich) was dissolved in previously prepared luciferase enzyme buffer (20 mM Tris [pH 7.4], 0.1 mM EDTA, 1 mM DTT, and 0.8 mg/mL BSA). D-thioluciferin, was prepared as a 10 µM solution in substrate buffer (20 mM Tris [pH 7.4], 0.1 mM EDTA, 8 mM $MgSO_4$, and 4 mM ATP) and D-thioluciferin thioacrylate was prepared as a 0.1 µM 1 µM and 10 µM solution in substrate buffer (20 mM Tris [pH 7.4], 0.1 mM EDTA, 8 mM $MgSO_4$, and 4 mM ATP). Starting solutions of 10 µM D-thioluciferin and increasing concentrations of D-thioluciferin thioacrylate were then prepared. 60 µL of a 1:1 solutions of 10 µM D-thioluciferin and 0.1 µM 1 µM and 10 µM D-thioluciferin thioacrylate were prepared. Inhibition assays were initiated by adding 30 µL of luciferase in luciferase enzyme buffer to 60 µL of a mixture of D-thioluciferin and D-thioluciferin thioacrylate in substrate buffer in a white 96-well plate (Costar 3915). Imaging was performed one minute after enzyme addition using a Luminoskan Ascent (detector 270 - 670 nm) and data acquisition and analyses were performed with Ascent Software version 2.6. Data are reported as RLU for each ROI corresponding to each well of the 96-well plate.

Live imaging of luciferase expression in N. Tabacum plants

Live imaging of luciferase expression: Luciferase expressing *N. Tabacum* plants were received from Dr. Suhail Rafudeen of the Plant Stress Research Unit at the University of Cape Town. The plants were transfected with a previously prepared luciferase coupled stress inducible promotor, *XvSap1*, isolated from *X. viscosa*. Luciferase expression was then induced by subjecting mature *N. Tabacum* plants were subjected to a 6 day dehydration period, after which leaves were taken from plants for bioluminescence imaging. leaves were individually sprayed and painted with equal amounts of 5 mM D-Luciferin (VivoGlo, Promega Corporation, USA). Luciferase activity was imaged with a 3D-luminometer consisting of a 0.5 square inch CCD camera and a field of view of 12.5 cm (Xenogen IVIS Lumina, Caliper, USA) at an exposure time of 300 s per leaf. Photon or count emission by luciferase expressing leaves was quantified using the Living Image software (Caliper, USA). The GFP assay was selected to negate any luminescence from chloroplasts.

Agrobacterium infection of leaf disks: Leaf disks were infected for 30 min in the dark with the *Agrobacterium* inoculum containing the promoter cassettes in sterile petri dishes. The petri dish was agitated once every 10 min. Thereafter, infected leaf disks were blot dried on sterile filter paper. Each infected explant was transferred to co-cultivation medium and incubated for 3 days at 23 ^{o}C (18 h light, 6 h dark; light intensity of 140 µmol/m2/s). The co-cultivation media comprised 28 hormone free

MS basal salts (Highveld Biological, South Africa) supplemented with B5 vitamins, 30 g/L sucrose, 0.1 mg/L α-naphthaleneacetic acid, 1 mg/L 6-benzylamino purine and 100 µM/l acetosyringone. The pH was adjusted to 5.4 with 1M KOH. Following the 3 day co-cultivation period, leaf discs were selected on shooting medium comprising hormone free MS basal salts supplemented with B5 vitamins, 30 g/L sucrose, 0.1 mg/L α-naphthaleneacetic acid, 1 mg/L 6-benzylamino purine, 10 µg/L nyastatin, 250 mg/L carbenicillin, and 3 mg/L BASTA (Bayer, South Africa). Leaf explants were placed under an 18 h light regime with light intensity of 140 µmol/m2/s at 28ºC. Putative transformants were subcultured fortnightly onto fresh media until sizable shoots were formed. BASTA resistant shoots were selected, excised and transferred to rooting media. The rooting media comprised half strength hormone free MS basal salts (Highveld Biological, South Africa) supplemented with 10 mg/L sucrose, 10 µg/L nyastatin, 250 mg/L carbenicillin and 3 mg/L BASTA (Bayer, South Africa). Putative transformants with well-established root systems were transferred to pots containing sterile potting soil and cultured with set conditions. The plants were covered with saran wrap for 8 days to assist acclimatisation and minimise dehydration. Once acclimatised, the putative transformants were transferred to 6 inch pots containing potting soil under normal growth conditions.

Dehydration of luciferase expressing transgenic tobacco plants: The dehydration treatments were carried out as described by Audran *et al* with the following modification: plants were dehydrated in soil instead of hydroponically. Prior to dehydration, plants were transferred to pots containing 800 g of soil and 200 ml water to allow for even drying rates. Plants were moved to Percival chambers (Percival Scientific Inc, USA) and incubated under set conditions (26 ^{o}C; 16 h day, 8 h night; 60% humidity; light intensity of 100 µmol/m2/s) for 1 week. Dehydration stress was carried out on whole plants and achieved by withholding water for 6 days. Day 0 of the dehydration treatment represents the first day after watering ceased. Stressed tobacco leaves were sampled every 24 hours. The sampled leaves were used to assay for luciferase activity.

Glutathione reductase assay using a GSH-Aldrithiol mixed disulfide substrate[23]

Glutathione reductase (GSR) activity was measured via the increase in absorbance at 340 nm over time as a result of 2-thiopyridine release upon GSR mediated GSH-Aldrithiol reduction. The assay was done in triplicate and kinetic data recorded on a Cary 60 eclipse UV-VIS spectrophotometer that had been blanked with distilled water. Absorbance was read at 340 nm over 30 min at 30 s intervals.

Sample preparation: Test samples were prepared by mixing 0.25 mL of 6 mM GSH-Aldrithiol disulfide in deionised water with 1 mL of previously prepared phosphate buffer (75 mM potassium phosphate monobasic with 0.15 % (w/v) Bovine Serum Albumin (BSA), pH 5.5), 0.15 mL deionised water, 0.05 mL

of 4.5 mM NADPH (b-Nicotanamide Adenine Dinucleotide Phosphate, reduced form, tetrasodium salt) in deionised water, to a final volume of 1.45 mL. The solution was incubated at 25 ^{o}C for 5 min, after which the absorbance was recorded at 340 nm on a UV-VIS spectrophotometer until a steady reading was observed. After a constant absorbance reading was achieved, 0.05 mL of GSR (0.5 unit/mL in deionised water) was then rapidly injected into the solution and it was immediately inverted to mix and then the change in absorbance at 340 nm was measured over a 30 min period.

Final assay concentrations: In a 1.5 mL reaction mixture, the final concentrations are 50 mM potassium phosphate, 1.0 mM GSH-Aldrithiol disulfide, 0.15 mM NADPH, 0.01 % (w/v) BSA, and 0.05 unit GSR. The assay was repeated at varying GSH-Aldrithiol concentrations (1.7 mM, 1.0 mM, 0.5 mM, 0.35 mM, 0.25 mM and 0.1 mM) adjusted accordingly with deionized water.

Rate determination and enzyme kinetics: The rates of disulfide reduction at each concentration (1.7 mM, 1.0 mM, 0.5 mM, 0.35 mM, 0.25 mM and 0.1 mM) were obtained from the gradient of the absorbance curves. The relative rates were then plotted against their corresponding substrate concentrations to generate a Michealis-Menton plot. Graph Pad Prism software version 5.0 was used to calculate the apparent Km and Vmax values through its non-linear regression Michealis-kinetics option. Km and Vmax are reported as ranges with a 95 % confidence interval.

Glutathione reductase assay using GSSG[24]

Glutathione reductase (GSR) activity was measured via the decrease in absorbance at 340 nm over time as a result of NADPH consumption upon GSR mediated GSSG reduction. The assay was done in triplicate and kinetic data recorded on a Cary 60 eclipse UV-VIS spectrophotometer that had been blanked with distilled water. Absorbance was read at 340 nm over 30 min at 30 s intervals.

Sample preparation: Test samples were prepared by mixing 0.25 mL of 6 mM GSSG in deionised water with 1 mL of previously prepared phosphate buffer (75 mM potassium phosphate monobasic with 0.15 % (w/v) Bovine Serum Albumin (BSA), pH 5.5), 0.15 mL deionised water, 0.05 mL of 4.5 mM NADPH (b-Nicotanamide Adenine Dinucleotide Phosphate, reduced form, tetrasodium salt) in deionised water, to a final volume of 1.45 mL. The solution was incubated at 25 ^{o}C for 5 min, after which the absorbance was recorded at 340 nm on a UV-VIS spectrophotometer until a steady reading was observed. After a constant absorbance reading was achieved, 0.05 mL of GSR (0.5 unit/mL in deionised water) was then rapidly injected into the solution and it was immediately inverted to mix and then the change in absorbance at 340 nm was measured over a 30 min period.

Final assay concentrations: In a 1.5 mL reaction mixture, the final concentrations are 50 mM potassium phosphate, 1.0 mM GSSG, 0.15 mM NADPH, 0.01 % (w/v) BSA, and 0.05 unit GSR. The assay was

repeated at varying GSSG concentrations (1.0 mM, 0.5 mM, 0.25 mM and 0.1 mM) adjusted accordingly with deionized water.

Rate determination and enzyme kinetics: The rates of disulfide reduction at each concentration (1.0 mM, 0.5 mM, 0.25 mM and 0.1 mM) were obtained from the gradient of the absorbance curves. The relative rates were then plotted against their corresponding substrate concentrations to generate a Michealis-Menton plot. Graph Pad Prism software version 5.0 was used to calculate the apparent Km and Vmax values through its non-linear regression Michealis-kinetics option. Km and Vmax are reported as ranges with a 95 % confidence interval.

Thiolate release assay

Potassium thiolates were reacted with vinyl sulfides to determine relative rates and to evaluate the effect of the potassium thiolate on the reaction rate. The vinylssulfide was measured at 340 and 380 nm using a Cary 60 eclipse UV-VIS spectrophotometer, that had been blanked with distilled water. The change in absorbance over time as a result of the addition of either potassium thioacetate or L-Cys/potassium carbonate was then measured.

Sample preparation: The vinyl sulfides, benzyl (E)-3-((4-aminophenyl)thio)acrylate and benzyl (E)-3-((4-(((Z)-4-chloro-5H-1,2,3-dithiazol-5-ylidene)amino)phenyl)thio)acrylate, were prepared as a 5 mM solution in 1:3 (v/v) H_2O:CH_3CN. Potassium thioacetate and 1:1 L-Cys:potassium carbonate were prepared as 5 mM solutions in deionized water.

Rate determinations: 0.05 mL of vinyl sulfide was added to 1.45 mL of 1:3 (v/v) H2O:CH3CN, and the absorbance was recorded until a constant reading was observed. 0.05 mL of the thiolate was then injected and the solution rapidly inverted to mix before reading the change in absorbance for 500 s at 10 second intervals. Benzyl (E)-3-((4-aminophenyl)thio)acrylate absorbance was read at 320 nm and benzyl (E)-3-((4-(((Z)-4-chloro-5H-1,2,3-dithiazol-5-ylidene)amino)phenyl)thio)acrylate was read at 380 nm, corresponding to their previously recorded absorbance maxima.

References

1. McCutcheon, D. C.; Paley, M. A.; Steinhardt, R. C.; Prescher, J. A., Expedient synthesis of electronically modified luciferins for bioluminescence imaging. Journal of the American Chemical Society 2012, 134 (18), 7604-7607.

2. Appel, R.; Janssen, H.; Siray, M.; Knoch, F., Synthesis and Reactions of 4,5-Dichloro-1,2,3-dithiazolium chlorides. Chemische Berichte 1985, 118 (4), 1632-1643.

3. Besson, T.; Rees, C. W., Some chemistry of 4, 5-dichloro-1, 2, 3-dithiazolium chloride and its derivatives. Journal of the Chemical Society, Perkin Transactions 1 1995, (13), 1659-1662.

4. Grabenko, A.; Pelkis, P., ISSLEDOVANIYA V RYADU ZAMESHCHENNYKH ARILAMIDOV DITIOKARBONOVYKH KISLOT. 1. SINTEZ ALKOKSIZAMESHCHENNYKH N-FENILDITIOOKSAMIDA. ZHURNAL OBSHCHEI KHIMII 1960, 30 (4), 1222-1226.

5. Mcelroy, W. D.; White, E. H., Hydroxybenzothiazoles and methods of preparing same. Google Patents: 1965.

6. White, E. H.; Wörther, H.; Field, G. F.; McElroy, W. D., Analogs of firefly luciferin. The Journal of Organic Chemistry 1965, 30 (7), 2344-2348.

7. Seliger, H.; McElroy, W.; White, E.; Field, G., Stereospecificity and firefly bioluminescence, a comparison of natural and synthetic luciferins. Proceedings of the National Academy of Sciences 1961, 47 (8), 1129-1134.

8. White, E. H.; Wörther, H.; Seliger, H. H.; McElroy, W. D., Amino Analogs of Firefly Luciferin and Biological Activity Thereof1. Journal of the American Chemical Society 1966, 88 (9), 2015-2019.

9. Porterfield, W. B.; Jones, K. A.; McCutcheon, D. C.; Prescher, J. A., A “Caged” Luciferin for Imaging Cell–Cell Contacts. Journal of the American Chemical Society 2015, 137 (27), 8656-8659.

10. Appel, R.; Janssen, H.; Siray, M.; Knoch, F., Synthese und Reaktionen des 4, 5-Dichlor-1, 2, 3-dithiazolium-chlorids. Chemische Berichte 1985, 118 (4), 1632-1643.

11. FRIEDRICH, K.; ZAMKANEI, M., DIELS-ALDER REACTIONS WITH CYANOTHIOFORMAMIDES. TETRAHEDRON LETTERS 1977, (25), 2139-2140.

12. Baker, A. E.; Marchal, E.; Lund, K.-l. A.; Thompson, A., The use of tin (IV) chloride to selectively cleave benzyl esters over benzyl ethers and benzyl amines. Canadian Journal of Chemistry 2014, 92 (12), 1175-1185.

13. Cossy, J.; Poitevin, C.; Pardo, D. G.; Peglion, J. L., An Easy and Efficient Access to 2-Bromo-4-methoxyaniline. Synthetic communications 1997, 27 (20), 3525-3527.

14. Roche, D.; Prasad, K.; Repic, O.; Blacklock, T. J., Mild and regioselective oxidative bromination of anilines using potassium bromide and sodium perborate. Tetrahedron letters 2000, 41 (13), 2083-2085.

15. Ando, W.; Tsumaki, H., Synthetic Application of Aminosilanes: Selective Bromination of Anilines via Reaction of Anilinosilanes with N-Bromosuccinimide. Synthesis 1982, 1982 (04), 263-264.

16. McKillop, A.; Koyuncu, D.; Krief, A.; Dumont, W.; Renier, P.; Trabelsi, M., Efficicient, high yield, oxidation of thiols and selenols to disulphides and diselenides. Tetrahedron Letters 1990, 31 (35), 5007-5010.

17. Lam, K.; Geiger, W. E., Anodic Oxidation of Disulfides: Detection and Reactions of Disulfide Radical Cations. The Journal of organic chemistry 2013, 78 (16), 8020-8027.

18. Santos, P. F.; Reis, L. V.; Duarte, I.; Serrano, J. P.; Almeida, P.; Oliveira, A. S.; Ferreira, L. F. V., Synthesis and photochemical evaluation of iodinated squarylium cyanine dyes. Helvetica chimica acta 2005, 88 (5), 1135-1143.

19. Quang, N.; Diêp, B. K.; Buu-Hoï, N., Orientation dans la Réaction de Friedel-Crafts D'acétylation des Bromofluorobenzènes. Recueil des Travaux Chimiques des Pays-Bas 1964, 83 (11), 1142-1148.

20. Stevens, T., Amine Oxidations with Iodine Pentafluoride. Preparation of Azoisobutane. The Journal of Organic Chemistry 1961, 26 (7), 2531-2533.

21. Cyanine dyes containing the triazolo [4, 3-alpha] quinoline or tetrazolo [alpha] quinoline nucleus. Google Patents: 1954.

22. Hrobárik, P.; Hrobáriková, V.; Sigmundová, I.; Zahradník, P.; Fakis, M.; Polyzos, I.; Persephonis, P., Benzothiazoles with tunable electron-withdrawing strength and reverse polarity: a route to triphenylamine-based chromophores with enhanced two-photon absorption. The Journal of organic chemistry 2011, 76 (21), 8726-8736.

23. Jones, L. R.; Goun, E. A.; Shinde, R.; Rothbard, J. B.; Contag, C. H.; Wender, P. A., Releasable luciferin-transporter conjugates: tools for the real-time analysis of cellular uptake and release. Journal of the American Chemical Society 2006, 128 (20), 6526-6527.

24. Carlberg, I.; Mannervik, B., [59] Glutathione reductase. Methods in enzymology 1985, 113, 484-490.